National Library of Canada
Canadian Theses Service
Ottawa, Canada
K1A 0N4

Bibliothèque nationale du Canada
Services des thèses canadiennes

CANADIAN THESES

THÈSES CANADIENNES

NOTICE

The quality of this microfiche is heavily dependent upon the quality of the original thesis submitted for microfilming. Every effort has been made to ensure the highest quality of reproduction possible.

If pages are missing, contact the university which granted the degree.

Some pages may have indistinct print especially if the original pages were typed with a poor typewriter ribbon or if the university sent us an inferior photocopy.

Previously copyrighted materials (journal articles, published tests, etc.) are not filmed.

Reproduction in full or in part of this film is governed by the Canadian Copyright Act, R.S.C. 1970, c. C-30.

AVIS

La qualité de cette microfiche dépend grandement de la qualité de la thèse soumise au microfilmage. Nous avons tout fait pour assurer une qualité supérieure de reproduction.

S'il manque des pages, veuillez communiquer avec l'université qui a conféré le grade.

La qualité d'impression de certaines pages peut laisser à désirer, surtout si les pages originales ont été dactylographiées à l'aide d'un ruban usé ou si l'université nous a fait parvenir une photocopie de qualité inférieure.

Les documents qui font déjà l'objet d'un droit d'auteur (articles de revue, examens publiés, etc.) ne sont pas microfilmés.

La reproduction, même partielle, de ce microfilm est soumise à la Loi canadienne sur le droit d'auteur, SRC 1970, c. C-30.

THIS DISSERTATION HAS BEEN MICROFILMED EXACTLY AS RECEIVED

LA THÈSE A ÉTÉ MICROFILMÉE TELLE QUE NOUS L'AVONS REÇUE

NL-339 (r. 86/06)

Canada

THE UNIVERSITY OF ALBERTA

Origin Of Gold In The White Channel Sediments Of The Klondike Region, Yukon Territory

by

Michael B. Dufresne

A THESIS

SUBMITTED TO THE FACULTY OF GRADUATE STUDIES AND RESEARCH

IN PARTIAL FULFILMENT OF THE REQUIREMENTS FOR THE DEGREE

OF Master of Science

Department of Geology

Edmonton, Alberta

Spring, 1987

Permission has been granted to the National Library of Canada to microfilm this thesis and to lend or sell copies of the film.

The author (copyright owner) has reserved other publication rights, and neither the thesis nor extensive extracts from it may be printed or otherwise reproduced without his/her written permission.

L'autorisation a été accordée à la Bibliothèque nationale du Canada de microfilmer cette thèse et de prêter ou de vendre des exemplaires du film.

L'auteur (titulaire du droit d'auteur) se réserve les autres droits de publication; ni la thèse ni de longs extraits de celle-ci ne doivent être imprimés ou autrement reproduits sans son autorisation écrite.

ISBN 0-315-37737-2

THE UNIVERSITY OF ALBERTA

RELEASE FORM

NAME OF AUTHOR Michael B. Dufresne

TITLE OF THESIS Origin Of Gold In The White Channel Sediments Of The Klondike Region, Yukon Territory

DEGREE FOR WHICH THESIS WAS PRESENTED Master of Science

YEAR THIS DEGREE GRANTED Spring, 1987

Permission is hereby granted to THE UNIVERSITY OF ALBERTA LIBRARY to reproduce single copies of this thesis and to lend or sell such copies for private, scholarly or scientific research purposes only.

The author reserves other publication rights, and neither the thesis nor extensive extracts from it may be printed or otherwise reproduced without the author's written permission.

(SIGNED) Michael B. Dufresne

PERMANENT ADDRESS:

3626 Bethel Rd.

Wilmington, N.C. 28403

U.S.A.

DATED March 3 1987

THE UNIVERSITY OF ALBERTA

FACULTY OF GRADUATE STUDIES AND RESEARCH

The undersigned certify that they have read, and recommend to the Faculty of Graduate Studies and Research, for acceptance, a thesis entitled Origin Of Gold In The White Channel Sediments Of The Klondike Region, Yukon Territory submitted by Michael B. Dufresne in partial fulfilment of the requirements for the degree of Master of Science.

Bruce Ventre
Supervisor

Fred Cook

Date June 23, 1986

DEDICATION

To my family, to all my friends and to all those people at the University of North Carolina Wilmington and the University of Alberta who pushed me into, and guided me through graduate school.

ABSTRACT

The field relationships and data collected from mineralogical, geochemical and fluid inclusion studies indicate that most of the gold mineralization in the clay-altered White Channel gravel of the Klondike district was formed directly from Plio-Pleistocene epithermal processes.

Post-depositional alteration in the Plio-Pleistocene White Channel deposit is divided into three zones: Bleached zone gravel, Iron zone gravel and altered Footwall zone rocks. Altered White Channel gravel in the uppermost zone (Bleached zone gravel) is white to grey, and contains secondary kaolinite and illite. The weight percentages of Fe_2O_3 (total Fe), MgO, Na_2O and K_2O are depleted and LOI (loss on ignition) is increased relative to unaltered White Channel gravel. Altered Iron zone gravel (the lowest 2-4 meters of gravel) is bright orange with secondary kaolinite, illite (and/or muscovite), goethite, lepidocrocite, hematite, adularia, gypsum and smectite group minerals. Kaolinite, illite, goethite and lepidocrocite are all highly crystalline. The weight percentage of Fe_2O_3 and LOI are increased, while other major oxides are unchanged relative to unaltered White Channel gravel. Anomalous concentrations of up to 6.55% MnO, 0.73% P_2O_5, 490ppm S, 15,900ppm Ba, 1,560ppm As, 45.5ppm Sb and 110ppm Co are present in this zone. Altered Footwall zone rocks below the gravel contact contain secondary minerals such as well crystallized kaolinite, illite and interstratified illite/smectite (or chlorite/smectite). The weight percentage of the major oxides generally decrease and LOI increases with increasing degree of alteration in this zone.

Three types of veins were emplaced during the alteration event. Type 1 veins contain quartz and/or chalcedony with vugs, banding, cockade, cockscomb and crustiform textures. Type 2 veins are composed of siderite and quartz, with botryoidal and concretionary growth structures. Type 3 veins consist of microfractures filled with either smectite group minerals and goethite, or amorphous silicates and goethite. Fluid inclusion analyses indicate that these veins were deposited from low temperature ($\simeq$125°C), low salinity ($\simeq$1-2wt.% equivalent NaCl) hydrothermal fluids. The veins contain anomalous concentrations of up to 1.86% MnO, 0.43% P_2O_5, 2,800ppm S, 5,410ppm Ba, 97ppm As, 27.9ppm Sb and 280ppb Au.

The greatest concentration of gold in unaltered White Channel gravel exists in the lowest 1-2 meters of gravel, where concentrations often exceed 1ppm. The concentration of gold in unaltered gravel that is greater than 4 four meters above the bedrock contact generally is <0.02ppm. Altered White Channel gravel contains economic concentrations of gold (0.3->1ppm) in gravel as high as 10 meters above the bedrock contact. The concentration of gold in altered gravel does not appear to fall below 0.1ppm even in gravel 20 meters above bedrock. In addition, gold in altered gravel is not specific to facies types in contrast to the distribution of gold in unaltered White Channel gravel.

Mineral equilibria in the system K_2O-SiO_2-Al_2O_3-H_2O, the high crystallinities of the secondary clay minerals, and vein phases, textures and fluid inclusion data indicate that the alteration of the White Channel deposit and the emplacement of types 1, 2 and 3 veins was caused by low temperature (120-130°C), low salinity (<1-2wt.% NaCl) aqueous fluids. These features, in addition to the presence of anomalous Au, As, Sb, Ba, Fe, Mn, S and P in the Iron zone gravel and veins, indicate that the ore-forming fluids were meteoric in origin and probably similar to the fluids involved in most precious-metal epithermal deposits and geothermal systems.

ACKNOWLEDGEMENTS

This thesis would not have been possible without the ideas, moral support and financial support of Bruce Nesbitt and Steve Morison. To these two people I extend special thanks. I would also like to thank Bob St.Louis, Fred Longstaffe and Diane Caird who provided invaluable advice and assistance in completing the laboratory studies. The field work would not have been a success without the support of my friend Rhys Hughes and the placer miners of Dawson City, especially Mike Stutter and Benny Warmsby.

I would like to gratefully acknowledge all the people and institutions that went out of their way to provide the necessary financial support for this project. Funding was provided by the Department of Indian Affairs and Northern Development; the Department of Energy, Mines and Resources; the Canadian Natural Science and Engineering Research Council; the Boreal Institute for Northern Studies and the Department of Geology at the University of Alberta.

Finally, I am grateful for the friendship of my fellow graduate students and the Department of Geology faculty at the University of Alberta. Mark Brearly, Louise De St.Jourre, Don Dingwell, Paul Lhotka, Chris Sayer and Lori Walton are thanked for their friendship and encouragement. Lastly, but not least, I would like to thank Jane Evens for her continuous patience, encouragement, support and friendship through the duration of this thesis.

Table of Contents

Chapter . Page

1. INTRODUCTION 1

1.1 General Background 1

1.2 Objectives Of The Alteration Study 4

1.3 Regional Geology 5

1.3.1 Geology of the Klondike district 5

1.3.2 Lode gold occurrences 9

1.4 Geology Of The Unconsolidated Sediments 10

2. FIELD RELATIONSHIPS, MINERALOGY AND CHEMISTRY OF ALTERATION IN THE WHITE CHANNEL DEPOSIT 16

2.1 Field Relationships 16

2.1.1 Degree of alteration and general distribution 16

2.1.2 Unaltered and Bleached zone gravel 19

2.1.3 Iron zone gravel 25

2.1.4 Footwall zone 27

2.2 Mineralogy 31

2.2.1 Unaltered and Bleached zone gravel 31

2.2.2 Iron zone gravel 38

2.2.3 Clasts from the White Channel deposit 41

2.2.4 Footwall zone 43

2.3 Chemistry 47

2.3.1 Unaltered and Bleached zone gravel 51

2.3.2 Iron zone 53

2.3.3 Clasts from the White Channel deposit 56

2.3.4 Footwall zone 60

2.3.5 Distribution of gold in the White Channel deposit 65

2.4 Discussion 69

2.4.1 Summary of data 69

2.4.2 Kaolinization related to weathering 70
2.4.3 Origin of kaolinization in the White Channel deposit 71
2.4.4 Origin of alteration in the White Channel deposit 73
2.4.4.1 Mineralogical features 73
2.4.4.2 Geochemical features 75
3. VEINS IN ALTERED FOOTWALL ROCKS 78
3.1 Field Relationships 78
3.1.1 Veins associated with Footwall zone alteration 78
3.1.2 Mesothermal, metamorphic and carbonate veins 85
3.2 Mineralogy And Textures 87
3.2.1 Veins associated with Footwall zone alteration 87
3.2.2 Mesothermal, metamorphic and carbonate veins 90
3.3 Fluid Inclusions 90
3.3.1 Petrography 90
3.3.1.1 Veins associated with Footwall zone alteration 91
3.3.1.2 Mesothermal, metamorphic and carbonate veins 91
3.3.2 Microthermometry 93
3.3.2.1 Veins associated with Footwall zone alteration 96
3.3.2.2 Mesothermal/metamorphic quartz veins 104
3.3.2.3 Carbonate veins associated with volcanics 105
3.4 Vein Chemistry 105
3.4.1 Type 1 quartz veins 108
3.4.2 Type 2 siderite+quartz veins 110
3.4.3 Type 3 veins 111
3.4.4 Carbonate veins associated with volcanics 112
3.4.5 Carbonate veins associated with shear zones 113
3.5 Discussion 114

3.5.1 Summary of data 114
3.5.1.1 Textures, mineralogy and geochemistry of types 1, 2 and 3 veins .. 114
3.5.1.2 Important field relationships of types 1, 2 and 3 veins 115
3.5.1.3 Type 1 veins contrasted with mesothermal/metamorphic veins 116
3.5.2 Discussion of the origin of types 1, 2 and 3 veins 117
3.5.2.1 Characteristics indicative of near-surface deposition 117
3.5.2.2 Geochemical characteristics of the vein fluid 119
3.5.2.3 A contrasting origin for the mesothermal/metamorphic veins 120
3.5.2.4 Origin of the carbonate veins 122
3.5.3 Conclusions 123
4. GENESIS OF THE DEPOSIT AND CONCLUSIONS 125
4.1 Summary Of Relevant Data 125
4.1.1 Alteration zones 125
4.1.2 Veins in altered Footwall zone rocks 126
4.1.3 Gold distribution 127
4.2 Genesis Of The Deposit 129
4.2.1 Environment of deposition 130
4.2.1.1 Types 1, 2 and 3 Veins 130
4.2.1.2 Hydrothermal alteration 131
4.2.2 Origin of the fluid 136
4.2.3 Transport and deposition of gold 137
4.2.3.1 Transport of gold 138
4.2.3.2 Deposition of gold 142
4.2.4 Comparison to hot-spring epithermal model 144
4.2.5 Age and extent of epithermal gold mineralization 146
4.3 Conclusions and Implications 148
4.3.1 Implications 149

REFERENCE LIST 151

5. APPENDICES 160

5.1 Scales Of Alteration 161

5.1.1 Scale of competence 161

5.1.2 Scale of gravel alteration 161

5.2 Sample List And Location Map 163

5.3 Hydrometer Analysis 173

5.3.1 Background 173

5.3.2 Sample preparation 174

5.3.3 Procedure 174

5.4 Clay Mineral Analysis 175

5.4.1 Background 175

5.4.2 Sample preparation 176

5.4.3 X-ray diffraction 177

5.4.4 Clay mineral abundances 177

5.4.5 Clay mineral crystallinities 178

5.5 Geochemical Analysis 180

5.5.1 X-Ray Fluorescence Analysis 180

5.5.1.1 Sample preparation 180

5.5.2 Instrumental Neutron Activation Analysis 180

5.5.2.1 Sample preparation 180

List of Tables

Table		Page
2.1	Normalized grain size distribution of the <2mm size fraction (wt.%) for selected samples of matrix and cobbles from White Channel sediments, and mica schist collected from Dago Hill.	32
2.2	Mineralogy of samples collected from the matrix (<2mm size fraction) of White Channel gravel at Dago Hill.	33
2.3	Mineralogy of rhyolite porphyry and mica schist cobbles (<2mm size fraction) collected from the White Channel gravel.	42
2.4	Mineralogy of samples (<2mm size fraction) collected from bedrock below the White Channel gravel.	44
2.5	Whole rock chemistry of samples collected from the matrix (<2mm size fraction) of White Channel gravel at Dago Hill.	49
2.6	Major oxide/Al_2O_3 ratios, LOI and trace element analyses of samples collected from the matrix (<2mm size fraction) of White Channel gravel at Dago Hill.	50
2.7	Whole rock chemistry of rhyolite and mica schist cobbles (<2mm size fraction) collected from the White Channel gravel at Dago Hill.	57
2.8	Major oxide/Al_2O_3 ratios, LOI and trace element analyses of rhyolite and mica schist cobbles (<2mm size fraction) collected from the White Channel gravel at Dago Hill.	58
2.9	Whole rock chemistry of samples (<2mm size fraction) collected from bedrock below the White Channel gravel.	61
2.10	Major oxide/Al_2O_3 ratios, LOI and trace element analyses of samples (<2mm size fraction) collected from bedrock below the White Channel gravel.	62
3.11	Homogenization and melting temperatures of fluid inclusions in selected samples of quartz and carbonate from types 1, 2, mesothermal/metamorphic and carbonate veins in the Klondike district.	97
3.12	Whole rock chemistry of types 2 and 3 veins in the clay-altered footwall rocks below the White Channel gravel.	106
3.13	Chemistry of selected vein and White Channel gravel (matrix) samples from the Klondike district.	107
5.14	Location and description of samples collected from the Klondike district.	163

List of Figures

Figure		Page
1.1	Location map for the Klondike district (modified after Morison, 1985)	2
1.2	A generalized tectonic map of the Yukon with the subdivisions of the ancient North American margin (shaded) and the elements of the southwestern accreted terranes (modified after Tempelman-Kluit, 1981 and 1980).	6
1.3	Bedrock geology of the Klondike district with reported lode gold occurrences (x) (modified after Bostock, 1942; Boyle, 1979; Debicki, 1985 and 1984).	7
1.4	Generalized section of gravel stratigraphy across a) lower Bonanza and Hunker valleys, and b) upper Bonanza valley (modified after McConnell, 1907).	12
2.5	Map showing the distribution of alteration in the White Channel sediments and the underlying bedrock in the Bonanza and Hunker Creek areas of the Klondike district.	18
2.6	An exposure at Dago Hill showing planar stratified fluvial gravel overlying sediments of the White Channel deposit. Note the presence of a post-depositional alteration contact within the White Channel sediments (modified after Dufresne and Morison, 1985).	20
2.7	Grain size distribution of the <2mm size fraction for slightly (2) altered (W-410) versus extremely (5) altered (A-403) gravel matrix. An incompetent {e} rhyolite cobble is included (A-410) for comparison.	35
2.8	Schematic section of the White Channel deposit at Dago Hill with three distinct alteration zones. The clay mineralogy of the <2μm size fraction and mineralogy of the 2μm-2mm size fraction is included (modified after Dufresne *et al.*, 1987).	36
2.9	Plot of the grain size distribution for samples of mica schist at Dago Hill. Samples range from breakable {b} to incompetent {e}.	46
2.10	Plot of log (oxide/Al_2O_3) and log LOI versus elevation for matrix samples above and below the alteration contact within the White Channel gravel at Dago Hill.	52
2.11	Plot of log (oxide/Al_2O_3) and log LOI versus elevation above bedrock for matrix samples within the White Channel gravel at Dago Hill.	54
2.12	Plot of log (oxide/Al_2O_3) versus log LOI for rhyolite cobbles within the White Channel gravel.	59
2.13	Plot of log (oxide/Al_2O_3) and log LOI versus depth below the gravel contact for samples of mica schist within the Footwall zone.	63

Figure — Page

2.14 Plot of log (oxide/Al_2O_3) and log LOI versus depth below the gravel contact for samples of diabase within the Footwall zone. 64

2.15 Schematic sections showing the vertical distribution of gold in the White Channel gravel of Trail and Lovett Hills versus Dago Hill. Data for Trail and Lovett Hills was calculated from the grades reported by McConnell (1907) and Gleeson (1970). Data for Dago Hill was calculated from grade estimates given by Stutter and Warmsby (*pers. comm.*, 1985). 66

3.16 Calibration curve for fluid inclusion analyses using the Chaixmeca apparatus at the University of Alberta (modified after Fluet, 1986). 99

3.17 Homogenization temperatures (Th) of fluid inclusions in quartz and carbonate from Types 1, 2, mesothermal/metamorphic and carbonate (associated with volcanics) veins. 100

3.18 Melting temperatures of ice (Tm-ice), CO_2 (Te-co_2) and CO_2-H_2O clathrates (Tm-clath) from fluid inclusions in quartz and carbonate from Types 1, 2, mesothermal/metamorphic and carbonate (associated with volcanics) veins. 102

4.19 A plot of temperature versus log (aK^+/aH^+) for the system K_2O-SiO_2-Al_2O_3-H_2O. Aluminum is conserved in the reactions and the activities of solids and H_2O are assumed to be 1. The data for the reactions is from Helgeson *et al.* (1978). 132

4.20 A plot of log aO_2 versus pH in the system Au-Fe-S-Cl-H_2O at 250°C (modified after Shenberger, 1985). 139

4.21 A plot of the solubility of gold as log($Au(HS)_2^-$) versus temperature in a solution buffered by the assemblage of quartz+K-feldspar+K-mica and SO_4^{2-}:H_2S(aq)=1 (modified after Shenberger, 1985). 140

4.22 A schematic model of hydrothermal alteration and mineralization for the White Channel deposit. 145

5.23 Location map for samples collected from the Klondike district. 172

List of Plates

Plate		Page
1.1	Photograph of mined White Channel gravel on an elevated bench at Paradise Hill approximately 100 meters above the creek bottom.	3
2.2	Photograph of Bleached and altered White Channel gravel at Dago Hill.	21
2.3	Photograph of slightly (2) altered White Channel gravel that overlies strongly (4) to extremely (5) altered Bleached zone gravel at Dago Hill.	22
2.4	Photograph that shows brown to yellow unaltered White Channel gravel above the brown colored alteration contact, and grey to white Bleached zone gravel below the contact (from Dago Hill).	23
2.5	Photograph of incompetent (e) clay-altered rhyolite clasts within Bleached zone White Channel gravel at Dago Hill.	24
2.6	Photograph of extremely (5) altered Iron zone gravel from the lowest 2-3 meters of White Channel gravel that is immediately above incompetent (e) bedrock at Dago Hill.	26
2.7	Photograph of cemented Iron zone gravel at Nugget Hill.	26
2.8	Photograph of incohesive (d) to incompetent (e) Footwall zone rocks below altered White Channel gravel at Dago Hill.	28
2.9	Photomicrograph (crossed polarized light) of cemented Iron zone gravel at Nugget Hill with botryoidal goethite cementing detrital quartz grains.	39
2.10	Photomicrograph (plane polarized light) of cemented Iron zone gravel at Nugget Hill with coarse 10Å mica (muscovite 1-2mm in length) rimming detrital quartz grains.	40
2.11	Photomicrograph (plane polarized light) of cemented Iron zone gravel at Nugget Hill with intergrown goethite and muscovite cementing the matrix of the gravel.	40
2.12	Photograph of a section of clay-altered bedrock at Trail Hill that was processed for significant amounts of gold.	68
3.13	Photograph of a type 1 quartz vein with open-space filled crystals. Note the bleached and clay-altered bedrock incorporated in the vein.	79
3.14	Photograph of a siderite+quartz concretion hosted in clay-altered mica schist at Jackson Hill. The concretion has cemented and partially replaced the schist.	80

Plate Page

3.15 Photograph of a siderite+quartz+gypsum concretion hosted in clay-altered diabase at Jackson Hill. The concretion has cemented and partially replaced the diabase, and is associated with type 2 veins. 81

3.16 Photograph of type 2 veins showing a horsetail veining pattern in clay-altered diabase. This outcrop of clay-altered bedrock is only 1-2 meters below the gravel contact at Jackson Hill. 83

3.17 Photograph of thin, type 1 quartz veins in iron-stained and clay-altered graphitic schist from Nugget Hill. 84

3.18 Photograph of a microfracture in the Bleached zone gravel of Nugget Hill that is filled with clay minerals (and amorphous silicates?). 86

3.19 Photograph of a type 1 quartz vein with banded chalcedony along the margins of the vein. 88

3.20 Photograph of a concretion related to type 2 siderite+quartz veins with euhedral quartz protruding into cavities of the concretion. 88

3.21 Photomicrograph of a 2 phase aqueous inclusion with a high L/V ratio from a type 1 quartz vein. 92

3.22 Photomicrograph of a 2 phase aqueous inclusion with a moderate L/V ratio in quartz from a mesothermal/metamorphic vein. 94

3.23 Photomicrograph of 2 phase CO_2-rich inclusions with ≈75-85% CO_2, in quartz from a mesothermal/metamorphic vein. 94

1. INTRODUCTION

1.1 General Background

Since the discovery of placer gold in 1896 at Bonanza Creek, more than 10 million ounces of fine gold are reported to have been recovered from the Klondike gold fields (Boyle, 1979). The most productive gravels in this district included those of Bonanza, Hunker, Eldorado, Dominion, Sulphur, Gold Run and Quartz Creeks, and gravel at the mouth of the Klondike River (figure 1.1). Today, producing gold mines generally are restricted to the Holocene gravel of tributary gulches throughout the district and the White Channel gravel on elevated, bedrock benches along the limits of Hunker, lower Bonanza and Quartz Creek valleys (plate 1.1). Much of the gold that was recovered from Bonanza and Hunker Creeks is reported to have been derived from the erosion of the White Channel gravel, a gold-bearing, high level bench gravel (Boyle, 1979).

Since the discovery of placer gold in this district prospectors have combed the hills in search of the hypogene lode source. However, to date, an insignificant amount of lode gold has been recovered from this district in comparison to the amount of gold recovered from placer deposits. Extensive exploration of mesothermal and/or metamorphic quartz veins in the Klondike Schist have failed to locate a significant lode source for gold that is contained in the White Channel gravel and the Holocene creek gravels (Boyle, 1979).

Recently, Dirk Tempelman-Kluit (1982) suggested that important concentrations of gold in the White Channel gravel may have been chemically precipitated during alteration of the gravel. If in fact this is correct, it has major ramifications for the source of gold in both the White Channel gravel and the Holocene creek gravels. Tempelman-Kluit's (1982) work on the White Channel gravel prompted this study of the geological and geochemical origin of alteration in the White Channel gravelly sediments, and the relationships between alteration and gold mineralization.

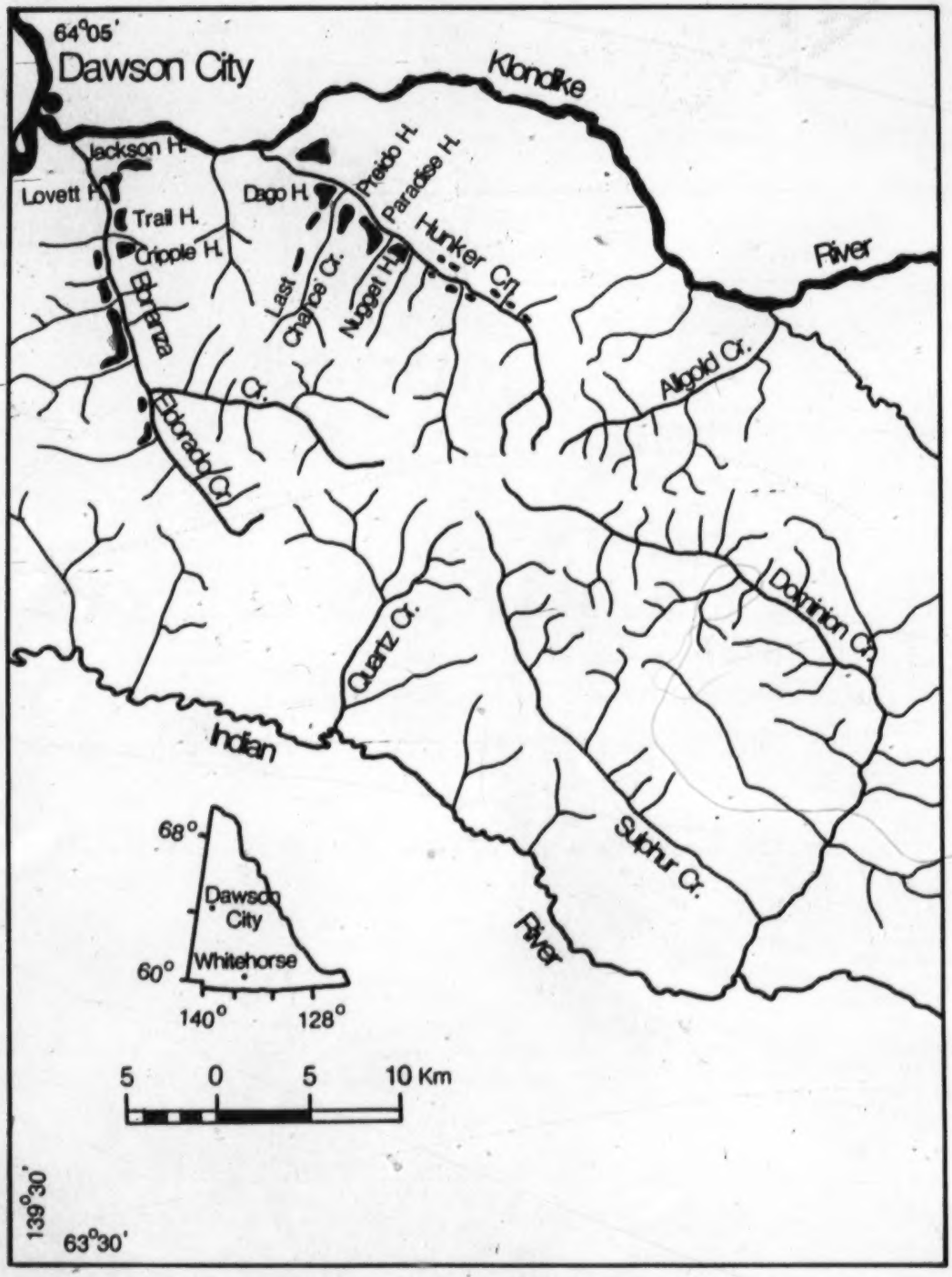

Figure 1.1 Location map for the Klondike district (modified after Morison, 1985)

Plate 1.1 Photograph of mined White Channel gravel on an elevated bench at Paradise Hill approximately 100 meters above the creek bottom.

1.2 Objectives Of The Alteration Study

Alteration in the White Channel gravel was first noted by McConnell in 1905. He described the White Channel gravel as having a white or light grey bleached appearance with schist pebbles that are decomposed and crumble when thawed. Brief descriptions of altered White Channel gravel and the altered underlying bedrock are presented by McConnell (1907) and Brock (1910).

More recently, Tempelman-Kluit (1982) described post-depositional alteration in the White Channel gravel and underlying bedrock of Dago Hill (figure 1.1). He described altered White Channel gravel as having a white bleached color with schist, gneiss and feldspar porphyry clasts that disintegrate and crumble upon thawing. Pervasive alteration is characterized by a complete replacement of feldspars and micas by clay minerals. Quartz clasts disintegrate on the first blow of a hammer. Schist and porphyry clasts are doughy or pulpy and easily penetrated by a knife (Tempelman-Kluit, 1982). In addition, he suggested that chemical processes responsible for the alteration may have contributed significant amounts of gold to the White Channel gravel during alteration at Dago Hill.

As a result of Tempelman-Kluit's ideas, this study was initiated with the following objectives:

1. To determine the origin of alteration in the Plio-Pleistocene White Channel sediments and bedrock with the use of field observations, mineralogical and geochemical analysis.
2. To coordinate the study with a sedimentological study of the White Channel gravel by S.R. Morison (1985), in an effort to determine the relationship between alteration and the distribution of gold in altered White Channel gravel.
3. To determine the origin and extent of the Plio-Pleistocene processes responsible for alteration of the White Channel sediments and the significance of these processes in creating a lode source of gold in the Klondike placer district.

1.3 Regional Geology

The Yukon can be divided into two major lithological components separated by the Tintina fault (figure 1.2). Northeast of the Tintina fault are strata that were deposited on the ancient North American continent. Southwest of the Tintina fault the rocks are part of an allochthonous Mesozoic island arc that is now accreted to North America (Tempelman-Kluit, 1981, 1979 and 1976). The Tintina and Denali-Shakwak faults are northwest-trending dextral strike slip faults (figure 1.2). At least 450km of movement (Roddick, 1967; Tempelman-Kluit, 1976) and possibly greater than 900km of relative displacement (Gabrielse, 1985) has been reported for the rocks adjacent to the Tintina fault. Tempelman-Kluit (1976) and Gabrielse (1985) suggest that major transcurrent movement occurred between the middle Cretaceous and late Eocene or Oligocene time.

1.3.1 Geology of the Klondike district

The Klondike district was first mapped by Bostock (1942), and more recently by Metcalfe (1981) and Debicki (1985 and 1984). The Klondike is situated approximately 2-5km southwest of the Tintina Trench within the Yukon Cataclastic Complex (figure 1.2). Normal faulting along the Tintina fault during the Pliocene is responsible for the formation of a physiographic trench (Tempelman-Kluit, 1981). Bedrock in the Klondike area is generally grouped into five major units which are, from oldest to youngest, the Nasina Series, the Klondike Series (Klondike Schist), the Moosehide Assemblage, early Tertiary volcanic/volcaniclastic rocks and Tertiary intrusive rocks (figure 1.3).

Rocks of the Nasina Series were first described by Spurr (1897) and McConnell (1905). Structurally, they are the lowermost and probably the oldest rock units in the Klondike area, consisting of graphitic schists, graphitic quartzites and siliceous marbles with minor chlorite schists and muscovite schists. Rocks of the Nasina Series have been metamorphosed to grades ranging from upper greenschist to middle amphibolite facies (Metcalfe, 1981). Tempelman-Kluit (1977) interprets the Nasina Series as metamorphosed outer shelf sediments of the ancient North American continent composed of siliceous

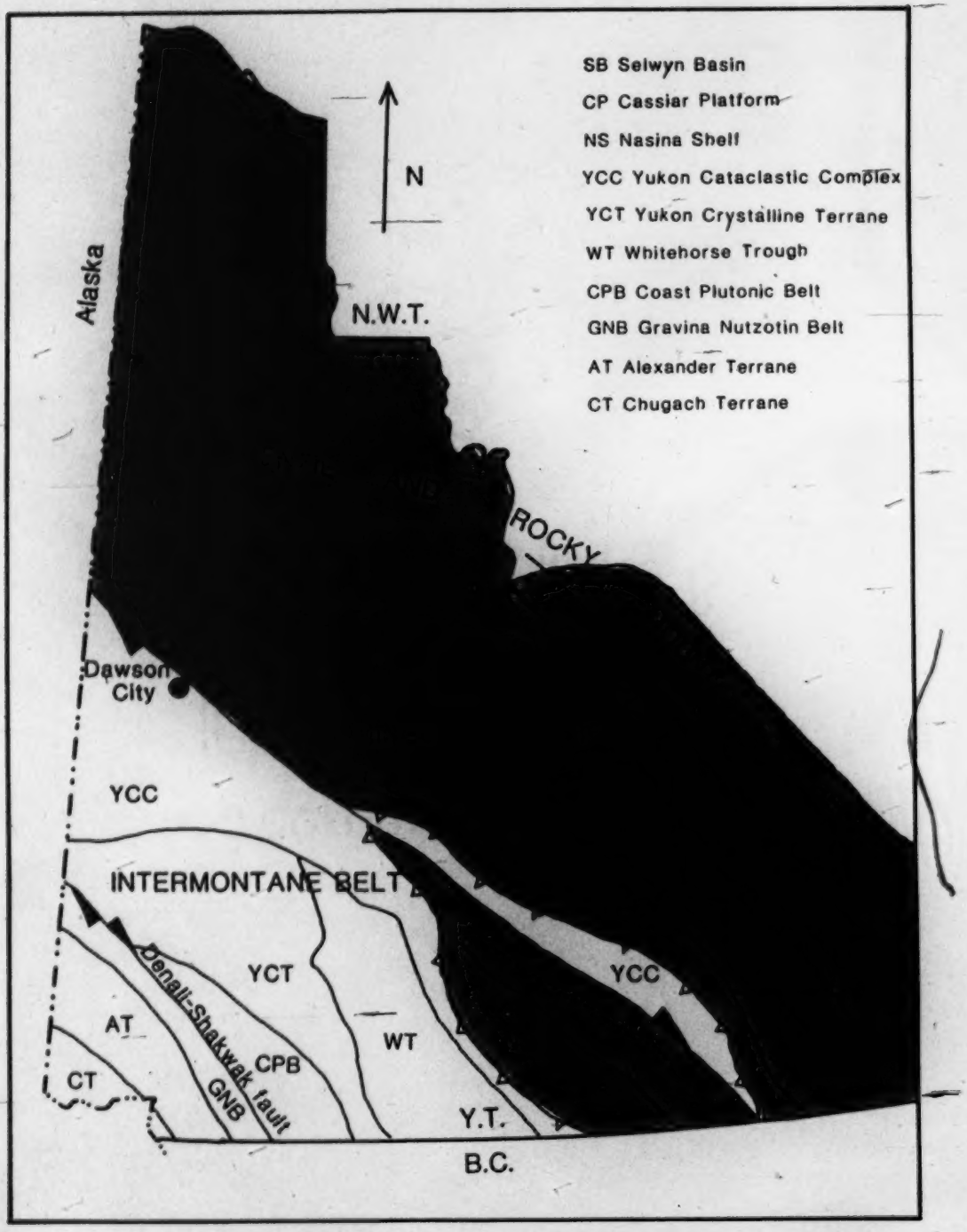

Figure 1.2 A generalized tectonic map of the Yukon with the subdivisions of the ancient North American margin (shaded) and the elements of the southwestern accreted terranes (modified after Tempelman-Kluit, 1981 and 1980).

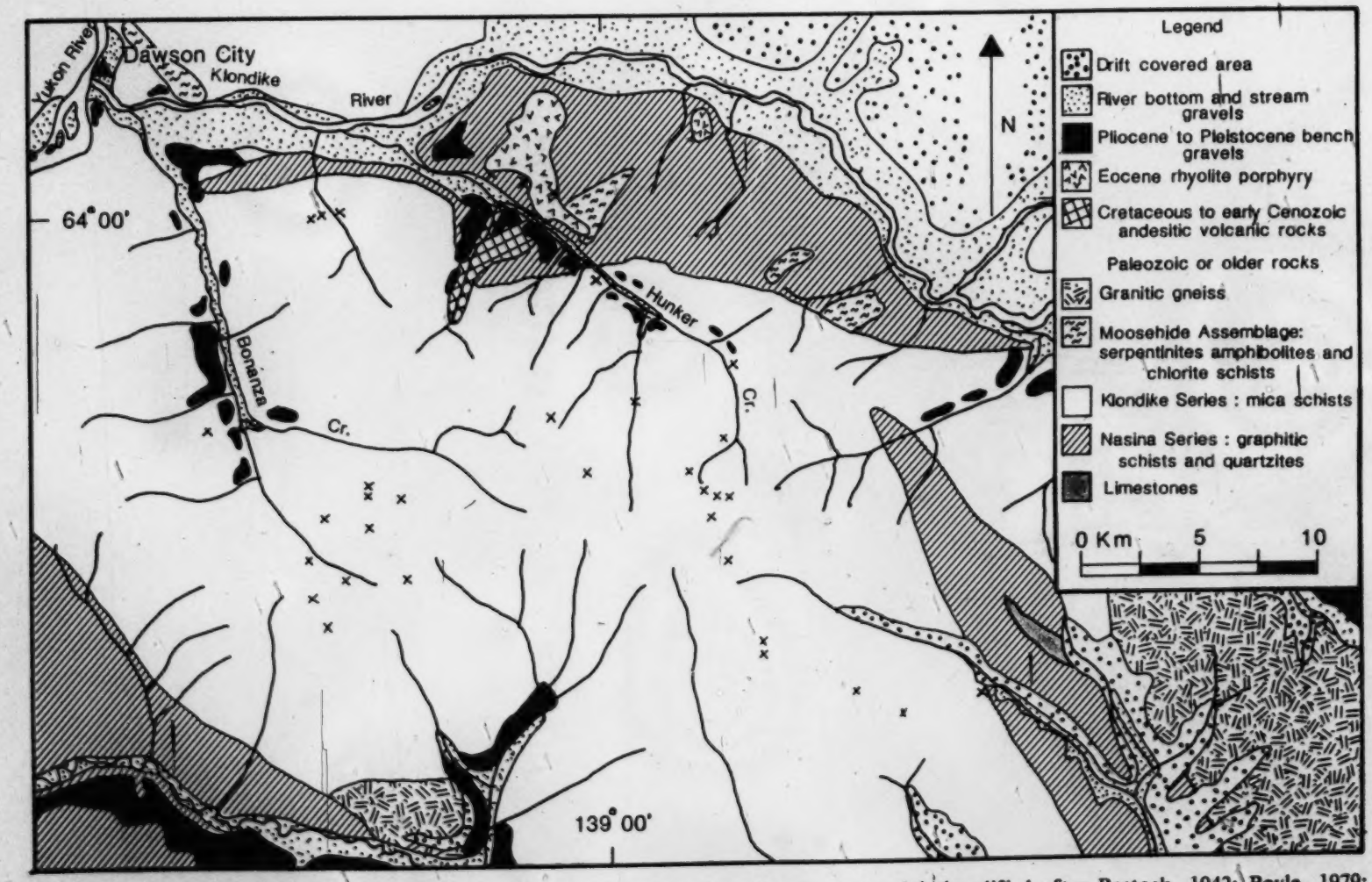

Figure 1.3 Bedrock geology of the Klondike district with reported lode gold occurrences (x) (modified after Bostock, 1942; Boyle, 1979; Debicki, 1985 and 1984).

limestones, sandstones and black shales. He correlates these rocks with the lower Paleozoic miogeosynclinal sedimentary succession of the Pelly-Cassiar Platform and Selwyn Basin in the Omineca Crystalline Belt (figure 1.2).

Most rocks exposed in the Klondike district belong to the Klondike Series (or Klondike Schist). McConnell (1905) first characterized the Klondike Series as being composed of light-colored sericite schists, sericite-feldspar schists and chlorite schists. Metcalfe (1981) and Tempelman-Kluit (1976) describe the Kondike Series rocks as being leucocratic quartz-feldspar-muscovite schists with prominent "eyes" of quartz and feldspar. The schists have been penetratively sheared as indicated by common cataclastic textures such as augen and flaser structures. Metcalfe (1981) groups Klondike Series rocks into two major lithologies; a quartz-plagioclase-mica schist with minor chlorite and blastomylonitic texture, and a quartz-K-feldspar schist which is mica poor with a protomylonitic texture. Petrography and chemistry of the schists indicates that the blastomylonitic mica-rich schists are metamorphosed sedimentary rocks, while the protomylonitic mica-poor schists are metamorphosed volcanic rocks (Metcalfe, 1981). Minor ferruginous quartzites and siliceous marbles are also present within the Klondike Series. These rocks have undergone upper greenschist to middle amphibolite grade metamorphism and at least four separate deformational events (Mortensen, 1984). Metcalfe and Clark (1983) report that the contact between the basal schist of the Klondike Series and graphitic schist of the Nasina Series is sheared. This in conjunction with discordant bedding and discordant cleavage in the underlying Nasina Series rocks suggest that the contact is a low angle thrust fault. Tempelman-Kluit (1979) suggests that the Klondike Series of rocks are similar to rocks of the Nisutlin Allochthonous Assemblage which have been thrust over Nasina Shelf strata.

Structurally overlying rocks of the Klondike and Nasina Series are sparse occurrences of mylonitized serpentinite, amphibolite, chlorite schist and talc schist. McConnell (1905) originally referred to these rocks as the Moosehide diabase. Metcalfe (1981) called this sequence of rocks the Moosehide Assemblage. Tempelman-Kluit (1981 and 1979) suggests that these rocks are similar to the Anvil Allochthonous Assemblage, a sheared ophiolite, that is

part of a structural stack which includes the Nisutlin Assemblage. He also suggests that this entire stack was thrust over ancient North American strata during the Jurassic.

Gently folded andesitic volcanic and volcaniclastic rocks are present in the Last Chance Creek area (figure 1.3). McConnell (1905) considered these rocks to be early Tertiary in age; however, recent work by Lowey (1984) on similar rocks in the Indian River area suggests that they are middle Cretaceous in age. Tertiary intrusive rocks are rare in the Klondike district except for a rhyolite porphyry stock that outcrops on the right limit (north bank) of lower Hunker Creek (figure 1.3). In addition, there are some outcrops of volcanic and volcaniclastic rocks associated with the rhyolite porphyry. Debicki (*pers. comm.*, 1985) indicates that the rhyolite porphyry has been isotopically dated at approximately 50 to 60 Ma.

1.3.2 Lode gold occurrences

Extensive exploration for lode sources of gold has failed to locate an economically significant, lode gold deposit in the Klondike district. There are many known lode gold occurrences (figure 1.3) which have been described and sampled by Cairnes (1912), Maclean (1914), Gleeson (1970) and Debicki (1984 and 1985). Most of these gold occurrences are associated with quartz veins in the Klondike Series rocks. At least four types of gold-bearing quartz veins have been recognized;

1. Gold associated with tabular and often discordant quartz veins that contain minor ferroan carbonates, barite and sulfides. These veins occur in a variety of Klondike Series lithologies and are clearly mesothermal in character (Mortensen, 1984). The Lone Star prospect is perhaps the best known example of this type of gold occurrence. The gold-bearing quartz vein at the Lone Star prospect has been folded, and was probably emplaced during or between late deformational (folding) events affecting the Klondike Schist (Mortensen, 1984).
2. Gold associated with milky white, rusty weathering and often base-metal rich quartz veins. These veins are discordant, with irregular thicknesses and they are usually hosted by Klondike Schist. As at the Mitchell claims, the quartz veins are typically barren of

mineralization, yet in places, the veins contain abundant pyrite, galena, sphalerite, chalcopyrite, tetrahedrite, arsenopyrite and significant amounts of gold. Alteration halos of ferroan carbonate and pyrite often extend several meters into the wallrocks (Debicki, 1984). The width, strike length and structural elements that control the gold-bearing quartz veins at the Mitchell claims are not well documented or understood.

3. Gold associated with carbonate ± quartz ± barite ± fluorite veins. These veins generally are vuggy with colloform banding and breccia textures, which are characteristic of carbonate veins in the upper zones of epithermal gold deposits. An example of this type of vein exists at the Unexpected claims. At these claims the carbonate veins are hosted by or they are spatially related to outcrops of rhyolite porphyry (Maclean, 1914; Debicki, 1984). The veins at the Unexpected claims are probably early Tertiary or younger in age.
4. Gold associated with thin quartz or quartz-chalcedony veins that contain minor amounts of muscovite, kaolinite, dickite, ferroan carbonate, hematite, goethite and pyrite. These veins, which were first recognized during the course of this study, usually occur in bleached and clay-altered bedrock of varying lithologies. Extensive colloform banding, vugs, crustiform and botryoidal textures characterize these veins as epithermal in nature. The veins are probably late Pliocene or early Pleistocene in age (described in chapter 3).

1.4 Geology Of The Unconsolidated Sediments

The Klondike placer district is situated in the Klondike Plateau, which is the northwestern portion of the unglaciated Yukon Plateau (Bostock, 1948). This area is thoroughly dissected with rounded hills and many gulches that are tributaries to the major creeks and rivers. The valleys are generally broad and flat, however, they narrow towards the headlands into steep-sided gulches (Bostock, 1948; Boyle, 1979). Elevations in the Klondike district range from 600 to 1800 meters above sea level. This mature landscape is the result of pervasive Tertiary weathering that ended around the Miocene (Tempelman-Kluit, 1980). During the early Tertiary, creeks and rivers drained predominantly to the southwest. Differential uplift of the Klondike Plateau occurred about the late Miocene or Pliocene time.

This resulted in renewed downcutting and a change in drainage direction (to the northwest) of the major creeks and rivers in the Klondike district (Hughes *et al.*, 1972; Tempelman-Kluit, 1980). These processes are responsible for the present day geomorphology of the area. The Quaternary geology and geomorphology of the Klondike Plateau has been described in detail by Foscolos *et al.* (1979), Hughes (1969), Hughes *et al.* (1972), Milner (1976), Rutter *et al.* (1978) and Tempelman-Kluit (1980).

The stratigraphy of the auriferous gravels of the Klondike district was originally described by McConnell and Tyrell (1898), and McConnell (1905 and 1907). McConnell (1905) divided the unconsolidated sediments of the region as follows;

Low level gravels	Gulch gravel
	Creek gravel
	River gravel
Gravels at intermediate levels	Terrace gravels
High level bench gravels	High level river gravel
	(Klondike gravel)
	White Channel gravel

The stratigraphic relationships of these gravels are shown in figure 1.4.

The White Channel sediments, also called the White Channel deposit, are the oldest unconsolidated sediments in the Klondike area. Morison (1985) reports that White Channel sediments are Pliocene in age based upon preliminary palynological evaluation of samples from overbank sediments. At the mouth of lower Bonanza Creek, the upper 10-20 meters of White Channel gravel are interbedded with early Pleistocene Klondike gravel. In addition, cryogenic features such as ice wedge pseudomorphs are present in the upper portions of the White Channel gravel (Milner, 1976; Morison, 1985). These features indicate that White Channel aggradation probably started during the late Pliocene (during an interglacial period) and continued into the early Pleistocene (Hughes *et al.*, 1972; Milner, 1976; Morison, 1985).

The White Channel gravelly sediments occur on bedrock benches approximately 50 to 100 meters above present day stream levels (plate 1.1). These sediments attain a maximum thickness of 45 to 50 meters. Morison (1985) distinguishes 14 lithofacies types in the White Channel sediments ranging from laminated silts and clays to massive and disorganized boulder gravel. Gravelly facies comprise approximately 80% of all sedimentary beds in the White

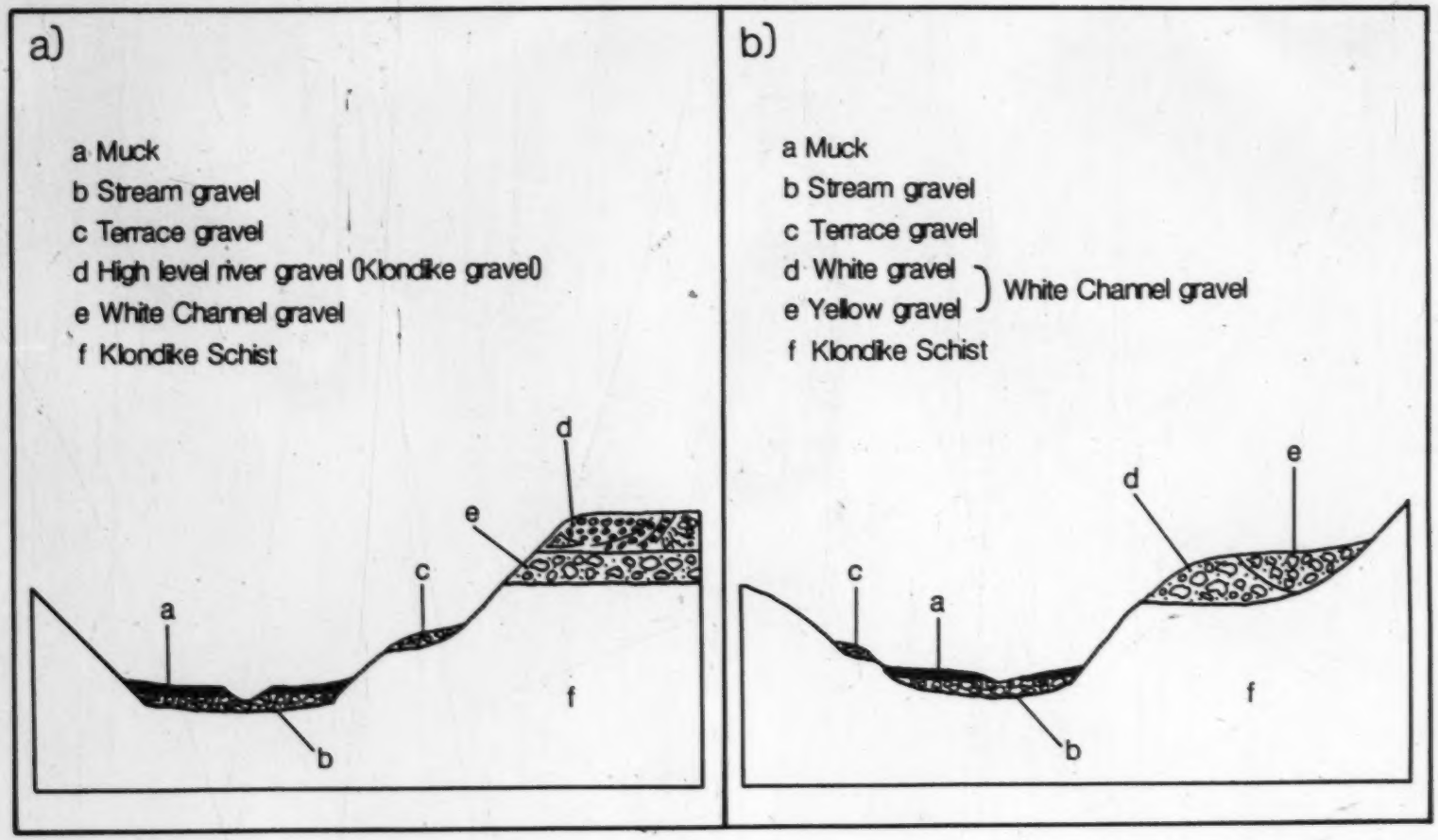

Figure 1.4 Generalized section of gravel stratigraphy across a) lower Bonanza and Hunker valleys, and b) upper Bonanza valley (modified after McConnell, 1907).

Channel deposit (Morison, 1985). The dominant lithofacies types are characterized as distinctly stratified and crudely stratified gravel which are both clast-supported and matrix filled. Basal sequences of the gravel are dominantly composed of poorly sorted, crudely stratified gravel and poorly sorted, chaotic gravel. In addition, poorly sorted, massive and disorganized gravel is occasionally present. As a result, Morison (1985) interprets the basal sequences as interbedded channel and bar deposits, in both deep and shallow channels, which were formed in a crudely braided fluvial environment. He also interprets the massive gravel facies as valley wall gravity flow deposits that are components of tributary alluvial fan deposits.

Middle to upper sequences of the White Channel deposit commonly show distinctly stratified gravel that is vertically associated with crudely stratified and chaotic gravel. The coarse-grained facies are often capped by laminated mud and fine sand (Morison, 1985). These sedimentary sequences are interpreted to be the result of crude depositional cycles of lateral migration, followed by abandonment of channels, which occurred in a multi-braided fluvial environment during White Channel aggradation (Morison, 1985).

At lower Bonanza Creek, the upper 10 meters of the White Channel deposit is interbedded with the Klondike gravel, a high level river gravel (unit e, figure 1.4). The Klondike gravel is generally characterized as a distinctly stratified to crudely stratified gravel which is clast-supported and matrix filled, and often interbedded with well sorted sands. The coarse-grained facies are usually well sorted, with well rounded pebbles and cobbles. These clasts, which are composed of quartzite, slate, chert, syenite, diabase and conglomerate, were probably derived from the Ogilvie Range (McConnell, 1905). The Klondike gravel is interpreted as a glaciofluvial deposit formed during pre-Reid (early Pleistocene) glacial activity (Hughes *et al.*, 1972; Morison, 1985; Rutter *et al.*, 1978).

Overlying the White Channel deposit, along the left bank of lower Hunker Creek (Dago, Preido and Paradise Hills, figure 1.1), is a stratigraphically younger, non-glacial gravel. This gravel unit has been called iron-stained fluvial gravel (Dufresne and Morison, 1985; Morison, 1985). The iron-stained fluvial gravel overlies White Channel silty clay

overbank sediment, with a continuous erosional contact that separates the two units. The gravel is clast-supported, matrix filled, well sorted and distinctly planar stratified (Morison, 1985). Well rounded clasts are dominantly composed of quartz, quartzite, mica schist and rhyolite porphyry, all of which are found locally in the Klondike district. Morison (1985) suggests that the iron-stained fluvial gravel is non-glacial and early Pleistocene in age.

Little work has been done on the terrace gravels (unit c, figure 1.4), as they are small in volume and they are of little economic importance. In general, the terrace gravels are similar to the low level creek gravel (Holocene gravel). The terraces are cut into bedrock of the valley slopes and they are remnants of ancient valley bottoms. These terraces probably formed during early Pleistocene downcutting after the deposition of the high level bench gravels (Morison, 1985). Mosquito Creek tephra, dated at 1.22 Ma. (Naeser *et al.*, 1982), was found on an intermediate terrace level. It gives a minimum date for the pre-Reid glacial activity responsible for the deposition of the glaciofluvial Klondike gravel; and the uplift responsible for the initial phase of downcutting and terrace gravel sedimentation (Hughes *et al.*, 1972; Morison, 1985).

A later period of Pleistocene uplift before Reid glacial activity, which is equivalent to Illinoian or early Wisconsin glacial activity, is responsible for the incision of the streams to present day base levels and the deposition of Holocene valley-bottom sediments (Hughes *et al.*, 1972; Morison, 1985; Rutter *et al.*, 1978). These low level, gravelly sediments (units a and b, figure 1.4) contained the most economically significant placer gold deposits in the Klondike district. Gold that was concentrated in the low level gravels was probably derived from both bedrock lode gold sources and the erosion of the gold-bearing White Channel gravel. Typically, the low level gravels are clast-supported and matrix filled with crude stratification. Gulch gravel is poorly sorted with angular to subangular clasts, while creek and river gravels are better sorted with well rounded clasts. Pebbles and cobbles from the low level gravels are composed of locally derived quartz, mica schist, quartzite and rhyolite porphyry. The creek gravel is usually less than 10 meters in thickness and is often capped by frozen, organic-rich muds that are often 30 meters in thickness (McConnell, 1905). Within the muds, are fossils

of extinct Pleistocene mammals (Harington, 1985). Radiocarbon dates of these fossils from the lower mud horizons indicate that the muds are 15,000 to >42,000 years old, while fossils from the upper mud horizons yield radicarbon ages of less than 10,000 years (Harington, 1985; Milner, 1976).

2. FIELD RELATIONSHIPS, MINERALOGY AND CHEMISTRY OF ALTERATION IN THE WHITE CHANNEL DEPOSIT

As a result of Tempelman-Kluit's (1982) initial work, this detailed study was undertaken in order to determine the field relationships, and mineralogical and geochemical characteristics of alteration within the White Channel deposit. This study was coordinated with a detailed sedimentological study of the White Channel sediments by S.R. Morison (1985) in order to evaluate the relationship between alteration and gold distribution.

2.1 Field Relationships

The distribution and intensity of alteration in the White Channel sediments and the underlying bedrock of Bonanza and Hunker Creeks was mapped during the 1983-84 field seasons. At Dago Hill approximately 25-30 meters of White Channel sediments (Plio-Pleistocene in age) are overlain by 2-5 meters of iron-stained Pleistocene fluvial gravel. A laterally continuous erosional contact separates the two units. Within the White Channel sediments, a distinct zone of alteration is recognizeable. The alteration zone ranges from 15 to 30 meters in thickness, and it extends down to bedrock, and 5-10 meters into the footwall rocks. This alteration zone is sub-divided into three zones which are named the Bleached zone, Iron zone and Footwall zone.

2.1.1 Degree of alteration and general distribution

Alteration in the White Channel sediments and the underlying footwall rocks is predominantly characterized by the progressive decompositon of feldspars, mica and mafic minerals to clay minerals. Clasts within altered gravel, and the altered bedrock which underlies the altered gravel, show an increase in the loss of competence with increased degree of alteration. A scale of competence, which ranges from competent (a) to incompetent (e), was constructed to describe the degree of clay alteration of clasts and/or bedrock (appendix 5.1). In addition, a scale of alteration, which ranges from unaltered (1) to altered (6), was used to describe the degree of alteration for exposures of White Channel gravel. This scale was

constructed based upon the degree of competence of 100 clasts, the amount of clay matrix present and the visible alteration state of quartz, feldspars, mica and mafic minerals within the White Channel gravel (appendix 5.1). Features affected by alteration such as color, texture, pH, plasticity and grain size were included in the descriptions of each outcrop examined.

The distribution of alteration in the White Channel sediments and the underlying bedrock along Bonanza and Hunker Creeks is shown in figure 2.5. Over 300 samples were collected from gravel matrix, cobbles and bedrock at Cripple, Dago, Discovery, Jackson, Lovett, Nugget, Paradise, Preido and Trail Hills. A sample list with brief descriptions is in appendix 5.2. The White Channel sediments at Dago Hill range from strongly (4) to extremely (5) altered, except for a thin horizon (2-3 meters) of unaltered (1) to slightly (2) altered sediments that cap the altered sediments. The White Channel gravel at Preido Hill ranges from moderately (3) to extremely (5) altered. Outcrops of strongly (4) to extremely (5) altered White Channel gravel are interbedded with altered debris flows at the east corner of Paradise Hill. At the southern, central and western faces of Paradise Hill are outcrops of unaltered (1) to slightly (2) altered White Channel gravel. All the outcrops of White Channel gravel at Nugget Hill exhibit strong (4) to extreme (5) alteration. Strong (4) to extreme (5) alteration in the White Channel deposit is restricted to Dago, Preido, Paradise and Nugget Hills. The White Channel gravel on other hills in the Bonanza and Hunker Creek areas contain unaltered (1) to moderately (3) altered gravel only. However, no reports exist that describe the vast amounts of White Channel sediments that were removed during mining. The brief descriptions by McConnell (1905 and 1907) and Brock (1910) all indicate that alteration was present.

Bedrock alteration is much more varied in distribution, as every hill that bears White Channel sediments has a range from competent (a) to incompetent (e) bedrock. Hills along Hunker Creek, including Dago, Preido, Paradise and Nugget, have a blanket of friable (incohesive, (d)) to incompetent (e) bedrock (5-10 meters in thickness) below intensely altered gravel. However, many hills along lower Bonanza Creek have large areas of friable

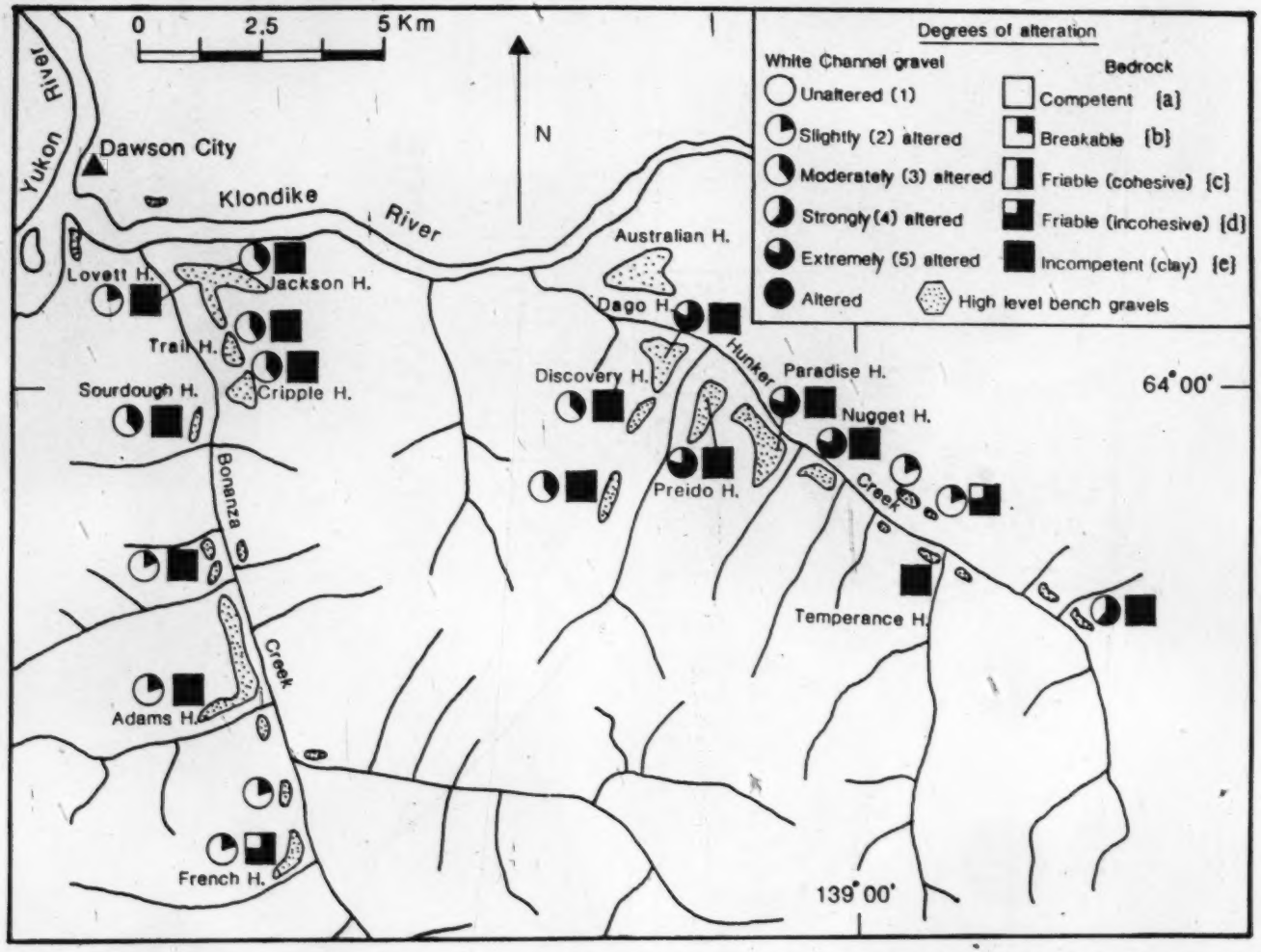

Figure 2.5 Map showing the distribution of alteration in the White Channel sediments and the underlying bedrock in the Bonanza and Hunker Creek areas of the Klondike district.

(incohesive, {d}) to incompetent {e} bedrock as well. In most cases, the overlying gravels have been removed from the bedrock benches of Bonanza Creek for a considerable period of time (since the early 1900's). As a result, it is unkown exactly how much weathering has affected these exposures, and if the overlying gravel (now removed) was altered.

2.1.2 Unaltered and Bleached zone gravel

At Dago Hill, the iron-stained fluvial gravel, which overlies the White Channel sediments, lacks significant clay alteration except at the surface in the recently developed soil horizon. Below the iron-stained fluvial gravel, separated by an unconformity, are unaltered (1) to slightly (2) altered White Channel sediments (figure 2.6). In general, slightly (2) altered White Channel gravel is yellow to light brown with lithofacies relationships and sedimentary structures clearly distinguishable (Dufresne and Morison, 1985). Within slightly (2) altered gravel the felsic porphyry and mica schist clasts are competent {a} to friable (cohesive, {c}) and they are often iron-stained. The gravel matrix contains little or no clay size material (Dufresne and Morison, 1985; Dufresne *et al.*, 1986).

Slightly (2) altered White Channel sediments are underlain by the uppermost zone of altered White Channel sediments called the Bleached zone (plate 2.2). A sharp (20-50cm thick), brown to purple alteration boundary separates the two units (plates 2.3 and 2.4). The alteration boundary cross-cuts lithofacies contacts and sedimentary structures within the White Channel sediments (Dufresne and Morison, 1985; Dufresne *et al.*, 1986). The alteration zone occurs within the White Channel sediments only, and it is completely isolated from the surficial weathering zone, except at the northern end of Dago Hill. At the north end, the iron-stained fluvial gravel cross-cuts Bleached zone White Channel sediments (figure 2.6). A bleached grey to white color is characteristic of the White Channel sediments in the Bleached zone (plates 2.3 and 2.4). Within the Bleached zone, felsic porphyry and mica schist clasts are generally friable (incohesive, {d}) to incompetent {e} and they are almost completely altered to clay minerals (plate 2.5). Lithofacies characteristics of the sediments in this zone have been masked or destroyed due to volume changes associated with pervasive secondary clay mineral

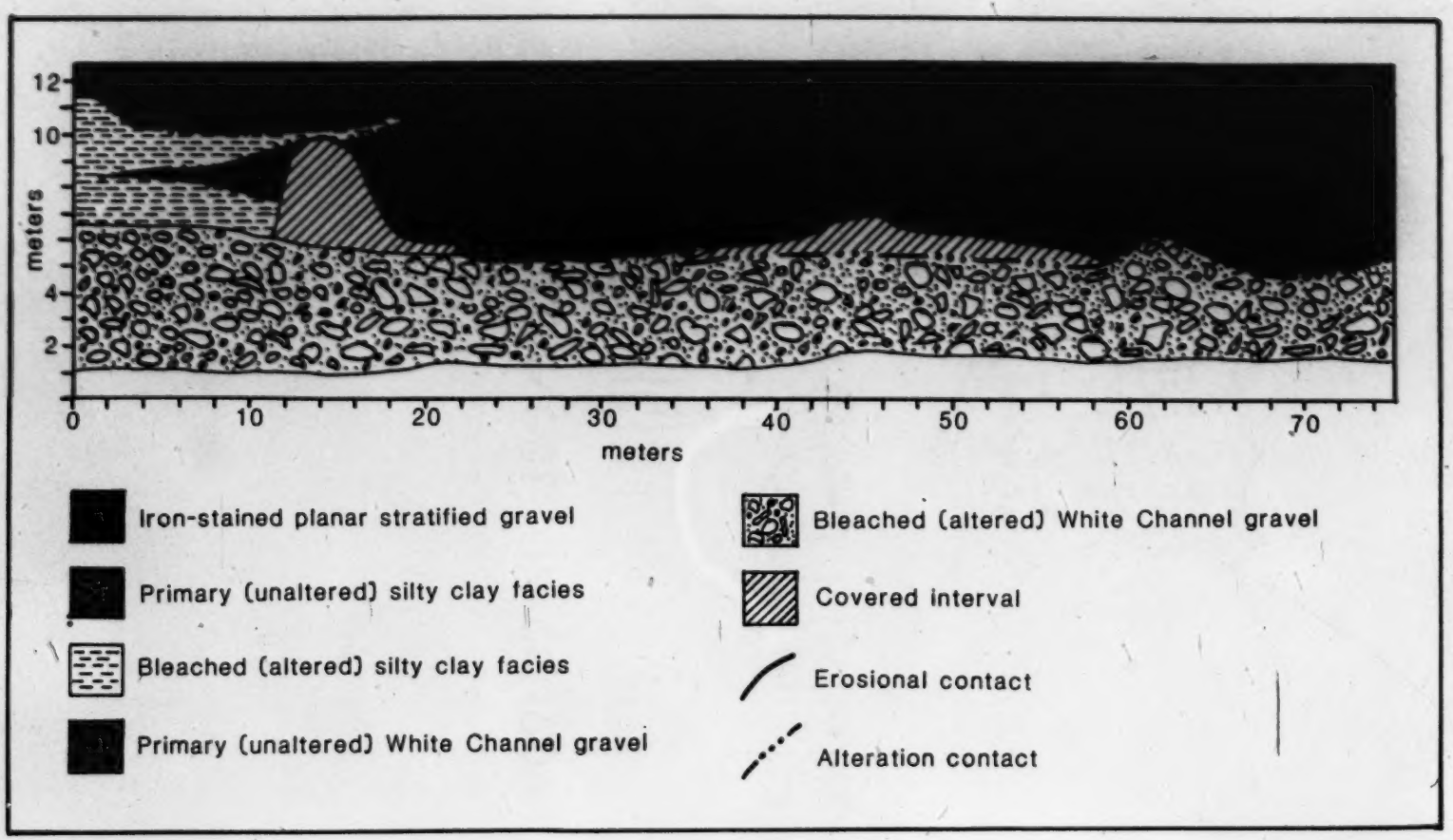

Figure 2.6 An exposure at Dago Hill showing planar stratified fluvial gravel overlying sediments of the White Channel deposit. Note the presence of a post-depositional alteration contact within the White Channel sediments (modified after Dufresne and Morison, 1985).

Plate 2.2 Photograph of Bleached and altered White Channel gravel at Dago Hill.

Plate 2.3 Photograph of slightly (2) altered White Channel gravel that overlies strongly (4) to extremely (5) altered Bleached zone gravel at Dago Hill.

Plate 2.4 Photograph that shows brown to yellow unaltered White Channel gravel above the brown colored alteration contact, and grey to white Bleached zone gravel below the contact (from Dago Hill).

Plate 2.5 Photograph of incompetent (e) clay-altered rhyolite clasts within Bleached zone White Channel gravel at Dago Hill.

development in the gravel matrix. The degree of alteration in the Bleached zone gravel fluctuates from strong (4) to extreme (5) both laterally and vertically with no regular pattern. The Bleached zone in the White Channel sediments at Dago Hill extends down to within 2-4 meters of bedrock.

At Dago Hill, a sub-horizontal zone (2-3 meters thick) of moderately (3) altered White Channel gravel exists within the Bleached zone. This zone is approximately 10 meters above bedrock. A light purple to grey contact separates gravel of the moderately (3) altered zone from strongly (4) altered gravel above and below this zone. The contacts of the zone appear to undulate and in places are stringer-like. Moderately (3) altered gravel within this zone is white to light grey but contains noticeably less clay matrix than White Channel gravel above or below.

2.1.3 Iron zone gravel

At Dago Hill, a 2-4 meter horizon of strongly (4) to extremely (5) altered and iron-stained gravel, which is immediately above bedrock, is called the Iron zone (plate 2.6). Similar to the overlying Bleached zone gravel, porphyry and schist clasts that are within this zone are friable (incohesive, {d}) to incompetent {e}. The gravel varies from bright orange to red in color. The development of secondary clay minerals and iron-hydroxides has masked or destroyed all lithofacies characteristics. The development of iron-staining appears to be directly related to clay alteration as hills with sections of unaltered (1) to slightly (2) altered White Channel gravel (*i.e.* Cripple, Jackson, Lovett and Trail Hills) lack intense iron-staining in the lower 2-3 meters of gravel.

Clay-altered boulders and altered bedrock intraclasts, which are within the Iron zone gravel, sit immediately above several meters of intensely clay-altered bedrock of the Footwall zone. If the clasts or bedrock were altered pre-deposition they would not have survived the high energy fluvial environment responsible for the deposition of the White Channel gravel (Dufresne and Morison, 1985). This indicates that both the gravel and the underlying footwall rocks were altered subsequent to deposition of the White Channel gravel.

Plate 2.6 Photograph of extremely (5) altered Iron zone gravel from the lowest 2-3 meters of White Channel gravel that is immediately above incompetent (e) bedrock at Dago Hill.

Plate 2.7 Photograph of cemented Iron zone gravel at Nugget Hill.

At Nugget Hill, an Iron zone similar to that at Dago Hill exists in the lower 2-3 meters of White Channel gravel. The Nugget Hill Iron zone consists of strongly (4) to extremely (5) altered and iron-stained gravel with pockets of cemented gravel that contain a range in degrees of clay alteration (plate 2.7). The cemented gravel is competent to friable and is cemented by limonite. In comparison to strongly (4) or extremely (5) altered gravel, lesser amounts of clay size material is present in the cemented gravel. Uncemented Iron zone gravel contains a significant amount of clay size material, as does the overlying Bleached zone gravel which is pervasively clay-altered (strongly (4) to extremely (5) altered).

Iron zone alteration exists in the lower 3-4 meters of White Channel gravel at Paradise Hill; however, poor exposure prevented a detailed investigation. Iron zone alteration at Preido Hill is variable. In a few areas on the northwest side of the Preido Hill bench facing Last Chance Creek the Iron zone is bright orange, occurs in a 2-3 meter horizon directly above bedrock, and is associated with strong (4) to extreme (5) alteration of the White Channel gravel. Further into the hillside, the iron-staining and the degree of alteration weaken in intensity. In addition, the Iron zone appears to thicken and become diffuse with several outcrops of gravel that show the Iron zone perched 2-5 meters above the bedrock contact. White Channel gravel below the perched Iron zone appears to be moderately (3) to strongly (4) altered. The development of Iron zone alteration appears to be restricted to Dago, Preido, Paradise and Nugget Hills, and it is always associated with strong (4) to extreme (5) alteration of the White Channel gravel near bedrock. The White Channel gravel at other hills in the Hunker and Bonanza Creek areas contain minor clay alteration and little or no iron-staining.

2.1.4 Footwall zone

The third zone of alteration, named the Footwall zone, occurs in bedrock directly below the White Channel gravel. Intense clay alteration is often visible 5-10 meters into the bedrock below the gravel contact (plate 2.8). At Dago and Nugget Hills, iron-staining exists below the gravel contact approximately 2-3 meters into clay-altered bedrock. At both of these

Plate 2.8 Photograph of incohesive {d} to incompetent {e} Footwall zone rocks below altered White Channel gravel at Dago Hill.

hills clay alteration of the Footwall zone rocks consistently extends 8-10 meters in depth below the gravel contact. As discussed in the previous section, intensely altered gravel is located above altered bedrock of the Footwall zone. Most of the clay material that would have been present prior to the deposition of the White Channel gravel, should have been eroded during the deposition of the gravel. Consequently, the gravel and bedrock had to have been altered following the deposition of the gravel.

In the Footwall zone, mica-feldspar schist has a bleached, light green to white color and ranges from incompetent {e} within 3-5 meters of the gravel contact to breakable {b} at approximately 10-20 meters below the contact. Graphitic quartzites and quartz-rich graphitic schists in the Footwall zone often have a bleached, light grey color but they are usually more competent. These quartz-rich rocks are often highly fractured with quartz that crumbles upon the blow of a hammer. Below the Footwall zone, which roughly parallels the gravel contact, pervasive footwall alteration and bleaching are associated with either highly fractured bedrock or remnant shear and/or fault zones. A similar footwall zonation also exists at Preido and Paradise Hills.

Intense Footwall zone alteration below the White Channel gravel of hills along upper Hunker and Bonanza Creeks is far more sporadic in comparison to the alteration in the Footwall zone at Dago Hill. At hills along Bonanza Creek such as Adams, American, Cheechako, Cripple, Lovett, Monte Cristo, Sourdough and Trail, areas of friable (incohesive, {d}) to incompetent {e} bedrock exist. However, these areas commonly occur where gravel has been removed. The zone of intense bedrock alteration usually extends 3-5 meters below the exposed surface, however, the original gravel contact at these hills was probably 2-5 meters above the present day surface. At most of these hills, little mining has occurred in the White Channel gravel since the early 1900's. However, bedrock exposed by mining at these hills during the early 1900's has undergone 80 years of surficial weathering and is often revegetated. As a result, it is difficult to determine the original extent and degree of Footwall zone alteration at these hills. Recently exposed bedrock at Jackson Hill consists of friable (incohesive, {d}) to incompetent {e} chlorite-mica-feldspar schist and intruded diabase dikes,

with the zone of clay alteration ranging from 3 to 6 meters in thickness. The gravel contact is estimated to have been 2-3 meters above the present day surface. Bedrock immediately below slightly (2) altered White Channel gravel at Cripple, Jackson, Trail and Sourdough Hills ranges from competent (a) to friable ((c) or (d)). Incompetent (e) bedrock found in place below slightly (2) altered gravel is rare at all of these hills.

Clay-altered bedrock in the Footwall zone occasionally contains quartz or siderite+quartz veins. The veins are thin (usually <1-2cm in thickness), and they cross-cut all metamorphic and deformational fabrics in Klondike Schist and associated units. These veins are easily distinguished from the more common metamorphic quartz veins present in the footwall rocks based upon their morphology, mineralogy and textures. Their morphology and apparent genetic association with intensely, clay-altered Footwall zone rocks suggests that they were emplaced during post-depositional alteration of the Footwall zone and the overlying White Channel gravel. The veins and their relationship to alteration are thoroughly discussed in chapter 3.

At the northeast corner of the Paradise Hill bench (facing Hunker Creek), a zone of silicified bedrock exists in the clay-altered Footwall zone. At this particular part of the bench, the White Channel gravel has been removed and mined. The Footwall zone rocks consist of graphitic schist, graphitic quartzite and serpentinite. A small zone of silicified rocks, approximately 10 meters in length and several meters in thickness, is present in a highly iron-stained and clay-altered portion of the serpentinite. Thin quartz and quartz-chalcedony veins with vuggy and cockscomb textures are present in the silicified zone. The surface of the Footwall zone is estimated to be approximately 2-5 meters below the former gravel contact. A pit approximately 100-150 meters south of the silicified serpentinite contains an exposure of intensely clay-altered bedrock and strongly (4) to extremely (5) altered Iron zone gravel overlying the Footwall zone. Similar to the Footwall zone alteration at other hills along Hunker Creek, it appears that clay alteration and iron-staining of the White Channel gravel and the underlying serpentinite occurred following the deposition of the gravel. In addition, the silicification and presence of associated quartz veins in the clay-altered and iron-stained

serpentinite suggests that they also are directly related to the post-depositional alteration. This relationship is further supported by the morphology, mineralogy and chemistry of the veins which are discussed in chapter 3.

2.2 Mineralogy

A distinct mineralogical variation is associated with the three visible alteration zones described in the previous section. Hydrometer, X-ray diffraction and petrographic analyses were used to determine the grain size distribution, mineralogy and kaolinite crystallinity of samples from the three alteration zones. The results are compared to analyses of stratigraphically and lithologically similar but less altered materials. Procedural techniques and calculations involved in the hydrometer and X-ray diffraction analyses are outlined in appendices 5.3 and 5.4, respectively. The following section describes the grain size distribution and mineralogy of unaltered White Channel sediments, Bleached zone gravel, Iron zone gravel, altered Footwall zone rocks and unaltered bedrock from Dago, Cripple, Jackson, Nugget, Paradise, Preido and Trail Hills.

2.2.1 Unaltered and Bleached zone gravel

Slightly (2) altered White Channel gravel overlying altered Bleached zone gravel at Dago Hill (figure 2.6) contains less than 1-2wt.% clay size material (<2μm size fraction) in the gravel matrix (table 2.1 and figure 2.7). Over 80wt.% of the gravel matrix (<2mm size fraction) occurs in the 100μm-2mm size fraction. The matrix is composed of abundant detrital quartz, muscovite (10Å mica), K-feldspar, plagioclase and minor chlorite. The clay mineralogy of the <2μm size fraction, shown in table 2.2 and figure 2.8, consists of approximately equal amounts of illite (10Å mica), kaolinite, smectite and occasionally abundant, randomly interstratified illite/smectite (as defined by Brindley and Brown, 1980; Hower, 1981; Reynolds and Hower, 1970; Srodon, 1984). In general, the diffraction patterns of these clay minerals consist of poorly developed peaks indicating that they have poor crystallinities. The Hinckley (1963) crystallinity index (HCI) for kaolinite from the slightly

Table 2.1 Normalized grain size distribution of the <2mm size fraction (wt.%) for selected samples of matrix and cobbles from White Channel sediments, and mica schist collected from Dago Hill.

Sample		2mm-100μm	100μm-20μm	20μm-5μm	5μm-2μm	<2μm
Primary Gravel Matrix						
W-414[1]	(≈23m, 2)	31	13	19	6	31
W-411	(≈21m, 2)	78	12	7	1	2
W-410	(≈20.5m, 2)	83	8	7	2	2
Bleached Zone						
A-407[1]	(≈22m, 5)	44	22	18	2	14
A-401	(≈20m, 3)	73	8	5	0	14
A-402	(≈19.5m, 5)	47	22	15	5	11
A-403	(≈17m, 5)	38	18	24	7	13
522	(≈8.5m, 4)	60	18	14	3	5
527	(≈6m, 4)	63	12	11	5	9
514	(≈3m, 4)	65	12	12	2	9
Iron Zone						
A-410[2]	(≈2.5m, {e})	0	15	40	14	31
517	(≈1m, 5)	60	18	13	3	6
W-404	(≈1m, 5)	57	17	16	3	7
516	(≈0.5m, 5)	37	19	24	6	14
908[3]	(≈1m, 4)	64	15	11	4	6
Bedrock						
515	(≈0.5m, {e})	40	14	22	5	9
502	(≈3-4m, {c})	78	11	7	0	4
503	(≈10m, {b})	74	18	7	0	1
HP-1[4]	({b})	74	12	8	5	1

The elevation above or below the gravel-bedrock contact and the degree of alteration (competence for bedrock and cobbles) of each sample are in parentheses. Analyses were performed using the hydrometer method (described in appendix 5.3).
[1]Samples from overbank sediments within the White Channel sediments. [2]Completely clay altered rhyolite porphyry cobble. [3]Sample from Nugget Hill. [4]Sample from the Hunker Creek rhyolite porphyry.

Table 2.2 Mineralogy of samples collected from the matrix (<2mm size fraction) of White Channel gravel at Dago Hill.

Sample		<2μm size fraction (clay minerals normalized to 100%) ka	ill	sm	chl	ill/sm	chl/sm	2μm-2mm size fraction normalized to 100% >10%	1-10%	<1%	
Primary Gravel											
W-413[1]	(≈22m, 2)	56	30	10	0	4	0	qz	-	-	qz(50), mc(38), ab(8), chl(2), ka(2), HCl<0.3
W-412[1]	(≈21m, 2)	30	60	6	0	4	0	-	qz,tc,pl	-	qz(63), mc(24), ab(11), chl(2), ka(<1)
W-411	(≈21m, 2)	40	44	16	0	tr	0	qz	pl	-	qz(70), mc(21), kf(4), ab(3), ka(<1), chl(<1)
W-410	(≈20.5m, 2)	38	46	16	0	0	0	-	qz	pl,kf	qz(61), pl(22), mc(14), kf(3), chl(<1), ka(<1), HCl<0.3
Bleached Zone											
A-407[1]	(≈22m, 5)	75	17	4	0	4	0	-	qz	fs	qz(77), mc(13), ka(6), pl(2), kf(1), sm(1), HCl=0.53
A-401	(≈20m, 3)	52	36	12	0	tr	0	-	qz	-	qz(73), mc(15), pl(11), ka(1)
A-402	(≈19.5m, 5)	67	28	tr	0	4	0	qz	-	fs	qz(87), mc(11), sa(2), ka(<1), HCl=0.51
A-405	(≈19m, 5)	77	21	1	0	1	0	-	qz	fs	qz(86), mc(8), ka(3), kf(2), pl(1), HCl<0.3
A-403	(≈17m, 5)	85	14	1	0	0	0	qz	tc	fs	qz(83), mc(14), ka(3), fs(<1), tc(<1), HCl=0.59
504	(≈11m, 3)	40	60	0	0	tr	0	qz	-	fs	qz(70), mc(18), ab(8), chl(2), ka(2)
524	(≈10m, 3)	44	56	0	0	0	0	qz	pl	kf	qz(69), mc(18), ab(7), mic(5), ka(1)
523	(≈9.5m, 4)	-	-	-	-	-	-	-	-	-	qz(86), mc(9), pl(4), kf(1)
522	(≈8.5m, 4)	74	26	0	0	0	0	-	qz	fs	-
W-407	(≈7m, 4)	81	16	3	0	0	0	-	qz,tc	-	qz(85), mc(14), kf(1), ka(<1)
A-416	(≈6m, 4)	83	17	0	0	0	0	-	qz	-	qz(65), mc(22), ka(10), kf(2), pl(1)
527	(≈6m, 4)	88	12	0	0	0	0	-	qz	-	HCl=0.61
514	(≈3m, 4)	79	21	0	0	0	0	-	qz	-	qz(82), mc(14), ka(2), pl(1), kf(1)

Iron Zone											
CN-01	(≈1.5m, 5)	-	-	-	-	-	-	-	-	-	qz(42), hm(28), ge(16), mc(13), ka(1)
517	(≈1m, 5)	70	25	0	0	5	0	-	qz	fs	qz(60), mc(25), pl(10), chl(3), kf(3), ka(2)
W-404	(≈1m, 5)	69	22	9	0	tr	0	-	qz	ge	qz(81), mc(17), ab(2), ka(<1), HCI=1.30
516	(≈0.5m, 5)	55	42	2	0	1	0	lp	qz,ge	-	qz(47), mc(28), kf(14), ka(11), lp(<1), HCI=1.59
908[2]	(≈1m, 4)	tr	tr	0	0	0	0	ad,qz	ge,pl	-	qz(84), mc(6), ge(5), pl(5), kf(<1)
Primary Gravel Near Bedrock											
405[3]	(≈1.5m, 2)	48	47	5	0	0	0	-	qz	-	qz(73), mc(19), ab(6), kf(1), ka(<1), chl(<1)
807[4]	(≈4m, 1)	43	45	0	5	0	7	qz	tc,pl,kf	sp	qz(73), mc(15), chl(7), pl(3), sp(2), ka(<1), kf(<1)
806[4]	(≈2m, 1)	52	38	0	tr	0	10	sp,qz	tc,pl	-	qz(45), sp(25), mc(20), chl(8), pl(2)
810[4]	(≈1m, 1)	24	53	0	4	0	19	sp,qz	pl,kf	-	qz(65), mc(15), chl(7), sp(6), pl(5), ka(2), hb(1), kf(<1)

The elevation above bedrock and the degree of alteration for each sample are in parentheses. Mineralogy of the <2μm size fraction was determined by XRD (clay minerals normalized to 100%) using a basal orientation technique. The mineralogy of the 2μm-2mm size fraction was determined by XRD using backpacked (randomly oriented) powders.

[1]Samples from overbank sediments within the White Channel sediments. [2]Sample from Nugget Hill. [3]Sample from Cripple Hill. [4]Samples from Paradise Hill.

Key to mineral abbreviations; ka=kaolinite, ill=illite (10Å mica), sm=smectite, chl=chlorite, ill/sm=interstratified illite/smectite, chl/sm=interstratified chlorite/smectite, qz=quartz, mc=muscovite (10Å mica), fs=feldspar, kf=k-feldspar, pl=plagioclase, sa=sanidine, mic=microcline, or=orthoclase, ad=adularia, ab=albite, lp=lepidocrocite (γFeOOH), ge=goethite (αFeOOH), hm=hematite, sp=serpentine, mg=margarite, tc=talc, hb=hornblende, tr=trace, HCI=Hinckley crystallinity index, XRD=X-ray diffraction.

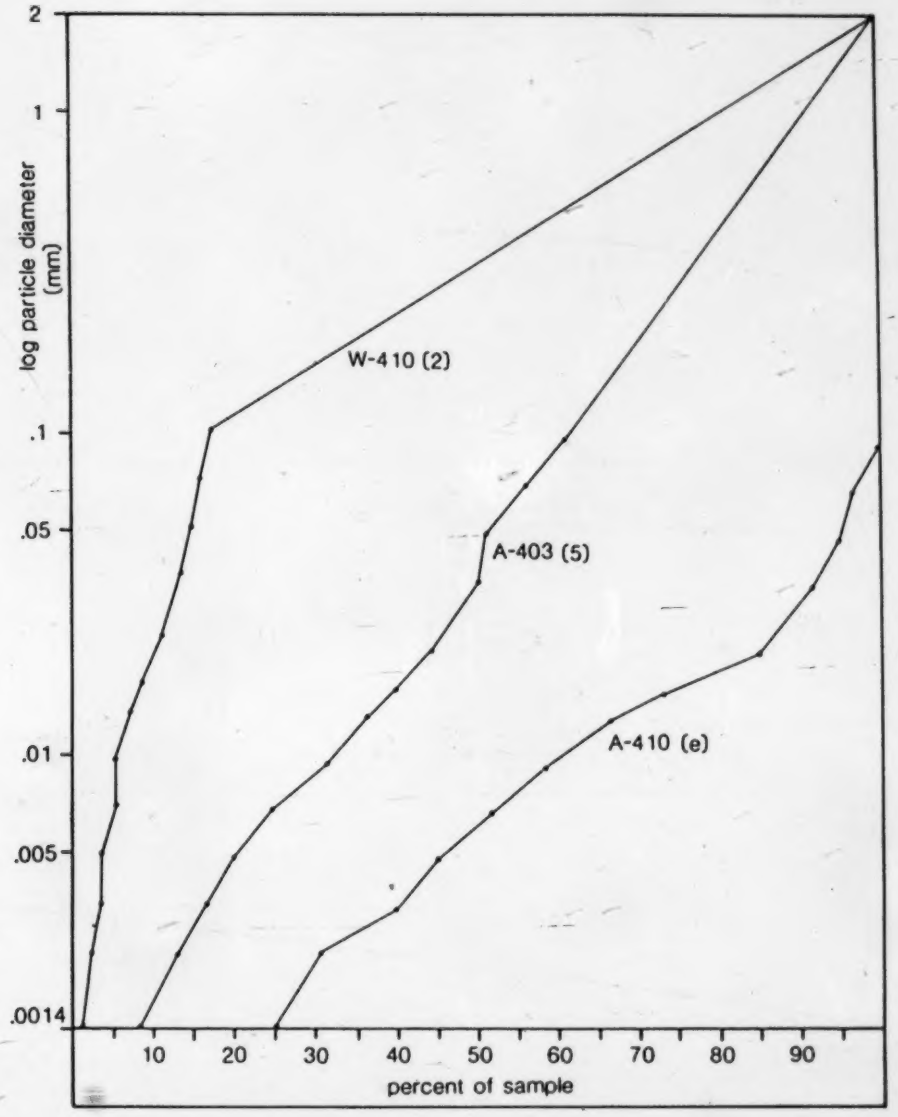

Figure 2.7 Grain size distribution of the <2mm size fraction for slightly (2) altered (W-410) versus extremely (5) altered (A-403) gravel matrix. An incompetent (e) rhyolite cobble is included (A-410) for comparison.

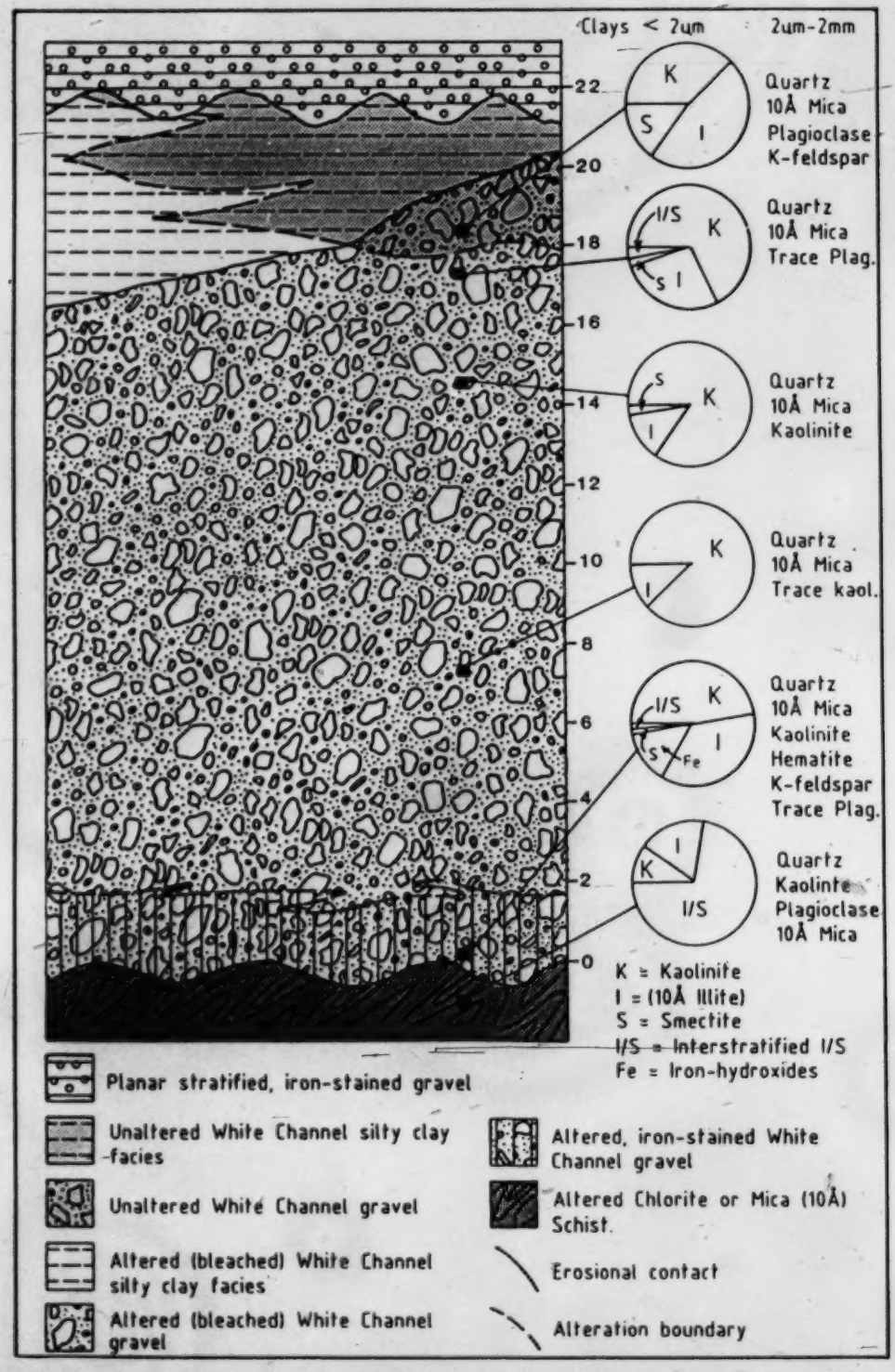

Figure 2.8 Schematic section of the White Channel deposit at Dago Hill with three distinct alteration zones. The clay mineralogy of the <2μm size fraction and mineralogy of the 2μm-2mm size fraction is included (modified after Dufresne *et al.*, 1987).

(2) altered gravel is generally $\leq$0.3 (table 2.2).

White Channel gravel in the Bleached zone that is directly below slightly (2) altered gravel contains 10-15wt.% clay size material (<2μm size fraction) in the gravel matrix (table 2.1 and figure 2.7). Only 35-50wt.% of the matrix is in the 100μm-2mm size fraction. The matrix is dominantly composed of quartz, muscovite and clay minerals (table 2.2 and figure 2.8). At Dago, Preido, Paradise and Nugget Hills vast amounts of volcanic smoky quartz are visible in the gravel matrix, probably derived from the rhyolite stock on lower Hunker Creek. Muscovite is usually abundant, with feldspars and chlorite present in trace amounts only. The clay mineralogy of the <2μm size fraction is generally characterized by the presence of abundant kaolinite (65-85%) and illite (15-30%). Smectite and interstratified illite/smectite occur in minor (1-5%) to trace quantities ($\leq$1%) close to the alteration contact. The high percentage of material in the <2μm size fraction of strongly (4) to extremely (5) altered gravel relative to slightly (2) altered gravel matrix indicates that most of the minerals in the <2μm size fraction are the product of secondary post-depositional alteration. At first glance, illite appears to be less abundant in the matrix of Bleached zone gravel (15-30%) than in the matrix of slightly (2) altered gravel ($\approx$45%) from just above the alteration contact (table 2.2). However, illite has actually increased in abundance as strongly (4) to extremely (5) altered gravel in the Bleached zone contains approximately five to ten times the amount of clay size material in the gravel matrix, compared to slightly (2) altered gravel (table 2.1). The increase in kaolinite and illite in the Bleached zone gravel is the result of post-depositional alteration processes. Kaolinite crystallinity in the upper regions of the Bleached zone varies from an HCl of $\leq$0.3 to $\approx$0.6 (table 2.2). In general, secondary kaolinite from strongly (4) to extremely (5) altered gravel matrix in the Bleached zone shows a slight increase in crystallinity relative to kaolinite from slightly (2) altered gravel. The crystallinity values are still low indicating poor crystal ordering and/or morphology.

The grain size distrbution and mineralogy of gravel matrix in the Bleached zone is relatively consistent throughout the Dago Hill section, except for a 2-3 meter thick horizon of moderately (3) altered gravel approximately 10-12m above bedrock. Gravel from within this

zone appears to contain less clay material in the matrix, as compared to strongly (4) altered gravel above and below. In addition, the clay mineralogy of the <2μm size fraction from the gravel matrix is characterized by approximately equal proportions of kaolinite and illite (table 2.2). The coarser size fractions contain abundant quartz, muscovite, plagioclase, K-feldspar and minor chlorite (table 2.2).

2.2.2 Iron zone gravel

Gravel matrix from the Iron zone of Dago Hill consists of 5-15wt.% clay size material (<2μm size fraction) with 35-60wt.% of the matrix in the 100μm-2mm size fraction (table 2.1). The mineralogy of the coarser size fractions is characterized by the presence of abundant quartz, muscovite, plagioclase and K-feldspar with minor to trace amounts of kaolinite, illite, smectite, hematite, lepidocrocite (γFeOOH), goethite (αFeOOH), gypsum and chlorite. Hematite occurs as a cement in a few outcrops of Iron zone gravel. The clay mineralogy of the <2μm size fraction is commonly dominated by kaolinite and illite with significant amounts of lepidocrocite and goethite. Interstratified illite/smectite, smectite, quartz and feldspars are usually present in minor to trace amounts (table 2.2 and figure 2.8). The HCI of kaolinite in one sample is 1.59 (table 2.2). In addition, illite, goethite and especially lepidocrocite exhibit sharp and symmetric peaks on the X-ray diffractogram patterns indicating that these minerals are well crystallized and ordered. The high percentages and high crystallinities of kaolinite, illite, and the iron-hydroxides in the <2μm size fraction, in comparison to unaltered White Channel gravel matrix, indicate that they are secondary and the product of post-depositional alteration of gravel matrix.

Cemented and iron-stained gravel from the White Channel deposit at Nugget Hill contains 6wt.% of the matrix in the <2μm size fraction, while 60-65wt.% of the matrix occurs in the 100μm-2mm size fraction. The 2μm-2mm size fraction is dominantly composed of quartz with minor muscovite, goethite, plagioclase and trace adularia. Thin-section textures indicate that botryoidal goethite is the dominant cement (plate 2.9). Coarse secondary muscovite (1-2mm in size, plate 2.10) is present as a minor cement, often rimming clasts and

Plate 2.9 Photomicrograph (crossed polarized light) of cemented Iron zone gravel at Nugget Hill with botryoidal goethite cementing detrital quartz grains.

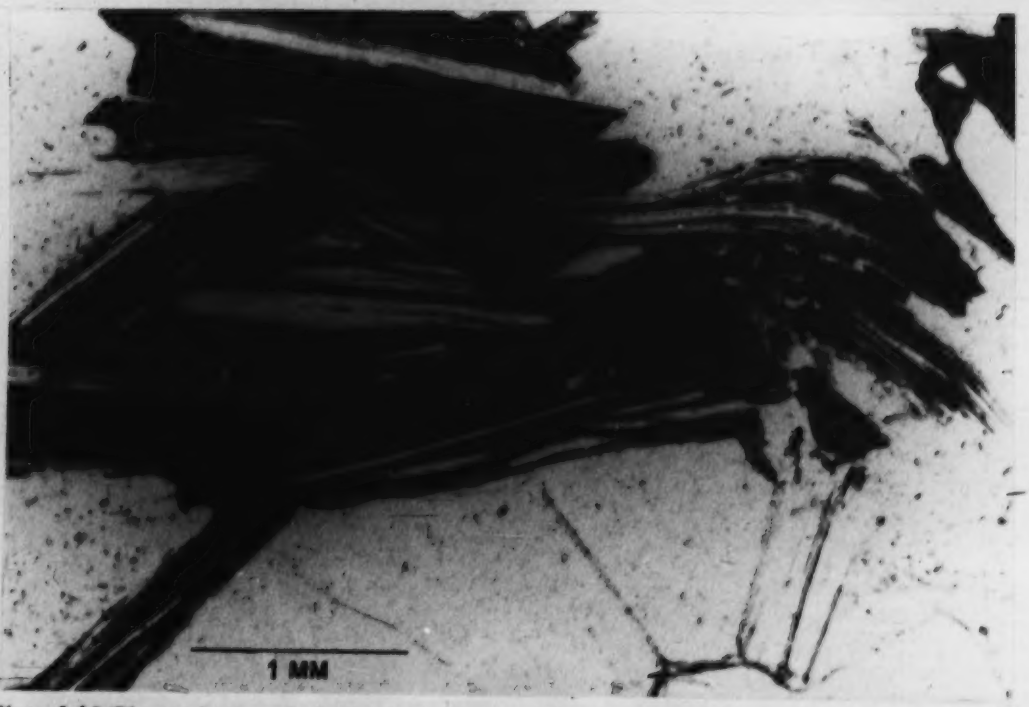

Plate 2.10 Photomicrograph (plane polarized light) of cemented Iron zone gravel at Nugget Hill with coarse 10Å mica (muscovite 1-2mm in length) rimming detrital quartz grains.

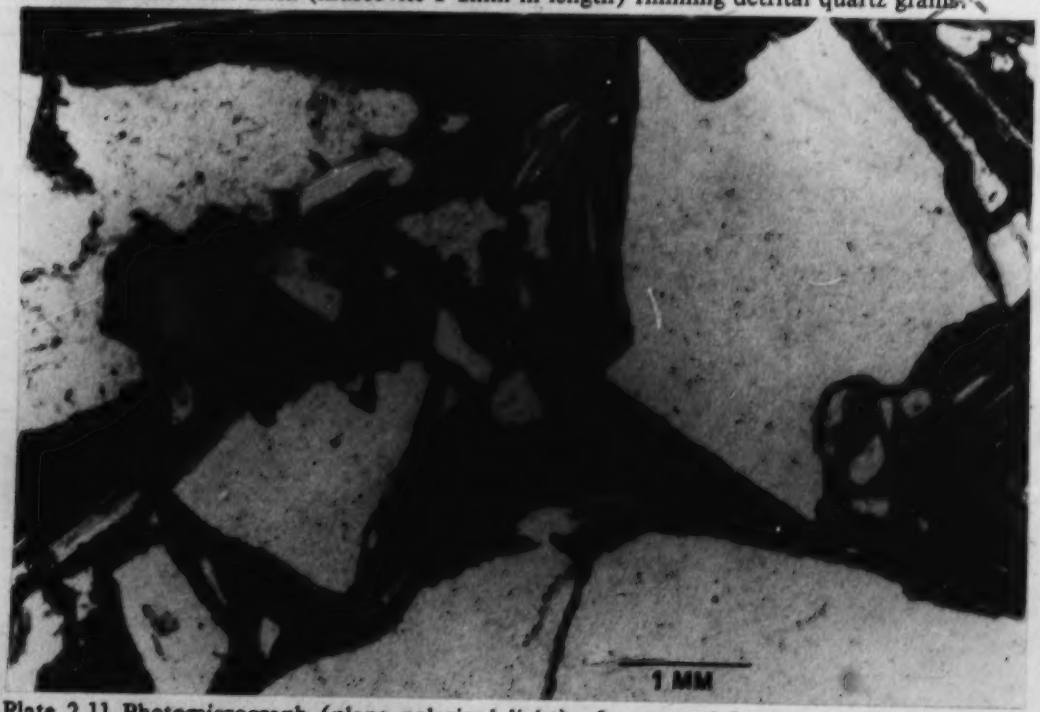

Plate 2.11 Photomicrograph (plane polarized light) of cemented Iron zone gravel at Nugget Hill with intergrown goethite and muscovite cementing the matrix of the gravel.

intergrown with botryoidal goethite (plate 2.11). In the <2μm size fraction, quartz, adularia and goethite are abundant with only trace amounts of clay minerals present. The abundance of adularia in the <2μm size fraction and its absence in the coarser size fractions suggests that it is secondary and the product of post-depositional alteration along with secondary goethite and muscovite.

2.2.3 Clasts from the White Channel deposit

Rhyolite porphyry clasts, from the White Channel gravel of Dago Hill, generally range from friable (incohesive, {d}) to incompetent {e} in their degree of competence (plate 2.5). Occasional friable (cohesive, {c}) clasts are also present. Competent {a} rhyolite porphyry clasts in the White Channel gravel of Preido and Dago Hills are petrographically similar to the Hunker Creek rhyolite porphyry on the right bank of lower Hunker Creek. The rhyolite porphyry is composed of quartz, orthoclase and/or sanidine phenocrysts in a groundmass of similar composition except for the presence of small quantities of plagioclase. Muscovite and amphibole are present in subordinate amounts in the groundmass. One incompetent {e} rhyolite clast from Dago Hill contains approximately 31wt.% of its material in the <2μm size fraction (table 2.1 and figure 2.7). At Preido Hill, rhyolite porphyry clasts generally range from breakable {b} to incompetent {e}, with an abundance of friable clasts present (both cohesive, {c} and incohesive, {d}). All the rhyolite porphyry clasts examined from within 3 meters of bedrock at Dago and Preido Hills are dominantly composed of quartz, adularia, kaolinite and varying amounts (usually minor) of orthoclase or sanidine (table 2.3). The clay mineralogy of the <2μm size fraction is dominated by kaolinite (often >80%) with minor to trace amounts of illite and smectite. In addition, quartz and adularia are usually abundant in this size fraction. In thin-section, irregardless of the degree of competence of the rhyolite cobble, K-feldspar phenocrysts and groundmass show at least incipient alteration and usually are strongly altered. Adularia is commonly regarded as a low temperature vein phase and not as a magmatic K-feldspar (Deer *et al.*, 1966). Consequently, adularia may have resulted from the alteration of primary volcanic sanidine and/or orthoclase

Table 2.3 Mineralogy of rhyolite porphyry and mica schist cobbles (<2mm size fraction) collected from the White Channel gravel.

		<2μm size fraction (clay minerals normalized to 100%)									2μm-2mm size fraction normalized to 100%
Sample		ka	ill	sm	chl	ill/sm	chl/sm	>10%	1-10%	<1%	
Rhyolite cobbles											
602[1]	(≈2-3m, {b})	80	17	3	0	0	0	qz,ad	-	-	qz(68), ad(32), ka(<1)
604[1]	(≈1.5m, {b})	96	4	0	tr	0	0	qz,ad	-	tc?	qz(79), ad(20), ka(1), HCI=1.30
508	(≈2-3m, {c})	88	9	0	3	0	0	qz,ad	pl?	-	qz(77), ad(23), ka(<1), HCI<0.3
W-401	(≈1-1.5m, {c})	95	4	0	1	0	0	qz,ad	-	-	qz(81), ad(16), ka(3), mc(<1), sa(<1), HCI=0.74
A-409	(≈1.5m, {d})	87	13	0	0	0	0	ad,qz	-	-	qz(79), ad(12), mic(6), mc(2), pl(1), ka(<1)
A-411	(≈2.5m, {d})	100	tr	0	0	0	0	qz	kf,pl?	-	qz(79), kf(20), ka(1)
614[1]	(≈1.5-2m, {e})	57	21	22	0	0	0	qz	kf	-	qz(91), ad(7), ka(2), mc(<1)
A-414	(≈6-7m, {e})	67	33	tr	0	0	0	-	qz	kf	qz(92), mc(8), ka(3), kf(3), mc(2)
A-410	(≈2.5m, {e})	86	4	tr	0	0	0	qz	mic?	-	-
Mica schist cobbles											
W-415	(≈20-21m, {b})	49	50	1	tr	0	0	qz	pl	-	mc(67), qz(33), ka(<1)
507	(≈10-12m, {b})	44	55	1	tr	0	0	qz,kf	pl	-	qz(60), mc(22), mic(15), pl(3)
406[2]	(≈1.5m, {c})	36	59	5	tr	0	0	qz,pl	kf	-	qz(58), ab(22), mc(12), mic(8), ka(<1)
W-405	(≈0.5m, {e})	85	15	0	tr	0	0	qz	pl	tc?	qz(51), mc(25), pl(17), kf(6), ka(1), HCI=0.63

The elevation above bedrock and the degree of competence of each cobble are in parentheses. Mineralogy of the <2μm size fraction was determined by XRD (clay minerals normalized to 100%) using a basal orientation technique. The mineralogy of the 2μm-2mm size fraction was determined by XRD using backpacked (randomly oriented) powders.

[1]Samples from Preido Hill. [2]Sample from Cripple Hill.

Key to mineral abbreviations; ka=kaolinite, ill=illite (10Å mica), sm=smectite, chl=chlorite, ill/sm=interstratified illite/smectite, chl/sm=interstratified chlorite/smectite, qz=quartz, mc=muscovite (10Å mica), fs=feldspar, kf=k-feldspar, pl=plagioclase, sa=sanidine, mic=microcline, or=orthoclase, ad=adularia, ab=albite, lp=lepidocrocite (γFeOOH), ge=goethite (αFeOOH), hm=hematite, sp=serpentine, mg=margarite, tc=talc, hb=hornblende, tr=trace, HCI=Hinckley crystallinity index, XRD=X-ray diffraction.

in these cobbles. It is not entirely clear whether adularia formed after incorporation into the White Channel gravel or before the cobbles were eroded from their source. One rhyolite cobble from 6-7 meters above bedrock at Dago Hill contains quartz with only minor to trace amounts of K-feldspar, kaolinite and muscovite in the 2μm-2mm size fraction. Adularia was not distinguished in the X-ray patterns of the 2μm-2mm or <2μm size fractions. One rhyolite cobble from 1.5-2 meters above bedrock at Preido Hill contains significant smectite in the clay size fraction.

The crystallinity of kaolinite is highly variable in the rhyolite cobbles. One rhyolite cobble contains kaolinite with a high HCI of ≈1.3, yet two cobbles contain kaolinite with intermediate crystallinities of approximately 0.6 and 0.7. Several cobbles contain kaolinite of poor crystallinity with HCI's ≤0.3 (table 2.3). One or two completely clay-altered cobbles contain a kaolin mineral resembling halloysite or an intergradient kaolinite/smectite mineral as the basal 001 and 002 reflections are poorly developed occurring in the 7.3-7.5Å and 3.57-3.60Å regions, respectively. In addition, K-feldspar is present in minor to trace amounts. Kaolinite and illite in the clay size fraction of these cobbles are the products of *in situ* alteration.

Mica schist cobbles ranging from breakable (b) to incompetent (e) show little variation in the mineralogy of the 2μm-2mm size fraction (table 2.3). Quartz, muscovite, plagioclase and microcline are the main constituents. In the <2μm size fraction breakable (b) to friable (cohesive, (c)) clasts contain approximately equal amounts of kaolinite and illite with minor to trace amounts of smectite. One incompetent (e) mica schist cobble contains approximately 85% kaolinite and 15% illite (table 2.3).

2.2.4 Footwall zone

Various degrees of altered bedrock in the Footwall zone were sampled and analysed using X-ray diffraction and petrography (table 2.4). A range in lithologies was also collected including mica schist, chlorite-mica schist, graphitic-mica schist and diabase. Clay-altered clasts of altered White Channel gravel sit immediately above intensely altered bedrock on

Table 2.4 Mineralogy of samples (<2mm size fraction) collected from bedrock below the White Channel gravel.

Sample		<2μm size fraction (clay minerals normalized to 100%) ka	ill	sm	chl	ill/sm	chl/sm	>10%	1-10%	<1%	2μm-2mm size fraction normalized to 100%
Mica schist[1]											
515	(≈0.5m, {e})	86	14	0	0	tr	0	-	qz	-	qz(60), mc(20), ka(13), ab(7), HCI=1.03
A-417	(≈2-3m, {e})	72	28	0	0	0	0	qz	pl	-	qz(62), mc(29), mic(6), ka(3), ab(<1)
502	(≈3-4m, {c})	2	98	0	0	tr	0	-	qz	-	qz(69), mc(29), pl(1), kf(1)
503	(≈10m, {b})	4	89	0	0	7	0	qz,pl	kf	-	qz(64), mc(28), pl(8), kf(<1)
Chlorite schist[2]											
105	(≈2-3m, {e})	56	15	0	tr	0	29	qz	pl	-	qz(77), mc(8), chl/sm(5), pl(5), ka(2), chl(2)
104	(≈6-7m, {d})	11	44	0	5	0	40	qz	pl	-	mc(46), qz(33), chl(16), pl(5)
103	(≈10-11m, {b})	15	32	0	4	0	49	qz	pl	-	qz(54), mc(27), chl(15), pl(3), ka(1)
Diabase[2]											
D-112	(≈2m, {e})	49	5	46	0	0	0	qz	pl,mg?	-	pl(60), qz(26), ka(8), mg?(6)
D-111	(≈3m, {d})	46	19	35	0	0	0	qz	pl,mg?	-	pl(69), qz(15), mg?(8), ka(5), mc(3)
D-101	(≈20-25m, {b})	46	7	0	7	0	40	qz,pl	-	-	pl(47), qz(47), ka(6), chl(<1)
Graphitic mica schist[3]											
A-351	(≈0.5m, {e})	10	17	0	0	73	0	qz	-	-	qz(69), ab(24), kf(4), mc(3)
A-335	(≈1m, {e})	27	36	34	0	3	0	qz	pl	-	qz(66), mc(20), ab(14)
A-331	(≈2m, {d})	47	28	15	0	10	0	qz	pl	-	qz(56), ab(36), mc(8), ka(<1)
402	(≈3-4m, {c})	37	60	tr	0	3	0	qz	pl	-	qz(80), mc(9), ab(8), kf(3)
401	(≈7-8m, {b})	32	65	3	0	0	0	qz,pl	kf	-	qz(65), mc(15), ab(15), kf(5)

The depth below the gravel contact and degree of clay alteration for each sample are in parentheses. Mineralogy of the <2μm size fraction was determined by XRD (clay minerals normalized to 100%) using a basal orientation technique. The mineralogy of the 2μm-2mm size fraction was determined by XRD using backpacked (randomly oriented) powders.

[1]Samples from Dago Hill. [2]Samples from Jackson Hill. [3]Samples from Cripple Hill.

Key to mineral abbreviations; ka=kaolinite, ill=illite (10Å mica), sm=smectite, chl=chlorite, ill/sm=interstratified illite/smectite, chl/sm=interstratified chlorite/smectite, qz=quartz, mc=muscovite (10Å mica), fs=feldspar, kf=k-feldspar, pl=plagioclase, sa=sanidine, mic=microcline, or=orthoclase, ad=adularia, ab=albite, lp=lepidocrocite (γFeOOH), ge=goethite (αFeOOH), hm=hematite, sp=serpentine, mg=margarite, tc=talc, hb=hornblende, tr=trace, HCI=Hinckley crystallinity index XRD=X-ray diffraction.

several Hunker Creek hills. The gravel and the underlying Footwall zone rocks are interpreted to have been post-depositionally altered, as previously discussed in section 2.1.3. Breakable {b} mica schist 10-20 meters below the White Channel gravel at Dago Hill is composed of quartz, muscovite, plagioclase and microcline in the 2μm-2mm size fraction. The clay minerals in <2μm size fraction consist of approximately 89% illite, 7% interstratified illite/smectite and 4% kaolinite (table 2.4). The grain size distribution (table 2.1 and figure 2.9) of breakable {b} mica schist (sample 503) shows approximately 1wt.% of the schist in the <2μm size fraction with almost 75wt.% of the schist in the 100μm-2mm size fraction. Incompetent {e} mica schist (samples 515 and A-417) from immediately below or within 2 meters of the gravel contact is composed of quartz, muscovite and kaolinite with minor to trace amounts of feldspar in the 2μm-2mm size fraction. In the clay size fraction, kaolinite (70-90%) and illite are the main constituents with trace amounts of interstratified illite/smectite (table 2.4). The grain size distribution (table 2.1 and figure 2.9) of sample 515 shows that considerably more material exists in the <2μm size fraction (9wt.%) of sample 515 than in samples 503 and 502. The decrease in percentage of illite in the <2μm size fraction of sample 515 (versus 503) reflects the increase in the kaolinite/illite ratio due to an increase in the degree of clay alteration. The absolute abundance of illite in sample 515 is actually greater than in sample 503 as the amount of clay size material has increased from approximately 1% in sample 503 to 9% in sample 515. During the initial stages of alteration (sample 503) randomly interstratified illite/smectite is present in the clay size fraction. As the degree of clay alteration increases, illite/smectite appears to be replaced by secondary kaolinite and illite. Kaolinite from the <2μm size fraction of sample 515 is well crystallized with an HCI of $\simeq$1.03.

Breakable {b} chlorite-mica schist at Jackson Hill is composed of quartz, muscovite and chlorite with minor plagioclase (sample 103, table 2.4). The clay mineralogy of the <2μm size fraction consists of approximately 49% randomly interstratified chlorite/smectite (as defined by Brindley and Brown, 1980; Tomita and Takahashi, 1985), 32% illite, 15% kaolinite and 4% chlorite. Incompetent {e} chlorite-mica schist (sample 105) contains significantly less muscovite and chlorite in the 2μm-2mm size fraction as compared to samples 103 and 104

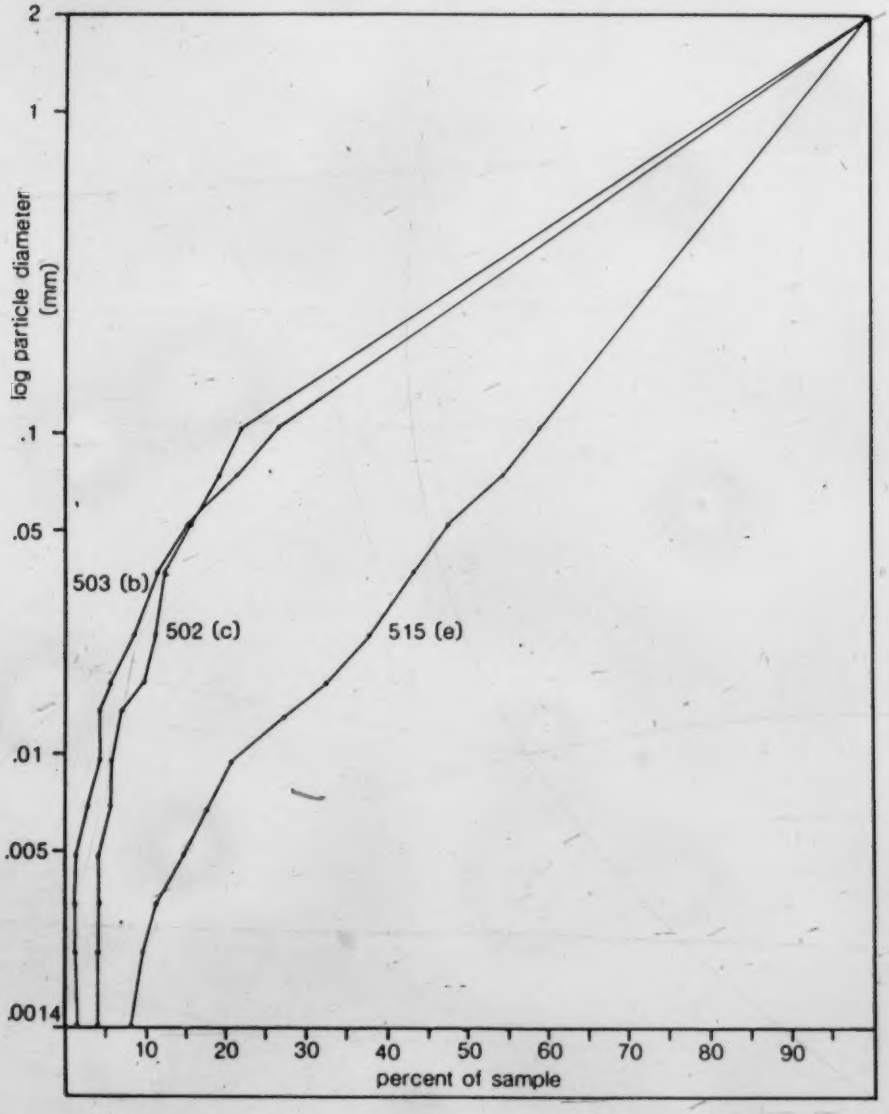

Figure 2.9 Plot of the grain size distribution for samples of mica schist at Dago Hill. Samples range from breakable (b) to incompetent (e).

(table 2.4). Sample 105 contains more quartz, interstratified chlorite/smectite and kaolinite in the 2μm-2mm size fraction in comparison to samples 103 and 104. The amount of plagioclase present does not appear to change significantly with increased degree of alteration. In the <2μm size fraction the amount of illite and interstratified chlorite/smectite appear to have decreased significantly with an increased degree of alteration due to the large increase in kaolinite. However, the absolute amount of illite, interstratified chlorite/smectite and kaolinite have all increased with the increased degree of alteration due to the large increase in the amount of clay size material in the <2μm size fraction. Similar patterns of alteration occur in the progressive alteration of diabase at Jackson Hill and graphitic-mica schist at Cripple Hill (table 2.4).

2.3 Chemistry

The distribution of major and trace elements in the Bleached, Iron and Footwall zones at Dago Hill was investigated in detail and compared to analyses of stratigraphically equivalent but less altered materials. In all, 49 samples of White Channel gravel and bedrock were analysed with 31 samples selected from Dago Hill and 18 from various locations on Cripple, Jackson, Nugget, Paradise, Preido and Trail Hills. The majority of major and trace element analyses were carried out using the X-ray fluorescence (XRF) technique at McMaster University. Several samples were analysed for trace elements, at a later date, using Instrumental Neutron Activation Analysis (INAA) at the SLOWPOKE II reactor, University of Alberta. Element concentrations obtained by the XRF method included Si, Al, Fe, Mg, Ca, Na, K, Ti, Mn, P, S, Ba, As and loss on ignition (LOI). Elements obtained by INAA included Fe, Na, Cr, U, Co, As, Sb and various rare earth elements (which are not reported). Details of the experimental procedure and estimates of error for both XRF and INAA methods are presented in appendix 5.5.

The clay alteration of the White Channel gravel matrix does not appear to have affected quartz significantly as quartz modes (determined by XRD) throughout the entire Dago Hill section are relatively consistent (table 2.2). The whole rock chemistry of the White

Channel gravel matrix is essentially a function of the quartz/(mica+feldspar+clay mineral) ratio, which was initially determined by the source rock and fluvial environment of deposition. This causes natural chemical inhomogeneities in the White Channel gravel matrix, which are dependent upon facies type. These inhomogeneities in the mineralogical content of each facies make it difficult to detect small changes that have occurred in the concentration of SiO_2 and/or the mobility of SiO_2 due to the alteration of the White Channel sediments. Nevertheless, it is still possible to chemically characterize the alteration process by comparing the major oxide chemistry (not including SiO_2), ratioed against Al_2O_3, of unaltered versus altered gravel matrix. This is possible, due to the fact that the most significant change during alteration is the transformation of feldspars, mica and trace amounts of mafic minerals to kaolinite and illite, essentially conserving alumina throughout these changes.

The major oxides of table 2.5 (excluding SiO_2) are ratioed against Al_2O_3 in table 2.6. Alumina is chosen for three major reasons. First, it is generally accepted that alumina is immobile during alteration by low temperature (<200°C) hydrothermal or supergene fluids (Kerrich and Fyfe, 1982). Consequently, the alteration of White Channel sediments should not have affected initial whole rock alumina concentrations. In addition, the ratios are also independent of volume changes due to the uptake of water (H_2O) during clay alteration. The third reason is that initial chemical inhomogeneities due to variations in the quartz/(mica+feldspar+clays) content of various sedimentary facies will not affect major oxide/Al_2O_3 ratios as long as there is a reasonably constant ratio between mica, feldspar and clays. This can be assumed in this study as throughout a section of White Channel gravel on any particular hill in the Klondike district, the distribution of, and ratio between mica schist, felsic porphyry and mafic clasts is reasonably consistent. This indicates that the matrix of the gravel will also bear a consistent ratio between micas, feldspars, mafic minerals and clay minerals. As a result, although the whole rock chemistry will vary between facies types depending upon the quartz/(other minerals) ratio, the initial oxide/Al_2O_3 ratios of any facies should be consistent. This should hold true as long as there is a consistent source of bedrock during erosion. The mineralogy and the oxide/Al_2O_3 ratios of primary unaltered White

Table 2.5 Whole rock chemistry of samples collected from the matrix (<2mm size fraction) of White Channel gravel at Dago Hill.

Sample		SiO_2	Al_2O_3	Fe_2O_3	MgO	CaO	Na_2O	K_2O	TiO_2	MnO	P_2O_5	LOI
Primary Gravel												
W-413[1]	(≈22m, 2)	68.71	16.83	2.39	1.45	0.04	1.52	3.60	0.48	0.00	0.01	4.94
W-411	(≈21m, 2)	83.86	7.53	1.72	0.88	0.17	0.72	2.81	0.25	0.01	0.03	2.02
W-410	(≈20.5m, 2)	86.20	7.12	1.29	0.88	0.03	0.74	2.15	0.20	0.00	0.00	1.48
Bleached Zone												
A-407[1]	(≈22m, 5)	82.12	11.79	0.72	0.59	0.03	0.40	1.96	0.16	0.00	0.00	2.22
A-401	(≈20m, 3)	84.18	7.86	1.35	0.95	0.03	0.93	1.95	0.18	0.00	0.01	2.52
A-402	(≈19.5m, 5)	77.12	13.12	1.20	1.19	0.03	0.28	2.27	0.59	0.00	0.00	4.15
A-403	(≈17m, 5)	67.88	19.02	1.24	1.45	0.04	0.13	2.09	0.91	0.00	0.04	7.18
504	(≈11m, 3)	79.88	11.33	1.10	0.06	0.09	1.36	2.99	0.29	0.02	0.02	2.86
524	(≈10m, 3)	84.54	8.84	0.93	0.03	0.08	1.07	2.71	0.22	0.01	0.01	1.56
525	(≈9-10m, 4)	87.34	7.89	0.60	0.03	0.09	0.38	1.07	0.26	0.01	0.02	2.31
523	(≈9.5m, 4)	81.61	8.39	0.96	0.02	0.09	0.77	1.62	0.20	0.01	0.02	2.63
522	(≈8.5m, 4)	85.50	9.58	0.75	0.04	0.08	0.47	2.46	0.24	0.01	0.01	0.86
527	(≈6m, 4)	83.53	9.70	0.64	0.76	0.03	0.48	1.67	0.33	0.00	0.00	2.85
514	(≈3m, 4)	84.00	9.74	0.70	0.05	0.09	0.54	1.83	0.31	0.01	0.02	2.71
Iron Zone												
CN-01[2]	(≈1.5m, 5)	na	na	53.31	na	na	0.04	na	na	na	na	na
517	(≈1-1.5m, 5)	79.65	10.48	2.13	1.16	0.07	0.85	2.29	0.41	0.05	0.01	2.86
516	(≈0.5m, 5)	69.04	13.55	8.13	0.64	0.09	0.48	2.82	0.36	0.02	0.08	4.79
622[3]	(≈8m, 4)	79.89	5.35	2.53	0.40	0.03	0.09	1.67	0.16	6.55	0.13	3.18
908[4]	(≈1m, 4)	58.55	5.05	26.16	0.47	0.03	1.06	1.59	0.25	0.39	0.73	5.72
302[5]	(≈2m, 2)	81.20	10.46	1.39	0.06	0.11	1.45	2.86	0.21	0.02	0.02	2.21

The elevation above bedrock and the degree of alteration of each sample are in parentheses. Analyses were performed by the XRF technique (data in % oxides and LOI, LOI=loss on ignition at 1040°C, Fe_2O_3=total iron, na=not analysed) and recalculated to 100% (except CN-01).
[1]Samples from overbank sediments within the White Channel sediments. [2]Analysis by INAA. [3]Sample from Preido Hill. [4]Sample from Nugget Hill. [5]Sample from Trail Hill.

Table 2.6 Major oxide/Al_2O_3 ratios, LOI and trace element analyses of samples collected from the matrix (<2mm size fraction) of White Channel gravel at Dago Hill.

Sample		$\frac{Fe_2O_3}{Al_2O_3}$	$\frac{MgO}{Al_2O_3}$	$\frac{CaO}{Al_2O_3}$	$\frac{Na_2O}{Al_2O_3}$	$\frac{K_2O}{Al_2O_3}$	LOI (%)	S (ppm)	Mn (ppm)	Ba (ppm)	As (ppm)	Sb (ppm)	Co (ppm)
Primary Sediments													
W-413[1]	(≈22m, 2)	0.142	0.086	0.002	0.090	0.214	4.94	95	283	380	20	na	na
W-411	(≈21m, 2)	0.228	0.117	0.023	0.096	0.373	2.02	na	na	na	na	na	na
W-410	(≈20.5m, 2)	0.181	0.124	0.004	0.104	0.302	1.48	50	165	2,740	21	na	na
Bleached zone													
A-407[1]	(≈22m, 5)	0.061	0.050	0.003	0.034	0.166	2.22	90	106	2,730	8	na	na
A-401	(≈20m, 3)	0.172	0.121	0.004	0.118	0.248	2.52	120	157	2,290	30	na	na
A-402	(≈19.5m, 5)	0.091	0.091	0.002	0.021	0.173	4.15	160	146	2,510	3	na	na
A-403	(≈17m, 5)	0.065	0.076	0.002	0.007	0.110	7.18	120	127	1,950	12	na	na
504	(≈11m, 3)	0.097	0.005	0.008	0.120	0.264	2.86	na	187	2,890	18	na	na
524	(≈10m, 3)	0.105	0.003	0.009	0.121	0.307	1.56	na	144	2,420	<2	na	na
525	(≈9-10m, 4)	0.076	0.004	0.011	0.048	0.136	2.31	na	92	125	16	na	na
523	(≈9.5m, 4)	0.114	0.002	0.011	0.092	0.193	2.63	na	109	215	15	na	na
522	(≈8.5m, 4)	0.078	0.004	0.008	0.049	0.257	0.86	na	105	2,100	13	na	na
527	(≈6m, 4)	0.066	0.078	0.003	0.049	0.172	2.85	75	116	1,690	12	na	na
514	(≈3m, 4)	0.072	0.005	0.009	0.055	0.188	2.71	na	100	1,750	5	na	na
Iron zone													
CN-01	(≈1.5m, 5)	na	na	na	na	na	na	na	na	na	[2]1,560	[2]45.5	[2]110
517	(≈1-1.5m, 5)	0.203	0.111	0.007	0.081	0.219	2.86	330	1,050	3,080	23	[2]3.7	[2]63
516	(≈0.5m, 5)	0.600	0.047	0.007	0.035	0.208	4.79	na	238	6,750	16	[2]1.8	[2]31
622[3]	(≈8m, 4)	0.473	0.075	0.006	0.017	0.312	3.18	140	65,000	15,900	109	na	na
908[4]	(≈2m, 4)	5.180	0.093	0.006	0.210	0.315	5.72	490	4,300	1,500	266	[2]7.2	[2]nd
302[5]	(≈1m, 2)	0.133	0.006	0.010	0.139	0.273	2.21	na	164	2,720	18	na	na

The elevation above bedrock and the degree of alteration of each sample are in parentheses. Analyses were performed by the XRF technique with LOI in percent and trace elements in parts per million (na=not analysed, nd=not detected).
[1]Samples from overbank sediments within the White Channel sediments. [2]Analyses by INAA. [3]Sample from Preido Hill. [4]Sample from Nugget Hill. [5]Sample from Trail Hill.

Channel sediments confirm these consistencies. In general, the oxide/Al_2O_3 ratios of slightly (2) altered gravel matrix (samples W-410, W-411, A-401 and 302) show a narrow range for most of the major oxides (table 2.5). However, the raw totals of Al_2O_3, Fe_2O_3, MgO, Na_2O and K_2O for sample W-413, which is from a primary unaltered silty clay facies, are higher then the raw oxide totals for samples of slightly (2) altered gravel matrix. In addition, the concentration of SiO_2 is significantly less. The SiO_2 and Al_2O_3 differences are the result of an increase in the detrital clay mineral content of the silty clay facies versus the gravel facies, which was the result of changes in the depositional environment. Nevertheless, all the major oxide/Al_2O_3 ratios of sample W-413 generally fall within the range of values for slightly (2) altered White Channel gravel matrix.

2.3.1 Unaltered and Bleached zone gravel

Whole rock major and trace element chemistry was performed on seven samples from Dago Hill that range from slightly (2) altered White Channel sediments (3 samples) above the alteration contact to extremely (5) altered sediments (4 samples) immediately below the alteration contact (figure 2.6). Two of the samples are from White Channel overbank sediments (W-413 and A-407). The remaining five samples (W-410, W-411, A-401, A-402 and A-403) are from White Channel gravel matrix. The major oxide chemistry and LOI results (normalized to 100%) are presented in table 2.5. Trace element concentrations and major oxide/Al_2O_3 ratios are listed in table 2.6. Figure 2.10 is a schematic diagram that shows the chemistry of the gravel matrix above and below the alteration contact in the White Channel gravel at Dago Hill. Log (oxide/Al_2O_3) and log LOI of the five samples of gravel matrix are plotted in relationship to vertical distance above or below the alteration contact. The matrix of the Bleached zone (A-402 and A-403) shows a significant depletion in Fe_2O_3/Al_2O_3, Na_2O/Al_2O_3, K_2O/Al_2O_3 ratios and a minor reduction in the MgO/Al_2O_3 ratio relative to primary (slightly (2) altered) White Channel gravel matrix. No increase occurs in the concentration of CaO; however, it is not possible to detect a decrease in the concentration of CaO due to the low values of CaO in the sediments. LOI values show a significant increase

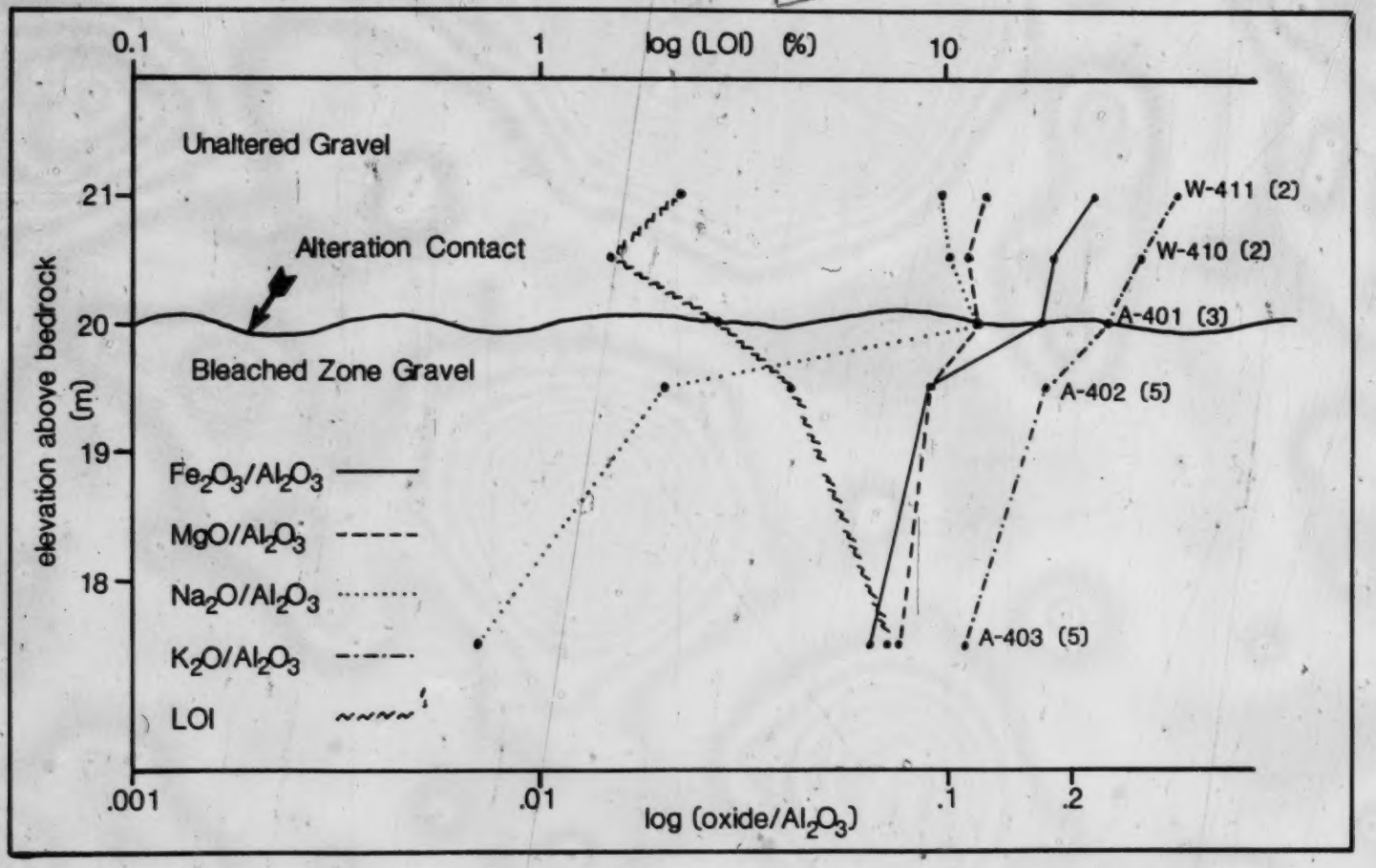

Figure 2.10 Plot of log (oxide/Al_2O_3) and log LOI versus elevation for matrix samples above and below the alteration contact within the White Channel gravel at Dago Hill.

due to the formation of secondary clay minerals in the Bleached zone. Minor and trace element concentrations (TiO_2, MnO, P_2O_5, S, Ba and As) appear to have been unaffected by Bleached zone alteration.

Moving vertically down the section in the Bleached zone (figure 2.11), the oxide/Al_2O_3 ratios are reasonably consistent for samples 523, 527 and 514. The Fe_2O_3/Al_2O_3 and K_2O/Al_2O_3 ratios are significantly depleted throughout the Bleached zone. The MgO/Al_2O_3 ratios of the upper Bleached zone gravel matrix are decreased significantly in comparison slightly (2) altered White Channel gravel matrix. The Na_2O/Al_2O_3 ratio is decreased compared to slightly (2) altered White Channel gravel but not as severely as the decrease in the Bleached zone gravel matrix directly below the alteration contact (figure 2.11). The values of LOI for samples 525, 523, 527 and 514, which are from the middle region of the Bleached zone, are slightly higher in comparison to LOI values for slightly (2) altered gravel matrix. As in the the uppermost region of the Bleached zone, the gravel from the middle region contains minor and trace element concentrations that are similar to values of primary White Channel gravel. Two samples (504 and 524) have anomalously high Na_2O/Al_2O_3 and K_2O/Al_2O_3 ratios compared to normal Bleached zone gravel. These two samples are from the sub-horizontal (2-3 meters thick) zone of moderately (3) altered gravel that appears to contain less secondary clay matrix than the gravel above or below the zone. Mineralogically, the samples from this zone contain a much higher illite/kaolinite ratio in the clay size fraction and higher (mica+albite)/quartz ratio in the 2μm-2mm size fraction compared to Bleached zone samples above and below. The higher abundance of the alkali-bearing minerals is probabaly a result of decreased intensity of alteration in this horizon.

2.3.2 Iron zone

The matrix of the Iron zone gravel at Dago Hill contains anomalously high Fe_2O_3/Al_2O_3 ratios and LOI values (samples 516 and 517) in comparison to the matrix of slightly (2) altered and Bleached zone gravel (table 2.6 and figure 2.11). Sample CN-01,

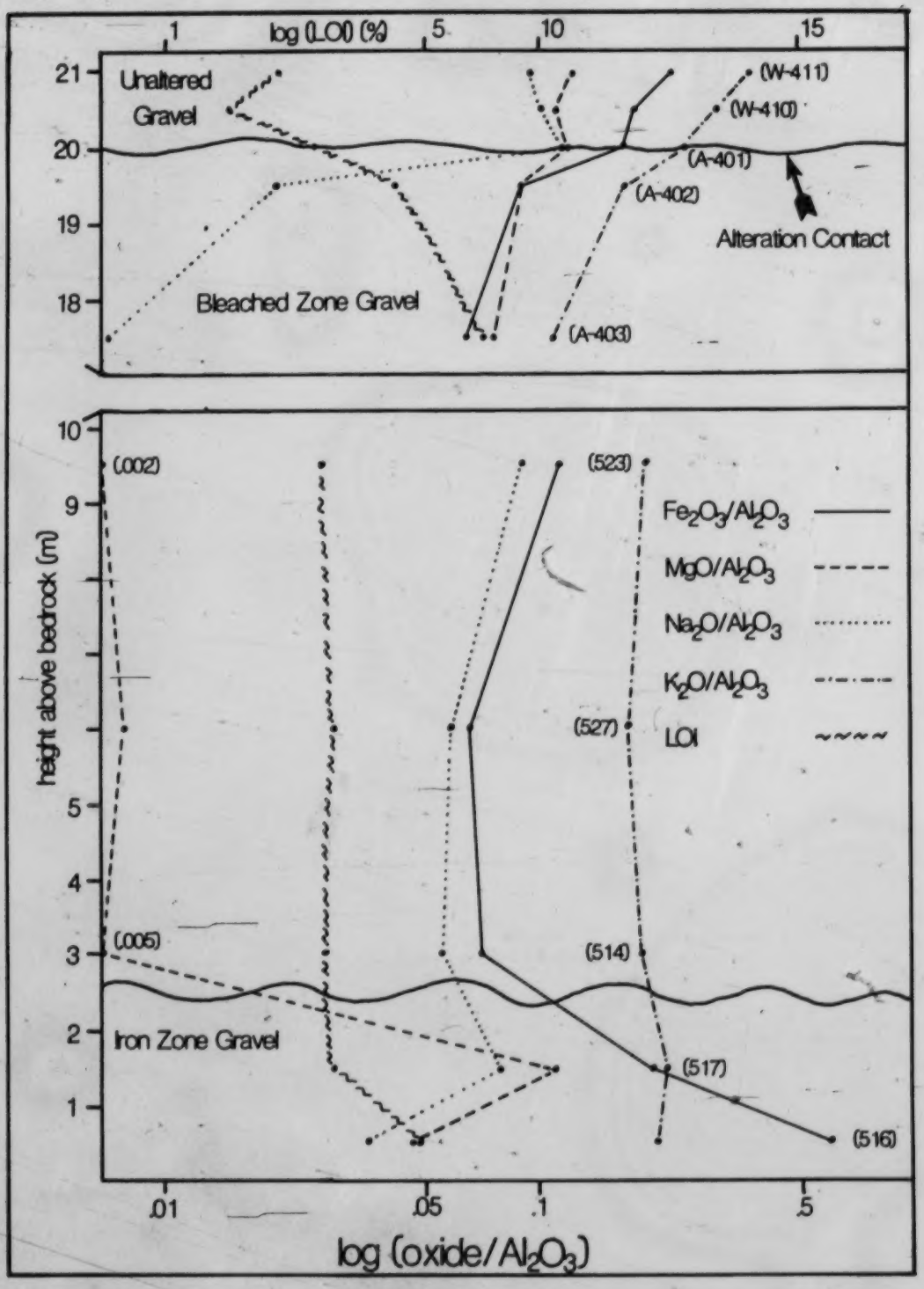

Figure 2.11 Plot of log (oxide/Al_2O_3) and log LOI versus elevation above bedrock for matrix samples within the White Channel gravel at Dago Hill.

which consists of hematite+goethite cemented matrix, contains ≈53wt.% Fe_2O_3. The K_2O/Al_2O_3 ratio is similar to values for slightly (2) altered and Bleached zone gravel matrix. The Na_2O/Al_2O_3 ratio is erratic while the MgO/Al_2O_3 ratio is increased dramatically compared to Bleached zone values, but is similar to values for slightly (2) altered gravel matrix. These trends also hold for samples from the Iron zone gravel matrix of Preido Hill (622) and Nugget Hill (908).

More significant is the trace element enrichment which occurs in the Iron zone gravel. The results for samples W-410, W-411 and 302, which are from the matrix of slightly (2) altered gravel at Dago and Trail Hills, indicate that normal background values of minor and trace elements for the matrix of primary gravel are close to as follows: <0.25wt.% TiO_2, <0.03wt.% P_2O_5, <50ppm S, <165ppm Mn, <2,740ppm Ba and <20ppm As (table 2.6). These samples were not analysed by the INAA method hence, values for Cr, Co and Sb are unavailable. Sample CN-01 from the gravel matrix of the Iron zone at Dago Hill contains over 1,500ppm As (table 2.6), approximately two orders of magnitude more As than the average value for slightly (2) altered or Bleached zone gravel matrix. In addition, extremely high concentrations of Sb (45.5ppm) and Co (110ppm) are present in CN-01. Sample 516 contains approximately 100% more Ba (6,750ppm) and P_2O_5 (0.08wt.%) relative to slightly (2) altered gravel matrix with significant Sb (1.8ppm) and Co (31ppm) present. Sample 517 contains approximately 100-200% more S (330ppm) and an order of magnitude more Mn (1,050ppm) than samples of slightly (2) altered or Bleached zone gravel matrix. High Sb (3.7ppm) and Co (63ppm) are also present in sample 517. Samples 622 and 908 from the Iron zone gravels of Preido and Nugget Hills respectively, contain orders of magnitude higher concentrations of P_2O_5, Mn, Ba, As with anomalous S and high Sb in comparison to the matrix of slightly (2) altered or Bleached zone gravel. The high concentrations of these elements in the matrix of the Iron zone gravel does not appear to be linked to an increase in the amount of placer heavy minerals at the bedrock contact. Matrix from unaltered (1) to slightly (2) altered gravel near the bedrock contact at other hills does not contain high concentrations of P_2O_5, S, Mn, Ba, As, Sb, Cr and Co. In addition, heavy mineral studies by

Gleeson (1970) and Morison (1985) show no major increases in the detrital heavies in the lower 1-2 meters of White Channel gravel at most hills. Consequently, The trace element enrichment of the Iron zone is believed to be the result of post-depositional alteration processes.

2.3.3 Clasts from the White Channel deposit

Nine rhyolite porphyry cobbles, and five cobbles of green mica schist at various stages of alteration were analysed for major, minor and trace element chemistry (tables 2.7 and 2.8). The cobbles were selected from various heights above bedrock (from Bleached and Iron zones) with a range of competences. The three rhyolite cobbles from Preido Hill (602, 604 and 608) were all obtained from within 3 meters of the bedrock contact in the Bleached zone. The cobbles are breakable {b}, yet the gravel host is moderately (3) to strongly (4) altered. The rhyolite cobbles in the White Channel gravel of Preido Hill generally are friable (both cohesive, {c} and incohesive, {d}). Four rhyolite cobbles from Dago Hill (samples 508, A-410, A-411 and A-414) were selected from the Bleached zone at various elevations above the bedrock contact and with a range of competences. The gravel host generally is strongly (4) to extremely (5) altered and the rhyolite cobbles range from friable (incohesive, {d}) to incompetent {e}. Two rhyolite cobbles were selected from extremely (5) altered Iron zone gravel (A-409 and W-401) within 2 meters of the bedrock contact at Dago Hill. The major element chemistry or oxide/Al_2O_3 ratios of the analysed cobbles appear to show no systematic changes with height above the bedrock contact. Consequently, log (oxide/Al_2O_3) ratios are plotted versus log LOI in figure 2.12. In general, increasing LOI parallels the loss of competence of these cobbles, as increased clay alteration involves an increased uptake of water. As a result, with increased LOI the K_2O/Al_2O_3 ratio decreases dramatically, while MgO/Al_2O_3 decreases to a minor degree. The Fe_2O_3/Al_2O_3 ratio increases significantly with increasing LOI, while the behaviour of the Na_2O/Al_2O_3 ratio is extremely irregular. The major element chemistry of the mica schist cobbles shows no systematic trends at all, hence it is probable that initial compositional inhomogeneities affected the results. No significant changes

Table 2.7 Whole rock chemistry of rhyolite and mica schist cobbles (<2mm size fraction) collected from the White Channel gravel at Dago Hill.

Sample	SiO_2	Al_2O_3	Fe_2O_3	MgO	CaO	Na_2O	K_2O	TiO_2	MnO	P_2O_5	LOI
Rhyolite cobbles											
HP-1[1] (bedrock, [b])	76.15	13.46	0.56	0.47	0.04	3.90	3.80	0.00	0.03	0.00	1.55
602[2] (≈2-3m, [b])	74.37	14.00	0.27	0.64	0.04	0.21	8.47	0.27	0.00	0.00	1.69
604[2] (≈1.5m, [b])	77.73	12.38	0.15	0.22	0.05	0.17	8.27	0.02	0.00	0.00	0.99
608[2] (≈1.5-2m, [b])	74.15	14.15	0.34	0.14	0.04	0.26	9.27	0.25	0.00	0.00	1.38
W-401 (≈1-1.5m, [c])	77.12	12.54	0.14	0.52	0.03	0.38	7.82	0.04	0.00	0.02	1.37
508 (≈2-3m, [c])	78.26	11.87	0.20	0.35	0.04	0.44	7.68	0.04	0.00	0.00	1.11
A-409 (≈1.5m, [d])	75.92	12.88	0.66	0.37	0.03	2.26	4.20	0.00	0.00	0.00	3.63
A-411 (≈2.5m, [d])	74.91	15.31	0.60	0.28	0.03	1.30	2.76	0.02	0.00	0.00	4.75
A-410 (≈2.5m, [e])	63.85	23.02	1.00	0.52	0.04	0.37	0.78	0.83	0.00	0.03	9.53
A-414 (≈6-7m, [e])	61.71	23.10	1.25	1.69	0.03	0.54	1.75	0.77	0.00	0.02	9.11
Mica schist cobbles											
W-415 (≈20-21m, [b])	74.88	12.40	2.36	2.15	0.02	0.17	5.23	0.28	0.02	0.00	2.48
507 (≈10-12m, [b])	76.77	12.42	1.10	0.85	0.04	0.63	6.69	0.22	0.00	0.00	1.25
406[3] (≈1.5m, [c])	76.44	12.70	0.93	0.77	0.04	4.39	3.63	0.12	0.00	0.00	0.96
506 (≈10-12m, [d])	77.97	11.79	1.43	1.00	0.03	1.64	4.29	0.25	0.00	0.00	1.57
W-405 (≈0.5m, [e])	80.88	10.76	1.12	1.07	0.02	0.79	3.21	0.18	0.00	0.00	1.94

The elevation above bedrock and the degree of competence of each cobble are in parentheses. Analyses were performed by the XRF technique (data in % oxides and LOI, LOI=loss on ignition at 1040°C, Fe_2O_3=total iron) and recalculated to 100%.
[1]Hunker Creek rhyolite porphyry. [2]Samples from Preido Hill. [3]Sample from Cripple Hill.

Table 2.8 Major oxide/Al_2O_3 ratios, LOI and trace element analyses of rhyolite and mica schist cobbles (<2mm size fraction) collected from the White Channel gravel at Dago Hill.

Sample	$\frac{Fe_2O_3}{Al_2O_3}$	$\frac{MgO}{Al_2O_3}$	$\frac{CaO}{Al_2O_3}$	$\frac{Na_2O}{Al_2O_3}$	$\frac{K_2O}{Al_2O_3}$	LOI (%)	S (ppm)	Mn (ppm)	Ba (ppm)	As (ppm)
Rhyolite cobbles										
HP-1[1] (bedrock, [b])	0.042	0.035	0.003	0.289	0.282	1.55	150	397	85	11
602[2] (≈2-3m, [b])	0.019	0.046	0.003	0.015	0.605	1.11	180	45	2,570	14
604[2] (≈1.5m, [b])	0.012	0.018	0.004	0.014	0.668	0.99	75	33	1,120	8
608[2] (≈1.5-2m, [b])	0.024	0.010	0.003	0.018	0.655	1.38	360	30	1,870	3
W-401 (≈1-1.5m, [c])	0.011	0.041	0.002	0.030	0.624	1.37	140	24	280	4
508 (≈2-3m, [c])	0.017	0.029	0.003	0.037	0.647	1.11	140	16	910	<2
A-409 (≈1.5m, [d])	0.051	0.029	0.002	0.175	0.326	3.63	90	142	140	11
A-411 (≈2.5m, [d])	0.039	0.018	0.002	0.085	0.180	4.75	70	120	127	14
A-410 (≈2.5m, [e])	0.043	0.023	0.002	0.016	0.034	9.53	140	120	1,460	7
A-414 (≈6-7m, [e])	0.054	0.073	0.001	0.023	0.076	9.11	20	108	730	10
Mica schist cobbles										
W-415 (≈20-21m, [b])	0.190	0.173	0.002	0.014	0.422	2.48	170	300	3,470	19
507 (≈10-12m, [b])	0.089	0.068	0.003	0.051	0.539	1.25	140	74	2,480	19
406[3] (≈1.5m, [c])	0.073	0.061	0.003	0.346	0.289	0.96	140	122	3,940	15
506 (≈10-12m, [d])	0.121	0.085	0.003	0.139	0.364	1.57	160	163	2,860	4
W-405 (≈0.5m, [e])	0.104	0.099	0.002	0.073	0.298	1.94	90	139	4,790	11

The elevation above bedrock and degree of competence of each cobble are in parentheses. The analyses were performed by the XRF technique with LOI in percent and trace elememts in parts per million.
[1]Hunker Creek rhyolite porphyry. [2]Samples from Preido Hill. [3]Sample from Cripple Hill.

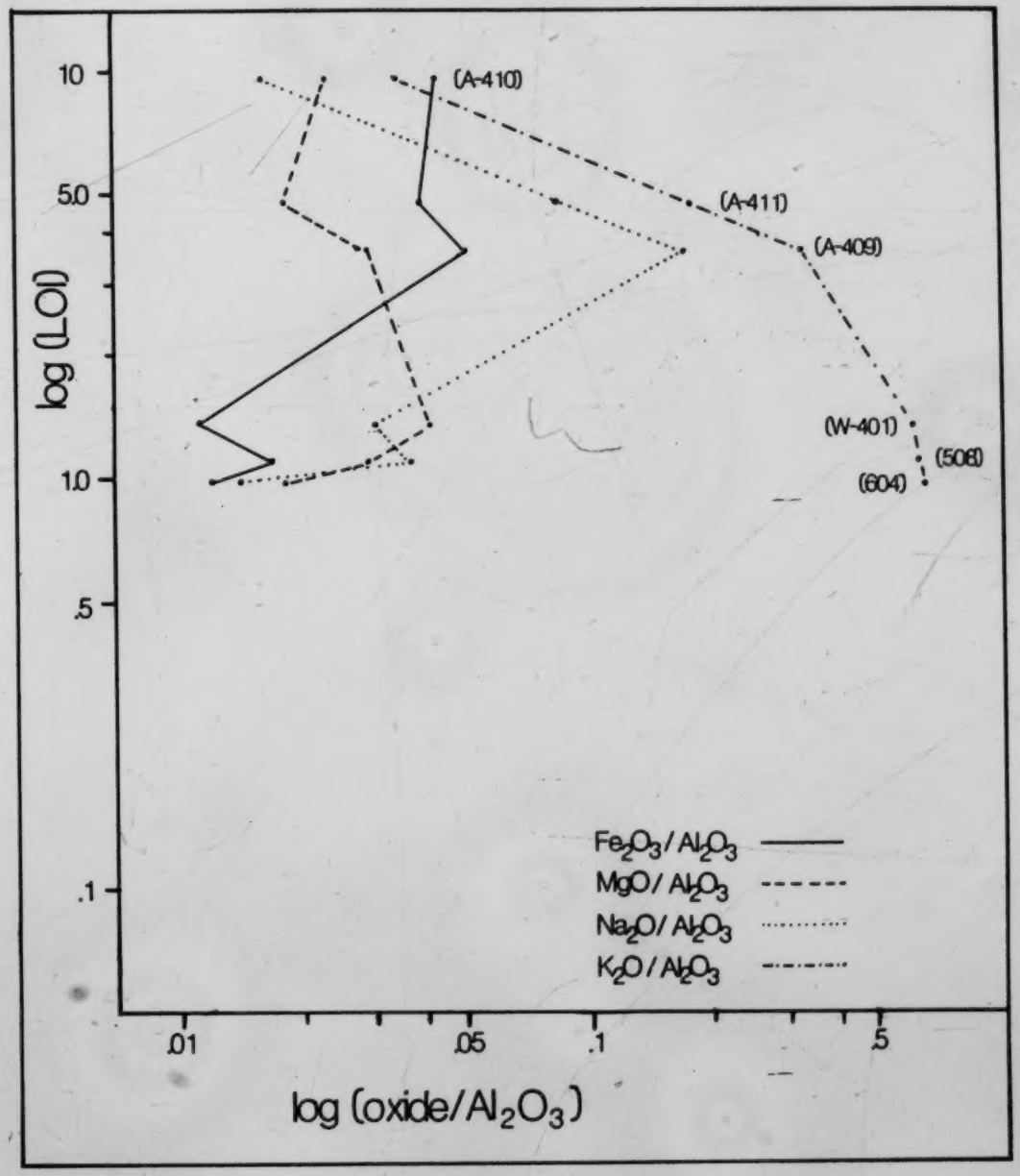

Figure 2.12 Plot of log (oxide/Al_2O_3) versus log LOI for rhyolite cobbles within the White Channel gravel.

occur in the trace element concentrations with increasing alteration (LOI) for either the rhyolite or mica schist cobbles.

2.3.4 Footwall zone

Bedrock in the Footwall zone below White Channel gravel shows depletion patterns similar to those of gravel matrix from the Bleached zone (tables 2.9 and 2.10). Green mica schist samples from Dago Hill show significant decreases in the Fe_2O_3/Al_2O_3, MgO/Al_2O_3, K_2O/Al_2O_3 ratios and an increase in LOI vertically from 8 meters to 0.5 meters below the Iron zone gravel contact (table 2.10 and figure 2.13). The Na_2O/Al_2O_3 ratio is more erratic but it also appears to decrease towards the gravel contact. The concentration of SiO_2 does not appear to have been affected to any great degree with increasing intensity of clay alteration, assuming the initial whole rock chemistry of the schist was consistent throughout the entire vertical section. The degree of competence of the mica schist decreases from breakable (b) at 8 meters depth to incompetent (e) immediately below the gravel contact. The progressive intensity of clay alteration parallels the increasing LOI values. Alteration of a diabase dike at Jackson Hill shows similar patterns to the alteration of the Dago Hill schist. All the major oxide/Al_2O_3 ratios (including CaO/Al_2O_3) decrease, while LOI increases in samples located closer to the gravel-bedrock contact (figure 2.14). Chlorite schist at Jackson Hill and graphitic-mica schist at Cripple Hill show erratic results of oxide/Al_2O_3 ratios and LOI plotted against depth below the gravel contact. In general, the oxide/Al_2O_3 ratios decrease with a progressive degree of clay alteration of bedrock on these two hills; however, this is not always the case. Initial chemical inhomogeneities or recent supergene processes may account for the variability in the oxide/Al_2O_3 patterns of bedrock on these two hills. The outcrops have been exposed for a considerable period of time (probably 50-80 years). The trace element patterns for all four types of bedrock sampled show no significant changes with increasing clay alteration (table 2.10).

Table 2.9 Whole rock chemistry of samples (<2mm size fraction) collected from bedrock below the White Channel gravel.

Sample		SiO_2	Al_2O_3	Fe_2O_3	MgO	CaO	Na_2O	K_2O	TiO_2	MnO	P_2O_5	LOI
Mica schist[1]												
515	(≈0.5m, {e})	77.84	13.59	0.86	0.80	0.03	0.90	1.73	0.35	0.00	0.02	3.84
A-417	(≈2-3m, {e})	75.44	14.06	1.21	1.26	0.03	0.01	4.46	0.08	0.00	0.00	3.42
502	(≈3-4m, {c})	77.58	12.79	1.21	1.33	0.03	0.05	4.53	0.06	0.02	0.00	2.34
503	(≈10m, {b})	78.67	11.66	1.16	1.29	0.03	2.71	3.00	0.07	0.00	0.00	1.37
Chlorite schist[2]												
105	(≈2-3m, {e})	73.33	12.38	3.42	1.86	1.57	0.86	1.40	0.66	0.04	0.02	4.44
104	(≈6-7m, {d})	58.53	19.76	4.80	4.23	0.06	0.10	6.18	1.15	0.03	0.32	4.81
103	(≈10-11m, {b})	67.03	15.11	4.79	3.49	0.06	0.65	3.90	0.84	0.04	0.25	3.82
Diabase[2]												
D-112	(≈2m, {e})	49.17	19.42	9.11	3.16	3.81	2.16	0.85	2.76	0.07	0.73	3.75
D-111	(≈3m, {d})	51.63	19.18	7.41	3.78	4.97	2.65	1.02	2.96	0.03	0.77	5.59
D-102	(≈10-15m, {b})	48.30	15.70	11.00	4.80	8.36	2.78	1.08	2.41	0.41	0.65	4.51
D-101	(≈20-25m, {b})	52.63	18.29	8.96	3.63	1.42	4.39	0.86	2.85	0.02	0.70	6.23
Graphitic mica schist[3]												
A-351	(≈0.5m, {e})	76.23	12.69	1.36	0.88	0.04	2.75	3.50	0.28	0.00	0.00	2.28
402	(≈3-4m, {c})	79.97	11.08	1.03	0.43	0.04	3.24	2.73	0.23	0.00	0.00	1.24
401	(≈7-8m, {b})	77.07	12.68	1.24	0.71	0.05	3.05	3.85	0.27	0.03	0.00	0.96

The depth below the gravel contact and degree of competence of each sample are parentheses. Analyses were performed by the XRF technique (data in % oxides and LOI, LOI=loss on ignition at 1040°C, Fe_2O_3=total iron) and recalculated to 100%.
[1]Samples from Dago Hill. [2]Samples from Jackson Hill. [3]Samples from Cripple Hill.

Table 2.10 Major oxide/Al_2O_3 ratios, LOI and trace element analyses of samples (<2mm size fraction) collected from bedrock below the White Channel gravel.

Sample	$\frac{Fe_2O_3}{Al_2O_3}$	$\frac{MgO}{Al_2O_3}$	$\frac{CaO}{Al_2O_3}$	$\frac{Na_2O}{Al_2O_3}$	$\frac{K_2O}{Al_2O_3}$	LOI (%)	S (ppm)	Mn (ppm)	Ba (ppm)	As (ppm)
Mica schist[1]										
515 (≈0.5m, {e})	0.063	0.059	0.002	0.066	0.127	3.84	270	183	3,340	5
A-417 (≈2-3m, {e})	0.086	0.090	0.002	0.001	0.317	3.42	60	205	2,840	8
502 (≈3-4m, {c})	0.095	0.104	0.002	0.004	0.354	2.34	430	250	2,220	10
503 (≈10m, {b})	0.099	0.111	0.002	0.232	0.257	1.37	140	176	2,600	7
Chlorite schist[2]										
105 (≈2-3m, {e})	0.276	0.150	0.127	0.069	0.113	4.44	360	400	3,220	9
104 (≈6-7m, {d})	0.243	0.214	0.003	0.005	0.313	4.81	2,550	590	7,480	13
103 (≈10-11m, {b})	0.317	0.231	0.004	0.043	0.258	3.82	2,700	630	5,240	28
Diabase dike[2]										
D-112 (≈2m, {e})	0.469	0.163	0.196	0.111	0.044	8.75	1,730	715	770	16
D-111 (≈3m, {d})	0.386	0.197	0.259	0.138	0.058	5.59	1,270	451	850	17
D-102 (≈10-15m, {b})	0.701	0.306	0.532	0.177	0.069	4.51	1,310	3,900	820	<2
D-101 (≈20-25m, {b})	0.490	0.198	0.078	0.240	0.047	6.23	1,910	302	1,610	9
Graphitic mica schist[3]										
A-351 (≈0.5m, {e})	0.107	0.069	0.003	0.217	0.276	2.28	125	155	340	6
402 (≈3-4m, {c})	0.092	0.039	0.004	0.292	0.246	1.24	230	83	2,540	11
401 (≈7-8m, {b})	0.098	0.056	0.004	0.241	0.304	0.96	110	92	30	6

The depth below the gravel contact and the degree of competence for each sample are in parentheses. Analyses were performed by the XRF technique with LOI in percent and trace elements in parts per million.
[1]Samples from Dago Hill. [2]Samples from Jackson Hill. [3]Samples from Cripple Hill.

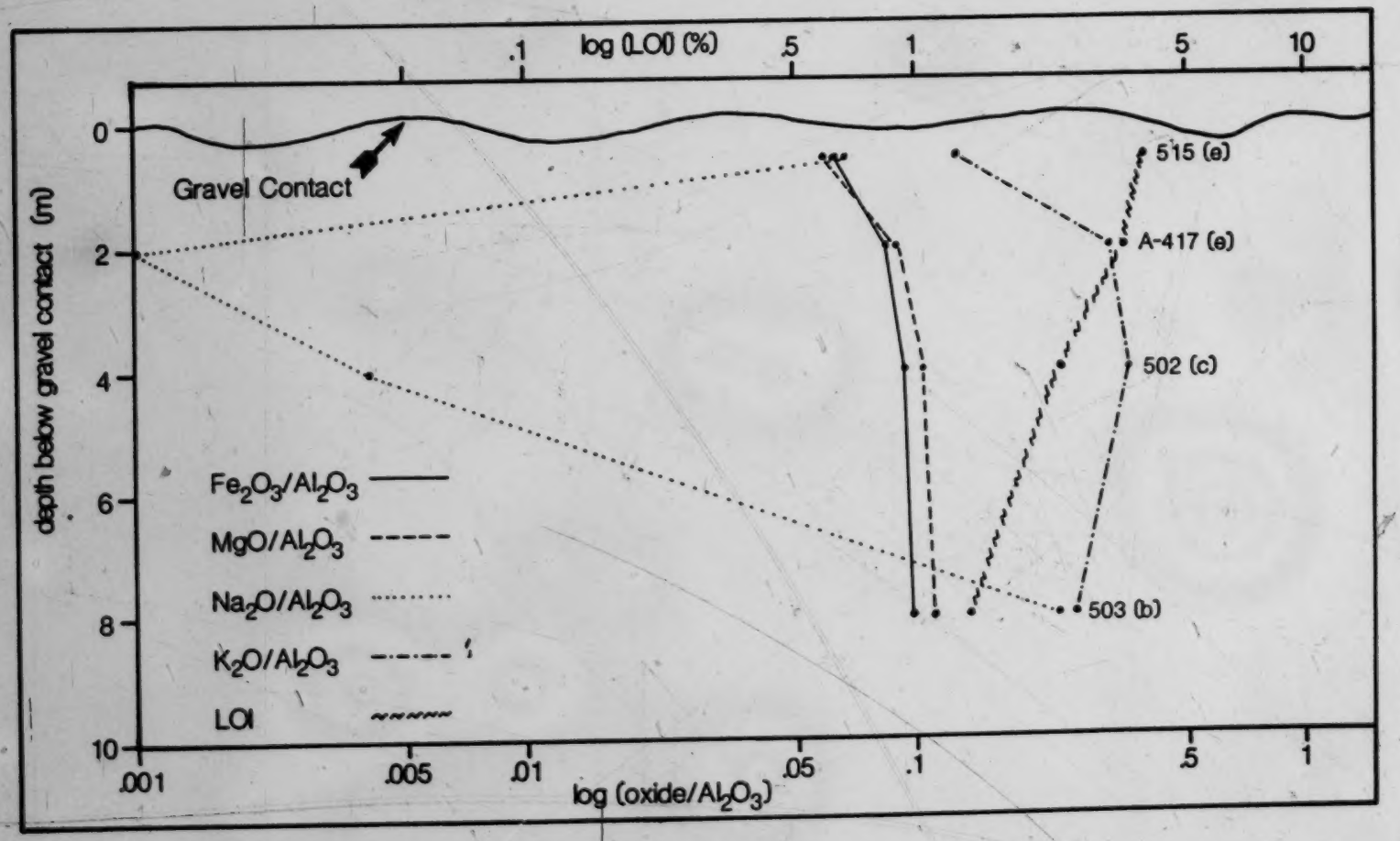

Figure 2.13 Plot of log (oxide/Al_2O_3) and log LOI versus depth below the gravel contact for samples of mica schist within the Footwall zone.

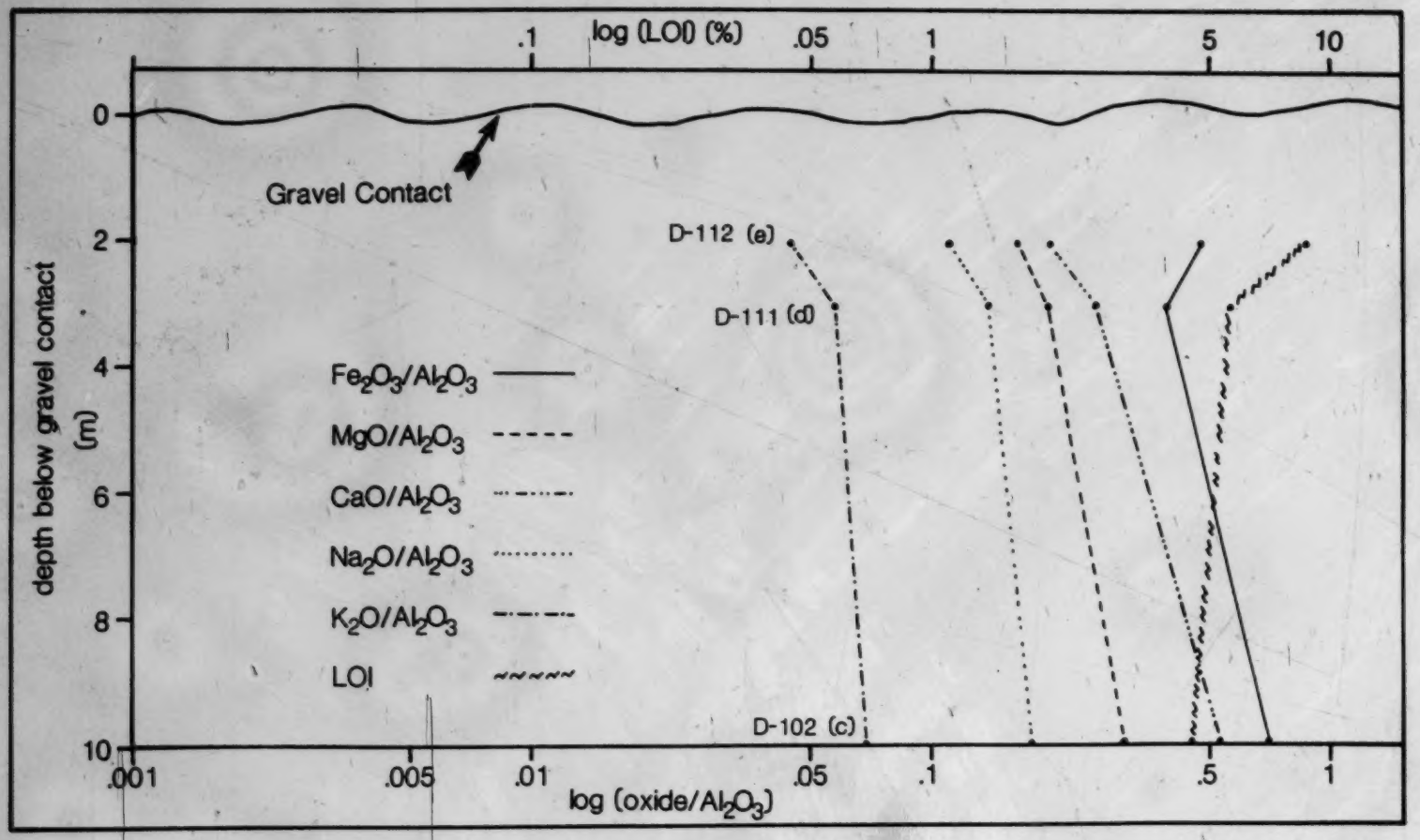

Figure 2.14 Plot of log (oxide/Al_2O_3) and log LOI versus depth below the gravel contact for samples of diabase within the Footwall zone.

2.3.5 Distribution of gold in the White Channel deposit

The greatest concentration of gold in unaltered White Channel gravel occurs in the lowest 1-2 meters of gravel and decreases dramatically upsection. Morison (1985) indicates that gold mineralization in unaltered White Channel gravel is entirely specific to certain gravelly facies. From calculations based upon the grades reported by Gleeson (1970) and McConnell (1907), unaltered White Channel gravel on Adams, Cripple, Lovett, Monte Cristo and Trail Hills usually contains concentrations of ≈0.1 to >1ppm gold in the lowest 1-2 meters of gravel (figure 2.15). In the 2-4 meter interval above bedrock the concentration of gold ranges from ≈0.02 to 0.1ppm. Above the 4 meter height, the gold values fall off to significantly less than 0.02ppm. This dramatic decrease in gold concentration up-section occurs even though the sedimentological concentrating mechanisms become more efficient (Morison, 1985). As a result, Morison (1985) suggests that the high concentration of gold at the bedrock contact are due to an increasing number of gold-bearing proximal facies, and the presence of available lode sources. He also suggests that the lode sources must have been depleted quickly with progressive erosion. At today's gold prices economic concentrations of gold occur in the lower 1-2 meters of unaltered White Channel gravel only. At present, little mining activity occurs in unaltered White Channel gravel due to the large amounts of overburden that must be removed in order to process this thin veneer of economic gravel.

In the altered White Channel gravel of Dago, Preido, Paradise and Nugget Hills the distribution of gold is not related to specific facies types. The White Channel gravel at Dago Hill was sampled for gold in a vertical section from bedrock (Iron zone gravel) through Bleached zone gravel, to primary unaltered gravel above the alteration contact (Morison, *pers. comm.*, 1986). Cubic foot samples were taken at 1 meter intervals and concentrated using a small sluice box. Visible gold was present in the concentrates throughout the entire section of altered gravel irregardless of facies type. Gold was not found in samples of unaltered gravel from above the alteration contact. Grades reported by McConnell (1907) indicate that gold values in White Channel gravel that is more than ≈4 meters above bedrock at Dago Hill are much higher than values for similar stratigraphic levels at Trail and Lovett Hills. McConnell

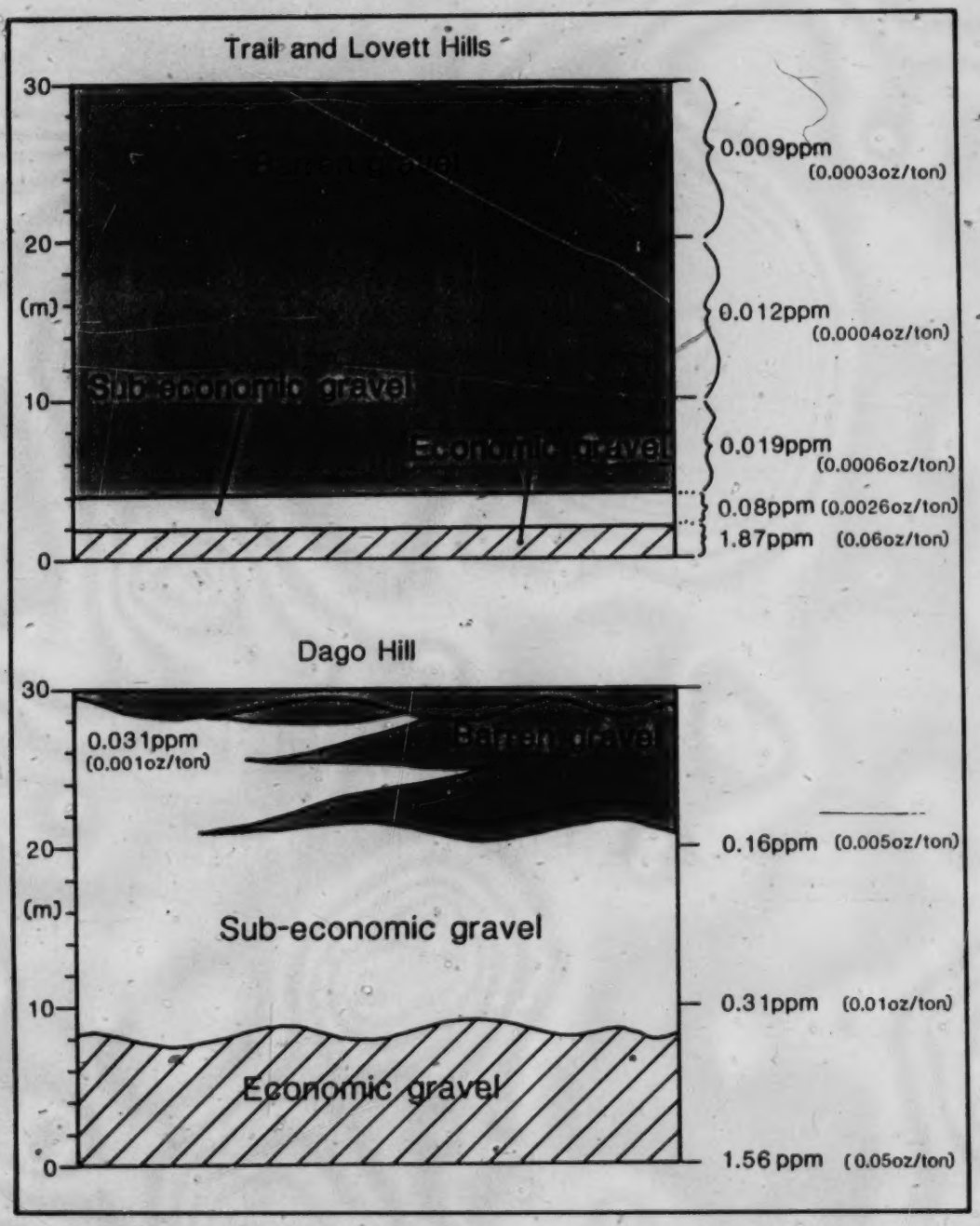

Figure 2.15 Schematic sections showing the vertical distribution of gold in the White Channel gravel of Trail and Lovett Hills versus Dago Hill. Data for Trail and Lovett Hills was calculated from the grades reported by McConnell (1907) and Gleeson (1970). Data for Dago Hill was calculated from grade estimates given by Stutter and Warmsby (*pers. comm.*, 1985).

(1907) also reports extremely high but sporadic gold values for a 5 to 6 meter section of White Channel gravel on the Paradise Hill bench just below Hester Creek. This section of gravel has been inspected and consists of extremely (5) altered gravel. Morison (1985) recovered gold from an altered debris flow of bedrock within the altered White Channel sequence at Paradise Hill. Figure 2.15 illustrates the distribution of gold in the altered White Channel gravel of Dago Hill. The concentrations were calculated from grade estimates provided by Stutter and Warmsby (*pers. comm.*, 1985) from mining at Dago Hill. The gold concentration decreases gradually from ≈1.5ppm at the bedrock contact to ≈0.3ppm at 8-10 meters above bedrock. The upper limit of gravel being actively mined occurs between 6-10 meters above bedrock. The concentration of gold in altered gravel does not fall to <0.1ppm except in gravel more than 20 meters above the bedrock contact (figure 2.15). This gradual decrease in the concentration of gold with elevation in sections of altered White Channel gravel contrasts distinctly with the normal distribution of placer gold in unaltered gravel (Morison *pers. comm.*, 1986). Consequently, as suggested by Tempelman-Kluit (1982), much of the gold in the altered White Channel gravel is interpreted to be genetically linked to alteration. Today, Large-scale gold mining in the White Channel gravel is restricted to sections of altered White Channel gravel at Dago, Nugget, Paradise and Preido Hills. The altered White Channel gravel at these hills contain large tonnages of low grade but economic gravel (*i.e.* McConnell (1907) estimated Dago Hill to have greater than 7 million cubic meters of gold-bearing gravel).

Intensely clay-altered bedrock immediately below the White Channel gravel has occasionally yielded several thousand ounces of gold from small outcrops such as the one pictured in plate 2.12 at Trail Hill (Morison *pers. comm.*, 1986). Gold was recovered from up to 10 meters depth in the clay-altered bedrock shown in plate 2.12. The gold extracted from this outcrop could not have been emplaced by placer processes. Placer gold is rarely found at more than 1-2 meters of depth in the bedrock in a normal placer environment (Morison *pers. comm.*, 1986). Consequently, the anomalous gold values in the clay-altered bedrock were either present prior to the deposition of the White Channel gravel or are genetically related to

Plate 2.12 Photograph of a section of clay-altered bedrock at Trail Hill that was processed for significant amounts of gold.

the alteration of the Footwall zone rocks.

2.4 Discussion

The observed field relationships, mineralogy and geochemistry of alteration in the White Channel deposit are compared and contrasted to the characteristics of alteration associated with many surficial deposits, epithermal precious-metal deposits and geothermal systems.

2.4.1 Summary of data

It is apparent from the results of this study that post-depositional alteration of the White Channel sediments and the underlying bedrock can be divided into three distinct zones: Bleached zone, Iron zone and altered Footwall zone. Pervasive clay alteration of the White Channel sediments is restricted to four hills along the lower left (south) bank of Hunker Creek. Intense footwall alteration is present below White Channel gravel at these four hills as well as hills at the mouth of the Klondike river and along Bonanza Creek.

In places, the Bleached zone reaches thicknesses of 20-25 meters in the White Channel sediments with a sharp, post-depositional, alteration contact separating altered sediments from the overlying unaltered sediments. The Bleached zone is characterized by extensive secondary clay mineral development (kaolinite and illite) in comparison to unaltered gravel matrix. Secondary kaolinite and illite are characterized by low crystallinities in unaltered and Bleached zone gravel matrix. Oxide/Al_2O_3 ratios such as Fe_2O_3/Al_2O_3, MgO/Al_2O_3, Na_2O/Al_2O_3 and K_2O/Al_2O_3 are depleted in the matrix of Bleached zone gravel relative to unaltered gravel matrix. Incompetent rhyolite and schist cobbles show similar patterns of oxide depletion relative to competent cobbles. The cobbles contain secondary kaolinite and minor illite, both with a range from low to high crystallinities. The rhyolite cobbles also contain abundant adularia that may be secondary and related to alteration. Minor and trace element concentrations, including TiO_2, P_2O_5, S, Mn, Ba and As, of both the Bleached zone gravel matrix and altered clasts show no significant changes in comparison to primary gravel

matrix or competent clasts.

The alteration of gravel matrix in the Iron zone at Dago Hill is characterized by the development of secondary kaolinite, illite and iron-hydroxides all with high crystallinities. Secondary hematite and gypsum are also present. The Nugget Hill Iron zone contains secondary goethite, muscovite and adularia as a cement in the gravel matrix. Values of LOI and Fe_2O_3 in the Iron zone gravel matrix at Nugget and Dago Hills are anomalously high relative to unaltered gravel matrix. Values of MgO, Na_2O and K_2O are similar to values obtained for unaltered gravel matrix. Concentrations of MnO, P_2O_5, S, Ba and As in the gravel matrix of the Iron zone are often enriched by severals orders of magnitude in comparison to the matrix of unaltered or Bleached zone sediments. In addition, high values of Sb and Co exist in the Iron zone gravel matrix.

Altered bedrock in the Footwall zone is characterized by the development of secondary kaolinite, illite and occasionally interstratified expandable minerals (illite/smectite or chlorite/smectite). Kaolinite and illite are well crystallized. Oxide concentrations of altered bedrock are decreased while LOI is increased relative to unaltered bedrock. No significant change occurs in the minor and trace element chemistry of altered bedrock in comparison to unaltered rocks. Intense clay alteration often extends 5-10 meters into the footwall rocks below the gravel contact.

2.4.2 Kaolinization related to weathering

In some respects, the intense kaolinization of all three alteration zones is similar to bauxitic or residual kaolin deposits (ball clay or soft flint clay deposits) and the lower zones of laterites developed from intense *in situ* leaching during weathering. Residual kaolin deposits and laterites in clastic sediments are found in such locations as the Tertiary sediments near Weipa, Queensland (Loughnan and Bayliss, 1961), Cretaceous-Paleocene sediments of the South Carolina and Georgia coastal plain (Harder, 1952; Hassanipak and Eslinger, 1985; Hinckley, 1963) and the Ordovician sandstones of the Châteaubriant area of Brittany (Esteoule-Choux, 1983). In all cases the kaolinized zones in these deposits form horizons in

the weathering profile that parallel surface topography and extend over vast regions. Bauxitic kaolin deposits and laterites always show a decrease in the intensity of alteration from the surface downward. This holds true whether the deposit occurs in semi-impermeable rocks such as granites or in highy permeable rocks such as sandstones and conglomerates. Kaolinization is usually accompanied by ironstone pisolites, concretions or intense iron-staining due to the formation of iron-oxides, iron-hydroxides and, occasionally, iron-carbonates during leaching. Quartz and illite are usually found in subordinate amounts, if at all. Kaolinite and the iron-rich minerals in these deposits are usually poorly crystalline with broad, ill-defined peaks on their X-ray diffraction patterns, or are amorphous yielding no X-ray patterns at all. The Hinckley (1963) crystallinity index (HCI) of the kaolinites in these deposits is usually $\leq$0.3, except in the case of the hard flint clays of Georgia (Hassanipak and Eslinger, 1985) where kaolinite exhibits an HCI$\approx$0.8. Kaolinite in the hard flint clay deposits of Georgia; however, was not formed from *in situ* weathering. The deposit has resulted from *in situ* recrystallization of kaolinite and illite that was initially transported in a fluvial system and deposited in a quiet water coastal environment (Keller, 1982 and 1968). Chemically, the kaolinized sediments of the residual deposits are characterized by strong residual enrichment of Al_2O_3, Fe_2O_3 (total iron) and TiO_2. The enrichment is caused dominantly by the removal of SiO_2 (often present in concentrations $<$20 wt.%). In addition, Mg, Ca, Na and K are also removed, usually completely.

2.4.3 Origin of kaolinization in the White Channel deposit

The field relationships and mineralogy of alteration in the White Channel sediments contrasts with the observed features of residual kaolin deposits. Bleached zone alteration in the White Channel sediments is completely isolated from the surficial weathering zone. In addition, unaltered White Channel sediments overlying altered sediments (with a sharp boundary separating the two units) are zoned in an opposite sense to kaolinized deposits formed as a result of *in situ* weathering. Alteration during surficial weathering results in a gradational change from altered to unaltered material with increasing depth below the surface

as in the sediments of the Weipa and Châteaubriant areas (Esteoule-Choux, 1983; Loughnan and Bayliss, 1961).

The mineralogy of the three alteration zones in the White Channel sediments is significantly different to the mineralogy that typically characterizes residual kaolin deposits. The gravel matrix of the Bleached zone contains abundant secondary kaolinite and illite in the clay size fraction. Quartz and muscovite are the dominant minerals in the coarser size fractions. The gravel matrix of the Iron zone consists of abundant seconday kaolinite, illite, lepidocrocite and goethite in the clay size fraction, with abundant quartz, muscovite, feldspars and hematite in the coarser size fractions. The gravel matrix of the Iron zone at Nugget Hill contains secondary goethite, muscovite and adularia. Detrital quartz and muscovite are also present in the coarser size fractions. The presence of secondary minerals such as illite, muscovite, lepidocrocite, adularia, and the apparent stability of primary detrital quartz, muscovite and feldspars in the coarser size fractions is completely atypical of residual kaolin deposits or laterites. The residual deposits generally contain minerals such as kaolinite, diaspore and gibbsite, with all the primary minerals completely removed due to alteration.

The high crystallinities exhibited by many of the secondary minerals in the matrix of altered White Channel gravel contrast with the low crystallinities of kaolinite and iron-hydroxides in most residual deposits. Kaolinite, illite and lepidocrocite from the Iron zone gravel of Dago Hill all have well-defined and extremely sharp peaks on their X-ray patterns indicating a high degree of crystallinity. The HCI of kaolinite in the $<2\mu$m size fraction of one sample analysed is $\approx$1.6, much higher than the crystallinities reported for kaolinite produced during the supergene alteration of clastic sediments of the Georgia and South Carolina coastal plain (Hassanipak and Eslinger, 1985; Hinckley, 1963; Keller, 1976a), the Châteaubriant area, Brittany (Esteoule-Choux, 1983; Keller, 1976b) and Devon, England (Vincent, 1983).

Alternate causes of alteration in the White Channel deposit may include circulating groundwater, as suggested by Tempelman-Kluit (1982), or a perched water table. In both cases the site of alteration would be confined to an interface between a permeable and

impermeable barrier, such as provided at a gravel-bedrock contact. Neither groundwater or a perched water table appear to have been responsible for alteration in the White Channel sediments due to several reasons. First, alteration in the White Channel sediments forms a zone 20-25 meters in thickness above the bedrock contact at Dago and Priedo Hills. The zone of alteration also terminates in a sharp upper contact (figures 2.6 and 2.8). This indicates that a 20-25 meter zone of gravel was saturated with a fluid for a considerable period of time. Gravitational considerations would prevent a fluid saturation zone or lateral migrational zone of 20-25 meters thickness in a such a permeable medium as gravel. In addition, no oxidation fronts due to seasonal water table fluctuations are visible and no impermeable barrier is present that would enable a perched water table to saturate the gravel at significant elevations above bedrock. Intense clay alteration of the White Channel sediments is restricted to four hills along the lower left bank of Hunker Creek. Alteration due to weathering or other related surficial processes should be present on a regional scale in such a permeable medium as the White Channel sediments; however, at least 15-20 hills in the Klondike area, which bear White Channel sediments, contain only limited alteration within the sediments. Alteration of the White Channel deposit must have occurred due to the vertical migration of an overpressurized fluid, one that exceeded its hydrostatic boiling pressure for a given temperature (White *et al.*, 1975), and which originated below the gravel-bedrock contact.

2.4.4 Origin of alteration in the White Channel deposit

Several mineralogical and geochemical features of alteration in the Iron zone gravel and Footwall zone of the White Channel deposit bear a distinct resemblance to the observed features of many precious-metal epithermal deposits and geothermal systems. These features, in association with the contrasting evidence that indicates the alteration is not related to surficial processes, seem to suggest that the alteration is hydrothermal in origin.

2.4.4.1 Mineralogical features

The gravel matrix in the Iron zone at Dago Hill contains extremely well crystallized kaolinite, illite and lepidocrocite. The high crystallinity of kaolinite (HCI=1.6) is similar to

hydrothermally produced kaolinite from Japan (Keller, 1977), Mexico (Hanson *et al.*, 1981; Keller and Hanson, 1975, 1969 and 1968), England (Bray and Spooner, 1983; Bristow, 1977; Vincent, 1983) and the United States (Droste, 1967; Schoen *et al.*, 1974; Schoen and White, 1967; Schroeder and Hayes, 1968). In addition, lepidocrocite in the Iron zone is similar to the well crystallized hydrothermal lepidocrocite that is reported to be present at the Enfield Bell mine by Birak and Hawkins (1985). As a result, the high crystallinities of these minerals in the Dago Hill Iron zone indicate that they are the products of hydrothermal processes.

The Iron zone gravel of Nugget Hill contains secondary botryoidal goethite intergrown with coarse muscovite as a cement. Goethite appears to be a direct precipitate from iron-bearing solutions as no relict sulphide textures are visible to indicate *in situ* oxidation as in a gossan. Therefore, the secondary goethite is "exotic" in origin (Blanchard, 1966), as the source of iron for the iron-rich solutions cannot be identified. The abundance of adularia in the $<2\mu m$ size fraction and absence in the coarser size fractions may indicate that it is secondary in origin. Adularia (K-feldspar) is commonly reported as a hydrothermal phase often associated with sericite (similar to muscovite) and occasionally kaolinite in hydrothermal vein deposits and upper levels of alteration halos associated with geothermal hot-spring deposits (Ashley, 1974; Berger, 1985; Bonham and Garside, 1979; Buchanan, 1981 and 1980; Masterton and Kyle, 1984; Schoen and White, 1967; Schroeter, 1984; Tingley and Berger, 1985). The mineralogy of the cemented and iron-stained gravel matrix at Nugget Hill appears to be the result of hydrothermal alteration of White Channel gravel.

Several rhyolite cobbles from within or just above the Iron zone gravel at Dago and Preido Hills contain secondary kaolinite with high crystallinity (HCI≈1.3) and adularia. The high kaolinite crystallinity is indicative of hydrothermal kaolinite as discussed previously. Relatively fresh rhyolite porphyry bedrock from the lower right bank of Hunker Creek contains abundant sanidine, orthoclase and albite but no adularia. The absence of adularia in unaltered porphyry samples may indicate that adularia in the rhyolite cobbles of altered White Channel gravel is secondary and hydrothermal in origin.

At Dago, Nugget, Paradise and Preido Hills, clay-altered Iron zone gravel directly overlies several meters of pervasively altered bedrock (Footwall zone). The gravel and bedrock were altered contemporaneously after deposition of the sediments. Clay-altered mica schist of the altered Footwall zone at Dago Hill contains abundant secondary kaolinite and illite. Randomly interstratified illite/smectite, in the $<2\mu$m size fraction, is present in samples of breakable (b) schist furthest from the gravel-bedrock contact. Samples with an increased degree of clay alteration (closer to the gravel-bedrock contact) contain kaolinite and illite as the stable secondary products in the clay size fraction. One sample (515) of incompetent (e) mica schist contained well-crystallized kaolinite (HCI≈1.03). The sample was taken from altered bedrock immediately below sample 516. Sample 516 was collected from gravel matrix of the Iron zone at Dago Hill and contains kaolinite with an HCI of ≈1.6. Interstratified expandable clay minerals and/or discrete smectite group (expandable) minerals are stable through all stages of progressive clay alteration of the footwall rocks. Incompetent (e) chlorite-mica schist from Jackson Hill contains secondary kaolinite, illite and randomly interstratified chlorite/smectite. Incompetent (e) graphitic-mica-feldspar schist from Cripple Hill contains mostly interstratified illite/smectite with minor kaolinite and illite. The expandable and interstratified expandable (illite/smectite or chlorite/smectite) clay minerals are most commonly found in well sorted fine-grained sediments (*i.e.* pelagic sediments) and the weathering environment. However, there are several occurrences of these minerals in altered wall rocks adjacent to hydrothermal veins (Horton, 1985), adjacent to massive sulphide deposits (Inoue and Utada, 1983) and in the upper levels of alteration halos associated with geothermal deposits (Eslinger and Sarin, 1973; McDowell and Elders, 1980; Steiner, 1968; Sumi, 1969).

2.4.4.2 Geochemical features

Trace element concentrations in the gravel matrix of the Iron zone at Dago, Preido and Nugget Hills are similar to the chemical signatures of many epithermal precious-metal deposits and geothermal systems. In most of these types of deposits a distinct zonation of trace elements exists usually with depth and/or temperature. The surface environment (within

100-150m depth) of active geothermal systems usually includes sinters, hot-spring pools and associated precipitates, and argillic alteration zones. The trace element content of most of these near-surface environments typically includes high levels of Au, As, Sb, Hg, Tl, Fe, Mn, Ba, Co, F, S and P (Ewers and Keays, 1979; Henley and Ellis, 1983; Weissberg *et al.*, 1979; White, 1985 and 1981). Precious-metal deposits contain a similar enrichment of these elements in veins and alteration zones formed near the paleosurface and/or at low temperatures (<200°C) (Berger, 1985; Buchanan, 1981). Similar to these environments, five samples collected from the gravel matrix of the Iron zone show significant values of up to ≈53% Fe_2O_3, ≈6.6% MnO, ≈0.73% P_2O_5, ≈490ppm S, ≈15,900ppm Ba and ≈1,560ppm As. These values generally are an order of magnitude greater than the background values for either unaltered White Channel gravel, or normal clastic sandstones (Turekian and Wedepohl, 1961). High values of Sb (≈46ppm) and Co (≈110ppm) in the matrix of the Iron zone gravel also exceed the values reported by Turekian and Wedepohl (1961) by orders of magnitude; however, no samples of primary White Channel gravel were analysed by INAA, hence background values for these elements are unavailable. The elements Hg and Tl were not available using the INAA method. Most of the other major element concentrations of altered White Channel gravel matrix are unchanged in comparison to unaltered White Channel gravel. This indicates that the increased concentrations of these trace elements in the Iron zone are the result of addition to White Channel gravel during alteration rather than enrichment due to severe leaching of other elements. Three samples (302, W-410 and W-411) of unaltered (1) to slightly (2) altered White Channel gravel were analysed for Fe, Mn, P, S, Ba and As, and contained levels several orders of magnitude lower than the highest concentrations recorded for the Iron zone gravel matrix. Although two samples (W-410 and W-411) were from 22 meters above bedrock at Dago Hill, sample 302 was taken from gold-bearing (sub-economic) placer gravel within 1-2 meters of bedrock at Trail Hill. This sample showed no evidence of chemical enrichment due to increased detrital heavies within the lower 1-2 meters of White Channel gravel. Consequently, chemical enrichment of the gravel matrix in the Iron zone is associated with post-depositional alteration rather than primary fluvial processes. The

similarities between the Iron zone trace element suite, and the trace elements commomly associated with epithermal precious-metal deposits or geothermal systems, lends further support to a hydrothermal origin for alteration in the White Channel deposit.

In summary, the field relationships, mineralogy and geochemistry of alteration in the White Channel deposit contrast distinctly with the characteristics of most residual kaolin deposits or other related surficial deposits. However, the mineralogical and geochemical signatures of altered Iron zone gravel and the underlying Footwall zone rocks bear a distinct resemblance to the characteristics of epithermal precious-metal deposits and geothermal systems. As a result, the alteration of the White Channel deposit is interpreted to have been the result of near-surface hydrothermal activity.

3. VEINS IN ALTERED FOOTWALL ROCKS

In the Klondike district altered Footwall rocks below the White Channel gravel contain thin, post-metamorphic quartz and/or Fe-carbonate±quartz veins. These veins can be divided into three types (1, 2 and 3) based upon the mineralogy and texture of the veins. These veins are distinct in comparison to typical mesothermal and/or metamorphic veins in the Klondike Schist, and carbonate veins associated with volcanics in the Hunker Creek area. The following chapter details the field relationships, mineralogy, textures and geochemistry of types 1, 2 and 3 veins, and the evidence that indicates that these veins are associated with the alteration of the Footwall zone rocks. In addition, these veins are compared and contrasted to mesothermal and/or metamorphic veins in the Klondike Schist, carbonate veins associated with the Hunker Creek area volcanics, and veins associated with epithermal precious-metal deposits.

3.1 Field Relationships

3.1.1 Veins associated with Footwall zone alteration

Three types of veins can be recognized that are associated with intensely clay-altered Footwall zone rocks below the White Channel sediments. Type 1 veins are composed of medium-grained quartz to cryptocrystalline quartz (chalcedony). The veins are usually <10-20cm in thickness and lack intense iron-staining. Type 1 veins are often banded with vuggy, cockscomb and crustiform textures. The presence of euhedral quartz crystals and vugs are common as shown in a sample from Paradise Hill in plate 3.13. Type 2 veins contain abundant Fe-carbonate (usually siderite) with variable amounts of quartz. The veins are usually <1-2cm in thickness and often highly iron-stained. Type 2 veins often exhibit botryoidal textures and associated "concretionary-like" nodules (plates 3.14 and 3.15). A third type of vein, which is minor in occurrence, consists of thin (<1-2cm thick) microfractures filled with either clay minerals±goethite or amorphous silicate phases±goethite. All three types of veins are associated with pervasively clay-altered bedrock in the Footwall zone. The veins cross-cut all metamorphic and deformational fabrics in the Klondike Schist and

Plate 3.13 Photograph of a type 1 quartz vein with open-space filled crystals. Note the bleached and clay-altered bedrock incorporated in the vein.

Plate 3.14 Photograph of a siderite+quartz concretion hosted in clay-altered mica schist at Jackson Hill. The concretion has cemented and partially replaced the schist.

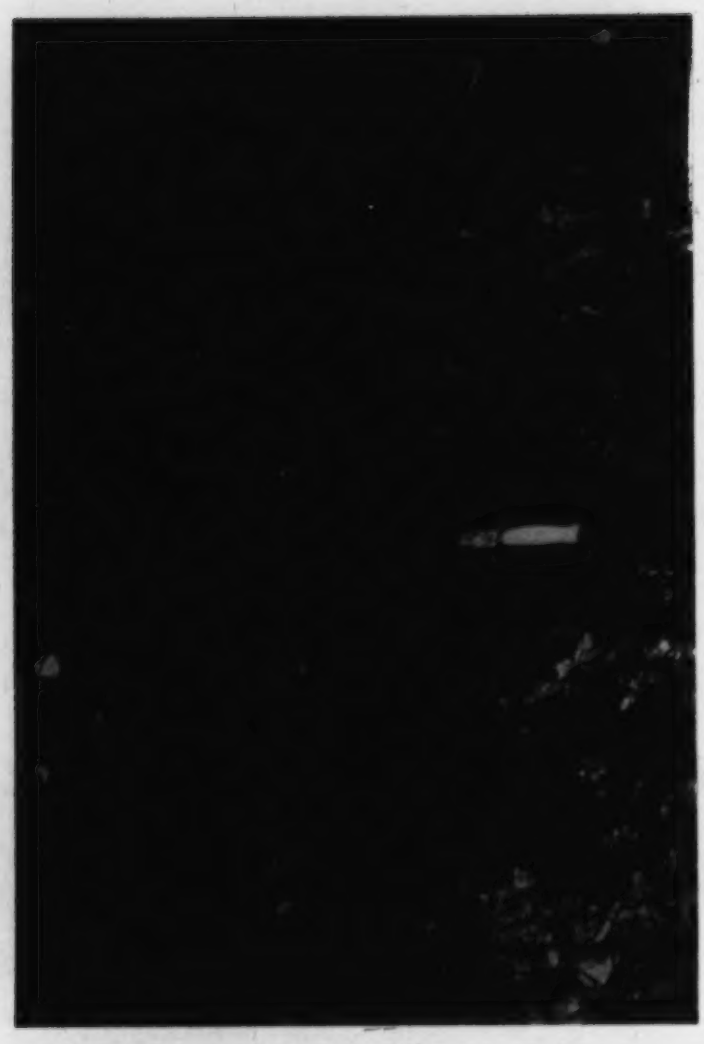

Plate 3.15 Photograph of a siderite + quartz + gypsum concretion hosted in clay-altered diabase at Jackson Hill. The concretion has cemented and partially replaced the diabase, and is associated with type 2 veins.

associated units.

The morphologies and field relationships of types 1 and 2 veins with respect to the clay-altered Footwall zone rocks are important indicators of the relationship between alteration and veining. Morphologically, types 1 and 2 veins typically exhibit delicate patterns of veining, such as the horsetail pattern shown in plate 3.16, where the veins are hosted by a completely altered diabase dike. Alteration of the footwall rocks in this area extends approximately 10 meters below the gravel contact. The diabase had to have been altered after deposition of the gravel or the clay zone would have been completely eroded during the deposition of the gravel. Folding and fractures that are visible in the unaltered diabase lower in the section have been completely obliterated by clay alteration in the Footwall zone. The obliteration of the folds and fractures has occurred in response to volume changes during intense clay alteration. Although the rocks are completely unrecognizeable after alteration, the veins in the altered dike, which is only 2-3 meters below the gravel contact, are clearly visible and appear to be unaffected by the intense clay alteration (plate 3.16). Types 1 and 2 veins are intimately associated with alteration as there is a good correlation of increasing degree of alteration with increasing density of vein occurrence. In addition, types 1 and 2 veins often appear to have incorporated and cemented fragments of partially bleached and clay-altered bedrock as shown in plate 3.13, or iron-stained and clay-altered bedrock as shown in plates 3.15 and 3.17. These types of field relationships indicate that the veins were emplaced during intense clay alteration of the Footwall zone rocks below the White Channel gravel.

Types 1 and 2 veins have been observed in clay-altered footwall rocks at most hills investigated along lower Hunker and lower Bonanza Creeks. At each hill the vein occurrences are usually rare, with erratic distribution and extent. The best occurrences of type 1 quartz veins are located on the southeast portion of the Trail Hill bedrock bench near Trail Gulch and the notheast corner of the Paradise Hill bench near Hester Creek. Type 1 quartz veins have also been observed and sampled in the altered bedrock of Dago, Jackson and Nugget Hills. Type 1 quartz veins at Paradise Hill are associated with a small zone of silicification in a clay-altered serpentinite. Both the quartz veins and silicification appear to have occurred

Plate 3.16 Photograph of type 2 veins showing a horsetail veining pattern in clay-altered diabase. This outcrop of clay-altered bedrock is only 1-2 meters below the gravel contact at Jackson Hill.

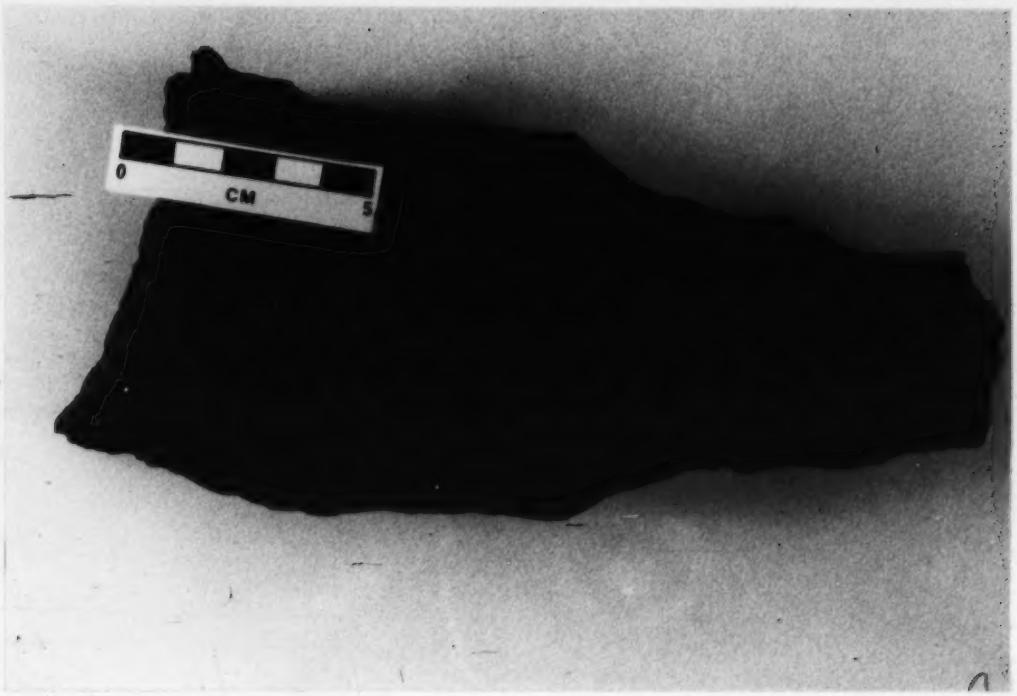

Plate 3.17 Photograph of thin, type 1 quartz veins in iron-stained and clay-altered graphitic schist from Nugget Hill.

during clay alteration of the serpentinite. Iron-stained type 2 veins are present in several areas of altered schist and diabase at Jackson Hill. Nodules of siderite-replaced bedrock are also abundant at Jackson Hill. Type 2 veins and associated nodules have also been observed in the altered footwall rocks of Dago, Paradise, Nugget and Trail Hill benches. Type 3 veins, consisting of clay minerals or amorphous silicate phases, are restricted to altered footwall rocks at Dago, Nugget and Trail Hills. These veins are very limited in their distribution at these hills. Perhaps more importantly type 3 veins are very similar in appearance and consequently may be related to microfractures (shear planes?) filled with clay minerals (and amorphous phases) in the clay-altered White Channel gravel of Dago and Nugget Hills (plate 3.18). However, this relationship is open to question.

3.1.2 Mesothermal, metamorphic and carbonate veins

Mesothermal and metamorphic quartz veins are common in the Footwall zone; however, they are easily distinguished from the veins related to alteration. The mesothermal quartz veins usually cross-cut the dominant foliation and layering within the Klondike Schist and associated units. In contrast to type 1 veins, they are commonly greater than 20cm in thickness and they are usually folded in large scale structures. In addition, the quartz is much coarser-grained and vugs, cockscomb, crustiform and botryoidal textures are rare. These veins do not increase in frequency with increasing degree of alteration of the host rocks.

The metamorphic quartz veins are easily recognized as they are present in the Klondike Schist as distinct bands of quartz completely concordant with the dominant foliation. The bands often pinch and swell similar to boudinage structure. The veins contain metamorphic mica and exhibit recrystallization textures, with thicknesses ranging from centimeters to meters.

Abundant carbonate veins are present in the Hunker Creek area. These veins contrast with the type 2 siderite±quartz veins as they have not been observed in altered Footwall zone rocks below the White Channel gravel. In addition, these veins are commonly greater than 20cm in thickness and they contain little siderite. Generally, these carbonate veins are spatially

Plate 3.18 Photograph of a microfracture in the Bleached zone gravel of Nugget Hill that is filled with clay minerals (and amorphous silicates?).

associated with volcanics in the Hunker Creek area.

3.2 Mineralogy And Textures

3.2.1 Veins associated with Footwall zone alteration

Each of the three vein types associated with altered footwall rocks can be distinguished based upon their mineralogy and textures. During the summers of 1983-85 approximately 150 samples of veins and associated wall rocks were collected. The samples are listed with brief descriptions and comments in appendix 5.2. The mineralogy of all samples used for fluid inclusion and/or chemical analysis was determined by X-ray diffraction and petrography.

Type 1 veins consist dominantly of medium-grained to cryptocrystalline quartz (chalcedony) with minor to trace quantities of Fe-carbonate, goethite, kaolinite, dickite, illite, smectite, gypsum, hematite, magnetite and pyrite (plate 3.19). Petrographically, the quartz is subhedral to euhedral with straight extinction and no evidence of strain. Visible growth lines are often present especially at the base of each crystal. Often associated with the quartz is extremely well crystallized kaolinite and/or dickite. Both kaolinite and dickite exhibit crystallinities comparable to or higher than that of kaolinite in the Iron zone gravel of Dago Hill. Kaolinite from sample DG-11 has an HCI ≈1.3. Secondary dickite, in sample DG-2, occurs between bands of metamorphic quartz. In addition, dickite is present as a pure and compact lining along the walls of the fracture that hosts the vein sampled in DG-2. In both cases the strong and sharp 110, $11\bar{2}$, 022 and all the 00*l* peaks on the diffractogram indicate that the dickite is highly crystalline. Typically, type 1 veins are vuggy, with euhedral dogtooth quartz, banding, cockscomb and cockade textures. The veins occasionally show crustiform growths with several generations of quartz and abundant vugs (plate 3.13). The veins are usually 2-3cm in thickness; however, quartz veins associated with wall rock silicification at Paradise Hill reach a thickness of 10-20cm. In addition, evidence of minor brecciation is present in the type 1 veins at Paradise Hill, as fragments of partially bleached and clay-altered

Plate 3.19 Photograph of a type 1 quartz vein with banded chalcedony along the margins of the vein.

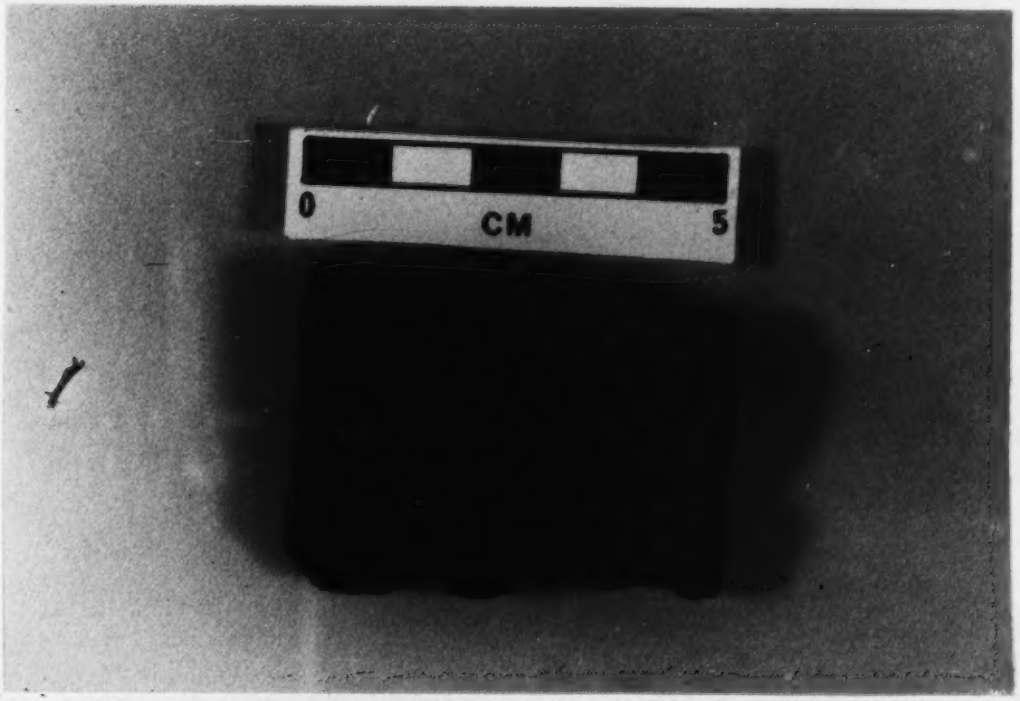

Plate 3.20 Photograph of a concretion related to type 2 siderite+quartz veins with euhedral quartz protruding into cavities of the concretion.

serpentinite have been incorporated into the quartz veins (cockade structure, plate 3.13).

Type 2 veins consist of siderite and variable amounts of quartz, with minor to trace quantities of ankerite, calcite, goethite, hematite, pyrite, gypsum and clay minerals. Generally, the siderite is extremely fine-grained and granular; however, small rhombs (0.2-0.5mm in length) of siderite and other carbonates can be seen in open spaces especially in the associated nodules. Quartz is usually minor and is found intergrown with siderite or lining open spaces as euhedral crystal aggregates (plate 3.20). Gypsum rosettes on the order of 1-2cm in diameter occasionally are present. Fe-staining is always intense causing difficulty in identification of minerals in the type 2 veins without the use of X-ray diffraction techniques. Texturally, type 2 veins exhibit botryoidal and concretionary structures. Concretion-like nodules are often associated with type 2 veins (plates 3.14 and 3.15). The nodules are usually composed of siderite which appears to have cemented and replaced clay-altered bedrock. Type 2 veins are generally <1-2cm in thickness; however, several of the siderite nodules attain thicknesses of 10-20cm.

The third type of vein (type 3) consists of microfractures filled with smectite (or interstratified illite/smectite) and goethite, or amorphous silicate phases (phases with no X-ray diffractogram pattern) and goethite. Trace amounts of kaolinite, illite and quartz have been detected in a few of the samples; however, it is unknown whether these minerals represent contamination from altered wall rocks or whether they are primary vein phases. Veins of this type at Trail Hill are 1-2cm thick. The veins at Trail Hill are composed dominantly of an amorphous phase that occurs in fibrous aggregates with low birefringence and a hardness of approximately 4-5 on Moh's hardness scale. The phase appears to be similar to the silicate named lussatite, a variety of opal (Kerr, 1974). Similar veins at Dago Hill are 1-2cm in thickness and composed dominantly of clay minerals and goethite with the vein material being very soft (<1 on Moh's hardness scale). X-ray diffractograms of the Dago Hill samples show only small quantities of clay minerals and goethite present indicating that amorphous phases are present. The softness of the material may indicate that the dominant phase is a poorly crystallized "sheet-like" silicate.

3.2.2 Mesothermal, metamorphic and carbonate veins

Mesothermal and/or metamorphic veins in the Klondike Schist are composed dominantly of quartz with minor to trace quantities of feldspar, muscovite, carbonate, apatite, zoisite, tourmaline, rutile, ilmentite, magnetite, pyrite, chalcopyrite, galena and sphalerite. The veins contain quartz which is usually more coarsely crystalline than quartz in the veins related to alteration. In addition, the quartz is usually anhedral to subhedral and shows weak to strong evidence of strain (undulatory extinction). Quartz grains from these veins often show triple point junctions, with rare vugs. Micas and chlorites usually show evidence of foliation or lineation and quartz is often segragated into distinct bands parallel to the foliation or lineation. The veins range from several meters in thickness (as at the Mitchell and Lone Star claims) to centimeters in thickness.

Veins hosted or associated with the Hunker Creek rhyolite porphyry are composed dominantly of carbonates including ankerite, dolomite, magnesite and calcite. Other phases present include minor to trace quantities of quartz, barite, fluorite, muscovite, Cr-mica (fuchsite), goethite and hematite with various unidentified opaque minerals. The carbonates range from fine-grained and granular to coarse-grained (5-10mm) euhedral rhombs. The veins commonly exhibit botryoidal and cockscomb textures with occasional cockade structures where wall rock has been incorporated into the veins. Euhedral carbonate crystals are common with paragenetically late quartz (minor quantities) occasionally lining open spaces. The veins are often slightly iron-stained and range from several meters thick (as at the Unexpected claims) to several centimeters thick.

3.3 Fluid Inclusions

3.3.1 Petrography

Petrographically, the veins associated with altered Footwall zone rocks, mesothermal and/or metamorphic quartz veins, and the carbonate veins associated with volcanics all contain distinct and unique sets of fluid inclusions. Approximately 50 samples of quartz and

carbonate from these veins were examined by thin-section before microthermometric work was carried out on representative samples.

3.3.1.1 Veins associated with Footwall zone alteration

Quartz from type 1 veins in altered footwall rocks contains aqueous fluid inclusions only. Primary inclusions usually exhibit either round or negative crystal shapes. Tabular and irregular shaped primary inclusions are often present. In general, the inclusions are small, usually ranging from <1 to 15μm, with an average diameter of 5-8μm. Primary aqueous inclusions contain one or two phases with one phase inclusions predominating. The two phase inclusions show very high liquid (L)/vapour (V) ratios with the vapour content $\leq$1-2% (plate 3.21). The L/V ratios of the two phase aqueous fluid inclusions are relatively consistent in each quartz grain within a sample and between samples from a vein. Occasionally, a quartz grain contains several inclusions with variable L/V filling ratios; however, these are rare. Liquid CO_2 or daughter crystals (salts) were not observed in any of the samples of type 1 quartz veins. Small secondary inclusions are common, usually occurring in linear arrays that often cross-cut grain boundaries. In some cases large irregular secondary inclusions are present. All of the secondary inclusions are one or two phase aqueous inclusions which in most cases are indistinguishable from the primary inclusions.

Quartz from type 2 siderite+quartz veins contains fluid inclusions with identical characteristics to the fluid inclusions of type 1 quartz veins. All the inclusions are one or two phase aqueous inclusions with no evidence of liquid CO_2 or daughter crystals. The L/V ratios of the two phase aqueous inclusions are generally high with $\leq$1-2% vapour.

3.3.1.2 Mesothermal, metamorphic and carbonate veins

Quartz from mesothermal and/or metamorphic veins contains primary fluid inclusions which range from dominantly aqueous to dominantly CO_2-rich. The primary inclusions from these types of veins are usually regular shaped (round or negative crystal shape) and often large, ranging from 5 to 50μm in diameter, commonly with averages of 10-20μm. The aqueous inclusions contain moderate L/V ratios ranging from $\approx$5 to 25% vapour with an

Plate 3.21 Photomicrograph of a 2 phase aqueous inclusion with a high L/V ratio from a type 1 quartz vein.

average of ≈10-15% vapour (plate 3.22). In samples that contain dominantly aqueous inclusions the filling ratios of the inclusions are usually very consistent. However, the few CO_2-rich inclusions present often show a wide range in the degree of filling. Compositionally, the inclusions range from almost pure CO_2 to either two or three phase inclusions, that range from CO_2-rich (plate 3.23) to CO_2-poor. Quartz from the mesothermal and/or metamorphic veins usually contains both aqueous inclusions and a variety of CO_2-rich inclusions. The dominant inclusion type varies from sample to sample; however, at least a few CO_2-rich inclusions usually are present in all the mesothermal and/or metamorphic quartz samples. Secondary inclusions in these veins are dominantly two phase aqueous inclusions with similar or higher L/V ratios than the primary aqueous inclusions. They are easily recognized as they are usually smaller than the primary inclusions and they are often arranged in planar arrays that cross-cut grain boundaries.

Ankerite, dolomite, calcite and magnesite from the carbonate veins associated with the Hunker Creek rhyolite porphyry or shear and fault zones in the Klondike Schist contain dominantly aqueous fluid inclusions. Primary inclusions usually show tabular, tubular or negative crystal shapes that range from 1-2μm to 50μm in length. The inclusions are usually very regular in shape and are oriented parallel to cleavage directions of the carbonate host. The aqueous inclusions are dominantly two phase with consistent L/V ratios throughout each sample ranging from ≈2 to 15% vapour, with an average of ≈5-10% vapour phase. No CO_2 or daughter crystals were observed in any of the carbonate samples. The secondary inclusions are generally small (<2-3μm) with similar L/V ratios to the primary inclusions.

3.3.2 Microthermometry

Heating measurements were completed on approximately 70 primary inclusions from 14 samples in order to provide information on the density and temperature of the fluid responsible for the deposition of each vein type. Microthermometric measurements were conducted on polished chips ranging from 0.2 to 0.5mm in thickness depending upon the clarity of each sample. The homogenization and melting temperatures were obtained on a

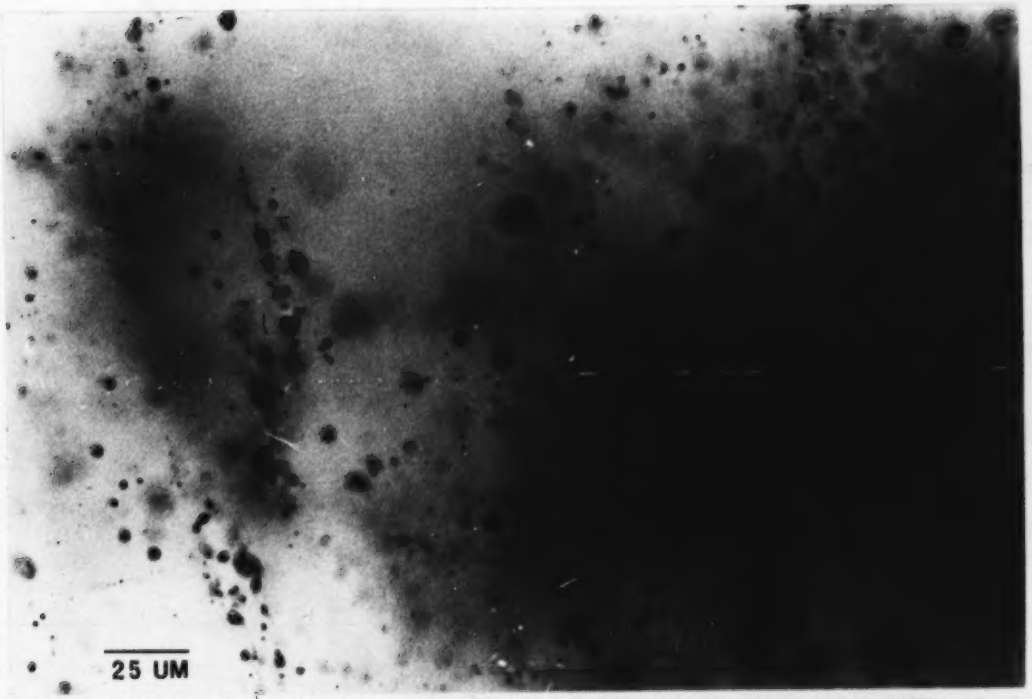

Plate 3.22 Photomicrograph of a 2 phase aqueous inclusion with a moderate L/V ratio in quartz from a mesothermal/metamorphic vein.

Plate 3.23 Photomicrograph of 2 phase CO_2-rich inclusions with ≃75-85% CO_2, in quartz from a mesothermal/metamorphic vein.

Chaixmeca heating- and cooling-stage (Poty *et al.*, 1976) attached to an Ortholux II Leitz microscope. The procedure and Chaixmeca apparatus at the University of Alberta are described in more detail by English (1981) and Fluet (1986). For extensive reviews of the methodology and applications of fluid inclusion analysis the reader is referred to Hollister and Crawford (1981), and Roedder (1984).

Homogenization temperatures of all the aqueous dominated inclusions with high L/V ratios were obtained first. The aqueous inclusions were then cooled to ≈-120°C in order to freeze the inclusions. The melting temperatures of ice and clathrates were then determined upon heating the frozen inclusions to room temperature. This order was employed as the cavities of the fluid inclusions with high L/V ratios can be stretched during the freezing stage of the procedure due to the volume expansion of ice. Stretching of the inclusion cavity would result in decreased L/V ratios and increased homogenization temperatures, if homogenization was performed following the freezing and melting stage. Little microthermometric data were obtained on the CO_2-rich inclusions from the mesothermal and/or metamorphic quartz veins as characterizing their microthermometric properties was beyond the scope of this study. CO_2-rich inclusions that were studied were frozen first, heated to room temperature and then homogenized. This order is generally used for CO_2-rich inclusions as homogenization is difficult to reach due to decrepitation of the inclusions (Roedder, 1984). Attempts were made, where applicable, to observe the following phase transformations:

Th = homogenization temperature of the aqueous phases
$Thco_2$ = homogenization temperature of CO_2
$Tmco_2$ = melting temperature of CO_2
Te = ice eutectic temperature
Tm-ice = melting temperature of ice
Tm-clath = melting temperature of H_2O-CO_2 clathrate

All measurements were usually repeated twice to check for reproducibility. Reasonably sized aqueous and CO_2-rich inclusions (>5-6μm in diameter) had homogenization and melting temperatures that were generally reproducible to within ±0.1°C.

Calibration of the thermometric apparatus was completed using solid melting point standards and distilled water. The standards used and calibration procedure are described by

English (1981) and Fluet (1986). The calibration curve indicates that the amount of necessary calibration increases with increasing temperature (figure 3.16, modified after Fluet, 1986). At 0°C the average temperature correction is ≃-0.7°C, at 100°C it is ≃-2°C and at 300°C it is ≃-4°C.

3.3.2.1 Veins associated with Footwall zone alteration

Seven samples of quartz from type 1 veins and 1 sample from a type 2 vein, which are all associated with the alteration of the Footwall zone rocks below the White Channel deposit, were used for microthermometric analysis. All the samples contained aqueous inclusions only, with the two phase inclusions possessing high L/V ratios ($\leq$1-2% vapour) and no visible CO_2. Homogenization temperatures ranged from ≃90°C to ≃160°C with an average Th of ≃122°C (table 3.11 and figure 3.17). One exception, sample DG-1, exhibits a range of homogenization temperatures from 157°C to 295°C. Homogenization in all the inclusions of type 1 quartz occurred to the liquid phase.

The average homogenization temperature (≃122°C) indicates the average density of the inclusion and the density isochore along which the fluid inclusion was trapped (Hollister and Crawford, 1981; Roedder, 1984). The maximum depth of formation of these veins is estimated to be no greater than 100-150 meters below the surface from paleoenvironmental reconstruction of the White Channel deposit (Morison, 1985). At 100-150 meters of depth, the maximum lithostatic pressure is approximately 35-40 bars (Hedenquist and Henley, 1985a). The maximum hydrostatic pressure for 100-150 meters of depth will be even less. As a result, the maximum pressure correction for Th to get the actual temperature of the fluid at the time of quartz deposition is $\leq$5°C (assuming the fluid contains minor salt). This indicates that the fluids responsible for the deposition of vein quartz and the surrounding clay alteration were approximately 120°C to 130°C.

One sample containing several small euhedral quartz crystals (sample 101) was taken from a siderite concretion associated with type 2 veins on Jackson Hill. The Th data for the aqueous inclusions (table 3.11) is similar to the range of Th measurements obtained for the seven samples of type 1 quartz veins. This indicates that the type 2 siderite+quartz veins were

Table 3.11 Homogenization and melting temperatures of fluid inclusions in selected samples of quartz and carbonate from types 1, 2, mesothermal/metamorphic and carbonate veins in the Klondike district.

Sample		Th(°C)	Tm-ice(°C)	Tm-clath(°C)	$Tmco_2$(°C)	Wt.% NaCl
Type 1 Veins						
109	(quartz)	124.8(L)	+1.2[1]	-	-	?
(Jackson Hill)		113.8(L)	+2.1[1]	-	-	?
		-	-0.1	-	-	0.2%
		103.0(L)	?[1]	-	-	?
		117.2(L)	-0.2	-	-	0.4%
TR-2	(quartz)	132.2(L)	+0.5[1]	-	-	?
(Trail Hill)		115.9(L)	-0.7	-	-	1.2%
		113.2(L)	0.0	-	-	0%
DG-1	(quartz)	163.7(L)	-	-	-	-
(Dago Hill)		167.2(L)	-2.7	-	-	4.5%
		186.9(L)	-2.2	-	-	3.7%
		210.4(L)	-1.8	-	-	3.1%
		295.0(L)	-2.5	-	-	4.2%
		215.6(L)	-2.8	-	-	4.6%
		221.0(L)	-	-	-	-
		157.6(L)	-1.6	-	-	2.7%
DG-2[2]	(quartz)	145.2(L)	-1.4	-	-	2.4%
(Dago Hill)		-	-2.0	-	-	3.4%
		-	-1.4	-	-	2.4%
		92.3(L)	+11.7[1]	-	-	?
		110.8(L)	-2.6	-	-	4.3%
		-	-2.3	-	-	3.9%
		117.3(L)	+13.9[1]	-	-	?
PD-8502	(quartz)	115.6(L)	-1.5	-	-	2.6%
(Paradise Hill)		102.4(L)	+1.0[1]	-	-	?
		122.7(L)	-0.1	-	-	0.2%
		131.7(L)	+0.4[1]	-	-	?
		132.5(L)	-0.3	-	-	0.5%
		135.7(L)	-0.3	-	-	0.5%
PD-8511	(quartz)	150.4(L)	+10.0[1]	-	-	?
(Paradise Hill)		109.5(L)	+4.9[1]	-	-	?
		128.7(L)	+5.5[1]	-	-	?
		117.7(L)	+3.3[1]	-	-	?
		108.2(L)	+5.3[1]	-	-	?
		111.2(L)	-0.8	-	-	1.4%
		117.6(L)	-0.9	-	-	1.6%
		150.7(L)	+11.0[1]	-	-	?
PD-8512	(quartz)	136.4(L)	?[1]	-	-	?

(Paradise Hill)		106.0(L)	-0.8	-	-	1.4%
		113.2(L)	-0.9	-	-	1.6%
Type 2 Vein						
101	(quartz)	128.7(L)	+1.9[1]	-	-	?
(Jackson Hill)		-	-1.1	-	-	1.9%
		153.4(L)	-1.7	-	-	2.9%
Mesothermal Or Metamorphic Veins						
DG-2[2]	(quartz)	241.7(L)	-1.9	-	-	3.2%
(Dago Hill)		238.8(L)	-3.0	-	-	4.9%
521	(quartz)	315.8(L)	-4 to -3.4?	-0.5?	-	?
(Dago Hill)		198.4(L)	-	+3.9	-	10.7%
		290.0(L)	-	+2.9	-	12.1%
		>371.6(V)	-	+6.1	-58.9	7.3%
TR-1	(quartz)	285.6(L)	-4.8	-	-	7.6%
(Trail Hill)						
TH-2	(quartz)	190.1(L)	-3.3	-	-	5.4%
(Trail Hill)		216.8(L)	-2.0	-	-	3.4%
		223.1(L)	-2.1	-	-	3.5%
		185.2(L)	-	-	-	-
		183.4(L)	-	-	-	-
		229.6(L)	-	-	-	-
LS-01	(quartz)	327.5(L)	-4.5	-	-	7.2%
(Lone Star Claims)		330.4(L)	-4.7	-	-	7.4%
		325-330(V)	-	+6 to +7?	-57.9	8.9%?
Carbonate Veins						
HN-02		236.1(L)	-	-	-	-
(Unexpected Claims)		237.3(L)	-7.6	-	-	11.2%
		238.2(L)	-8.1	-	-	11.8%
		240.6(L)	-	-	-	-
706		176.5(L)	-	-	-	-
(Discovery Hill)		176.4(L)	-2.1	-	-	3.5%
		171.5(L)	-2.5	-	-	4.2%
		167.1(L)	-2.3	-	-	3.9%
		168.5(L)	-	-	-	-
		166.1(L)	-3.5	-	-	5.7%

Microthermometric analyses were completed using a Chaixmeca heating-cooling stage attached to an OrtholuxII Leitz microscope.
Th = temperature of homogenization, Tm-ice = melting temperature of ice, Tm-clath = melting temperature of H_2O-CO_2 clathrate, $Tmco_2$ = melting temperature of CO_2, Wt.% NaCl = salinity in equivalent weight(%) of NaCl, (L) = homogenization into the liquid phase, (V) = homogenization into the vapour phase.
[1]Positive melting temperatures of ice occur in these inclusions due to metastable conditions that are created upon the complete elimination of vapour space during freezing.
[2]Sample includes distinct bands of strained metamorphic quartz (high homogenization temperatures) and secondary unstrained quartz (low homogenization temperatures).

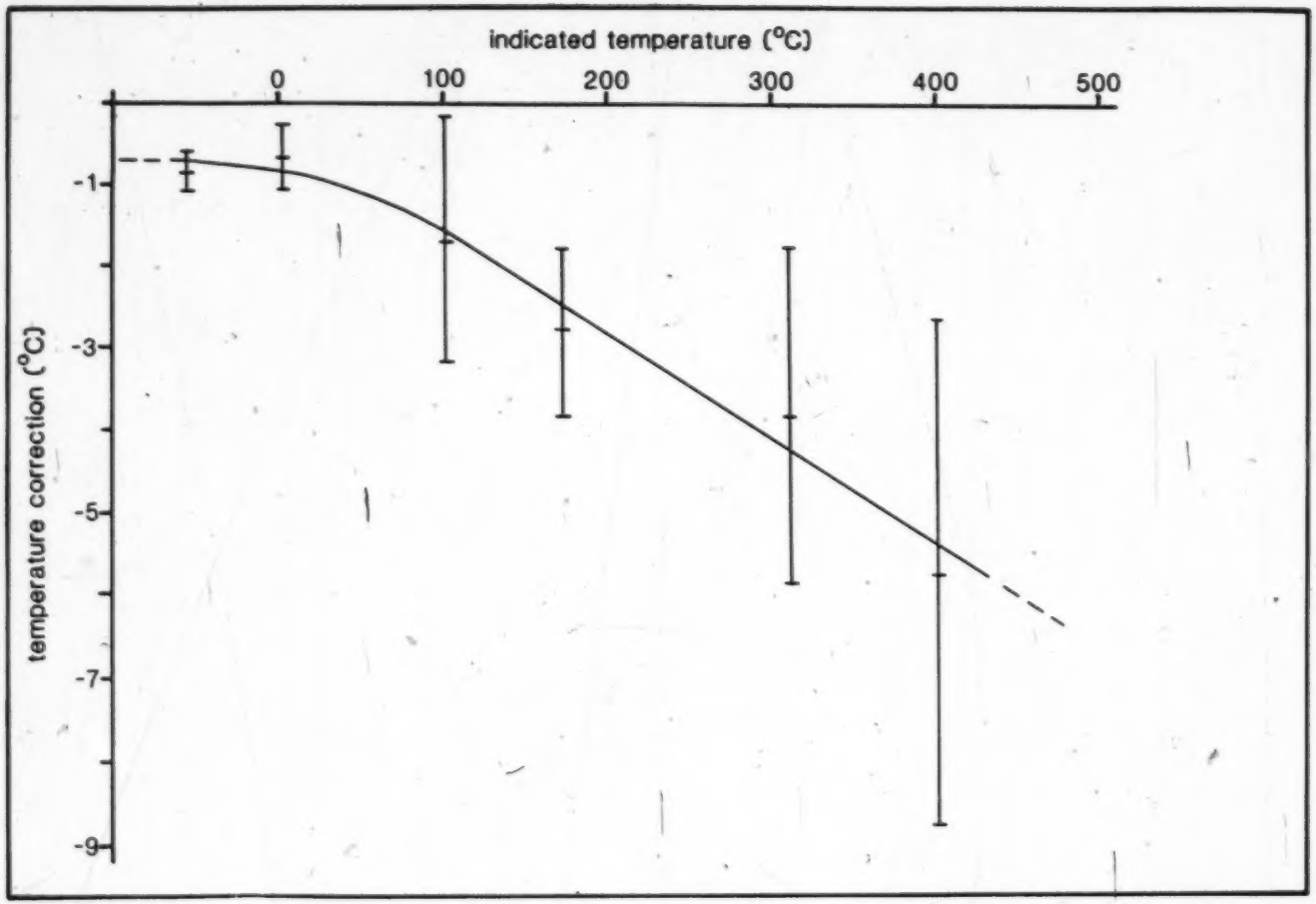

Figure 3.16 Calibration curve for fluid inclusion analyses using the Chaixmeca apparatus at the University of Alberta (modified after Fluet, 1986).

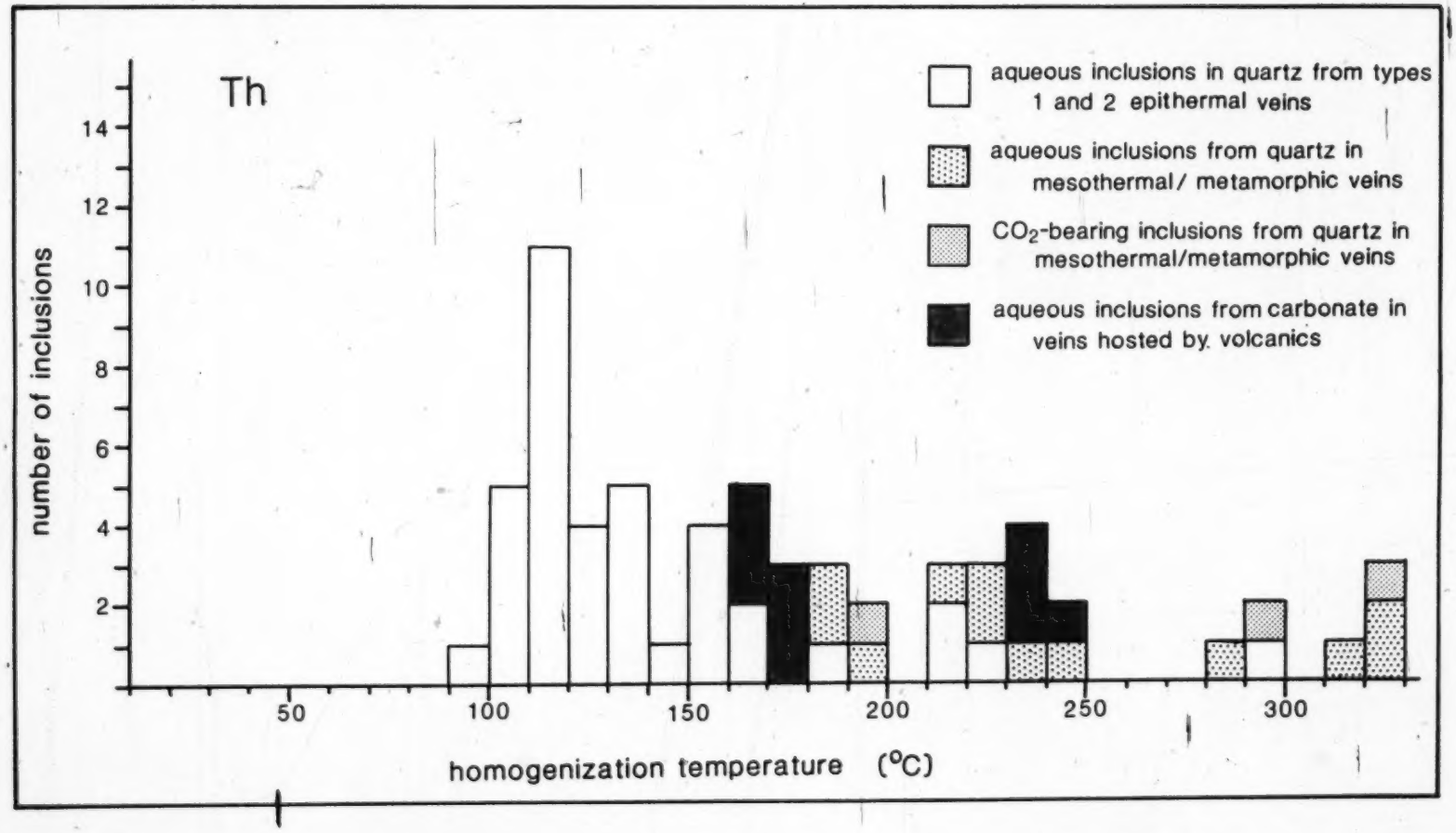

Figure 3.17 Homogenization temperatures (Th) of fluid inclusions in quartz and carbonate from Types 1, 2, mesothermal/metamorphic and carbonate (associated with volcanics) veins.

probably formed from a fluid similar to that responsible for the deposition of the type 1 quartz veins.

The composition of the aqueous fluid can be determined by Te and Tm-ice measurements. Depression of the melting point of ice is a direct function of increasing salinity and the dissolved CO_2 content of the fluid (Hedenquist and Henley, 1985a; Hollister and Crawford, 1981; Roedder, 1984). The presence of appreciable amounts of discrete CO_2 and/or dissolved CH_4 increases the apparent melting point of ice due to the formation of clathrates (Hollister and Crawford, 1981; Roedder, 1984).

The Tm-ice temperatures of the fluid inclusions in quartz from type 1 and 2 veins ranged from -2.8°C to +13.9°C (table 3.11 and figure 3.18), with an average Tm-ice of ≃-1.0°C for those aqueous inclusions that had ice that melted below 0°C. Eutectic melting (Te) was not observed in these inclusions. No CO_2 phase is visible in any of the fluid inclusions in quartz from type 1 or 2 veins. However, many Tm-ice temperatures of the H_2O-rich inclusions are well above the melting point of pure ice (0°C). This effect is most often attributed to the formation of CO_2-H_2O or CH_4-H_2O clathrates (Hollister and Crawford, 1981; Roedder, 1984). At room temperature the amount of dissolved CO_2 in the H_2O-rich inclusions of these quartz samples will be less than 5.45 wt.% CO_2 (Hollister and Crawford, 1981; Roedder, 1984). In addition, CH_4 was not detected during crushing. The low CO_2 and CH_4 content of these inclusions indicates that the amount of CO_2-H_2O or CH_4-H_2O clathrates formed were negligible hence, apparent Tm-ice temperatures should not have been affected. As a result, the amount of CO_2 or CH_4 present in the fluid inclusions in quartz from types 1 and 2 veins cannot account for the numerous positive Tm-ice temperatures obtained.

The range of melting temperatures above 0°C are most likely explained by nucleation problems incurred during heating of the ice. Hollister and Crawford (1981), and Roedder (1984) report ice melting temperatures of up to +6.5°C can occur in low salinity, water-rich inclusions. Unpublished data by Murck and coworkers (Hollister and Crawford, 1981) indicate that superheated (metastable) ice can be present in small inclusions at temperatures

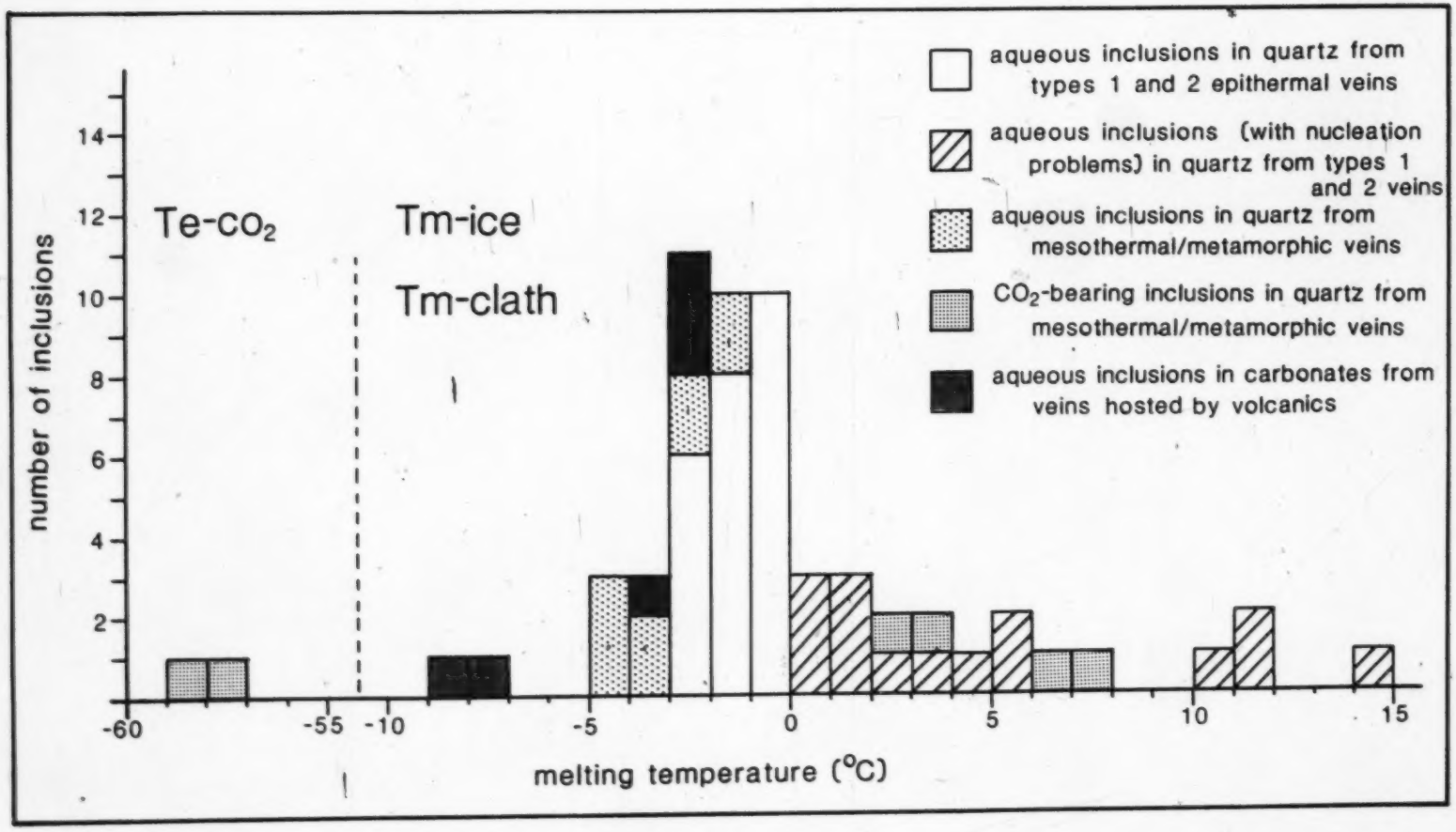

Figure 3.18 Melting temperatures of ice (Tm-ice), CO_2 (Te-co_2) and CO_2-H_2O clathrates (Tm-clath) from fluid inclusions in quartz and carbonate from Types 1, 2, mesothermal/metamorphic and carbonate (associated with volcanics) veins.

as high as +20°C. The high melting temperatures of ice (0°C to 14°C) in the inclusions with high L/V ratios in this study resulted from the complete elimination of the vapour phase due to the expansion of ice during supercooling. The presence of metastable ice above 0°C is indicated when the last remnant of ice melts and almost simultaneously a vapour bubble nucleates in the inclusion. Roedder (1984) explains that as long as nuclei for a vapour phase are absent in the inclusion, ice will melt to the liquid phase only. At a certain point the liquid phase is stretched over a larger volume than that of equilibrium conditions (where ice + liquid + vapour are present) resulting in metastable ice and liquid. This situation persists upon heating until the last ice melts and/or a vapour bubble nucleates. Inclusions exhibiting these phenomena cannot be used to determine the composition (salinity) of the contained fluid.

The salinity of the water-rich inclusions can be obtained using Tm-ice temperatures of inclusions that nucleate a vapour phase before the contained ice melts completely. The range of Tm-ice temperatures for inclusions in which metastability was not apparent is from -2.8°C to 0°C. These small values of freezing point depression indicate that a low salinity fluid exists in the water-rich inclusions. The eutectic temperature (Te) was not observed and as a result, the liquid phase of the aqueous inclusions is assumed to be a dilute NaCl brine. The salinities are calculated (based upon Tm-ice temperatures) using the formula of Potter *et al.* (1978):

$$W = 0.00 + 1.76958T - (4.2384 \times 10^{-2})T^2 + (5.2778 \times 10^{-4})T^3$$

where,

W = weight percent equivalent NaCl in solution (wt.% NaCl)
T = freezing point depression (°C) = 0 - (Tm-ice)

At a maximum freezing point depression of 2.8°C, the salinity of the liquid phase of the inclusion is 4.6±1.1 wt.% NaCl. At final melting temperatures of 0°C the salinity is negligible. The average salinity of the low temperature aqueous inclusions in type 1 quartz veins is 1.7±1.1 wt.% NaCl. Fluid inclusions in quartz from sample 101 show a similar range of Tm-ice temperatures indicating that the fluid responsible for the deposition of the type 2

siderite+quartz veins was similar in composition to the low salinity fluid that deposited the type 1 quartz veins.

3.3.2.2 Mesothermal/metamorphic quartz veins

Fluid inclusions in five samples from mesothermal and/or metamorphic quartz veins show Th and Tm-ice temperatures that differ vastly from the low temperature types 1 and 2 veins. One sample is from a known gold-bearing vein system (LS-1), while the remaining four samples (DG-1, DG-2, TR-1 and TH-2) are from metamorphic quartz bands and/or veins in clay-altered Klondike Schist. All of the quartz samples used contained both aqueous inclusions and CO_2-rich inclusions. Only a limited amount of data were collected from these types of inclusions in order to compare Th and Tm-ice temperatures to the low temperature type 1 quartz veins. Petrographic and microthermometric data collected in this study were not sufficient to adequately characterize the different types of mesothermal or metamorphic quartz samples within this group. The homogenization temperatures of the aqueous dominated inclusions ranged from 160°C to 330°C with an average Th of ≃241°C (table 3.11 and figure 3.17). Aqueous inclusions with no visible liquid CO_2 had Tm-ice temperatures that ranged from -5°C to -2°C with an average Tm-ice of ≃-3.5°C (table 3.11 and figure 3.18). Inclusions with visible liquid CO_2 had variable Tm-clath temperatures ranging from +3°C to +7°C; however, little microthermometric work was done on the CO_2-rich inclusions. More work on both the aqueous and CO_2-rich inclusions in this group of veins is necessary to estimate the pressures and temperatures of trapping in these samples. Nevertheless, it is clear that the fluids trapped by either the mesothermal or metamorphic quartz samples were much hotter than the fluid trapped in types 1 and 2 veins.

Salinity determinations in the system H_2O-NaCl-CO_2 are even more complex as NaCl and CO_2 have opposite effects on the melting point of ice due to the formation of salt-hydrates and CO_2-hydrates (clathrates). A qualitative estimate of salinities using the equation of Potter *et al.* (1978) for inclusions with no visible CO_2 indicate salinities no greater than 7-8 wt.% NaCl. A similar estimate of salinity can be made using the equation reported by Collins (1979) for the melting point depression of clathrates. This calculation indicates

salinities between 5 and 12 wt.% NaCl for the CO_2-rich inclusions. In general, the fluids responsible for the formation of either the mesothermal or the metamorphic quartz samples were higher in salinity and CO_2 than the fluids trapped in types 1 and 2 veins.

3.3.2.3 Carbonate veins associated with volcanics

Fluid inclusions in two samples of carbonate from the veins associated with the Hunker Creek rhyolite porphyry and Last Chance Creek volcanics show Th and Tm-ice temperatures quite different from those of types 1 and 2 veins. The inclusions within the carbonate samples are all 2 phase aqueous inclusions. The average homogenization temperature and resultant minimum trapping temperature for samples HN-02 and 706 is approximately 235°C and 171°C respectively. The average Tm-ice temperatures are approximately -7.5°C and -2.6°C respectively. This yields average salinities of approximately 11 and 4.3 wt.% equivalent NaCl for the two samples using the equation of Potter *et al.* (1978). Although the origin of these veins is unclear, the trapped fluids appear to have been slightly hotter and more saline than the fluids trapped by types 1 and 2 veins.

3.4 Vein Chemistry

Major and trace element analyses were conducted on 30 vein samples from types 1, 2 and 3 veins, mesothermal/metamorphic quartz veins and volcanic-associated carbonate veins. Analyses of major elements plus S, Ba and As for the samples listed in table 3.12 were performed by the XRF method at McMaster University. Analyses of Fe, Na, Cr, U, Co, As, Sb and Au for the samples listed in table 3.13 were performed by the INAA method at the SLOWPOKE II reactor, Univeristy of Alberta. Details of the experimental procedure and estimates of error for both XRF and INAA methods are presented in appendix 5.5. The analyses of types 2 and 3 veins, along with the majority of the gravel and bedrock samples, were performed by the XRF method in the early stages of the study. Adequate samples of type 1 veins were obtained at a later stage after the XRF analyses were completed hence, the samples were analysed using INAA at the University of Alberta due to time constraints.

Table 3.12 Whole rock chemistry of types 2 and 3 veins in the clay-altered footwall rocks below the White Channel gravel.

Sample		SiO_2 (%)	Al_2O_3 (%)	Fe_2O_3 (%)	MgO (%)	CaO (%)	Na_2O (%)	K_2O (%)	TiO_2 (%)	MnO (%)	P_2O_5 (%)	LOI (%)	S (ppm)	Mn (ppm)	Ba (ppm)	As (ppm)
Jackson Hill																
101	(type 2)	8.84	0.75	61.99	0.65	0.59	0.03	0.13	0.00	1.17	0.00	25.81	1,520	1.31%	5,410	<2
107	(")	6.72	2.11	62.25	1.18	0.99	0.25	0.16	0.35	0.76	0.12	25.12	2,110	0.81%	430	<2
113	(")	23.88	4.46	45.85	0.55	0.97	0.29	0.99	0.24	0.35	0.20	22.23	1,360	0.36%	2,400	<2
115	(")	15.52	3.07	49.35	0.58	1.25	0.27	1.03	0.16	0.66	0.05	28.04	2,800	0.65%	1,420	<2
Trail Hill																
309	(type 3)	4.88	3.20	73.78	0.50	0.03	0.09	0.15	0.00	1.86	0.09	15.41	890	1.82%	330	<2
320	(")	27.86	10.82	43.03	0.29	0.06	0.11	1.01	1.19	0.45	0.43	14.74	650	0.43%	315	<2
321	(")	54.13	18.46	7.12	2.09	1.00	0.87	0.62	1.37	0.06	0.42	13.85	260	635	610	36
Dago Hill																
501	(")	75.59	14.90	0.90	1.03	0.03	0.31	3.33	0.00	0.01	0.00	3.84	340	199	1,020	15
528	(")	7.52	5.32	68.65	0.61	0.03	0.49	0.14	0.00	0.47	0.21	16.54	900	0.49%	265	<2
Discovery Hill																
705[1]		90.05	3.62	3.17	0.36	0.03	0.05	0.45	0.16	0.13	0.07	1.87	120	1,660	1,770	13
706[1]		3.76	0.89	5.40	14.83	33.05	0.09	0.12	0.01	0.29	0.00	41.54	840	2,980	2,540	<2

Analyses were performed by the XRF technique (major elements in % oxides, LOI in % and trace elements in ppm, LOI=loss on ignition at 1040°C, Fe_2O_3=total iron) and recalculated to 100%. Vein type is indicated in parenthesis.
[1]Samples from veins hosted by andesitic volcanics on Last Chance Creek.

Table 3.13 Chemistry of selected vein and White Channel gravel (matrix) samples from the Klondike district.

Sample		Fe_2O_3 (%)	Na_2O (%)	Cr_2O_3 (ppm)	U (ppm)	Co (ppm)	As (ppm)	Sb (ppm)	Au (ppb)
Dago Hill (veins)									
DG-2	(type 1?)	1.46	0.03	nd	3.0	nd	9	0.7	26
DG-3	(type 2?)	3.79	0.02	50	3.8	nd	17	1.2	nd
DG-4	(carbonate)	4.19	0.03	4,060	nd	135	900	9.8	nd
DG-9	(carbonate)	5.73	0.02	3,550	nd	95	220	3.8	nd
DG-10	(carbonate)	4.88	0.04	nd	nd	nd	71	1.3	nd
DG-11	(type 1?)	3.50	0.03	nd	0.9	5	97	3.4	280
DG-15	(type 3?)	73.32	0.01	340	23.2	190	38	0.8	nd
DG-16	(carbonate)	13.74	0.04	1,910	nd	1,520	9,024	143.1	nd
Paradise Hill (veins)									
PD-8502	(type 1?)	3.19	0.03	2,460	1	16	32	27.9	nd
PD-8507	(type 3?)	63.26	0.04	190	6.4	190	4	1.4	nd
PD-8509	(type 1?)	23.09	0.01	≈37%	nd	260	53	25.3	nd
PD-8511	(type 1)	3.46	0.01	3,270	nd	24	21	15.1	nd
PD-8512	(type 1)	0.57	0.01	100	nd	4	47	12.9	nd
PD-8513	(type 1)	3.23	0.02	14,990	nd	48	70	8.8	80
Nugget Hill (vein)									
NH-8513	(type 1)	8.44	0.05	160	21.5	12	81	2.3	nd
Discovery Hill (veins)									
DH-02	(carbonate)	2.03	0.06	10	nd	nd	1	0.2	nd
DH-03	(carbonate)	3.29	0.02	nd	7.1	nd	nd	2.1	nd
Hunker Creek (veins)									
HN-03	(carbonate)	2.73	0.03	1,050	1.1	9.2	14	0.5	22
HN-04	(carbonate)	1.22	0.03	15	0.5	nd	7	0.2	nd
Gravel matrix									
516[1]	(Iron zone)	8.29	0.22	nd	14.5	31	13	1.8	nd
517[1]	(")	2.02	0.65	nd	5.9	63	7	3.7	nd
CN-01[1]	(")	53.31	0.04	810	31.8	110	1,560	45.5	nd
908[2]	(")	24.66	nd	nd	22.8	nd	220	7.2	nd

Analyses were performed by the INAA technique (outlined in appendix 5.5) at the SLOWPOKE II reactor, University of Alberta. Vein type is indicated in parentheses.
[1]Samples from Dago Hill. [2]Sample from Nugget Hill. nd=not detected

3.4.1 Type 1 quartz veins

Eight, type 1 quartz veins were analysed using INAA. Five samples were selected from Paradise Hill (PD-8502, 09, 11, 12, 13), two samples from Dago Hill (DG-2, DG-11) and one sample from Nugget Hill (NH-8513). Significant amounts of wall rock were incorporated into six of the samples during crushing (PD-8502, PD-8509, PD-8513, DG-2, DG-11 and NH-8513). The remaining two samples (PD-8511 and PD-8512) were relatively pure vein material (more than 98% quartz). Sample PD-8502 consists of chalcedony from a vein (≈75-85% quartz) within a silicified serpentinite. Material from the silicified serpentinite was included in the crushed sample used for analysis (≈15-25%). Sample PD-8509 dominantly consists of intensely clay-altered and iron-stained wall rock with 40-50% macroscopic magnetite and chromite and a thin (<2-3mm) quartz veinlet. The parent rock was probably serpentinite. Sample PD-8513 contains mostly quartz (>85-95%) from several veinlets in a sample of completely clay-altered and iron-stained serpentinite. The sample contains secondary minerals, in relationship to the host unit, which are dominantly quartz, Fe-hydroxides and clay minerals. The textures and minerals of the original host rock have been completely obliterated. The Dago Hill samples are dominantly composed of banded metamorphic quartz with secondary minerals present that are related to type 1 veins in the clay-altered and bleached mica schist. In sample DG-2, the secondary minerals present include quartz and dickite (≈10-20% of the sample). In sample DG-11, the secondary minerals quartz, kaolinite and ankerite are present. The secondary minerals in DG-11 approach 30-40% of the crushed sample. Sample NH-8513 (from the Nugget Hill Footwall zone) is composed of intensely clay-altered and iron-stained graphitic-mica schist with significant amounts of quartz (≈30-50%) from a thin (<3-5mm) type 1 vein.

The chemistries of all eight samples analysed by the INAA technique are listed in table 3.13. No samples of unaltered serpentinite were analysed in this study; however, average concentrations for the elements of interest in ultramafic rocks are 3,140ppm Cr_2O_3, 150ppm Co, 1ppm As (4ppm for serpentinites), 0.1ppm Sb and 6ppb Au (Turekian and Wedepohl, 1961). Background As values for unaltered schist at Dago Hill and several other hills in the

Klondike area are generally <10 ppm. Average concentrations of As, Sb and Au for mica schists (felsic rocks or mature clastic sandstones) reported by Turekian and Wedepohl (1961) include 1-2ppm As, 0.01-0.2ppm Sb and 1-9ppb Au. Two of the Paradise Hill Samples (PD-8511 and PD-8512), which are hosted by the altered serpentinite, are the best indicators of the chemistry of type 1 quartz veins, as they are entirely composed of vein material (>98% quartz). Both samples contain high As (21 and 47 ppm) and Sb (15.1 and 12.9 ppm) values. Sample Pd-8513 contains similar high values for As and Sb (70 and 8.8 ppm respectively) in addition to detectable amounts of anomalous Au (80ppb). All five samples from Paradise Hill show consistently high As and Sb values which are similar to those in the pure type 1 vein samples. This seems to indicate that the concentrations of As and Sb are not affected significantly by the amount of wallrock that was incorporated during crushing. The amount of altered serpentinite wallrock incorporated into each sample appears to be reflected in the Fe_2O_3, Cr_2O_3 and Co values (table 3.13). As a result, the consistently high As and Sb values are probably a reflection of the chemistry of the quartz veins rather than the original serpentinite host.

Sample DG-2, with ≈80-90% metamorphic minerals and 10-20% secondary quartz and dickite related to a type 1 vein, contains only background levels of As (9ppm) and Sb (0.7ppm), but it does contain anomalous Au (26ppb). Probably more significant are the higher values obtained for DG-11, which are 97ppm As, 3.4ppm Sb and 280ppb Au. In addition, DG-11 contains a higher precentage of secondary quartz, kaolinite and ankerite (≈30-50%) related to a type 1 vein. Sample NH-8513, with 50-70% clay-minerals and iron-hydroxides, and 30-50% quartz from a type 1 vein, contains anomalous Fe_2O_3 (8.44%), As (81ppm) and Sb (2.3ppm). These results indicate that the anomalously high As, Sb and Au values of the Dago Hill samples (DG-2 and DG-11) are linked to the secondary minerals of the type 1 veins and associated clay alteration of the mica schist.

Four samples of Iron zone gravel matrix were analysed by INAA. These samples are also discussed in 2.3.2. The anomalous values of Fe_2O_3, As and Sb in several of the type 1 quartz veins and associated clay-altered host rocks are similar to values obtained for the same

elements in Iron zone White Channel gravel. Matrix samples CN-01 and 908 are from Iron zone gravel at Dago and Nugget Hills, respectively. Both samples have extremely high values of Fe_2O_3 (53.31 and 24.66%), As (1,560 and 220 ppm) and Sb (45.5 and 7.2 ppm). Samples 516 and 517 from the Iron zone gravel at Dago Hill contain high Fe_2O_3 values but only background As values in comparison to unaltered White Channel gravel matrix (table 2.6). All four matrix samples contain no detectable Au; however, they are all from areas of economic gravel (Stutter and Warmsby *pers. comm.*, 1985). The lack of detectable Au is attributed to the small sample size and the high background during counting after irradiation. It is generally well accepted that in assaying gravel for Au at least one cubic foot of material (≃75kg) should be crushed and entirely assayed (Morison *pers. comm.*, 1986). For these samples approximately 250-500 grams of each sample were crushed, from which ≃100 mg was extracted and irradiated. In addition, the gravel samples were crushed using a tungsten carbide swing mill contributing significant amounts of tungsten to each sample. As a result, tungsten along with high values of Fe and Ba that are present in these four samples creates high radioactive background levels after irradiation which significantly reduces the detection level of the trace elements, especially Au. In the four gravel samples the detection limit of Au is probably on the order of 500-1000 ppb Au by the INAA method without using preconcentration (St. Louis *pers. comm.*, 1985).

3.4.2 Type 2 siderite+quartz veins

Four, type 2 siderite+quartz veins and/or concretions were analysed for major and some trace elements using the XRD method at McMaster Univeristy. All four samples (101, 107, 113 and 115) were selected from intensely altered footwall rocks at Jackson Hill. Samples 101 and 107 contain approximately 70-90% siderite, 10-20% quartz and 10-20% goethite. Both samples are concretions related to type 2 veins with siderite, quartz and goethite that have almost completely replaced the original diabase host. Samples 113 and 115 are from siderite concretions in altered mica-chlorite-plagioclase schist. These samples contain less siderite than samples 101 and 107 and significantly more quartz. Most of the quartz appears to be primary

metamorphic in origin, as it is associated with mica, plagioclase, apatite and zoisite, and it usually exhibits undulatory extinction in thin-section. The chemistry of all four samples (table 3.12), in comparison to the chemistries of unaltered diabase and schist bedrock reported in table 2.10, is characterized by high values of Fe_2O_3, MnO and LOI, with only background values for S, Ba and As. The S and Ba concentrations for samples 101 and 107 (1,520 and 2,110ppm S, 430 and 5,410ppm Ba, respectively), however, may be anomalous as the samples are entirely vein material. These four samples, in addition to several other similar samples, were assayed for Au by Bondar-Clegg of Vancouver. All the samples contained Au values at or just above the detection limit (5-10ppb). The samples were assayed by preconcentration fire assay coupled with Atomic Absorption Analysis. The low concentrations of Au indicate that it is either in low abundance in the type 2 veins, or that the small amount of sample crushed and analysed was inadequate to cope with the nugget effect.

3.4.3 Type 3 veins

Five samples of the type 3 veins were analysed for major and a few trace elements by the XRF technique at McMaster University (table 3.12). Three samples from veins in altered schist and diabase at Trail Hill (309, 320 and 321) are composed of amorphous silicates and/or goethite. All three samples contain high values of Fe_2O_3 and LOI. Sample 309, composed of mostly goethite, contains a high value for MnO, but all other cations are present in minor concentrations. Samples 320 and 321 are dominantly composed of amorphous silicates (probably lussatite or opal) with goethite and minor, poorly crystalline clay minerals. The major element chemistry of both samples is quite irregular (table 3.12) and as a result difficult to characterize. All three Trail Hill samples appear to contain low S, Ba and As values except sample 321 which contains 36ppm As.

Samples 501 and 528 from Dago Hill contain variable major element chemistries. Sample 501 contains high values of SiO_2, Al_2O_3 and K_2O due to the presence of quartz and clay minerals. The amount of vein material present in 501 is unknown. Sample 528, composed of goethite and minor amounts of amorphous silicates, contains high values of Fe_2O_3 and

LOI. Both samples contain low values of S, Ba and As.

3.4.4 Carbonate veins associated with volcanics

Six samples from veins (mostly carbonate-rich) associated with either the Hunker Creek rhyolite porphyry or Last Chance Creek andesite volcanic/volcaniclastic rocks were selected for major and trace element analysis. The analyses of two samples from Discovery Hill (705 and 706) were performed by XRF (table 3.12). Analyses of the remaining four samples (DH-02 and DH-03 from Discovery Hill, HN-03 and HN-04 from Hunker Creek) were performed by INAA (table 3.13). Macroscopically, samples 706, DH-02 and DH-03 are all very similar. All three vein samples are hosted by andesitic volcanic rocks at Discovery Hill. Each sample is composed dominantly of coarse botryoidal carbonates (mostly calcite, ankerite and dolomite). Sample 706 (analysed by XRF) contains high values of Fe_2O_3, MgO, CaO and LOI with significant values of Mn (2,980ppm) and Ba (3,540ppm). Samples DH-02 and DH-03 (analysed by INAA) contain Fe_2O_3 and little else except 2.1ppm Sb in sample DH-03. These two samples, however, probably contain significant values of MgO and CaO which were unobtainable from the short irradiation count used in the INAA analysis. Sample 705 is composed dominantly of quartz associated with the carbonate veins at Discovery Hill. The sample contains only minor concentrations of most cations other than SiO_2, but significant amounts of Mn (1,660ppm), Ba (1,770ppm) and As (13ppm) are present.

Samples HN-03 and HN-04 from the Unexpected claims hosted by the Hunker Creek rhyolite prophyry were selected for chemical analysis by INAA. Both samples are composed dominantly of fine-grained carbonate with evidence of local brecciation and recementation. Sample HN-03 contains trace amounts of an emerald green mica, probably fuchsite (Cr-mica). The chemistry of HN-03 is characterized by anomalous concentrations (in comparison to felsic rocks) of Fe_2O_3, Cr_2O_3, Co, As and Au. The small amount of Au (22 ppb) was detectable due to extremely low background radioactivity during INAA counting. Sample HN-04 contains insignificant values for most of these same elements.

3.4.5 Carbonate veins associated with shear zones

Four samples (DG-4, DG-9, DG-10 and DG-16) from the carbonate veins hosted by shear and/or fault zones at Dago Hill were selected for INAA analysis. The presence of fault zones is characterized by [illegible]heared and juxtaposed mica schist and graphitic schist. Small pods of serpentinite are often spatially coincident with these shear zones. Samples DG-4 and DG-9 are composed dominantly of medium- to coarse-grained dolomite and/or ankerite with quartz and fuchsite. Carbonate in these samples occurs as a partial to near complete replacement of serpentinite within the fault zones. Sample DG-10 consists of dolomite and/or ankerite from an isolated carbonate vein within partially altered mica schist. Sample DG-16 is composed of fine-grained, massive to spherulitic magnesite, quartz, dolomite (or ankerite?) fuchsite and possibly minor rhodochrosite. The sample appears to be related to a fault zone and associated serpentinite. All four samples appear to be either unaffected by, or they are associated with alteration of the host footwall rocks. The samples were taken from a significant distance below the bedrock gravel contact (≈ 35-50 meters) at Dago Hill. The chemistry of the three samples associated with the fault zones is almost identical with high values of Cr_2O_3 (1,910-4,060ppm), Co (95-1,520ppm), As (220-9,024ppm) and Sb (3.8-143.1ppm). Sample DG-10, not visibly associated with a fault zone or serpentinite pod, contains similar values for As and Sb; however, Cr_2O_3 and Co are not detectable. This may indicate that the high values of Cr_2O_3 and Co in the other samples are related to the presence of altered serpentinite and fuchsite that is often visible throughout the shear zones. The high values of As and Sb are unaffected by the presence or absence of serpentinite and/or fuchsite. As a result, As and Sb are probably related to the introduction of carbonate in the veins or as a replacement. The actual relationship of these carbonate-rich veins to types 1, 2 and 3 veins associated with Footwall zone clay alteration immediately below the White Channel gravel is unclear and in need of further work.

3.5 Discussion

The observed field relationships, mineralogy and geochemistry of types 1, 2 and 3 veins, and associated alteration are compared and contrasted to the characteristics of epithermal precious-metal deposits and geothermal systems.

3.5.1 Summary of data

3.5.1.1 Textures, mineralogy and geochemistry of types 1, 2 and 3 veins

Types 1, 2 and 3 veins in clay-altered Footwall zone rocks immediately below the White Channel gravel are distinct in morphological, mineralogical and geochemical characteristics. Type 1 quartz veins are usually thin (<10-20cm in thickness), lack iron-stain and are banded, with cockscomb and crustiform textures common. The quartz varies from medium-grained, euhedral (often protruding into open spaces) to fine-grained and chalcedonic. Fluid inclusions in the quartz are dominantly one or two phase aqueous inclusions with an average Th of ≃120-130°C and an average Tm-ice of ≃-1.0°C (average salinity ≃1.7wt.% equivalent NaCl). Maximum concentrations of the trace elements analysed in 4 or 5 relatively pure type 1 quartz veins include 97ppm As, 27.9ppm Sb and 280ppb Au.

Type 2 siderite+quartz veins are usually thin (<1-2cm in thickness), highly iron-stained and exhibit botryoidal and banded growth structures. Occasionally the veins are associated with siderite+quartz replaced, clay-altered bedrock, forming 10-30cm diameter "concretionary-like" nodules. One sample of quartz from a type 2 vein contains one and two phase aqueous inclusions, with homogenization (Th) and melting (Tm-ice) temperatures well within the range of temperatures for the type 1 quartz vein samples. The chemistry of these veins is characterized by extremely high values for Fe_2O_3, MnO and LOI with 5,410ppm Ba, 1,520ppm S and low As(<2 ppm). Several samples assayed for Au contained values at or less than detection limits (<5 ppb); however, the small sample size did not allow for an accurate trace element characterization of these veins.

Type 3 veins are characterized by the presence of amorphous silicate phases, Fe-hydroxides and clay minerals filling fractures. The veins or fractures are usually <1-2cm

in thickness, with the amorphous vein material exhibiting a variety of hardnesses from as low as <1 up to 4 or 5 on Moh's hardness scale. The harder material is extremely fine-grained, fibrous, banded and possibly similar to lussatite (a variety of opal). Fluid inclusions were not visible. The chemistry of these veins is highly variable ranging from Fe-rich, Si- and Al-poor to Si- and Al-rich, and Fe-poor. Values of S and Ba tend to be low while LOI, Mn, Ti, and P are usually high. Two samples contain significant As (15 and 36ppm).

3.5.1.2 Important field relationships of types 1, 2 and 3 veins

Types 1, 2 and 3 veins clearly cross-cut all structural fabrics in the Klondike Schist and appear to have been emplaced during the alteration of the Footwall zone rocks and the overlying White Channel sediments. Several relationships between types 1 and 2 veins, and altered to partially altered footwall rocks, suggest that vein emplacement and clay alteration were essentially penecontemporaneous. Type 1 quartz veins and type 2 siderite+quartz veins in clay-altered footwall rocks occasionally contain fragments of partially clay-altered bedrock. In addition, several siderite+quartz concretions associated with type 2 veins at Jackson Hill have almost entirely replaced the clay-altered schist and/or diabase bedrock. Cementation and/or replacement of the clay-altered or partially clay-altered bedrock must have occurred during or shortly after clay alteration.

Types 1 and 2 veins are usually thin (<2-3cm thick) and exhibit delicate patterns of veining in completely altered footwall rocks, in some cases only 2-3 meters below the gravel-bedrock contact. The Footwall zone of clay alteration and associated veins must have formed after the deposition of the gravel as the entire zone would have been eroded during deposition of the gravel, if it had been present previous to the fluvial event. All folding and fractures that are visible in the unaltered diabase (lower in the section) have been completely destroyed due to volume changes associated with intense clay alteration. However, types 1 and 2 veins are clearly visible and unaffected by the intense alteration of the Footwall zone rocks. In addition, there is a good correlation between increased alteration and the increased occurrence of these veins. These types of relationships indicate that types 1, 2 and 3 veins were actively forming during alteration of the Footwall zone rocks after deposition of the

White Channel gravel.

3.5.1.3 Type 1 veins contrasted with mesothermal/metamorphic veins

The textural and mineralogical characteristics of type 1 quartz veins distinctly contrast with the characteristics of typical mesothermal and/or metamorphic quartz veins hosted by the Klondike Schist in this district. The mesothermal/metamorphic quartz veins are usually thick (10's of centimeters to meters) with coarse-grained quartz. The veins are rarely associated with clay alteration of the host rock. The accessory mineral suite of the mesothermal/metamorphic quartz veins usually consists of coarse-grained feldspar, muscovite, carbonate, with trace amounts of apatite, zoisite, tourmaline, rutile, ilmenite, magnetite and pyrite. Most of these minerals have not been observed in type 1 quartz veins. Quartz in the mesothermal/metamorphic veins usually exhibits undulatory extinction in thin-section, indicative of strain, in contrast to quartz from type 1 veins that show straight extinction only. In addition, quartz grains in the mesothermal/metamorphic veins are often joined at triple points with rare vugs. Type 1 quartz veins usually contain substantial amounts of vugs filled with euhedral quartz and no triple point junctions between grains.

The petrography and microthermometry of fluid inclusions in the mesothermal and/or metamorphic quartz veins differ significantly from the characteristics of fluid inclusions in quartz of types 1 and 2 veins. Mesothermal/metamorphic quartz usually contains both aqueous and CO_2-rich inclusions. In addition, the aqueous inclusions have moderate L/V ratios averaging ≈10-15% vapour. In contrast, quartz from types 1 and 2 veins contain aqueous inclusions only, with high L/V ratios averaging ≈1-2% vapour. As a result, considerable differences occur in the microthermometric measurements of the two vein types. Aqueous dominated inclusions in mesothermal/metamorphic quartz have a wide range of homogenization temperatures (≈160-330°C) with an average Th of ≈240°C. Depending upon the depth of formation (and the resultant pressure correction) and the composition of the fluid that formed these veins, the actual trapping temperatures of the fluids were probably 50-100°C hotter than the average Th. The average Tm-ice of the aqueous-dominated inclusions from mesothermal/metamorphic quartz is ≈-3.5°C, corresponding to approximately

7-8wt.% equivalent NaCl using the equation of Potter *et al.* (1978). In contrast the aqueous inclusions of type 1 quartz veins have a narrow range of homogenization temperatures with an average Th of ≈120-130°C. In addition, the average Tm-ice is higher at ≈-1.0°C, indicating low salinities which average <1-2 wt.% equivalent NaCl.

3.5.2 Discussion of the origin of types 1, 2 and 3 veins

3.5.2.1 Characteristics indicative of near-surface deposition

The textural, mineralogical and geochemical characteristics of types 1, 2 and 3 veins are important indicators of the depth and environment of formation. Many of the mineralogical characteristics of types 1 and 2 veins are similar to features observed in precious-metal veins and veins which are associated with geothermal systems formed within 100-200m of the paleosurface (Berger, 1985; Hedenquist and Henley, 1985b). As previously discussed, the alteration and partial replacement of clay-altered bedrock by types 1 and 2 veins indicate that they were emplaced during the alteration of Footwall zone rocks and the overlying White Channel gravel. Maximum thicknesses of unconsolidated sediments overlying the altered Footwall zone and associated veins are estimated to have been 100-150m from paleoenvironmental reconstruction (Morison *pers. comm.*, 1986). Distinct banding and vugs are common in types 1 and 2 veins in addition to cockscomb, crustiform and botryoidal textures. Such features, according to Buchanan (1981), are characteristic of epithermal vein deposits formed near the surface (within 200-500m). Chalcedony is commonly present in several type 1 veins found in intensely clay-altered Footwall zone rocks. At Trail Hill a hard amorphous and fibrous silicate similar to lussatite (a variety of opal) is associated with several type 1 quartz/chalcedony veins. Chalcedony and amorphous hydrous-silica (opal) are rarely, if ever, formed above 150°C (Hedenquist and Henley, 1985b; Fournier, 1985). Fluids between 100 to 150°C in geothermal systems usually exist at no greater depths than 100-200m below the surface. Hedenquist and Henley (1985b) report that in the Waiotapu geothermal system of New Zealand, quartz is deposited as a cement and in veins at depths greater than 100m below the surface, while chalcedony is deposited within 100m of the surface only. At

Steamboat Springs chalcedony is actively cementing unconsolidated alluvium and is precipitating in sinters within 40-50m of the surface (Schoen and White, 1967; Schoen *et al.*, 1974; Sigvaldson and White, 1962). The formation of amorphous hydrated silica (opalization) is a common feature of pool precipitates and sinters associated with active geothermal systems usually forming at or within several meters of the surface (Fournier, 1985; Henely and Ellis, 1983). Opalization (often referred to as part of a jasperoid cement) occurs in the near-surface environment of many precious-metal deposits in Nevada (*i.e.* the Goldfield district, Ashley, 1974; the Borealis deposit, Strachan, 1985 and the Enfield Bell mine, Birak and Hawkins, 1985) all of which are considered to be remnant geothermal systems. The Hearts Peak deposit in northwest B.C. contains significant amounts of opal as part of the surface expression of a Plio-Pleistocene geothermal or epithermal system (Schroeter, 1985). These relationships in epithermal and geothermal systems suggest that the textural and mineralogical features of type 1 veins are the result of near-surface, low temperature, hydrothermal activity.

Well crystallized dickite and kaolinite, which are present in several of the type 1 quartz veins, also indicate a near surface, low temperature, origin for the veins. As discussed in chapter 2, well crystallized kaolin minerals are common in the upper levels of alteration halos associated with geothermal hot-spring deposits (Keller, 1982; Keller and Hanson, 1969 and 1968). In addition, kaolin minerals often are the dominant mineral phase (usually with sulphates or illite) in near-surface, "blanket-like", low pH alteration halos (argillic alteration) capping epithermal precious-metal deposits (Berger, 1985; Buchanan, 1981; Tooker, 1985). Kaolin-rich alteration zones also are often spatially associated with many precious-metal epithermal veins in the North American Cordillera (Buchanan, 1981). Much experimental work on kaolin synthesis indicates that at surface pressures, and during high water/rock and H^+/K^+ ratios, kaolinite is not stable with respect to pyrophyllite in the presence of dilute hydrothermal fluids and at temperatures greater than approximately 150-225°C (Hurst and Kunkle, 1985; Dekimpe *et al.*, 1981). As a result, these relationships indicate that crystalline kaolinite and dickite in type 1 quartz veins were formed from low

temperature hydrothermal fluids.

The mineralogy and textures of type 2 siderite+quartz veins appear to indicate that these veins were also formed in the near-surface environment at low temperatures. Siderite concretions, related to type 2 veins, contain vuggy and botryoidal textures. Gautier (1982) describes morphologically similar siderite+calcite concretions in the Gammon Shale (northern Great Plains). He suggests that the concretions formed during diagenesis somewhere near the onset of methane formation at ≈100-150°C. This is consistent with the formation temperatures indicated by the results of fluid inclusion microthermometry on quartz from the siderite concretions in the altered Footwall zone. Hydrothermal siderite is also common in several precious-metal deposits, usually associated with the formation of jasperoid (opal+hematite) near the paleosurface, as in the Tonopah Mining District (Bonham and Garside, 1979).

3.5.2.2 Geochemical characteristics of the vein fluid

In order to better understand the origin of the alteration and gold-bearing fluids, it is important to compare the fluid chemistry of types 1 and 2 veins to that of fluids in better known precious-metal and geothermal systems. In several reviews of the characteristics of geothermal systems and epithermal precious-metal deposits (Ellis, 1979; Ellis and Mahon, 1977; Henley and Ellis, 1983; White, 1981), fluids from geothermal wells and epithermal quartz veins, respectively, are described as having temperatures below 150°C with low salinities. Fluids at temperatures below 150°C are observed at or within 100-200m of the surface. Hedenquist and Henley (1985a) review most of the fluid inclusion data from many epithermal precious-metal deposits. They indicate that apparent salinities in these deposits are very low, ranging from 0 to 3 wt.% equivalent NaCl and averaging less than 1.5 wt.% equivalent NaCl. The average salinity (1.7 wt.% equivalent NaCl) and lack of significant amounts of CO_2 in the fluids trapped by quartz from type 1 and 2 veins bear a distinct resemblance to near-surface geothermal fluids and fluids trapped in inclusions of epithermal precious-metal deposits.

Trace element concentrations of types 1 and 2 veins are similar to the chemical signatures of many near-surface veins and alteration zones associated with geothermal systems

and precious-metal deposits. In most of these types of deposits a distinct zonation of trace elements, usually with depth, is present. The surface environment (within 50-100m depth) of active geothermal systems usually includes sinters, hot-spring pools, argillic alteration zones and some evidence of silicification/opalization. The trace element content of most of these surface (or near-surface) environments typically includes Au, As, Sb, Hg, Tl, Fe, Mn, Ba, F, S, P and occasionally Ag, Mo, W, Co, B (Ewers and Keays, 1977; Hedenquist and Henley, 1985b, Stauffer and Thompson, 1984; Weissberg *et al.*, 1979). This assemblage of elements is often referred to as the epithermal suite. Precious-metal deposits contain a similar enrichment of these metals in veins and alteration zones formed near the paleosurface and/or at low temperatures (Berger, 1985; Buchanan, 1981). At greater depths below the surface and higher temperatures (>100-200m and >200°C) both geothermal systems and precious-metal deposits show a gradation from the epithermal suite to the base metal suite of elements. The base metal suite of elements usually consists of Ag, Pb, Zn, Cu, Fe, Cr, Co, Se, Te, Bi, S and occasionally Au (Berger, 1985; Buchanan, 1981; Ewers and Keays, 1977; Weissberg *et al.*, 1979). Type 1 and 2 veins in the clay-altered Footwall zone rocks below the White Channel sediments contain anomalous Au, As, Sb, Ba, Fe, Mn, P, S and possibly Co and Cr. Analyses of Hg and Tl were not conducted. This suite of elements is similar to the diagnostic suite of epithermal elements. Not only are these elements present in the veins and clay-altered bedrock near the White Channel gravel contact, but anomalous As, Sb, Fe, Mn, Ba, Co and S values are also present in the gold-bearing Iron zone gravel at several hills in the Klondike district. This suite of trace elements in types 1 and 2 veins, and the Iron zone gravel, suggests that the fluid responsible for the deposition of the veins and associated alteration was similar to near-surface, low temperature geothermal fluids.

3.5.2.3 A contrasting origin for the mesothermal/metamorphic veins

In contrast to type 1 and 2 veins, the textural, mineralogical and geochemical characteristics of the mesothermal/metamorphic veins indicate a distinctly different origin. These veins contain none of the textural characteristics associated with epithermal veins such as vugs, cockscomb, crustiform and botryoidal textures. None of the typical minerals

associated with type 1 and 2 veins or epithermal veins are present such as chalcedony, opal, kaolinite, dickite and adularia. In addition, no major clay alteration envelope or low pH alteration cap is spatially associated with the mesothermal or the metamorphic veins. The assemblage of quartz, muscovite, plagioclase, apatite, zoisite, tourmaline, rutile, ilmenite, magnetite and pyrite is much more characteristic of the greenschist facies Klondike Series rocks (Turner, 1981). In addition, the quartz that is present is usually strained indicating that it was formed pre- or syn-deformation of the Klondike Schist (late Mesozoic to early Tertiary).

The geochemistry of the mesothermal and/or metamorphic veins (and vein fluids) is significantly different, in comparison to types 1 and 2 veins, indicating a contrasting origin for their formation. Quartz from the mesothermal/metamorphic veins contains higher temperature and higher salinity fluid inclusions in comparison to quartz from type 1 and 2 veins. In addition, abundant CO_2-rich inclusions are often present. The trace element suite is variable depending upon whether the quartz belongs to primary concordant metamorphic bands or to cross-cutting but structurally controlled (by late deformation folding) mesothermal veins in Klondike Schist bearing some form of metalliferous mineralization. Quartz from metamorphic bands that are distinctly syn-metamorphic usually contains trace element concentrations (Debicki *pers. comm.*, 1986) comparable to background values for chemically similar pelitic rocks reported by Turekian and Wedepohl (1961). These quartz bands or veins were formed from greenschist metamorphism during peak deformation of the Klondike Series rocks (middle to late Mesozoic). The mesothermal veins are commonly characterized by anomalous concentrations of the base metal suite of trace elements including Ag, Pb, Zn, Cu, Cr, Co, Se, Te, Bi and minor Au (Debicki *pers. comm.*, 1986). Most of the mesothermal veins are structurally controlled, many of them having been involved in late Cretaceous or early Tertiary folding (Mortensen, 1984). These veins were probably emplaced at much greater depths before or during the last stages of late Mesozoic ductile deformation.

3.5.2.4 Origin of the carbonate veins

Preliminary work on two distinct types of carbonate veins in the Hunker Creek area appears to indicate that these veins are not genetically related to Plio-Pleistocene epithermal activity; however, their origin is as of yet undetermined. The two vein types include carbonate veins hosted by the Hunker Creek rhyolite porphyry or Last Chance Creek volcanics, and carbonate veins hosted by, or associated with, fuchsite-bearing shear zones within schistose units. Veins associated with the volcanics consist of calcite and ankerite with minor barite, fluorite, quartz, chalcedony, Fe-oxides, Fe-hydroxides and pyrite. Classic epithermal textures are common including vugs, brecciation, cockscomb, crustiform and botryoidal textures. In addition, the veins occasionally exhibit clay alteration envelopes. The fluids responsible for deposition of the veins were dominantly CO_2-poor aqueous fluids with moderate salinities (4-12wt.% equivalent NaCl) and homogenization temperatures ranging from 150-250°C. Chemically, the veins contain elements from the epithermal trace element suite including anomalous Au, As, Sb, Hg, Ba, F and S (Debicki *pers. comm.*, 1986). The veins were emplaced post major deformation of the Klondike Schist and bear many similarities to precious-metal veins (Buchanan, 1981). However, it is not clear whether these veins were emplaced in association with an early Tertiary volcanic event or whether they are related to types 1 and 2 veins emplaced during the Plio-Pleistocene alteration of the White Channel deposit.

The carbonate veins associated with shear zones in schistose units differ in textures, mineralogy and trace element chemistry to the volcanic associated carbonate veins. Commonly these veins are associated with sheared contacts between mica-schist (Klondike Schist) and graphitic schist (Nasina Series rocks). Pods of replaced or altered serpentinite are often present in the shear zones. The veins often consist of magnesite and/or dolomite with minor calcite, ankerite and quartz. Fuchsite (Cr-mica) appears to be ubiquitous in both the veins and shear zones. Textually, the veins rarely show any of the classic textures associated with epithermal deposits that types 1, 2 and the volcanic-associated carbonate veins exhibit. The veins are often associated with massive carbonate replacement of serpentinite and occasionally

minor clay alteration of the enclosing host rocks. No fluid inclusion data are available for these veins at present. Several INAA analyses of samples from these veins indicate that Cr, Co, As and Sb are extremely anomalous. In fact three samples analysed with visible fuchsite contained the highest concentrations of Co, As and Sb reported in this study. The origin of these veins, however, is even more unclear than the volcanic-associated veins. Their chemistry and genetic association with shear zones and serpentinite bear a significant resemblance to many of the Au-quartz-carbonate vein deposits described by Nesbitt *et al.* (1986).

3.5.3 Conclusions

Types 1, 2 and 3 veins in the altered footwall rocks below the White Channel gravel are distinct texturally, mineralogically and geochemically from mesothermal and/or metamorphic quartz veins or carbonate veins from around the Klondike district. The field relationships and textures of types 1 and 2 veins indicate that they were emplaced during intense clay alteration of the Footwall zone rocks and overlying Plio-Pleistocene White Channel gravel. These veins also contain classic epithermal textures such as euhedral crystals in vugs, banding, cockscomb, crustiform and botryoidal textures. Type 1 veins consist of quartz and/or chalcedony. Type 2 veins contain siderite and quartz with minor goethite, gypsum and pyrite. Type 3 veins consist of amorphous silicates (opal and poorly crystalline sheet-like silicates), goethite and clay minerals. Fluid inclusion data indicate that the fluid responsible for the deposition of types 1 and 2 veins was a dominantly low salinity (≈1-2wt.% equivalent NaCl), CO_2-poor, aqueous fluid with an average trapping temperature of ≈120-130°C. Anomalous concentrations of Au, As, Sb, Fe, Mn, Ba, P, and S (Co?, Cr?) are present in these veins. The textures, mineralogy, geochemistry and associated clay alteration of these veins is consistent with the characteristics of near-surface (within 100-200m of the surface) geothermal hot-spring deposits, and the upper, near-surface zones of precious-metal deposits. As a result, types 1, 2 and 3 veins and associated alteration are interpreted to be the result of near-surface hydrothermal activity.

In contrast, mesothermal and/or metamorphic quartz veins hosted by the Klondike Schist display characteristics associated with veins formed at higher temperatures and pressures. Typically, these veins contain abundant feldspar, muscovite, zoisite, apatite, tourmaline, rutile, ilmenite and pyrite, with rare open-space and none of the classic epithermal textures. The quartz is usually strained and the platy minerals often show evidence of foliation. In addition, argillic alteration in the surrounding wallrocks is rare. Preliminary fluid inclusion results indicate that the trapped fluid responsible for deposition of these veins is characterized by moderate salinity (5-12wt.% equivalent NaCl), sporadic but usually abundant CO_2, and temperatures ranging from 160-330°C (without pressure corrections). The metalliferous mesothermal veins are usually characterized by anomalous concentrations of the "base-metal" trace element suite. The metamorphic quartz veins typically contain negligible amounts of most trace elements. The extent of the mesothermal and/or metamorphic quartz veins is dominantly controlled by late stage metamorphic and/or deformational fabrics (Mortenson, 1984) within the Klondike Schist indicating that these veins were emplaced during late stage orogenic events. The mineralogy, textures and geochemistry of these veins is consistent with either quartz veins emplaced during regional metamorphism and deformation (sometime during the middle to late Mesozoic) or base-metal mesothermal veins emplaced during the later stages of deformation.

4. GENESIS OF THE DEPOSIT AND CONCLUSIONS

4.1 Summary Of Relevant Data

4.1.1 Alteration zones

Post-depositional hydrothermal alteration of the Plio-Pleistocene White Channel gravel and the underlying bedrock can be divided mineralogically and chemically into three zones; Bleached zone gravel, Iron zone gravel and altered Footwall zone rocks. Alteration in all three zones is characterized by intense secondary clay mineral development with a ten to twenty fold increase in the amount of material in the clay size fraction (the $<2\mu m$ size fraction) relative to unaltered gravel or bedrock. Alteration in the uppermost zone (Bleached zone gravel) is characterized by the presence of secondary kaolinite and minor illite, both with poor to moderate crystallinities. The oxides Fe_2O_3 (total Fe), MgO, Na_2O and K_2O generally are depleted while LOI (loss on ignition) is increased relative to unaltered gravel. The trace element chemistry of the Bleached zone gravel is the same in comparison to unaltered gravel.

Alteration in the Iron zone gravel (2-4 meter zone directly above bedrock) is dominantly characterized by the presence of secondary kaolinite, illite (and/or muscovite), goethite, lepidocrocite, hematite, smectite, gypsum and adularia. The clay minerals kaolinite and illite, in addition to the Fe-hydroxides (goethite and lepidocrocite), are all highly crystalline. The major oxide chemistry is irregular, as Fe_2O_3 and LOI values are increased dramatically, and MgO, Na_2O and K_2O values fluctuate from unchanged to depleted in comparison to unaltered gravel. Concentrations of the elements (maximum concentrations detected are in parentheses) MnO (6.55%), P_2O_5 (0.73%), S (490ppm), Ba(15,000ppm) and As (1,560ppm) are significantly higher than the values obtained for unaltered gravel. In addition, anomalous concentrations of Sb (45.5ppm), Co (110ppm) and Cr_2O_3 (810ppm) were detected in this zone.

Intense clay alteration often extends 5-10 meters into the footwall rocks below the gravel contact. Pervasively altered cobbles and gravel directly overlying altered bedrock

indicate that both units were altered contemporaneously after the deposition of the gravel. Altered bedrock in the Footwall zone contains secondary kaolinite, illite and interstratified expandable minerals (either illite/smectite or chlorite/smectite). In general, kaolinite and illite are well crystallized. The major oxide concentrations generally decrease with increasing LOI and the corresponding increase in degree of clay alteration. Little change is evident in the concentrations of P_2O_5, S, Mn, Ba, and As with increasing clay alteration of the bedrock below the gravel contact.

4.1.2 Veins in altered Footwall zone rocks

Three types of veins appear to have been emplaced during hydrothermal alteration of the Footwall zone rocks and the overlying White Channel gravel. Replacement textures, incorporated clay-altered bedrock and the morphologies of these veins indicate that they were emplaced during the alteration of the footwall rocks. The division of the three vein types is based upon mineralogy, textures and morphology. These syn-alteration veins are easily distinguished from mesothermal and/or metamorphic quartz veins which are also present within the host footwall rocks.

Type 1 veins contain quartz and chalcedony with minor kaolinite, dickite, illite, Fe-hydroxides, hematite, Fe-carbonate and pyrite. The veins are generally <2-3cm in thickness (occasionally 10-20cm thick) and show characteristic epithermal textures including vugs with euhedral quartz, cockscomb, cockade and crustiform textures. Fluid inclusion analyses indicate that type 1 veins were formed from a low salinity (≈1.7wt.% equivalent NaCl), CO_2-poor aqueous fluid that was trapped at an average temperature of 120-130°C. Significant concentrations of Au (280ppb), As (97ppm), Sb (27.9ppm) and Fe_2O_3 (8.44%) (Hg, Tl, Ba, Mn, P and S were not analysed) have been detected in the veins and the clay-altered host rock immediately adjacent to type 1 veins (maximum concentrations detected are in parentheses).

Type 2 veins are composed of siderite and quartz with minor amounts of ankerite, calcite, goethite, gypsum, hematite, pyrite and clay minerals. Type 2 veins are generally

<1-2cm in thickness; however, associated concretions attain thicknesses of 10-30cm. Common textures in the type 2 veins include botryoidal growth structures, replacement and banding with minor vugs. Fluid inclusion measurements on associated quartz indicate that the veins formed from a fluid similar to that responsible for type 1 veins with <1-2wt.% equivalent NaCl, no visible CO_2 and average temperatures of 120-130°C. Anomalous concentrations of Fe_2O_3 (62.25%), MnO (1.17%), P_2O_5 (0.20%), S (2,800ppm) and Ba (5,410ppm) with minor As (<2ppm) were detected (Sb, Hg and Tl were not analysed). Several samples assayed for Au contained negligible concentrations (<5ppb)

Type 3 veins consist of microfractures in clay-altered footwall rocks containing smectite (or an interstratified smectite mineral) and either goethite or amorphous silicates. The microfractures are generally <1-2cm in thickness. Samples from Trail Hill contain a hard (4-5 on Moh's hardness scale), fibrous, amorphous silicate similar to lussatite (a variety of opal). Samples from Dago Hill contain a soft material which is also amorphous. The softness of the material indicates that the amorphous phases are probably poorly crystalline "clay-like" minerals. Anomalous concentrations of Fe_2O_3 (73.78%), MnO (1.86%), P_2O_5 (0.43%), S (900ppm), Ba (1,020ppm) and As (36ppm) were detected. Concentrations of Au were negligible (Sb, Hg, Tl, Co and Cr were not analysed).

4.1.3 Gold distribution

Significant differences occur in the distribution of gold in altered versus unaltered White Channel gravel. The greatest concentration of gold present in unaltered White Channel gravel is present in the lowest 1-2 meters of gravel and decreases dramatically upsection. Unaltered (1) to slightly (2) altered White Channel gravel at Adams, Cripple, Lovett, Monte Cristo and Trail Hills often contains concentrations of 0.1 to >1ppm gold in the lower 1-2 meters of gravel. In the 2-4 meter interval above bedrock gold concentrations usually range from approximately 0.02-0.1ppm. Above the lower 4 meter zone, gravel generally contains concentrations significantly less than 0.02ppm gold (calculations based upon the data of Gleeson, 1970; McConnell, 1907). Morison (1985) indicates that gold concentrations in the

unaltered White Channel gravel of these hills is restricted to specific gravel facies types. In addition, he suggests that high concentrations of gold at or near the bedrock surface are the result of an increase in the number of proximal facies types that contain placer gold and the presence of available lode sources (local point sources). The concentration of gold decreases up-section in unaltered gravel; however, the concentrating processes improve up-section indicating that initial lode sources of gold were depleted quickly with progressive erosion (Morison, 1985).

In contrast to unaltered White Channel gravel, the distribution of gold in altered gravel appears to be more uniform throughout a section and not related to specific facies types. Sampling of altered gravel at Dago Hill (Morison *pers. comm.*, 1986) shows that visible gold was found in all samples of strong (4) to extremely (5) altered gravel that were sluiced, irregardless of sedimentary facies type. Above the alteration contact, in primary White Channel gravel, the samples were barren of visible gold. Concentrations in similar sections of altered gravel at Dago Hill were calculated from gold grade estimates provided by Stutter and Warmsby (*pers. comm.*, 1985). Gold concentrations in altered gravel decrease gradually from ≈1.5ppm at the bedrock contact to ≈0.3ppm at 10 meters above bedrock. The upper limit of the actively mined ore zone occurs between 6-10 meters above the bedrock contact. The gold concentration is ≈0.15ppm at 20 meters above bedrock. The concentration of gold in altered gravel does not fall significantly below 0.1ppm except in gravel more than 20 meters above the bedrock contact. This gradual decrease in the gold concentration of altered gravel with elevation above bedrock sharply contrasts with the gold distribution in unaltered gravel. The concentration of gold at hills with unaltered gravel drops below 0.1ppm at 2-4 meters above bedrock. As a result, the distribution of gold in altered White Channel gravel is interpreted to be genetically related to alteration.

Mineable gold concentrations have been found to occur in outcrops of intensely clay-altered bedrock. Although no quantitative data are available to characterize the distribution of gold in altered Footwall zone rocks below the White Channel gravel, several observations have been made. Firstly, gold has been recovered from altered bedrock below the

White Channel gravel at several hills including the section described at Trail Hill (chapter 2). Gold was recovered in economic proportions (several thousand ounces) from 10-12 meters of depth into intensely clay-altered bedrock from the Trail Hill section (Morison *pers. comm.*, 1986). In addition, type 1 veins at Dago and Paradise Hills contain anomalous values of gold. This indicates that some gold exists in, and is genetically related to alteration of the Footwall zone rocks. The actual concentration and distribution of gold in relationship to hydrothermally altered bedrock below the White Channel deposit is sporadic and not well documented.

The significant increase in the concentration of gold in clay-altered White Channel gravel and, occasionally, in altered footwall rocks is interpreted to be the result of post-depositional hydrothermal activity in the White Channel deposit. This interpretation is supported by several pieces of evidence including the following;

1. The distibution of gold in altered White Channel sediments is atypical of the normal placer gold distribution in unaltered gravel from around the Klondike district.
2. The White Channel deposit has undergone a post-depositional, Plio-Pleistocene hydrothermal event with anomalous concentrations of As, Sb, Ba, Fe, Mn, P and S having been detected in altered Iron zone gravel.
3. Low-temperature, epithermal veins emplaced during the alteration of the Footwall zone rocks and the overlying White Channel gravel contain anomalous concentrations of Au, As, Sb, Ba, Fe, Mn, P and S. Not only is this trace element pattern similar to that of the Iron zone gravel, but these elements are common indicators of epithermal gold mineralization throughout the American and Canadian Cordillera (Berger, 1985; Buchanan, 1981).

4.2 Genesis Of The Deposit

Based upon the mineralogical and geochemical features of alteration and associated veining in the White Channel deposit, it is possible to place constraints on the origin of the fluid involved in this Plio-Pleistocene hydrothermal event. In addition, it is possible to

speculate on the probable transport and depositional mechanisms of the gold based upon the geochemical characteristics and the similarities of the fluids responsible for alteration of the White Channel deposit to the fluids involved in many hot-spring epithermal deposits and geothermal systems.

4.2.1 Environment of deposition

4.2.1.1 Types 1, 2 and 3 Veins

The timing of emplacement, textures and mineralogy of types 1, 2 and 3 veins suggest that they were formed in the near-surface environment. Partial replacement and cementation of the clay-altered bedrock by types 1 and 2 veins indicates that emplacement of the veins occurred during alteration of the Footwall zone rocks and the overlying White Channel gravel. The White Channel deposit probably reached a maximum thickness of 100-150 meters, constraining the maximum depth of emplacement for types 1, 2 and 3 veins to ≈150-175 meters. Characteristic epithermal textures such as vugs with euhedral quartz, banding, cockscomb, crustiform and cockade textures support a near-surface origin for these veins (Buchanan, 1981). In addition, the presence in these veins of phases such as chalcedony and lussatite (amorphous silica similar to opal) indicate a maximum depth of formation of 100-200 meters for types 1, 2 and 3 veins (Hedenquist and Henley, 1985b).

The mineralogy and fluid inclusion data indicate that types 1, 2 and 3 veins were formed from low temperature, low salinity, aqueous fluids that were close to saturation with respect to amorphous silica. The average trapping temperature for inclusions in quartz from types 1 and 2 veins is ≈120-130°C and the average salinity is ≈1.7wt.% equivalent NaCl. The majority of the samples show consistent inclusion filling ratios and therefore little evidence of boiling. One or two samples showed variable inclusion filling ratios and homogenization temperatures which might indicate localized boiling. Vein phases such as chalcedony, lussatite, kaolinite, dickite, and Fe-hydroxides are also indicative of deposition at temperatures in the range of 100-150°C. At these temperatures the fluids were probably close to saturation with amorphous silica (oversaturated with respect to quartz) as indicated by the presence of

amorphous silicates in type 3 veins. However, quartz veining and silicification (either opal or quartz dominated) in the Footwall zone rocks is minor in relationship to the amount of clay alteration present. There are at least two reasons for the minor quantities of quartz veining and silicification. First, is the kinetic problems associated with the precipitation of SiO_2 phases from fluids at temperatures less than 150°C without extreme supersaturation with respect to each of the phases (Fournier, 1985). The other problem would have involved the high permeability of the units being altered (especially the White Channel gravel) causing the dispersion of the fluid over a large area.

The trace element geochemistry of types 1, 2 and 3 veins bears a distinct resemblance to the trace element patterns associated with active geothermal systems and precious-metal deposits (Berger, 1985; Buchanan, 1981; Ewers and Keays, 1977; Weissberg *et al.*, 1979). Substantial trace element enrichments of Au, As, Sb, Ba, Mn, P and S are similar to concentrations of elements (Au, Ag, As, Sb, Hg, Tl, Ba, Fe, Mn, P and S) in the geothermal waters and surface precipitates of Broadlands and Warakei, New Zealand (Ewers and Keays, 1977; Weissberg et al., 1979), Reykjavik, Iceland (Olafsson and Riley, 1978) and Steamboat Springs, U.S.A. (Stauffer et al., 1980; Stauffer and Thompson, 1984). In addition, this suite of elements is commonly found in association with many epithermal gold deposits of Nevada, U.S.A. (Berger, 1985; Buchanan, 1981). In most of the deposits mentioned above, highly anomalous concentrations of Au, As, Sb, Hg and Tl are usually restricted to geothermal fluids, pool and well precipitates, alteration zones and veins that are present or were deposited within several hundred meters of the paleosurface. This is consistent with the concentrations of trace elements that exist in, and the depth of formation proposed for types 1, 2 and 3 veins.

4.2.1.2 Hydrothermal alteration

Mineral equilibria in the system K_2O-Al_2O_3-SiO_2-H_2O suggest that either a decrease in the temperature of the mineralizing fluid and/or oxidation of Fe^{2+} to Fe^{3+} is responsible for the mineral zonation observed in the White Channel deposit. A temperature versus log (aK^+/aH^+) diagram (figure 4.19) was constructed using thermodynamic data from Helgeson *et*

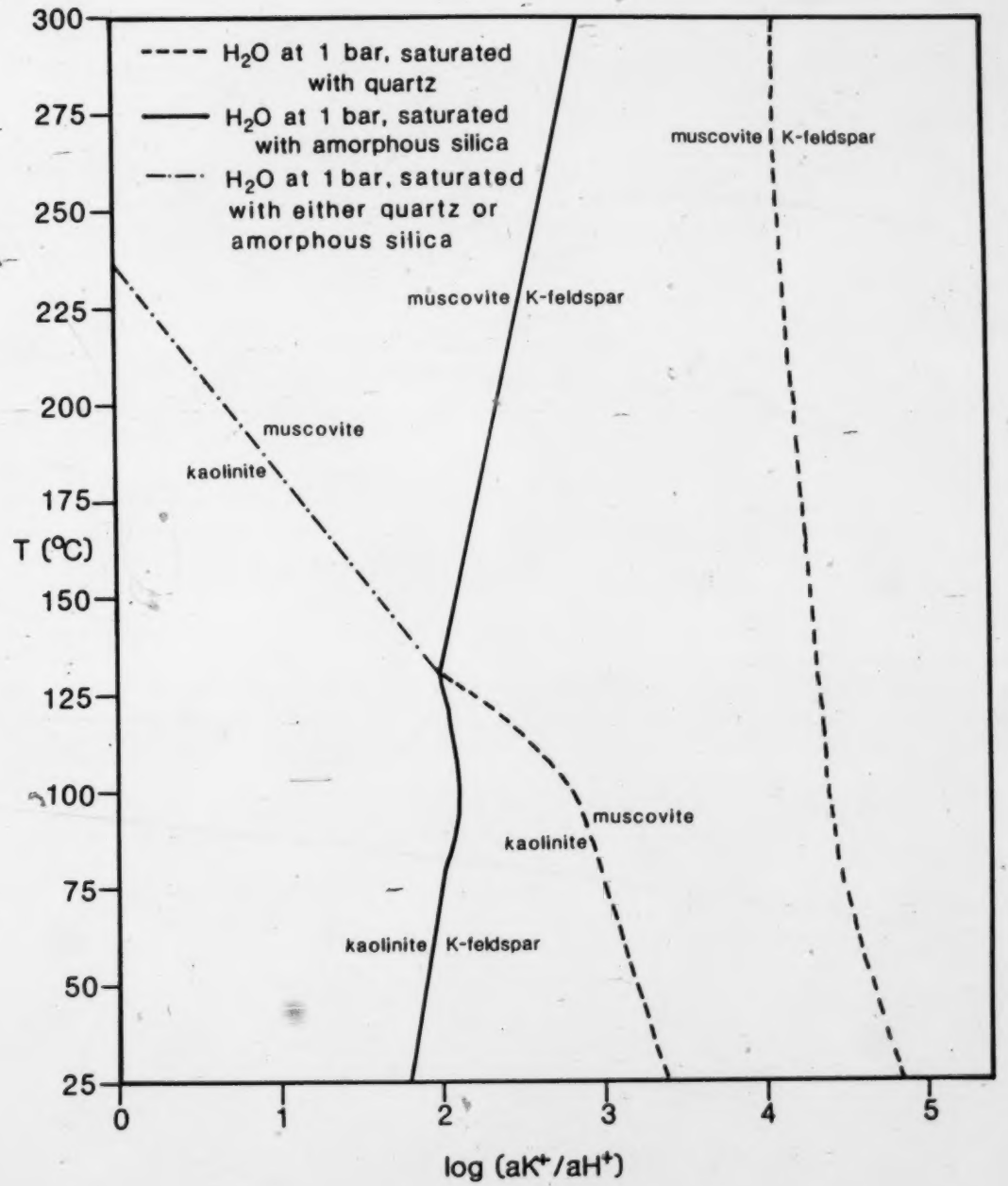

Figure 4.19 A plot of temperature versus log (aK^+/aH^+) for the system K_2O-SiO_2-Al_2O_3-H_2O. Aluminum is conserved in the reactions and the activities of solids and H_2O are assumed to be 1. The data for the reactions is from Helgeson *et al.* (1978).

al. (1978) and the SUPCRT program. The solid boundaries represent equilibrium reactions in the presence of excess amorphous silica and water. Dashed boundaries represent saturation with quartz and water. All the reactions assume conservation of aluminum between the reacting phases. Phases bearing Mg, Ca and Na were purposely avoided in figure 4.19 as these phases are usually minor if present at all. In addition, bulk chemistry indicates the presence of minor concentrations of Mg, Ca and Na in comparision to K. Thermodynamic data for muscovite are used to approximate the thermodynamic properties of illite due to the lack of quality data for illite and for the reason of simplicity. The data used for K-feldspar in the diagram is that of adularia. The diagram is constructed for 1 bar pressure, as little change occurs in the thermodynamic data for pressures up to 40 bars (the maximum pressure estimate for hydrothermal alteration of the White Channel deposit). The dominant secondary mineral assemblage in the altered Footwall zone rocks and the Iron zone gravel consists of kaolinite + muscovite(and/or illite) ± adularia. Abundant primary detrital quartz is also present. Figure 4.19 (solid boundaries) shows an invariant point at ≈125-130°C and log (aK^+/aH^+) equal to 2 where all three of the above mentioned secondary phases are stable in a fluid saturated with respect to amorphous silica. The temperature indicated by the alteration assemblage is consistent with the average temperatures obtained from fluid inclusions in type 1 quartz/chalcedony veins. In addition, these temperatures are required to produce the high crystallinities of kaolinite, muscovite (and/or illite) and lepidocrocite present in the two alteration zones. A fluid saturated with amorphous silica was chosen in constructing this diagram for two reasons. First, a fluid saturated with respect to quartz (dashed boundaries) fails to explain the observed secondary mineral assemblage in the two lowermost zones of alteration. Secondly, evidence of saturation with amorphous silica is present in types 1 and 3 veins, as chalcedony, lussatite (a form of opal) and other unidentifiable amorphous silicates have been observed.

The secondary mineral assemblage in the gravel of the overlying Bleached zone can be explained by a number of fluid changes upon migration of the fluid from the bedrock-gravel contact upwards. The secondary mineral assemblage of the Bleached zone gravel consists of

kaolinite with minor amounts of illite. In places, illite occurs in significant amounts; however, a corresponding decrease in the degree of alteration leaves doubt as to whether the illite is secondary or detrital in origin.

Although several possibilities exist, three major processes that occurred at the site of alteration in the Iron zone can explain the changes in the fluid parameters that resulted in the secondary mineral assemblage of the overlying Bleached zone. First, a drop in temperature must have occurred as the hydrothermal fluid either (a) mixed with cool, near-surface, meteoric water, and/or (b) cooled in response to interaction with the host units. The second process that occurred at the site of alteration in the Iron zone consisted of an increase in the aH^+ (decrease in pH), which probably resulted in a decrease in the aK^+/aH^+ ratio. This process occurred in response to the oxidation of Fe^{2+} carried by the hydrothermal fluid. The Iron zone gravel contains highly anomalous amounts of total Fe in the form of Fe-hydroxides. Textures and their high crystallinities indicate that the Fe-hydroxides were precipitated directly from solution rather than forming as *in situ* oxidation products of other minerals. The oxidation of Fe^{2+} probably occurred, as illustrated in the reaction below, during mixing of oxygenated meteoric and Fe-bearing hydrothermal fluids.

$$Fe^{2+} + 3H_2O \rightarrow Fe(OH)_3 + 3H^+ + 1e^-$$

A third, minor process that probably occurred during Iron zone alteration invloved a decrease in the aK^+ due to the formation of K-bearing minerals. This would also have resulted in a decrease of the pH and the aK^+/aH^+ ratio.

The presence of well crystallized, secondary lepidocrocite ($\gamma FeOOH$) within the Iron zone gravel indicates that the hydrothermal fluid met certain conditions at the site of deposition. Experimental work on the formation of lepidocrocite (Schwertmann and Taylor, 1972a and 1972b; Schwertmann and Thalmann, 1976) indicates that it only forms between pH's of 5-7. In addition, it only forms during rapid oxidation of Fe^{2+} in solution. Field observations support the experimental results in that lepidocrocite is exclusively found in hydromorphic soils where Fe^{2+} is formed during anaerobic conditions due to bacterial activity (Schwertmann and Fitzpatrick, 1977). This suggests that the hydrothemal fluid responsible for

the alteration of the gravel in the Iron zone contained an aH^+ between 10^{-5} and 10^{-7}. In addition, Fe^{2+} in solution, was oxidized quickly, probably due to the mixing of the Fe^{2+}-bearing hydrothermal fluid with near-surface meteoric water.

The secondary mineral assemblage of gravel in the Bleached zone indicates that at least two and probably all three of the above mentioned changes in the fluid parameters occurred. Several clay-altered rhyolite cobbles from 2-4 meters above the bedrock contact, within the Bleached zone gravel, contain secondary kaolinite and adularia. This assemblage is easily explained in figure 4.19 by a decrease in the temperature of a fluid at a relatively constant aK^+/aH^+ ratio. This process causes the fluid chemistry to shift from the invariant point at ≈125-130°C along the unvariant curve where kaolinite and adularia coexist. This assemblage also supports the interpretation that the hydrothermal fluid was close to saturation with respect to amorphous silica, as kaolinite+adularia would not be a stable assemblage in a fluid saturated with quartz only (dashed boundaries in figure 4.19). Alteration of gravel in the Bleached zone, however, is dominantly characterized by kaolinite with minor illite. The kaolinite dominated alteration can be explained by a simple decrease in the aK^+/aH^+ ratio, or probably more realistically by a decrease in this ratio and a decrease in temperature. The decrease in the aK^+/aH^+ is easily facilitated by the oxidation of Fe^{2+} and HS^- which in turn produces significant amounts of H^+. This would have caused the fluid composition to migrate into the kaolinite field, resulting in the metastablility of illite and K-feldspar. One other possible scenario exists that explains the coexistence of secondary kaolinite and illite. A decrease in the concentration of $SiO_2(aq)$ would shift the kaolinite+K-feldspar curve to a higher aK^+/aH^+ ratio. This coupled with a simple temperature decrease would explain the formation of coexisting secondary kaolinite and illite. This scenario could explain the small pockets of altered gravel in the Bleached zone where kaolinite and illite occur in approximately equal proportions.

Alteration in the White Channel deposit lacks the sulphate-bearing minerals that are common to many of the near-surface geothermal systems and precious-metal deposits. Minerals such as alunite ($KAl_3(SO_4)_2(OH)_6$) and jarosite ($KFe_3(SO_4)_2(OH)_6$) commonly

occur with kaolinite in an alteration zone that is often termed a low pH cap or acid-sulphate cap in these types of deposits. Both sulphate phases are most stable at ambient temperatures, decreasing in stability with increasing temperatures (Knight, 1977). The equilibration of alunite or jarosite in a solution saturated or oversaturated with quartz requires large values of aH^+ and aSO_4^{2-} regardless of temperature. In the case of alunite it is suggested that at surface temperatures continuous fluid conditions of pH<4 and SO_4^{2-} >100ppm are necessary to produce significant amounts of alunite (Knight, 1977). The activities of H^+ and SO_4^{2-} must be even greater to form alunite at higher temperatures. The chemistry of the Iron zone gravel indicates that an increase of S did occur during alteration. However, alunite or jarosite are not present, probably because the pH of the mineralizing fluid was to high and/or the concentration of SO_4^{2-} was too low.

4.2.2 Origin of the fluid

Unpublished oxygen isotope data on quartz from types 1 and 2 veins indicate a range of $\delta^{18}O$ (relative to SMOW) values between -3 and +7‰, with an average of ≈+4‰ (Dufresne, Longstaffe and Nesbitt, in prep.). These results, in conjunction with fluid inclusion analyses that indicate a trapping temperature of ≈125°C, suggest that the mineralizing fluid had a $\delta^{18}O$ range from -22 to -12‰, with an average of approximately -15‰ (Dufresne, Longstaffe and Nesbitt, in prep.). Comparison of these $\delta^{18}O$ values with the meteoric water line (Taylor, 1979) and unpublished values for meteoric fluids in the Klondike district (performed by F.A. Michel at the University of Waterloo) indicate that the mineralizing fluid responsible for the deposition of types 1 and 2 veins, and the associated clay alteration, was meteoric in origin with a slight to moderate enrichment of ^{18}O. Oxygen isotope studies from a variety of epithermal gold deposits in the western United States and the Canadian Cordillera show a similar involvement of isotopically unchanged meteoric water responsible for mineralization and alteration (Nesbitt *et al.*, 1986; O'Neil and Silberman, 1974; Taylor, 1979).

The suite of trace elements present in types 1 and 2 veins, and the Iron zone gravel is also indicative of meteoric water dominated geothermal systems and epithermal precious-metal deposits. Anomalous values of Au, As, Sb, Ba, Fe, Mn, P and S (also Co?, Cr?) are present in the veins and the Iron zone gravel (Hg and Tl not analysed). This suite of elements is very similar to the precious-metal suite of elements found in surface precipitates and pool waters of many geothermal systems (Berger, 1985; Ewers and Keays, 1977; Weissberg *et al.*, 1979; White, 1985). In addition, the precious-metal suite of elements are ubiquitous in veins and associated alteration zones formed either in the near-surface and/or low temperature environment of most epithermal precious-metal deposits derived from meteoric fluids (Berger, 1985; Buchanan, 1981; Tooker, 1985).

4.2.3 Transport and deposition of gold

The distribution of gold in the altered White Channel gravel of Dago, Preido, Paradise and Nugget Hills appears to indicate a genetic relationship between alteration and gold distribution. Significant amounts of gold appear to have been added to altered gravel, and in places Footwall zone rocks during hydrothermal alteration; however, quantifying the actual amount of gold added during alteration is impossible at this stage without a more detailed characterization of the extent, distribution and types of gold present in the White Channel deposit. Nevertheless, several questions remain such as; was the fluid that was responsible for alteration capable of transporting and depositing gold in the White Channel deposit? If so, what were the mechanisms of gold transport and deposition of the ore-forming fluid? These questions are not only important in determining the genesis of this deposit, but they have major implications for exploration targets in the Klondike and other districts where similar processes may have been active. These types of questions can be answered with a few assumptions based upon the characteristics of the mineralizing fluid and knowledge of the solubility of gold in certain hydrothermal environments.

4.2.3.1 Transport of gold

The amount of gold that this fluid was capable of transporting can be qualitatively examined using certain characteristics of the fluid at the site of deposition, well known geochemical characteristics of similar geothermal fluids, and assuming that the transporting fluids were probably in equilibrium with the Klondike Schist. The solubility of gold is presented in a log aO_2 versus pH diagram (figure 4.20) and a log $a\text{Au(HS)}_2^-$ versus temperature diagram (figure 4.21). Both diagrams have been taken from Shenberger (1985) and modified to fit the probable geological and geochemical conditions of the fluid involved in the alteration of the White Channel deposit. The assumptions that have been made about the ore-forming fluids in order to construct these diagrams are detailed in the following section.

The dominantly meteoric fluid responsible for alteration in the White Channel deposit was characterized by low salinities. As a result, gold-chloride complexing was probably not a significant factor in the transport of gold. Figure 4.20 shows that given the right conditions significant amounts of gold (>1ppm Au) can be transported as a gold-bisulphide complex in a hydrothermal fluid. Sulphur is anomalous in the Iron zone gravel and in types 1, 2 and 3 veins associated with the alteration of the White Channel deposit. This indicates that the gold-bisulphide complex was the likely transporting agent in the gold-bearing fluids.

In figure 4.21, Shenberger (1985) illustrates gold solubility as a function of temperature under reasonable geological and geochemical conditions. He calculates gold solubility in a solution containing total sulphur=0.01m (≈320ppm), total K^+=0.1m (≈4,000ppm), and saturated with respect to quartz. In addition, he uses the presence of K-feldspar and K-mica to buffer the pH of the solution (at ≈5.5), and a ratio of SO_4^{2-}: HS^- of 1 to buffer the activity of oxygen in the solution. Under these conditions the solubility of gold is ≈200ppb at high temperature (250°C). The solubility increases with decreasing temperature, peaking with a maximum gold solubility of 300-400ppb at approximately 150°C (figure 4.21). Below approximately 100°C the solubility of gold drops off significantly assuming the fluid composition remains constant. The fluid he has described in this situation could easily form a precious-metal deposit providing that hydrological processes are able to

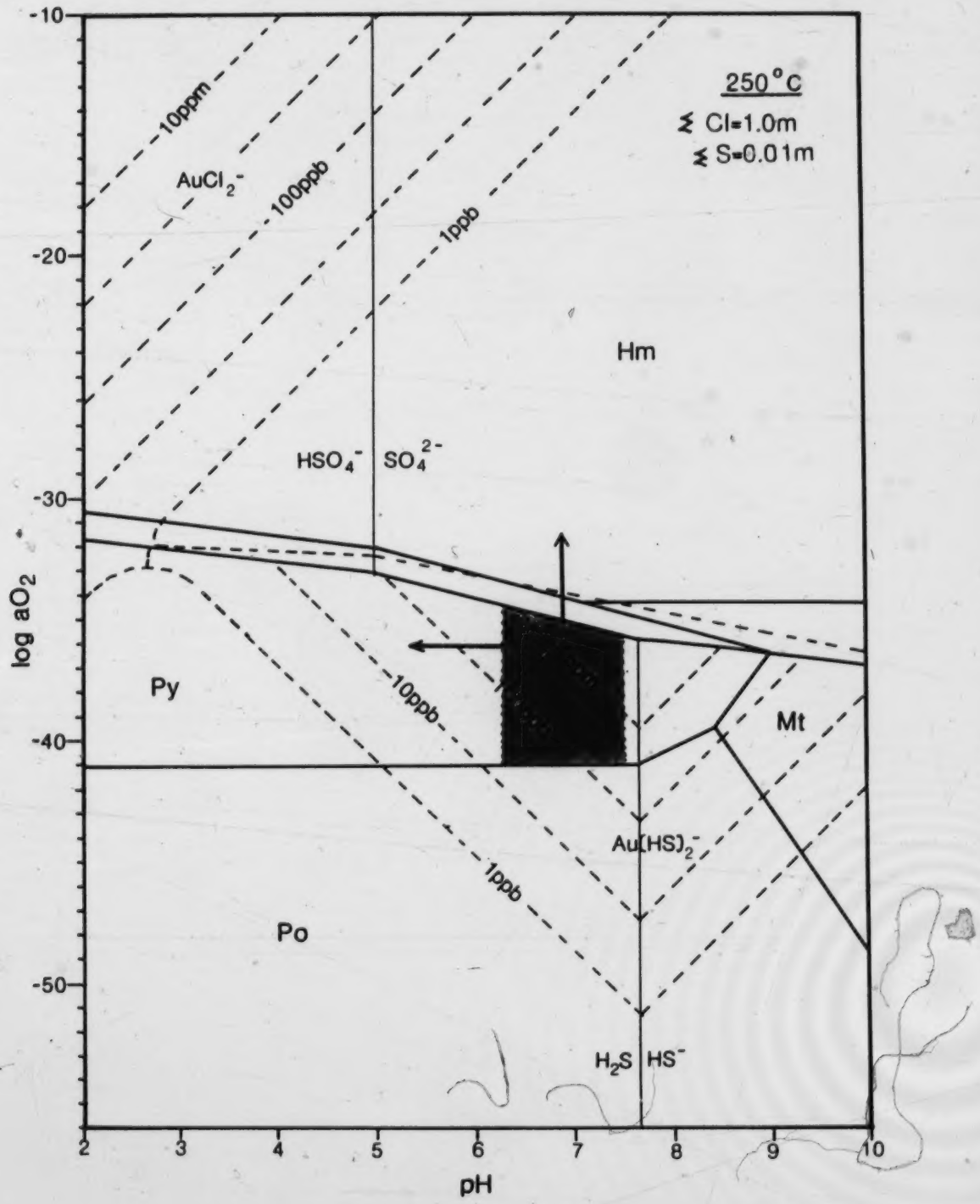

Figure 4.20 A plot of log aO_2 versus pH in the system Au-Fe-S-Cl-H_2O at 250°C (modified after Shenberger, 1985).

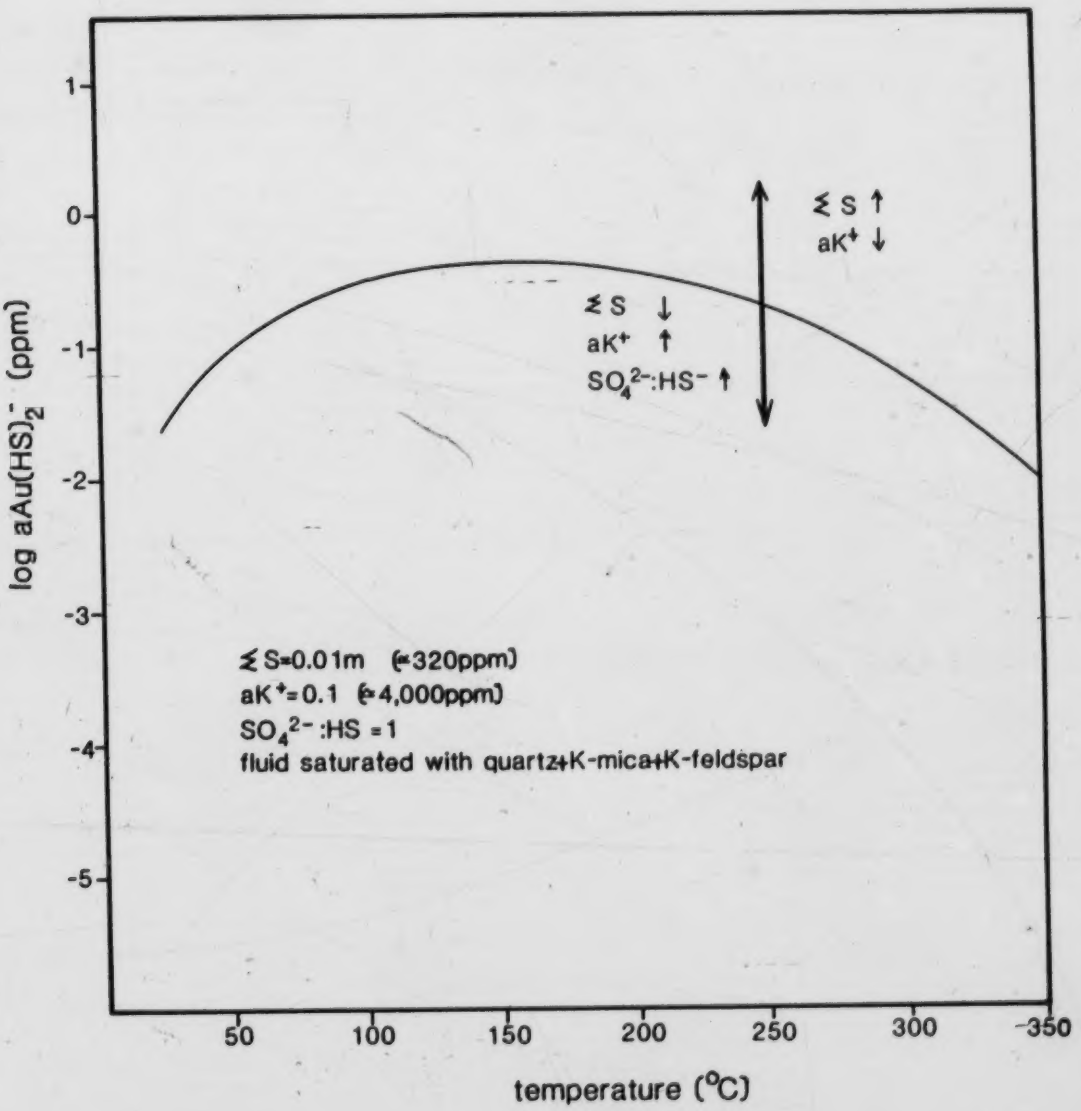

Figure 4.21 A plot of the solubility of gold as $\log(Au(HS)_2^-)$ versus temperature in a solution buffered by the assemblage of quartz+K-feldspar+K-mica and $SO_4^{2-}:H_2S(aq)=1$ (modified after Shenberger, 1985).

spatially concentrate the gold-bearing fluid, and suitable depositional mechanisms are able to precipitate the gold in a small volume of rock.

The geochemical characteristics of the mineralizing fluid involved in the alteration of the White Channel deposit suggest that it also could have been responsible for the transport of significant amount of gold in solution. The fluid contained approximately 1.7wt.% equivalent NaCl. Similar low salinity fluids in many meteorie-dominated geothermal systems usually contain anywhere between 50 and 500ppm K^+ (1.25×10^{-2}-1.25×10^{-1}m) in solution (Ellis, 1979). The total amount of sulphur in solution was probably similar to the concentration Shenberger (1985) selected ($\Sigma S = 0.01$m, ≈320ppm S), as the sulphur content of reported geothermal fluids ranges from approximately 20 to 800ppm (Ellis, 1979). If it is assumed that these fluids reached equilibrium with the Klondike Schist during fluid circulation and migration, then the fluids were probably buffered by the assemblage of quartz, K-mica, K-feldspar, albite and pyrite. Assuming $\Sigma S = 0.01$m than the shaded box in figure 4.20 approximates the range of solubilities for gold in a solution that contains 20-500ppm K^+, and is in equilibrium with quartz+K-mica+K-feldspar at 250°C. The pH of the fluid would be buffered by a constant aK^+/aH^+ ratio. Between 300°C and 100°C the log (aK^+/aH^+) ratio is relatively constant for coexisting K-mica+K-feldspar varying from ≈4.1 to 4.4 respectively. A solution containing 20 or 500ppm K^+ at 250°C would have pH's of 7.5 and 6.1 respectively. This pH range is consistent with pH's of dilute meteoric-dominated geothermal fluids at 250°C (Ellis, 1979). In addition, the deposition of lepidocrocite during alteration indicates a pH range of 5-7 for the mineralizing fluid (Schwertmann and Thalmann, 1976). The upper boundary of the shaded region indicates a high gold solubility in a solution that is buffered with a $H_2S(aq):SO_4^{2-}$ ratio of 1. The lower boundary represents a solution that is buffered by the presence of pyrite and pyrrhotite. A shallow circulating meteoric fluid in equilibrium with the Klondike Schist would probably have been buffered in the pyrite field somewhere between the two extremes of $H_2S(aq):SO_4^{2-}$ ratios described above. As a result, a fluid that reached equilibrium with the Klondike Schist under the conditions discussed above would plot within the shaded area of figure 4.20. Depending upon the duration of the geothermal event, fluid

flow rates and the efficiency of the depositional mechanism a resonable sized gold deposit could be formed from this fluid even at the low end of the solubility region. For instance, a fluid carrying 10ppb gold at a reasonable geothermal fluid flow rate of $3.7x10^{-3}km^3$/year (White, 1981) could deposit 10 million troy ounces of gold (the recorded production for the Klondike district) in approximately 16,800 years, given that 50% of the gold carried in solution is deposited in close spatial association. White (1981) indicates that realistic lifetimes for geothermal systems probably range from 10,000-1,000,000 years, providing more than enough time to form an ore deposit of the magnitude that must have been present in the Klondike.

4.2.3.2 Deposition of gold

A significant amount of finely disseminated gold appears to have been added to the White Channel sediments during alteration. In addition, small concentrations of gold were added to the altered footwall rocks and associated veins. Several processes during alteration could have triggered gold deposition from the ore-forming fluids and explain the apparent genetic relationship between gold and alteration within the White Channel deposit. However, at this stage with a relatively poor understanding of the exact distribution of gold it is difficult to narrow the triggering mechanism to one process from geological and geochemical evidence at the site of deposition.

The two major processes that occurred at the site of deposition in the White Channel gravel include a temperature decrease and oxidation. No real evidence is present that indicates significant boiling of the mineralizing fluid occurred. The decrease in temperature of the ore-forming fluid probably occurred in response to water-wall rock interaction and mixing with a cool, near-surface meteoric fluid. Significant oxidation of Fe^{2+} and HS^- probably occurred in response to mixing with a well oxygenated meteoric fluid as well. The result of oxidation is an increased activity of H^+ which probably caused a drop in pH at the site of deposition.

Even though figure 4.20 is constructed for Au solubility data at 250°C, in principle mechanisms that can cause precipitation of gold at that temperature should also be viable

mechanisms at 150 to 25°C. Perhaps the quickest and easiest method of gold deposition evident from figure 4.20 is simply oxidation. At a pH of ≃7 and SO_4^{2-}:H_2S(aq) ratio of ≃1, gold is soluble as an $Au(HS)_2^-$ complex to concentrations >1ppm. An increase in the activity of O_2 of approximately 1 to 2 log units would dramatically increase the SO_4^{2-}: H_2S(aq) ratio, resulting in the complete destabilization of the $Au(HS)_2^-$ complex, dropping the concentration of $Au(HS)_2^-$ to ≃1ppb. This mechanism could easily have been responsible for gold deposition in the White Channel gravel during fluid mixing in the Iron zone gravel.

Oxidation also results in a significant increase in the activity of H^+. In a solution in equilibrium with pyrite+pyrrhotite an increase in the activity of H^+ equivalent to ≃1 pH unit would drop the solubility of gold from ≃100ppb (at a pH of ≃7.1) to a solubility of ≃10ppb (at a pH of ≃6.1) resulting in the precipitation of 90% of the gold in solution. If significant amounts of H^+ were produced quickly during mixing of shallow meteoric fluid and the ascending ore-forming fluid, then pH decreases could also have been an adequate mechanism of gold deposition. In addition, mixing of the ore-forming fluid with dilute surface waters would decrease the activity of sulphur, causing a decrease in the activity of the gold-bisulfide complex, resulting in the precipitation of gold also.

A fourth possible mechanism for gold deposition involves simply a decrease in temperature of the ore-forming fluid. Figure 4.21 shows that gold solubility in the ore-forming fluid probably peaked at ≃225-125°C. Below 125°C and down to 25°C the solubility of gold drops off dramatically from ≃0.5ppm to ≃0.01-0.02ppm. A drop in temperature of the ore-forming fluid obviously occurred; however, it is difficult to determine whether the observed gold distribution in altered White Channel gravel was a function of decreasing temperature, oxidation of $Au(HS)_2^-$ or decreasing pH. In fact, it is quite possible that all of these mechanisms contributed significantly to the deposition of gold in the White Channel deposit.

4.2.4 Comparison to hot-spring epithermal model

Alteration and mineralization in the White Channel deposit bear many similarities to precious-metal deposits formed in hot-spring environments. Berger (1985) and Tooker (1985) describe many of the characteristics of the precious-metal, hot-spring model applied to many of the Nevada epithermal gold deposits. A schematic diagram (figure 4.22) shows all the major mineral and geochemical characteristics of alteration and ore-formation in the White Channel deposit. Some of the similarities between the model involved for the formation of the White Channel deposit and the hot-spring model (Berger, 1985; Tooker, 1985) described for many of the sediment-hosted, epithermal gold deposits of Nevada include the following characteristics;

1. Permeable host for mineralization.
2. A low temperature, near-surface, argillic (clay) alteration envelope consisting of kaolinite ± illite ± adularia ± Fe-oxides ± Fe-hydroxides.
3. Disseminated gold associated with argillic alteration,
4. Precious-metal suite of elements closely associated with gold mineralization (As, Sb, Ba, Fe, Mn, P, S and Co?, Cr?).
5. Low temperature (≈125°C), low salinity fluids (≈1.7wt.% equivalent NaCl), probably meteoric in origin ($\delta^{18}O(SMOW) \simeq -15‰$).
6. Gold carried as a gold-bisulphide complex with deposition due to a decrease in temperature, decrease in pH or oxidation.

Many of the differences in comparison to the Nevada hot-spring model include the following characteristics;

1. Permeable host is unconsolidated Plio-Pleistocene gravelly sediment.
2. Only minor silicification and/or opalization.
3. Little evidence of brecciation.
4. No low pH (acid) alteration cap that usually includes sulphate minerals such as alunite and jarosite.
5. Mineralization not directly associated with volcanics or an eruptive volcanic event,

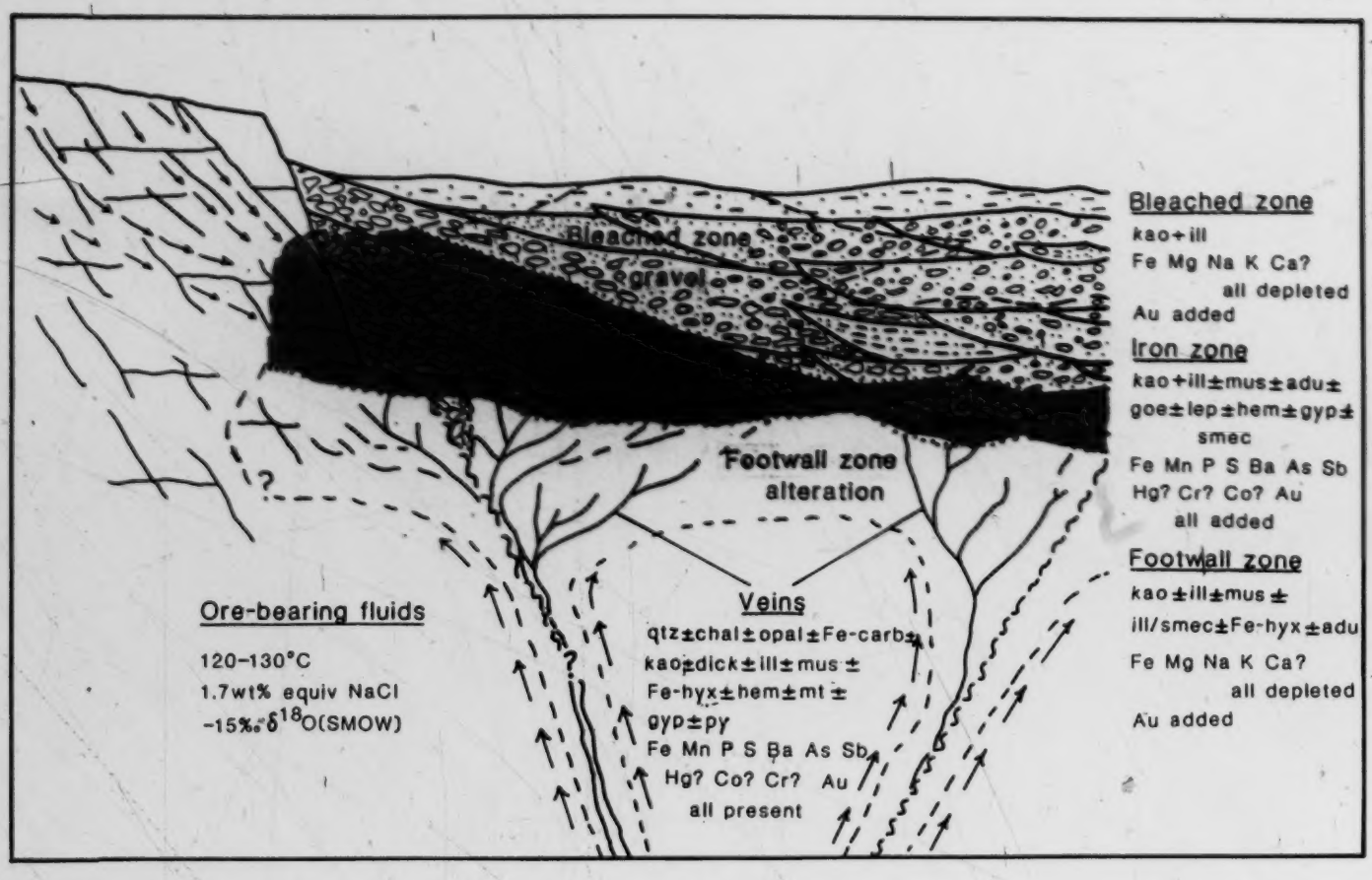

Figure 4.22 A schematic model of hydrothermal alteration and mineralization for the White Channel deposit.

although, several of the sediment-hosted Nevada deposits are not directly associated with volcanics as well.

4.2.5 Age and extent of epithermal gold mineralization

The age of the White Channel deposit and the onset of downcutting by current creeks in the Klondike bracket the age of epithermal activity in the deposit. The White Channel sediments are late Pliocene to early Pleistocene in age based upon pollen and cryogenic features found within the deposit (Morison, 1985). As a result, post-depositional hydrothermal alteration and mineralization in the sediments and the underlying footwall rocks is probably a maximum of 1.8-2 million years old (Plio-Pleistocene boundary at 1.8 Ma.). Altered White Channel sediments at Dago Hill are cross-cut by the overlying planar-stratified, iron-stained gravel indicating that alteration occurred before the deposition of the iron-stained gravel. This constrains the hydrothermal event to a minimum of 1.2 Ma. as a younger intermediate bench at Bonanza Creek contains the Mosquito Creek tephra dated at 1.2 Ma. by Naeser *et al.* (1982). A reworked ash, possibly related to the Mosquito Creek tephra, was also found during the summer of 1985 on a stratigraphically similar bench along the right bank of lower Hunker Creek opposite Paradise Hill.

Today, hydrothermal clay alteration and associated gold mineralization in the White Channel deposit is restricted to the sediments at four hills along the left (south) bank of lower Hunker Creek. However, sporadically distributed alteration and gold mineralization is present in the footwall rocks, not only below the sediments of these four hills, but also at several benches along Bonanza Creek where the White Channel gravel has been removed and processed for gold. White Channel gravel that exists today on most of the Bonanza Creek hills usually lacks intense alteration. McConnell (1907 and 1905), and Brock (1910) both noted alteration in the White Channel sediments being mined at those hills at the time; however, the exact degree of alteration, and the distribution of gold relative to alteration is impossible to determine from their descriptions. As a result, the relative extent and importance of hydrothermal alteration and ore-formation in much of the Bonanza Creek bench gravels that

were mined during the early 1900's is difficult to ascertain. However, there is little doubt that gold, which was added during post-depositional hydrothermal alteration of the White Channel sediments along Hunker Creek, is important economically as only those deposits with evidence of alteration are mined actively today.

Speculations can be made as to the heat source responsible for driving the hydrothermal system in addition to the possible structures used as conduits by the fluids; however, an accurate determination of these factors needs further work. The hydrothermal system that was responsible for epithemal alteration and mineralization in the White Channel deposit is not visibly linked to any Plio-Pleistocene volcanism. However, Pleistocene basalt flows commonly associated with the Tintina Trench, in addition to the presence of the Mosquito Creek tephra (1.2 Ma.), indicate that early Pleistocene volcanic activity could have provided a heat source. An alternate heat source may have been provided by a deep seated pluton underlying the Klondike district. Pleistocene uplift and/or transcurrent movement along the Tintina Trench could have served to fault rocks overlying the pluton, allowing sizeable stocks of hot magma to be emplaced at higher levels periodically.

Several structures in the Klondike district could easily have provided the necessary conduits to control fluid flow and mineralization during a Plio-Pleistocene hydrothermal event. The lower half of Hunker Creek essentially marks the contact between Klondike Series schists to the south and Nasina Series graphitic schists and quartzites to the north. The contacts between these two units are commonly exposed below the White Channel deposit in drainage ditches at Dago, Paradise and Nugget Hills. The contacts are often highly sheared, with pods of serpentinite and envelopes of intense clay alteration. These shear zones, whether the result of former thrust fault activity or more recent transcurrent movement, probably served as conduits for migrating fluids during Plio-Pleistocene hydrothermal activity. In addition, uplift and normal faulting responsible for the onset of White Channel erosion followed by downcutting to current base levels, may have also provided adequate structures for the migration of hydrothermal fluids.

4.3 Conclusions and Implications

The White Channel deposit in the Klondike district of west-central Yukon, consists of unconsolidated, dominantly gravelly sediments of Plio-Pleistocene age. Tempelman-Kluit (1982) first recognized post-depositional alteration in the White Channel sediments at Dago Hill. Based upon the work of this study, post-depositional argillic alteration of the sediments and the underlying bedrock in the Hunker Creek area is divided into three zones including the uppermost Bleached zone gravel, Iron zone gravel and the underlying Footwall zone rocks. The coexistence of kaolinite+illite(and/or muscovite)±adularia in the Iron zone gravel and altered footwall rocks indicates a temperature of alteration of ≈120-130°C. In addition, the fluid responsible for alteration must have had a log (aK^+/aH^+) ratio of approximately 2 and was probably close to saturation with amorphous silica. The high crystallinities of secondary kaolinite, illite and lepidocrocite in the Iron zone gravel and altered footwall rocks is consistent with a hydrothermal origin for alteration in the White Channel deposit.

Suggested first by Tempelman-Kluit (1982) and supported by the work of Morison (1985), the distribution of gold in the altered White Channel gravel is atypical of the normal placer distribution and appears to indicate a genetic relationship to alteration. In the clay-altered gravel of Dago Hill gold occurs in economic concentrations up to 8-10 meters above the bedrock contact. In addition, gold unrelated to placer processes, occasionally occurs in intensely clay-altered Footwall zone rocks and veins that were emplaced during the alteration of these rocks. These relationships suggest that significant amounts of gold were added to the White Channel deposit during post-depositional hydrothermal alteration.

Field relationships and textural characteristics indicate that three types of veins (types 1, 2 and 3) were emplaced during the hydrothermal alteration of the Footwall zone rocks and the overlying White Channel sediments. Fluid inclusions from quartz in types 1 and 2 veins indicate that the veins and associated alteration envelopes were formed from fluids at ≈120-130°C with low salinities of ≈1.7wt.% equivalent NaCl and no visible CO_2. The presence of chalcedony, amorphous silicates, well-crystallized kaolinite and dickite, in addition to vugs with euhedral quartz, banding, cockscomb, cockade, crustiform and botryoidal textures is

consistent with the low temperature hydrothermal origin for these veins indicated by the fluid inclusion analyses. Unpublished oxygen isotope data indicate that the hydrothermal fluids were dominantly meteoric in origin with a $\delta^{18}O$ of approximately -15‰. Paleoreconstruction of the overlying sediments suggests that the veins were probably emplaced within 100-150 meters of the surface.

Anomalous concentrations of the precious-metal suite of trace elements including As, Sb, Ba, Fe, Mn, P and S are present in the Iron zone gravel, occasional pockets of altered footwall rocks and in types 1, 2 and 3 veins. This suite of trace elements along with the characteristics described above indicate that the fluid responsible for alteration of the White Channel deposit bears many distinct similarities to fluids of active geothermal systems and epithermal precious-metal deposits. As a result, a similar origin is proposed for the hydrothermal fluids responsible for alteration and the associated gold distribution in the White Channel deposit.

4.3.1 Implications

Recognition of hydrothermal alteration, associated veins and epithermal gold mineralization in the White Channel deposit has several implications including the following;

1. The addition of gold directly into the White Channel deposit during hydrothermal activity may partially explain why no major lode sources of gold have been found from extensive exploration of mesothermal and/or metamorphic quartz veins in the Klondike Schist.
2. A model of Plio-Pleistocene epithermal mineralization changes much of the focus on future exploration targets as the associated alteration and veins have different geochemical signatures to the mesothermal and/or metamorphic quartz veins. The epithermal veins are distinct in hand sample, petrographic and geochemical characteristics.
3. Future targets based upon a Plio-Pleistocene epithermal mineralizing event include; (a) clay-altered Footwall zone rocks below the White Channel gravel, (b) clay-altered shear zones at depth, and (c) epithermal veins associated with shear zones and other major

structures in the district.

4. Current gravitational techniques employed in the evaluation and mining of clay-altered White Channel gravel and footwall rocks are vastly inadequate to recover the large amount of fine-grained hydrothermal gold suspected to be present in these units. Alternate methods of recovery may include chemical heap leach techniques.
5. Regional exploration for similar Plio-Pleistocene hydrothermal activity should be undertaken in unglaciated, central Yukon areas with adequate structures such as major faults, and suitable host units such as sedimentary and volcanic rocks. Other similar disticts where hydrothermal clay alteration has been noted include the Clear Creek and 60 Mile River placer districts, and the Grew Creek area.

REFERENCE LIST

Ashley, R.P., 1974. Goldfield mining district *in* Guidebook to the geology of the four Tertiary volcanic centers in central Nevada; Nevada Bureau of Mines and Geology, Report 19, Mackay School of Mines, University of Nevada, Reno, p. 49-66.

Berger, B.R., 1985. Geological-geochemical features of hot-spring precious-metal deposits *in* Geologic characteristics of sediment- and volcanic-hosted disseminated gold deposits - Search for an occurrence model; Tooker, E.W. (ed.), United States Geological Survey Bulletin 1646, p. 47-54.

Birak, D.J. and Hawkins, R.J., 1985. The geology of the Enfield Bell mine and the Jerritt Canyon district, Elko County, Nevada *in* Geologic characteristics of sediment- and volcanic-hosted disseminated gold deposits - Search for an occurrence model; Tooker, E.W. (ed.), United States Geological Survey Bulletin 1646, p. 95-106.

Biscaye, P.E., 1965. Mineralogy and sedimention of recent deep sea clays in the Atlantic Ocean and adjacent seas and oceans; Geological Society of America Bulletin, vol. 76, p. 803-832.

Blanchard, R., 1968. Interpretation of leached outcrops; Nevada Bureau of Mines Bulletin 66, Mackay School of Mines, University of Nevada, Reno, 196 pp.

Blatt, H., Middleton, G. and Murray, R., 1980. Origin of sedimentary rocks; Prentice Hall, Inc., Englewood Cliffs, New Jersey, 782 pp.

Bonham, H.F., 1985. Characteristics of bulk-mineable gold-silver deposits in Cordilleran and island-arc settings *in* Geologic characteristics of sediment- and volcanic-hosted disseminated gold deposits - Search for an occurrence model; Tooker, E.W. (ed.), United States Geological Survey Bulletin 1646, p. 71-78.

Bonham, H.F. (Jr.) and Garside, L.J., 1979. Geology of the Tonopah, Lone Mountain, Klondike, and Northern Mud Lake Quadrangles, Nevada; Nevada Bureau of Mines and Geology, Bulletin 92, Mackay School of Mines, University of Nevada, Reno, 142 pp.

Bostock, H.S., 1948. Physiography of the Canadian Cordillera, with special referrence to the area north of the fifty-fifth parallel; Geological Survey of Canada Memoir 247, 101 pp.

Bostock, H.S., 1942. Ogilivie map-sheet; Geological Survey of Canada Map 711A.

Boyle, R.W., 1979. The geochemistry of gold and its deposits; Geological Survey of Canada Bulletin 280, 584 pp.

Bray, C.J. and Spooner, T.C., 1983. Sheeted vein Sn-W mineralization and greissenization associated with economic kaolinization, Goonbarrow china clay pit, St. Austell, Cornwall, England: geologic relationships and geochronology; Economic Geology, vol. 78, p. 1064-1089.

Brindley, G.W. and Brown, G., 1980. Crystal structures of clay minerals and their X-ray identification; Mineralogical Society Monograph no. 5, London, England, 495 pp.

Bristow, C.M., 1977. A review of the evidence of the origin of kaolin deposits of southwest England *in* Proceedings of the 8th International Kaolin Symposium Mtg. Alunite, Madrid

Rome; p. 1-19.

Brock, R.W., 1910. Yukon Territory; Geological Survey of Canada, Summary Report for 1909, p. 2, 3, 9, 14-26, 47-60.

Buchanan, L.J., 1980. Ore controls of vertically stacked deposits, Guanajuato, Mexico; Society of Mining Engineers of A.I.M.E., Preprint no. 80-82, 16 pp.

Buchanan, L.J., 1981. Precious metal deposits associated with volcanic environments in the southwest *in* Relationships of tectonics to ore deposits in the southern Cordillera; W.R. Dickinson and W.D. Payne (eds.), Arizona Geological Society Digest volume XIV, Tucson, Arizona, p. 237-262.

Cairns, D.D., 1912. Quartz mining in the Klondike; Geological Survey of Canada, Summary Report for 1911, p. 4, 17-40.

Collins, P.L.F., 1979. Gas hydrates in CO_2-bearing fluid inclusions and the use of freezing data for estimation of salinity; Economic Geology, vol. 74, p. 1435-1444.

Debicki, R.L., 1984. Bedrock geology and mineralization of the Klondike area (west), 115 0/14,15 and 16 B/2,3, Open File, 1:50,000 scale map with marginal notes; Exploration and Geological Services Division, D.I.A.N.D., Yukon.

Debicki, R.L., 1985. Bedrock geology and mineralization of the Klondike area (east), 115 0/9, 10, 11, 14, 15, 16 and 116 B/2, Open File, 1:50,000 scale map with marginal notes; Exploration and Geological Services Division, D.I.A.N.D., Yukon.

DeKimpe, C.R., Kodama, H. and Rivard, R., 1981. Hydrothermal formation of a kaolinite-like product from non-crystalline aluminosilicate gels; Clays and Clay Minerals, vol. 29, no. 6, p. 446-450.

Deer, W.A., Howie, R.A. and Zussman, J., 1966. An introduction to the rock-forming minerals; Longman Group Ltd., Essex, England, 528 pp.

Droste, J.B., 1967. Clay mineral formation in Mud Pots, Yellowstone National park, Wyoming *in* Clays and Clay Minerals, Proceedings of the 15th National Conference on Clays and Clay Minerals; p. 409-422.

Dufresne, M.B., and Morison, S.R., 1985. Stratigraphy and alteration of the White Channel Gravel at Dago Hill, a progress report, Klondike area, Yukon *in* Yukon Exploration and Geology 1983; Exploration and Geological Services Division, D.I.A.N.D., p. 55-59.

Dufresne, M.B., Morison, S.R. and Nesbitt, B.E., 1987. Evidence of hydrothermal alteration in the White Channel sediments and bedrock of the Klondike region *in* Yukon Exploration and Geology 1984; Exploration and Geological Services Division, D.I.A.N.D.

Dunnoyer de Segonzac, G., 1970. The transformation of clay minerals during diagenesis and low-grade metamorphism: A review; Sedimentology, vol. 15, p. 281-346.

Ellis, A.J., 1979. Explored geothermal systems *in* Geochemistry of hydrothermal ore deposits; Barnes, H.L. (ed.), John Wiley and Sons, Inc., p. 632-683.

Ellis, A.J. and Mahon, W.A.J., 1977. Chemistry and geothermal systems; New York, Academic Press, 392 pp.

English, P.J., 1981. Gold-quartz veins in metasediments of the Yellowknife Supergroup,

Northwest Territories: A fluid inclusion study; Unpublished M.Sc. thesis, University of Alberta, 107 pp.

Eslinger, E.V. and Savin, S.M., 1973. Mineralogy and oxygen isotope geochemistry of the hydrothermally altered rocks of the Ohaki-Broadlands, New Zealand geothermal area; American Journal of Science, vol. 273, p. 240-267.

Esteoule-Choux, J., 1983. Kaolinite weathering profiles in Brittany: genesis and economic importance *in* Residual deposits: Surface related weathering processes and materials; Geological Society Special Publications Number 11, Wilson, P.C.L. (ed.), Blackwell Science Publications, p. 33-38.

Ewers, G.R. and Keays, R.R., 1977. Volatile and precious metal zoning in the Broadlands geothermal field, New Zealand; Economic Geology, vol. 72, p. 1337-1354.

Fluet, D.W., 1986. Genesis of the Deer Trail Zn-Pb-Ag vein deposit, Washington, United States; Unpublished M.Sc. thesis, University of Alberta, 129 pp.

Foscolos, A.E., Rutter, N.W. and Hughes, O.L., 1977. The use of pedological studies in interpreting the Quaternary history of central Yukon Territory; Geological Survey of Canada Bulletin 271, 48 pp.

Fournier, R.O., 1985. Silica minerals as indicators of conditions during gold deposition *in* Geologic characteristics of sediment- and volcanic-hosted disseminated gold deposits - Search for an occurrence model; Tooker, E.W. (ed.), United States Geological Survey Bulletin 1646, p. 15-26.

Gabrielse, H., 1985. Major dextral transcurrent displacements along the Northern Rocky Mountain Trench and related lineaments in north-central British Columbia; Geological Society of America Bulletin, vol. 96, p. 1-14.

Gautier, D.L., 1982. Siderite concretions: Indications of early diagenesis in the Gammon Shale (Cretaceous); Journal of Sedimentary Petrology, vol. 52, no. 3, p. 859-871.

Gleeson, C.F., 1970. Heavy mineral studies in the Klondike area, Yukon Territory; Geological Survey of Canada Bulletin 173, 63 pp.

Grim, R.E., 1968. Clay mineralogy; McGraw-Hill Book Co., 596 pp.

Hanson, R.F., Zamora, R. and Keller, W.D., 1981. Nacrite, dickite and kaolinite in one deposit in Nayarit, Mexico; Clays and Clay Minerals, vol. 29, no. 6, p. 451-453.

Harder, E.C., 1952. Examples of bauxite deposits illustrating variations in origin *in* Problems of clay and laterite genesis; Symposium at the Annual Meeting of American Institute of Metallurgy and Mineral Engineering, St. Louis, Missouri, February 19-22, 1951, Published by A.I.M.E., p. 35-64.

Harington, C.R., 1985. Comments on Canadian Pleistocene mammals; Acta Zoologica Fennica, vol. 70, p. 193-197.

Hassanipak, A.A. and Eslinger, E., 1985. Mineralogy, crystallinity, O^{18}/O^{16} and D/H of Georgia kaolins; Clays and Clay Minerals, vol. 33, no. 2, p. 99-106.

Hedenquist, J.W. and Henley, R.W., 1985a. The importance of CO_2 on freezing point measurements of fluid inclusions: Evidence from active geothermal systems and implications for epithermal ore deposition; Economic Geology, vol. 80, p. 1379-1407.

Hedenquist, J.W. and Henley, R.W., 1985b. Hydrothermal eruptions in the Waiotapu geothermal system, New Zealand: Their origin, associated breccias, and relation to precious metal mineralization; Economic Geology, vol. 80, p. 1640-1668.

Helgeson, H.C., Delany, J.M., Nesbitt, H.W. and Bird, D.R., 1978. Summary and critique of the thermodynamic properties of rock forming minerals; American Journal of Science, 278A, 229 pp.

Henley, R.W. and Ellis, A.J., 1983. Geothermal systems ancient and modern: a geochemical reveiw; Earth Sciences Reviews, vol. 19, p. 1-50.

Hinckley, D.N., 1963. Variability in "crystallinity" values among the kaolin deposits of the coastal plain of Georgia and South Carolina; Clays and Clay Minerals, Monograph no.13, Proceedings of the eleventh National Conference on Clays and Clay Minerals, Ottawa, Ontario, Canada, August 13-17, 1962, p. 229-235.

Hollister, L.S. and Crawford, M.L. (eds.), 1981. Fluid inclusions: Applications to petrology; Mineral Association of Canada, Short Course Handbook, vol. 6, Calagry, May, 1981, 304 pp.

Horton, D.G., 1985. Mixed-layer illite/smectite as a paleotemperature indicator in the Amethyst vein system, Creede district, Colorado, U.S.A.; Contributions to Mineralogy and Petrology, vol. 91, p. 171-179.

Hughes, O.L., Rampton, V.N. and Rutter, N.W., 1972. Quaternary geology and geomorphology, southern and central Yukon (Northern Canada); XXIV International Geologial Conferrence, Montreal, 1972, Excursion A11 Guidebook, 59 pp.

Hughes, O.L., Campbell, R.B., Muller, J.E. and Wheeler, J.O., 1969. Glacial limits and flow patterns, Yukon Territory, south of sixty-five degrees north latitude; Geological Survey of Canada Paper 68-34, 9 pp.

Hurst, V.J. and Kunkle, A.C., 1985. Dehydroxylation, rehydroxylation, and stability of kaolinite; Clays and Clay Minerals, vol. 33, no. 1, p. 1-14.

Ignasiak, T.M., Kotlyar, L., Longstaffe, F.J., Strausz, O.P. and Montgomery, D.S., 1983. Separation and characterization of clay from Athabasca asphaltene; Fuel, vol. 62, p. 353-362.

Inoue, A. and Utada, M., 1983. Further investigations of a conversion series of dioctahedral mica/smectites in the Shinzan hydrothermal alteration area, northeast Japan; Clays and Clay Minerals, vol. 31, no. 6, p. 401-412.

Johns, W.D., Grim, R.E. and Bradley, W.F., 1954. Quantitative estimations of clay minerals by diffraction methods; Journal of Sedimentary Petrology, vol. 24, p. 242-251.

Keller, W.D., 1968. Flint clay and flint-clay facies; Clays and Clay Minerals, vol. 16, p. 113-128.

Keller, W.D., 1976a. Scan electron micrographs of kaolins collected from diverse environments of origin -I; Clays and Clay Minerals, vol. 24, p. 107-113.

Keller, W.D., 1976b. Scan electron micrographs of kaolins collected from diverse environments of origin -II; Clays and Clay Minerals, vol. 24, p. 114-117.

Keller, W.D., 1977. Scan electron micrographs of kaolins collected from diverse environments of origin -V. Kaolins collected in Australia and Japan on field trips of the sixth and seventh clay conferences; Clays and Clay Minerals, vol. 25, p. 347-364.

Keller, W.D., 1982. Kaolin - A most diverse rock in genesis, texture, physical properties and uses; Geological Society of America Bulletin, vol. 93, p. 27-36.

Keller, W.D. and Hanson, R.F., 1968. Hydrothermal alteration of a rhyolite flow breccia near San Luis Potosi, Mexico to refractory kaolin; Clays and Clay Minerals, vol. 46, p. 223-229.

Keller, W.D. and Hanson, R.F., 1969. Hydrothermal argillation of volcanic pipes in limestone, Mexico; Clays and Clay Minerals, vol. 17, p. 9-12.

Kerr, P.F., 1977. Optical Mineralogy; McGraw-Hill Book Co., 280 pp.

Kerrich, R. and Fyfe, W.S., 1981. The gold-carbonate association: source of CO_2 and CO_2 fixation reactions in Archean lode deposits; Chemical Geology, vol. 33, p. 265-294.

Kinter, E.B. and Diamond, S., 1956. A new method for preparation and treatment of oriented aggregate samples of soil clays for X-ray diffraction analysis; Soil Science, vol. 81, p. 111-120.

Knight, J.E., 1977. A thermochemical study of alunite, enargite, luzonite and tennantite deposits; Economic Geology, vol. 72, p. 1321-1336.

Krumbein, W.C. and Sloss, L.L., 1963. Stratigraphy and sedimentation; W.H. Freeman and Co., San Francisco, 660 pp.

Kwong, Y.T.J. and Crocket, J.H., 1978. Background and anomalous gold in rocks of an Archean greenstone assemblage, Kakagi Lake area, northwestern Ontario; Economic Geology, vol. 73, p. 50-63.

Longstaffe, F.J., 1978. Oxygen isotope and elemental geochemistry of Archean silicate rocks from northern Ontario; Unpublished Ph.D. thesis, McMaster University, Hamilton, Ontario, 546 pp.

Longstaffe, F.J., 1984. The role of metoric water in diagenesis of shallow sandstones: Stable isotope studies of the Milk River aquifer and gas pool, southern Alberta *in* Clastic Diagenesis; American Association of Petroleum Geologists, Memoir 37, MacDonald, D.A. and Surdon, R.C. (eds.), Published by American Association of Petroleum Geologists, p. 81-98.

Loughnan, F.C. and Bayliss, P., 1961. The mineralogy of the bauxite deposits near Weipa, Queensland; American Mineralogist, vol. 46, p. 209-217.

Lowey, G.W., 1984. The stratigraphy and sedimentology of siliciclastic rocks, west-central Yukon, and their tectonic implications; Unpublished Ph.D. thesis, University of Calgary, Calgary, Alberta, 329 pp.

MacLean, M.E., 1914. Lode Mining in Yukon: an investigation of quartz deposits in the Klondike division; Publication no. 222, Mines Branch, Canadian Department of Mines, 205 pp.

Masterton, W.D. and Kyle, R.J., 1984. Geological, geochemical, stable isotope, and fluid inclusion characteristics of epithermal gold mineralization, Velvet didstrict, Nevada;

Journal of Geochemical Exploration, vol. 20, p. 55-74.

McConnell, R.G., 1905. Report on the Klondike gold fields *in* Annual Report for 1901, vol. XIV, pt. B, Geological Survey of Canada Publication No. 884, p. 1-71.

McConnell, R.G., 1907. Report on gold values in the Klondike High Level Gravels; Geological Survey of Canada Publication No. 979, 34 pp.

McConnell, R.G. and Tyrell, J.B., 1898. Preliminary note on the gold deposits and gold mining in the Klondike region *in* Gological Survey of Canada Summary Report for 1898 (1899) and Annual Report, vol. XI, 1898, pt. A, p. 24, 36-62 (1901).

McDowell, S.D. and Elders, W.A., 1980. Authigenic layer silicate minerals in borehole Elmore I, Salton Sea geothermal field, California, U.S.A.; Contributions to Mineralogy and Petrology, vol. 74, p. 293-310.

Metcalfe, P., 1981. Petrogenesis of the Klondike Formation, Yukon Territory; Unpublished M.Sc. thesis, University of Manitoba, Winnipeg, Manitoba, 103 pp.

Metcalfe, P. and Clark, G.S., 1983. Rb-Sr whole-rock age of the Klondike Schist, Yukon Territory; Canadian Journal of Earth Sciences, vol. 20, no. 5, p. 886-891.

Morison, S.R., 1985. Sedimentology of White Channel placer deposits, Klondike area, west-central Yukon; Unpublished M.Sc. thesis, University of Alberta, Edmonton, Alberta, 149 pp.

Milner, M.W., 1976. Geomorphology of the Klondike placer goldfields; Final Report, Contract OSV 5-0047, Exploration and Geological Services Division, D.I.A.N.D., Yukon, 157 pp.

Mortensen, J.A., 1984. Bedrock geology of the Klondike placer district and evidence for structural controls on lode gold mineralization; Geological Association of Canada, Abstracts for Geological Association of Canada Conference in Vancouver, B.C.

Naeser, N.D., Westgate, J.A., Hughes, O.L. and Péwé, T.L., 1982. Fission-track ages of late Cenozoic distal tephra beds in the Yukon Territory and Alaska; Canadian Journal of Earth Sciences, vol. 19, p. 2167-2178.

Nesbitt, B.E., Murowchick, J.B. and Muelenbachs, K., 1986. Dual origins of lode gold deposits in the Canadian Cordillera; Geology, vol. 14, p. 506-509.

Olafsson, J. and Riley, J.P., 1978. Geochemical studies on the thermal brine from Reykjanes, Iceland; Chemical Geology, vol. 21, p. 219-237.

O'Neil, J.R. and Silberman, M.L., 1974. Stable isotope relations in epithermal Au-Ag deposits; Economic Geology, vol. 69, p. 902-909.

Potter, R.W., II, Clynne, M.A. and Brown, D.L., 1978. Freezing point depression of aqueous sodium chloride solutions; Economic Geology, vol. 73, p. 284-285.

Poty, B., Leroy, J. and Jachimowicz, L., 1976. A new device for measuring temperature under the microscope: the Chaixmeca microthermometry apparatus; COFFI Fluid Inclusion Research, vol. 9, p. 173-178.

Roddick, J.A., 1967. Tintina Trench; Journal of Geology, vol. 75, no. 1, p. 23-33.

Roedder, E., 1984. Fluid inclusions; Mineralogical Society of America, Reviews in Mineralogy, vol. 12, 644 pp.

Rutter, N.W., Foscolos, A.E. and Hughes, O.L., 1978. Climate trends during the Quaternary in central Yukon based upon pedological and geomorphological evidence *in* Quaternary Soils; reprinted from the Third York Quaternary Symposium, Published by Geological Abstracts, Norwich, England, p. 309-359.

Schoen, R. and White, D.E., 1967. Hydrothermal alteration of basaltic andesite and other rocks in drill hole GS-6, Steamboat Springs, Nevada; United States Geological Survey Professional Paper 575-B, p. B110-B119.

Schoen, R., White, D.E. and Hemley, J.J., 1974. Argillization by descending acid at Steamboat Springs, Nevada; Clays and Clay Minerals, vol. 22, p. 1-22.

Schroeder, R.J. and Hayes, J.B., 1968. Dickite and kaolinite in Pennslyvanian limestones of southeastern Kansas; Clays and Clay Minerals, vol. 16, p. 41-49.

Schroeter, T.G., 1985. Heart Peaks prospect (104K/9E) *in* Geological framework, 1984, A summary of field activities and current research, paper 1985-1; Geological Branch of the Mineral Resources Division, Ministry of Energy, Mines and Petroleum Resources, p. 359-364.

Schwertmann, U. and Fitzpatrick, R.W., 1977. Occurrence of lepidocrocite and its association with goethite in Natal soils; Soil Science Society of America Journal, vol. 14, p. 1013-1018.

Schwertmann, U. and Taylor, R.M., 1972a. The transformation of lepidocrocite to goethite; Clays and Clay Minerals, vol. 20, p. 151-158.

Schwertmann, U. and Taylor, R.M., 1972b. The influence of silicate in the transformation of lepidocrocite to goethite; Clays and Clay Minerals, vol. 20, p. 159-164.

Schwertmann, U. and Thalmann, H., 1976. The influence of [Fe(II)], [Si], and pH on the formation of lepidocrocite and ferrihydrite during oxidation of aqueous $FeCl_2$ solutions; Clay Minerals, vol. 11, p. 189-200.

Shenberger, D.M., 1985. Gold solubility in aqueous sulfide solutions; Unpublished M.Sc. thesis, Pennsylvania State University, 102 pp.

Sigvaldason, G.E. and White, D.E., 1962. Hydrothermal alteration in drill holes G.S.-5 and G.S.-7, Steamboat Springs, Nevada; United States Geological Survey Professional Paper 450-D, D113-D117.

Sparr, J.E., 1897. Geology of the Yukon gold district, Alaska. United States Geological Survey 18th Annual Report, Part 3, p. 87-392.

Stauffer, R.E., Jenne, E.A. and Ball, J.W., 1980. Chemical studies of selected trace elements in hot spring drainages of Yellowstone National Park; United States Geological Survey Professional Paper 1044F, 20 pp.

Stanton, R.L., 1972. Ore petrology; McGraw-Hill Book Co., 713 pp.

Stauffer, R.E. and Thompson, J.M., 1984. Arsenic and antimony in geothermal waters of Yellowstone National Park, Wyoming, U.S.A.; Geochimica et Cosmochimica Acta, vol. 48, p. 2547-2561.

Steiner, A., 1968. Clay minerals in hydrothermally altered rocks at Wairakei, New Zealand; Clays and Clay Minerals, vol. 16, p. 193-213.

St. Louis, R.M., 1984. Geochemistry of the platinum group elements in the Tulameen Ultramafic Complex, British Columbia; Unpublished M.Sc. thesis, University of Alberta, Edmonton, Alberta, 120 pp.

Strachan, D.G., 1985. Geologic discussion of the Borealis gold-deposit, Mineral County, Nevada *in* Geologic characteristics of sediment- and volcanic-hosted disseminated gold deposits - Search for an occurrence model; Tooker, E.W. (ed.), United States Geological Survey Bulletin 1646, p. 89-94.

Sumi, K., 1969. Zonal distribution of clay minerals in the Matsukawa goethermal area, Japan *in* Proceedings of the International Clay Conference; Tokyo, Japan, 1969, September 5-10, vol. 1, p. 501-512.

Taylor, H.P., 1979. Oxygen and hydrogen isotope relationships in hydrothermal mineral deposits *in* Geochemistry of hydrothermal ore deposits; Barnes, H.L., (ed.), John Wiley and Sons, Inc., p. 236-272.

Tempelman-Kluit, D.J., 1976. The Yukon Crystalline Terrane: enigma in the Canadian Cordillera; Geological Society of America Bulletin, vol. 87, p. 1343-1357.

Tempelman-Kluit, D.J., 1977. Stratigraphic and structural relations between Selwyn basin, Pelly-Cassiar Platform and Yukon Crystalline Terrain in the Pelly Mountains, Yukon; Report of Activities, Part A, Geological Survey of Canada Paper 77-1A, p. 223-227.

Tempelman-Kluit, 1979. Transported cataclastic, ophiolite and granodiorite in Yukon: evidence of arc-continent collision; Geological Survey of Canada Paper 79-14, 27 pp.

Tempelman-Kluit, D.J., 1980. Evolution of the physiography and drainage in southern Yukon; Canadian Journal of Earth Sciences, vol. 17, no. 19, p. 1189-1203.

Tempelman-Kluit, D.J., 1981. Geology and mineral deposits of southern Yukon *in* Yukon Exloration and Geology 1979-80; Exploration and Geological Services Division, D.I.A.N.D., p. 7-31.

Tempelman-Kluit, D.J., 1982. White Channel gravel of the Klondike *in* Yukon Exploration and Geology 1981; Exploration and Geological Services Division, D.I.A.N.D., p. 74-79.

Tingley, J.V. and Berger, B.R., 1985. Lode gold deposits of Round Mountain, Nevada; Nevada Bureau of Mines and Geology, Bulletin 100, Mackay School of Mines, University of Nevada, Reno. 62 pp.

Thorez, J., 1976. Practical identification of clay minerals; Lelotte, Dison, Belgium, 90 pp.

Tomita, K. and Takahashi, H., 1985. curves for the quantification of mica/smectite and chlorite/smectite interstratifications by X-ray powder diffraction; Clays and Clay Minerals, vol. 33, no. 5, p. 379-390.

Tooker, E.W., 1985. Discussion of the disseminated-gold-ore-occurrence model *in* Geologic characteristics of sediment- and volcanic-hosted disseminated gold deposits - Search for an occurrence model; Tooker, E.W. (ed.), United States Geological Survey Bulletin 1646, p. 107-149.

Turekian, K.K. and Wedepohl, K.H., 1961. Distribution of the elements in some major units of the earth's crust; Geological Society of America Bulletin, vol. 72, p. 175-192.

Vincent, A., 1983. The origin and occurrence of Devon ball clays *in* Residual deposits: surface related weathering and materials; Geological Society Special Publications, no. 11, Wilson, R.C.L. (ed.), Blackwell Science Publications, p. 39-45.

Weissberg, B.C., Brown, P.R.L. and Seward, T.M., 1979. Ore metals in active geothermal systems *in* Geochemistry of hydrothermal ore deposits; Barnes, H.L. (ed.), John Wiley and Sons, Inc., p. 738-780.

White, D.E., 1981. Active geothermal systems and hydrothermal ore deposits *in* Seventy-fifth Aniversary Volume, 1905-1980; Skinner, B.J. (ed.), Economic Geology Publishing Company, El Paso, Texas, p. 392-423.

White, D.E., 1985. Summary of Steamboat Springs geothermal area, Nevada, with attached road-log commentary *in* Geologic characteristics of sediment- and volcanic-hosted disseminated gold deposits - Search for an occurrence model; Tooker, E.W. (ed.), United States Geological Survey, Bulletin 1646, p. 79-88.

White, D.E., Fournier, R.O., Muffler, L.J.P. and Truesdell, A.H., 1975. Physical results of research drilling in thermal areas of Yellowstone National Park, Wyoming; United States Geological Survey Professional Paper 892, 70 pp.

5. APPENDICES

5.1 Scales Of Alteration

5.1.1 Scale of competence

Alteration in the White Channel gravel and underlying bedrock is characterized by the progressive replacement of feldspars, mica and mafic minerals by clay minerals. As a result, the basic component of the alteration scales used in classifying the degree of alteration in either the White Channel gravel or the underlying bedrock is the degree of competence of cobbles within the gravel and the degree of competence of the bedrock, respectively. The following scale of competence is the observed degree of decomposition (or extent of clay mineral development) of clasts or bedrock.

(a) Competent: requires several blows with a hammer before fracturing.

(b) Breakable: competent but requires less than 1 or 2 blows with a hammer to cause fracturing.

(c) Friable (cohesive): this applies to semi-competent clasts or bedrock that can be moved without falling apart, but will partially disintegrate when pressure is applied.

(d) Friable (incohesive): incompetent clasts or bedrock that maintain minor cohesion but disintegrate when any pressure is applied.

(e) Incompetent (clay): clasts or bedrock that completely disintegrate when touched (when dry) or when wet are sticky and are easily penetrated by a knife.

Several factors affect the decomposition of clasts and bedrock including lithology, structure, mineral assemblage and grain size. As a result, this type of information was recorded and used in classifying the degree of competence of a clast or bedrock.

5.1.2 Scale of gravel alteration

In assessing the degree of alteration in the White Channel gravel approximately 100 clasts were randomly selected. The degree of competence of each clast was compiled versus the lithologic type. The alteration state of such minerals as feldspars, mica, mafic minerals and quartz was also noted. In addition, the amount of clay matrix was roughly estimated. Each outcrop of gravel was then categorized as follows;

(1) Unaltered: Clasts are competent (a) with little or no visible alteration of mafic minerals or feldspars within the clasts or matrix. Matrix is entirely primary (no clay size material present) with sedimentary structures clearly distinguishable.

(2) Slightly altered: Clasts predominantly competent (a) with occasional breakable (b) or friable (cohesive, (c)) clasts. Incipient alteration of mafic minerals and feldspars is visible. Matrix is primary (no clay size material present) with sedimentary structures clearly distinguishable.

(3) Moderately altered: Clasts are predominantly breakable (b) and friable (cohesive, (c)) with occasional friable (incohesive, (d)) or incompetent (e) clasts present (usually mafic-rich clasts). The mafic minerals are replaced while the feldspars are often chalky. The matrix is dominantly primary with incipient clay mineral development. Sedimentary structures are clearly distinguishable.

(4) Strongly altered: Clasts range from breakable (b) to incompetent (clay, (e)). Clasts dominantly composed of mafic minerals, feldspars and micas are usually friable

(incohesive, {d}) to incompetent (clay, {e}). Quartz-rich clasts are usually breakable {b} to friable (cohesive, {c}). Massive quartz clasts are usually competent {a}. Mafic minerals and feldspars are replaced while micas show incipient alteration. The matrix contains significant amounts of clay size material (≃2-10%) dominantly composed of secondary clay minerals. Sedimentary structures are visible to partly masked or destroyed.

(5) Extremely altered: Clasts are dominantly friable (incohesive, {d}) and incompetent (clay, {e}). Quartz-rich clasts or massive quartz is often breakable {b} and fractured in place. Mafic minerals, feldspars and micas are replaced. The matrix consists of >10% clay size material with the development of secondary clay minerals having masked or destroyed sedimentary structures beyond recognition.

(6) Altered: All clasts are friable (incohesive, {d}) to incompetent (clay, {e}) with massive quartz and quartz-rich clasts breakable {b} to friable (incohesive, {d}) or incompetent (clay, {e}). All structures of the former host material are completely obliterated. All primary minerals, except minor quartz, are altered to clay minerals and residual hydroxides.

5.2 Sample List And Location Map

Table 5.14 Location and description of samples collected from the Klondike district.

Sample #	Location and Description
	Adams Creek - 1985 Samples
AC-01	Quartz-carbonate veins in graphitic schist.
	Bear Creek - 1985 Samples
BC-01	Quartz vein in mica-feldspar schist, east bank opposite Discovery Pup.
	Bonanza Creek - 1985 Samples
BZ-01	Quartz veins in feldspar-mica schist, east bank near 49 Hill.
	Cripple Hill - 1983 Samples
A-301	Mica schist, quartz-rich fragments, Footwall zone.
A-302	Mica schist, {e}, Footwall zone.
A-303	Mica schist, {e}, Footwall zone.
A-304	Mica schist, {e}, Footwall zone.
A-305	Quartz boudin in Mica schist {e}, Footwall zone.
A-306	Mica schist, {e}, Footwall zone.
A-307	Mica schist, {e}, Footwall zone.
A-308	Mica schist, {e}, Footwall zone.
A-309	Mica schist, {e}, Footwall zone.
A-310	Mica schist, {e}, Footwall zone.
A-311	Mica schist, {e}, Footwall zone.
A-312	Mica schist, {e}, Footwall zone.
A-313	Mica schist, {e}, Footwall zone.
A-314	Mica schist, {c}-{d}, Footwall zone.
A-315	Mica schist, {c}-{d}, Footwall zone.
A-316	Mica schist with quartz boudin, {e}, Footwall zone.
A-317	Mica schist, {e}, Footwall zone.
A-318	Mica schist, {c}-{d}, Footwall zone.
A-319	Mica schist, {d}-{e}, Footwall zone.
A-320	Mica schist, {d}-{e}, Footwall zone.
A-321	Mica schist with quartz boudin, {e}, Footwall zone.
A-322	Mica schist, {e}, Footwall zone.
A-323	Mica schist, {e}, Footwall zone.
A-324	Mica schist with quartz vein, {e}, Footwall zone.
A-325	Mica schist with quartz vein, {e}, Footwall zone.
A-326	Fe-stained fragments of mica-schist, alt. ctk. in Footwall zone.
A-327	Mica schist, {d}-{e}, 34-41cm below alt. ctk. in Footwall zone.
A-328	Mica schist, {d}-{e}, 4-11cm below alt. ctk. in Footwall zone.
A-329	Mica schist, {e}, 6-11cm above alt. ctk. in Footwall zone.
A-330	Mica schist, {e}, 37-42cm above alt. ctk. in Footwall zone.
A-331	Mica schist, {c}-{d}, 62-72cm below alt. ctk. in Footwall zone.
A-332	Mica schist, {c}-{d}, 21-29cm below alt. ctk. in Footwall zone.
A-333	Mica schist, {c}-{d}, 4-9cm below alt. ctk. in Footwall zone.
A-334	Mica schist, {e}, 18-26cm above alt. ctk. in Footwall zone.
A-335	Mica schist, {e}, 66-74cm above alt. ctk. in Footwall zone.
A-336	Mica schist, {c}-{d}, 85-92cm below alt. ctk. in Footwall zone.
A-337	Mica schist, {c}-{d}, 26-33cm below alt. ctk. in Footwall zone.
A-338	Mica schist, {c}-{d}, 3-8cm below alt. ctk. in Footwall zone.
A-339	Mica schist, {e}, 12-18cm above alt. ctk. in Footwall zone.
A-340	Mica schist, {e}, 58-64cm above alt. ctk. in Footwall zone.
A-341	Mica schist, {c}-{d}, 110-125cm below alt. ctk. in Footwall zone.
A-342	Mica schist, {c}-{d}, 115-130cm below alt. ctk. in Footwall zone.

A-343	Mica schist, {c}-{d}, 95-100cm below alt. ctk. in Footwall zone.
A-344	Mica schist, {c}-{d}, 25-32cm below alt. ctk. in Footwall zone.
A-345	Mica schist, {c}-{d}, 2-9cm below alt. ctk. in Footwall zone.
A-346	Mica schist, {e}, 10-15cm above alt. ctk. in Footwall zone.
A-347	Mica schist, {e}, 52-60cm above alt. ctk. in Footwall zone.
A-348	Mica schist, {c}-{d}, 0-15cm below WCG ctk.
A-349	Graphitic mica schist, {d}-{e}, 90-100cm below WCG ctk.
A-350	Graphitic mica schist, {d}-{e}, 30-40cm below WCG ctk.
A-351	Graphitic mica schist, {d}-{e}, 5-10cm below WCG ctk.
A-352	Feldspar-mica schist, {d}-{e}, 80-90cm below WCG ctk.
A-353	Feldspar-mica schist, {d}-{e}, 30-40cm below WCG ctk.
A-354	Feldspar-mica schist, {d}-{e}, 5-10cm below WCG ctk.
A-355	Graphitic mica schist, {d}-{e}, 15-30cm below WCG ctk.
A-356	Graphitic mica schist, {d}-{e}, 15-25cm below WCG ctk.
B-301	Feldspar-mica schist, {b}-{c}, ?
B-302	Feldspar-mica schist, {d}-{e}, 1.9m below WCG ctk.
B-303	Feldspar-mica schist, {d}-{e}, 2.4m below WCG ctk.
B-304	Feldspar-mica schist, {c}-{d}, 3.3m below WCG ctk.
B-305	Feldspar-mica schist, {c}-{d}, 3.0m below WCG ctk.
B-306	Graphitic feldspar-mica schist, {d}-{e}, 2.5m below WCG ctk.
B-307	Graphitic feldspar-mica schist, {d}-{e}, 2.4m below WCG ctk.
B-308	Graphitic feldspar-mica schist, {c}-{d}, 3.6m below WCG ctk.
B-309	Graphitic feldspar-mica schist, {a}-{b}, 11m below WCG ctk.
B-310	Feldspar-mica schist, {c}-{d}, 3.6m below WCG ctk.
W-301	Pebbles w/ matrix, WCG (2)-(3) 0-15cm above brx.
W-302	Sandy matrix, WCG (2)-(3) 0-15cm above brx.
W-303	Mn-stained matrix, WCG (2)-(3) 40-55cm above brx.
W-304	Matrix w/ cobbles, WCG (2)-(3) 85-100cm above brx.
	Cripple Hill - 1984 Samples
401	Graphitic feldspar-mica schist, {a}-{b}, 7m below WCG ctk.
402	Graphitic feldspar-mica schist, {b}-{c}, 3-4m below WCG ctk.
403	Rhyolite clasts, {a}-{b}, WCG (2)-(3) 1-1.5m above brx.
404	Mica schist clasts, {a}-{b}, WCG (2)-(3) 1-1.5m above brx.
405	Matrix, WCG (2)-(3) 1-1.5m above brx.
406	Mica schist clasts, {b}-{c}, WCG (2)-(3) 1.5m above brx.
407	Mica schist clasts, {c}-{d}, WCG (2)-(3) 3-4m above brx.
	Dago Hill - 1983 Samples
W-401	Various clasts, {a}-{c}, Iron zone gravel (5) 0.5-1.5m above brx.
W-402	Quartz clast with vugs, Iron zone gravel (5).
W-403	Rhyolite clast, {d}-{e}, Iron zone gravel (5) 1.2m above brx.
W-404	Matrix, (4)-(5), Iron zone gravel (5) 1m above brx.
W-405	Mica schist clast, {d}-{e}, Iron zone gravel (5) 0.5m above brx.
W-406	Rhyolite clasts, {a}-{b}, Bleached zone gravel (4)-(5) 7-8m above brx.
W-407	Matrix, (4)-(5), Bleached zone gravel 7m above brx.
W-408	Rhyolite clasts, {d}-{e}, Bleached zone gravel (4)-(5) 7-8m above brx.
W-409	Matrix? rhyolite clast?, (4)-(5), Bleached zone gravel 7m above brx.
W-410	Matrix, WCG (1)-(2) 0.5m above Bleached zone gravel.
W-411	Matrix w/ pebbles, WCG (1)-(2) 0.5m above Bleached zone gravel.
W-412	Silts and clays, WCG (1)-(2) 1m above Bleached zone f.g. sediments.
W-413	Silts and clays, WCG (1)-(2) 1-2m above Bleached zone f.g. sediments.
W-414	Silts and clays, WCG (1)-(2) 2.5m above Bleached zone f.g. sediments.
W-415	Mica schist clast, {a}-{b}, White Channel gravel (1)-(2) 0.5m above Bleached zone gravel.
A-401	Matrix, stained WCG (3)-(5) from contact between unaltered and Bleached zone gravel.
A-402	Matrix, Bleached zone gravel (4)-(5) 0.5m below Unaltered gravel.

A-403	Matrix, Bleached zone gravel (4)-(5) 2.5m below Unaltered gravel.
A-404	Matrix w/ pebbles, Bleached zone gravel (4)-(5) 2.5-3m below Unaltered gravel.
A-405	Matrix w/ pebbles, Bleached zone gravel (4)-(5) 0.5m below Unaltered gravel.
A-406	Quartz sand, {e}? (formerly a quartz clast?), Bleached zone f.g. sediments.
A-407	Silts and clays, Bleached zone f.g. sediments (4)-(5).
A-408	Silts and clays, Bleached zone f.g. sediments (4)-(5).
A-409	Rhyolite clast, {d}-{e}, Iron zone gravel (5) 1.5m above brx.
A-410	Rhyolite clast, {e}, Bleached zone gravel (5) 2.5-3m above brx.
A-411	Rhyolite clast, {d}-{e}, Bleached zone gravel (5) 2.5-3m above brx.
A-412	Rhyolite clasts, {a}-{b}, Bleached zone gravel (5) 2.5-3m above brx.
A-413	Mica schist clast, {d}-{e}, Bleached zone gravel (5) 2.5-3m above brx.
A-414	Rhyolite clast, {d}-{e}, Bleached zone gravel (4)-(5) 6-7m above brx.
A-415	Rhyolite clasts, {a}-{b}, Bleached zone gravel (4)-(5) 6-7m above brx.
A-416	Matrix, Bleached zone gravel (4)-(5) 6-7m above brx.
A-417	Mica schist, {e}, Footwall zone 2m? below gravel contact.
B-401	Graphitic quartzite, {b}, Footwall zone 0.5m below gravel contact.
B-402	Mica schist, from conduit on south side.
Y-401	Various clasts, {a}, Yellow gravel unit.
Y-402	Silts and clays, Yellow gravel f.g. sediments.

Dago Hill - 1984 Samples

501	Clay, from fracture in mica schist 2-4m below gravel contact.
502	Mica schist, {b}-{c}, Footwall zone 3-4m below gravel contact on north side.
503	Mica schist, {a}-{b}, Bedrock below colluvial horizon on north side.
504	Matrix, Bleached zone gravel (3) 10-12m above brx.
505	Matrix, Bleached zone gravel (2)-(3) 10-12m above brx.
506	Mica schist clasts, {c}-{d}, Bleached zone gravel (4)-(5) 10-12m above brx.
507	Mica schist clasts, {a}-{b}, Bleached zone gravel (4)-(5) 10-12m above brx.
508	Rhyolite cobble, {c}-{d}, Bleached zone gravel (5) 2-4m above brx.
509	Rhyolite cobble, {b}, Bleached zone gravel (5) 3-4m above brx.
510	Matrix, Bleached zone gravel (4)-(5) 3-4m above brx.
510a	Rhyolite cobbles, {b}-{c}, Bleached zone gravel (4)-(5) 4-5m above brx.
511	Rhyolite cobbles, {b}-{c}, Bleached zone gravel (4)-(5) 4-5m above brx.
512	Rhyolite cobble, {e}, Bleached zone gravel (4)-(5) 5-6m above brx.
513	Matrix, Bleached zone gravel (4)-(5) 6-7m above brx.
514	Matrix, Bleached zone gravel (4)-(5) 3m above brx.
515	Mica schist, {e}, Footwall zone 0-0.5m below gravel contact.
516	Matrix, Iron zone gravel (5) 10cm above brx.
517	Matrix, Iron zone gravel (5) 1m above brx.
518	Rhyolite cobble, {d}-{e}, Bleached zone gravel (5) 1.5m above brx.
519	Clay from fracture in mica schist ({c}-{d}), Footwall zone 1-2m below gravel contact.
520	Chalcedony/quartz (Fe-stained) vein in mica schist ({d}-{e}), Footwall zone 1-2m below gravel contact.
521	Quartz (chalcedony ?) vein in mica schist ({d}-{e}), Footwall zone 2-4m below gravel contact.
522	Matrix, Bleached zone gravel (4) 8-9m above brx. and 1m below purple stain.
523	Matrix, Bleached zone gravel (4) 9-10m above brx. and includes purple stained material.
524	Matrix, Bleached zone gravel (3) 10-11m above brx. and 0.5m above purple stain.
525	Matrix, Bleached zone gravel (3) 9-10m above brx. and includes purple stained material.
526	Matrix, Bleached zone gravel (4) 7-8m above brx.
527	Matrix, Bleached zone gravel (4) 5-6m above brx.
528	Chalcedony ? (Fe-stained) vein in mica schist ({d}-{e}), Footwall zone 3-4m below gravel contact.

Dago Hill - 1985 Samples

CN-01	Matrix, hematite-cemented Iron zone gravel (5) 1-1.5m above brx.
DG-1	Quartz vein in mica schist, conduit on south side.
DG-2	Quartz-kaolinite vein in mica schist, conduit on south side.
DG-3	Quartz vein in mica schist, conduit on south side.
DG-4	Carbonate vein in mica schist, conduit on south side.
DG-5	Carbonate vein in serpentinite, conduit on south side.
DG-6	Silicified fault breccia? conduit on south side.
DG-7	Carbonate vein in mica schist, conduit on south side.
DG-8	Mafic dike, conduit on south side.
DG-9	Carbonate replaced serpentinite, conduit on south side.
DG-10	Carbonate vein in faulted graphitic schist, conduit on south side.
DG-11	Silicified mica schist in fault zone, conduit on south side.
DG-12	Carbonate vein in mica schist, conduit on south side.
DG-13	Foliform quartz in mica schist, conduit on south side.
DG-14	Graphitic quartzite w/ pyrite, (d)-(e), 2-4m below WCG on north side.
DG-15	Iron-stained concretion, float, conduit on south side.
DG-16	Carbonate cemented breccia, conduit on south side.
DG-17	Serpentinite near fault zone, conduit on south side.
DG-18	Clay-altered serpentinite, conduit on south side.
DGF	Silicified breccia w/ cockscomb texture, float from south side.

Dawson Dome - 1985 Samples

DW-01	Quartz veins in mica schist underlying glaciofluvial gravel.

Discovery Hill - 1984 Samples

701	Basaltic volcanics, conduit on front side.
702	Chalcedonic veinlet in basaltic volcanics, conduit on front side.
703	Breccia in basaltic volcanics, conduit on front side.
704	Carbonate vein in altered volcanics, conduit on front side.
705	Carbonate vein in altered volcanics, conduit on front side.
706	Carbonate vein in altered volcanics, conduit on front side.

Discovery Hill - 1985 Samples

DH-01	Carbonate vein in altered volcanics, conduit on front side.
DH-02	Carbonate vein in altered volcanics, conduit on front side.
DH-03	Barite-carbonate vein in altered volcanics, conduit on front side.
DH-04	Fault breccia in altered volcanics, conduit on front side.
DH-05	Quartz-carbonate replaced volcanics, conduit on front side.

Discovery Pup - 1985 Samples

DP-01	Quartz vein w/ pyrite in mica schist, on brx. bench north bank.
DP-02	Quartz vein w/ pyrite in mica schist, on brx. bench north bank.

49 Hill - 1985 Samples

FH-01	Metamorphic quartz veins in mica schist, 4-8m below WCG ctk.

French Gulch - 1985 Samples

FG-01	Mesothermal quartz veins in mica schist, southeast corner of French Hill brx. bench.
FG-02	Mesothermal quartz veins in mica schist, southeast corner of French Hill brx. bench.
FG-03	Foliform quartz w/ sulphides in graphitic schist, float from mouth of gulch.
FG-04	Foliform quartz in graphitic schist, mouth of gulch.

Henry Gulch - 1985 Samples

85010-03a	Mesothermal? quartz-carbonate vein in feldspar-mica schist, mouth of gulch.
85010-03b	Mesothermal? quartz-carbonate vein w/ sulphides in feldspar-mica schist, mouth of gulch.
85010-04	Clay-altered schist around the quartz vein sampled in 85010-03a, mouth of gulch.
85010-05	Foliform quartz in feldspar-mica schist, mouth of gulch.

Hester Creek - 1985 Samples

HC-01	Foliform quartz vein in graphitic schist, mouth of creek.
HC-02	Fe-stained? mud from bottom of placer pit, mouth of creek.

Hunker Creek - 1985 Samples

HN-01	Carbonate±quartz vein in rhyolite porphyry, near Unexpected claims opposite Paradise Hill.
HN-02	Carbonate±quartz vein in rhyolite porphyry, near Unexpected claims opposite Paradise Hill.
HN-03	Carbonate±quartz vein in rhyolite porphyry, near Unexpected claims opposite Paradise Hill.
HN-04	Carbonate±quartz vein in rhyolite porphyry, near Unexpected claims opposite Paradise Hill.
HN-05	Carbonate±quartz vein in rhyolite porphyry, near Unexpected claims opposite Paradise Hill.
HN-06	Carbonate±quartz vein in rhyolite porphyry, near Unexpected claims opposite Paradise Hill.
HN-07	Carbonate±quartz vein in rhyolite porphyry, near Unexpected claims opposite Paradise Hill.
HN-08	Carbonate±quartz vein in rhyolite porphyry, near Unexpected claims opposite Paradise Hill.
HN-08	Carbonate±quartz vein in rhyolite porphyry, near Unexpected claims opposite Paradise Hill.
HN-10	Carbonate±quartz vein in rhyolite porphyry, near Unexpected claims opposite Paradise Hill.
HN-11	Carbonate±quartz vein in rhyolite porphyry, near Unexpected claims opposite Paradise Hill.
HN-12	Carbonate±quartz vein in rhyolite porphyry, near Unexpected claims opposite Paradise Hill.
HN-13	Carbonate±quartz vein in rhyolite porphyry, near Unexpected claims opposite Paradise Hill.

Hunker Porphyry - 1984 Samples

HP-01	Rhyolite porphyry, east bank opposite Independance Creek.
HP-02	Rhyolite porphyry, east bank opposite Independance Creek.
HP-03	Rhyolite porphyry, east bank opposite Independance Creek.

Jackson Hill - 1983 Samples

A-101	Diabase dike, {e}, 2-4m below WCG ctk? west side of bench.
A-102	Diabase dike, {e}, 2-4m below WCG ctk? west side of bench.
A-103	Diabase dike w/ gypsum, {e}, 2-4m below WCG ctk.? east side of bench.
B-101	Graphitic schist, {b}-{c}, 30-40m below WCG ctk. west side of bench.
B-102	Mica schist, {a}-{b}, 25-30m below WCG ctk. west side of bench.
B-103	Graphitic mica schist, {a}-{b}, west side of bench.
B-104	Mica schist, {b}-{c}, 2.5m below WCG ctk. west side of bench.
B-105	Mica schist, {b}-{c}, 1.5m below WCG ctk. west side of bench.
B-106	Serpentinite w/ Cr-mica, float from west side of bench.
B-107	Fe-concretions in altered diabase, east side of bench.
D-101	Diabase dike, {b}, 20-25m below WCG ctk. west side of bench.
D-102	Diabase dike, {a}-{b}, 10-15m below WCG ctk. west side of bench.
D-103	Diabase dike, {b}, 10-15m below WCG ctk. west side of bench.
D-104	Diabase dike, {b}, 4m below colluvium west side of bench.
D-105	Diabase dike, {c}-{d}, 2.5m below colluvium west side of bench.
D-106	Diabase dike, {b}-{c}, 1m below colluvium west side of bench.
D-107	Diabase dike, {d}-{e}, 0.5m below colluvium west side of bench.
D-108	Diabase dike, {a}-{b}, 7m below WCG ctk. west side of bench.
D-109	Diabase dike, {b}, 6m below WCG ctk. west side of bench.
D-110	Diabase dike, {c}-{d}, 3m below WCG ctk. west side of bench.
D-111	Diabase dike, {d}, 3m below WCG ctk. west side of bench.

D-112	Diabase dike, {e}, 2.5m below WCG ctk. west side of bench.
D-113	Diabase dike, {e}, 2m below WCG ctk. west side of bench.

Jackson Hill - 1984 Samples

101	Siderite-quartz vein in altered diabase, west side of bench.
102	Chlorite-schist, {a}-{b}, west side of bench.
103	Chlorite-schist, {b}, 8-10m below 105 east side of bench.
104	Chlorite-schist, {c}-{d}, 5m below 105 east side of bench.
105	Chlorite-schist, {d}-{e}, 2-5m below WCG ctk. east side of bench.
106	Siderite concretion in altered diabase, east side of bench.
107	Siderite concretion in altered diabase, west side of bench.
108	Carbonate-quartz-gypsum vein in altered diabase, west side of bench.
109	Quartz-gypsum vein in altered diabase, west side of bench.
110	Carbonate-quartz veinlet in altered diabase, west side of bench.
111	Metamorphic quartz vein in mica schist, west side of bench.
112	Siderite concretion in altered diabase, west side of bench.
113	Siderite concretion in altered mica-schist, east side of bench.
114	Metamorphic quartz vein in altered mica schist, east side of bench.
115	Metamorphic quartz vein w/ secondary siderite in altered mica schist, east side of bench.
116	Metamorphic quartz vein w/ secondary siderite in altered mica schist, east side of bench.

Lovett Hill - 1983 Samples

A-201	Altered schist from colluvial horizon? south side of bench.
A-202	Altered schist from colluvial horizon? south side of bench.
A-203	Altered schist from colluvial horizon? south side of bench.
A-204	Altered schist from colluvial horizon? south side of bench.
A-205	Altered schist from colluvial horizon? south side of bench.
A-206	Altered schist from colluvial horizon? south side of bench.
A-207	Altered schist from colluvial horizon? south side of bench.
A-208	Altered schist from colluvial horizon? south side of bench.
A-209	Altered schist from colluvial horizon? south side of bench.
A-210	Altered schist from colluvial horizon? south side of bench.
A-211	Altered schist from colluvial horizon? south side of bench.
A-212	Altered schist from colluvial horizon? south side of bench.
A-213	Altered schist from colluvial horizon? south side of bench.
A-214	Altered schist from colluvial horizon? south side of bench.
A-215	Altered schist from colluvial horizon? south side of bench.
A-216	Altered schist from colluvial horizon? south side of bench.
A-217	Altered schist from colluvial horizon? south side of bench.
A-218	Altered schist from colluvial horizon? south side of bench.
A-219	Altered schist from colluvial horizon? south side of bench.
A-220	Altered schist from colluvial horizon? south side of bench.
A-221	Altered schist from colluvial horizon? south side of bench.
A-222	Altered schist from colluvial horizon? south side of bench.
A-223	Altered schist from colluvial horizon? south side of bench.
A-224	Altered schist from colluvial horizon? south side of bench.
A-225	Altered schist from colluvial horizon? south side of bench.
A-226	Altered schist from colluvial horizon? south side of bench.
A-227	Altered schist from colluvial horizon? south side of bench.
A-228	Altered schist from colluvial horizon? south side of bench.
A-229	Altered schist from colluvial horizon? south side of bench.
A-230	Altered schist from colluvial horizon? south side of bench.
A-231	Altered schist from colluvial horizon? south side of bench.
A-232	Altered schist from colluvial horizon? south side of bench.
A-233	Altered schist from colluvial horizon? south side of bench.
A-234	Altered schist from colluvial horizon? south side of bench.

A-235	Altered schist from colluvial horizon? south side of bench.
A-236	Altered schist from colluvial horizon? south side of bench.
B-201	Altered schist from colluvial horizon? south side of bench.
	Mitchell Prospect - 1985 Samples
MP-01	Mesothermal quartz vein w/ sulphides, north of King Solomans Dome.
MP-02	Mesothermal quartz vein w/ sulphides, north of King Solomans Dome.
MP-03	Mesothermal quartz vein w/ sulphides, north of King Solomans Dome.
MP-04	Mesothermal quartz vein w/ sulphides, north of King Solomans Dome.
MP-05	Mesothermal quartz vein w/ sulphides, north of King Solomans Dome.
MP-06	Mesothermal quartz vein w/ sulphides, north of King Solomans Dome.
	Nugget Hill - 1984 Samples
901	Fe-cemented sand, Iron zone gravel (2)-(5) 0.5-1m above brx. east pit.
902	Fe-stained matrix, Iron zone gravel (2)-(5) 0.5m above brx. east pit.
903	Matrix, Bleached zone gravel (4)-(5) 3m above brx. east pit.
904	Clay in microfracture, Bleached zone gravel (5) 3m above brx. east pit.
905	Matrix, Bleached zone gravel (5) 2m above brx. east pit.
906	Mica schist clast, {e}, Bleached zone gravel (5) 3m above brx. east pit.
907	Matrix, Bleached zone gravel (5) 4m above brx. east pit.
908	Fe-cemented gravel, Iron zone gravel (2)-(5) 1m above brx. east pit.
909	Fe-cemented gravel, Iron zone gravel (2)-(5) 1m above brx. east pit.
	Nugget Hill - 1985 Samples
NH-8501	Quartz vein in graphitic schist, northeast corner of bench.
NH-8502	Quartz vein in graphitic schist, northeast corner of bench.
NH-8503	Foliform quartz vein in graphitic schist, northeast corner of bench.
NH-8504	Foliform quartz vein in graphitic schist, northeast corner of bench.
NH-8505	Quartz vein in graphitic schist, northeast corner of bench.
NH-8506	Foliform quartz vein in graphitic schist, northeast corner of bench.
NH-8507	Foliform quartz vein in graphitic schist, northeast corner of bench.
NH-8508	Quartz vein in graphitic schist, northeast corner of bench.
NH-8509	Quartz vein in altered graphitic schist, northeast corner of bench.
NH-8510	Quartz vein in altered graphitic schist, northeast corner of bench.
NH-8511	Quartz vein in graphitic schist, northeast corner of bench.
NH-8512	Quartz vein in altered graphitic schist, northeast corner of bench.
NH-8513	Quartz vein in altered graphitic schist, northeast corner of bench.
	Paradise Hill - 1984 Samples
801	Rhyolite cobbles, {a}-{b}, WCG (1)-(2) northcentral part of bench.
802	Wood from WCG.
803	Quartz vein in mica schist, south part of bench.
804	Graphitic quartzite, {b}-{c}, south part of bench.
805	Mica schist, {d}-{e}, south part of bench.
806	Matrix, WCG (1)-(2) 2m above brx. northwest part of bench.
807	Matrix, WCG (1)-(2) 4m above brx. northwest part of bench.
808	Matrix, WCG (1)-(2) 6m above brx. northwest part of bench.
809	Matrix, WCG (1)-(2) 8m above brx. northwest part of bench.
810	Matrix, WCG (1)-(2) 1m above brx. northwest part of bench.
811	Mica schist clast, {e}, WCG debris flow (5) south part of bench.
812	Rhyolite clast, {e}, WCG debris flow (5) south part of bench.
813	Matrix, WCG debris flow (5) south part of bench.
814	Mica schist clast, {a}, WCG (2) 1m above brx. northwest part of bench.
815	Rhyolite clast, {a}, WCG (2) 1m above brx. northwest part of bench.
816	Gypsum in a microfracture in WCG debris flow (5), northeast corner of bench.
817	Rhyolite unit, WCG debris flow (5) northeast corner of bench.
	Paradise Hill - 1985 Samples,
PD-8501	Magnetite-bearing serpentinite, northeast corner of bench.
PD-8502	Silicified and quartz-veined serpentinite, northeast corner of bench.
PD-8503	Silicified and quartz-veined serpentinite, float from northeast corner of bench.

PD-8504	Silicified and quartz-veined serpentinite, northeast corner of bench.
PD-8505	Silicified serpentinite, northeast corner of bench.
PD-8506	Silicified serpentinite, northeast corner of bench.
PD-8507	Fe-Mn-stained and silicified concretion, northeast corner of bench.
PD-8508	Bleached and altered magnetite-bearing serpentinite? northeast corner of bench.
PD-8509	Bleached and altered magnetite-bearing serpentinite w/ quartz veins, northeast corner of bench.
PD-8510	Quartz veins in bleached and silicified host rock? northeast corner of bench.
PD-8511	Quartz veins in altered serpentinite, northeast corner of bench.
PD-8512	Quartz veins in altered serpentinite, northeast corner of bench.
PD-8513	Quartz veins in altered serpentinite, northeast corner of bench.
PD-8514	Magnetite-bearing serpentinite, northeast corner of bench.
PD-8515	Magnetite-bearing serpentinite, northeast corner of bench.
PD-8516	?
PD-8517	Chalcedony w/ hematite in gossaned serpentinite, northeast corner of bench.

Preido Hill - 1984 Samples

601	Rhyolite porphyry and mica schist clasts, {a}-{b}, WCG (3)-(4) 2-3m above brx. south pit.
602	Rhyolite porphyry clasts, {a}-{b}, WCG (3)-(4) 2-3m above brx. south pit.
603	Rhyolite porphyry clasts, {a}-{b}, WCG (3)-(4) 8-12m above brx. south pit.
604	Rhyolite porphyry clast, {b}, WCG (3)-(4) 1.5m above brx. south pit.
605	Rhyolite porphyry clast, {d}-{e}, WCG (3)-(4) 1.5m above brx. south pit.
606	Rhyolite porphyry clast, {b}-{c}, WCG (3)-(4) 1.5-2m above brx. south pit.
607	Rhyolite porphyry clast, {a}-{b}, WCG (3)-(4) 1.5-2m above brx. south pit.
608	Rhyolite porphyry clast, {b}, WCG (3)-(4) 1.5-2m above brx. south pit.
609	Rhyolite porphyry clast, {e}, WCG (3)-(4) 1.5-2m above brx. south pit.
610	Rhyolite porphyry clast, {b}-{c}, WCG (3)-(4) 1.5-2m above brx. south pit.
611	Rhyolite porphyry clast, {a}-{b}, WCG (3)-(4) 1.5-2m above brx. south pit.
612	Rhyolite porphyry clast, {e}, WCG (3)-(4) 1.5-2m above brx. south pit.
613	Rhyolite porphyry clast, {a}-{b}, WCG (3)-(4) 1.5-2m above brx. south pit.
614	Rhyolite porphyry clast, {e}, WCG (3)-(4) 1.5-2m above brx. south pit.
615	Sandy matrix, WCG (3)-(4) 1m above brx. north pit.
616	Mn-stained matrix, WCG (3)-(4) 5-6m above brx. north pit.
617	Mn-stained matrix, WCG (3)-(4) 5-6m above brx. north pit.
618	Mn-stained matrix, WCG (3)-(4) 5-6m above brx. north pit.
619	Matrix, WCG (3)-(4) 4-5m above brx. north pit.
620	Matrix, WCG (3)-(4) 6-7m above brx. north pit.
621	Matrix, WCG (3)-(4) 8-9m above brx. north pit.
622	Fe-stained matrix, WCG (3)-(4) 8-9m above brx. north pit.
623	Silts and clays, WCG? (3)-(4) 12m above brx. north pit.
624	Silts and clays, WCG? (3)-(4) 12m above brx. north pit.
625	Silts and clays, WCG? (2) 12.5m above brx. north pit.
626	Matrix, WCG? (2) 12.5m above brx. north pit.
627	Red quartz clast, WCG (3)-(4) 4-5m above brx. north pit.

Quartz Creek - 1984 Samples

1101	Rhyolite porphyry and mica schist clasts, {a}-{b}, intermediate bench gravel.

Sourdough Hill - 1985 Samples

SD-01	Quartz-carbonate vein in deformed felsite, south of the gulch mouth.
SD-02	Deformed felsite, south of the gulch mouth.

Sulphur Creek - 1985 Samples

SC-01	Quartz vein in chlorite-mica schist, south bank opposite Green gulch.
SC-02	Quartz vein in chlorite-mica schist, south bank opposite Green gulch.
SC-03	Foliform quartz vein in chlorite-mica schist, south bank opposite Green gulch.
SC-04	Foliform quartz vein in chlorite-mica schist, south bank opposite Green gulch.

Trail Hill - 1984 Samples

301	Matrix, WCG (2)-(3) 2-3m above brx. south side near Trail gulch.

302	Matrix, Fe-Mn-stained WCG (2)-(3) 2-3m above brx. south side near Trail gulch.
303	Matrix, WCG (2) 3-4m above brx. south side near Trail gulch.
304	Graphitic schist clast, {e}, WCG (2)-(3) 0.5m above brx. south side near Trail gulch.
305	Cr-mica schist and basalt dike, south side of bench.
306	Basalt dike and pod of serpentinite, south side of bench.
307	Felsic volcanics or dike?, south side of bench.
308	Fe-stained chalcedony? amorphous material? in vein in talc-amphibole schist, 4-8m below WCG south side of bench.
309	Fe-stained chalcedony? amorphous material? in vein in talc-amphibole schist, 4-8m below WCG south side of bench.
310	Talc-amphibole schist, 4-8m below WCG south side of bench.
311	Talc-like clay in fractures of talc-amphibole schist, 4-8m below WCG south side of bench.
312	Andesite, {a}-{b}, 4-8m below WCG south side of bench.
313	Chalcedony/quartz vein (w/ amorphous material) in altered andesite, south side of bench.
314	Andesite, {d}-{e}, 4-8m below WCG south side of bench.
315	Altered chalcedony/quartz vein (w/ amorphous material) in altered andesite, 4-8m below WCG south side of bench.
316	Chalcedony/quartz vein (w/ amorphous material) in altered andesite, 4-8m below WCG south side of bench.
317	Altered volcanics w/ clays in fractures, 3-5m below WCG south side of bench.
318	Chalcedony/quartz vein (w/ amorphous material) in altered basalt dike, 4-8m below WCG south side of bench.
319	Fe-stained chalcedony/quartz vein (w/ amorphous material) in altered basalt dike, 4-8m below WCG south side of bench.
320	Fe-stained chalcedony/quartz vein (w/ amorphous material) in altered basalt dike, 8-10m below WCG south side of bench.
321	Banded chalcedony/quartz vein (w/ amorphous material) in altered basalt dike, 8-10m below WCG south side of bench.
TR-1	Quartz vein in altered brx., collected by B.N. from south side of bench.
TR-2	Quartz vein in altered brx., collected by B.N. from south side of bench.
TR-3	Quartz vein in altered brx., collected by B.N. from south side of bench.
TH-1	Quartz vein in altered brx., collected by B.N. from south side of bench.
TH-2	Quartz vein in altered brx., collected by B.N. from south side of bench.
TH-3	Quartz vein in altered brx., collected by B.N. from south side of bench.
TH-4	Quartz vein in altered brx., collected by B.N. from south side of bench.

Trail Hill - 1985 Samples

TR-8501	Plagioclase and quartz in open spaces of mica schist, 4-8m below WCG south side of bench.
TR-8502	Plagioclase and quartz in open spaces of mica schist, 4-8m below WCG south side of bench.

Key to abbreviations: alt.=alteration, brx.=bedrock, ctk.=contact, f.g.=fine-grained, w/=with, WCG=White Channel gravel.

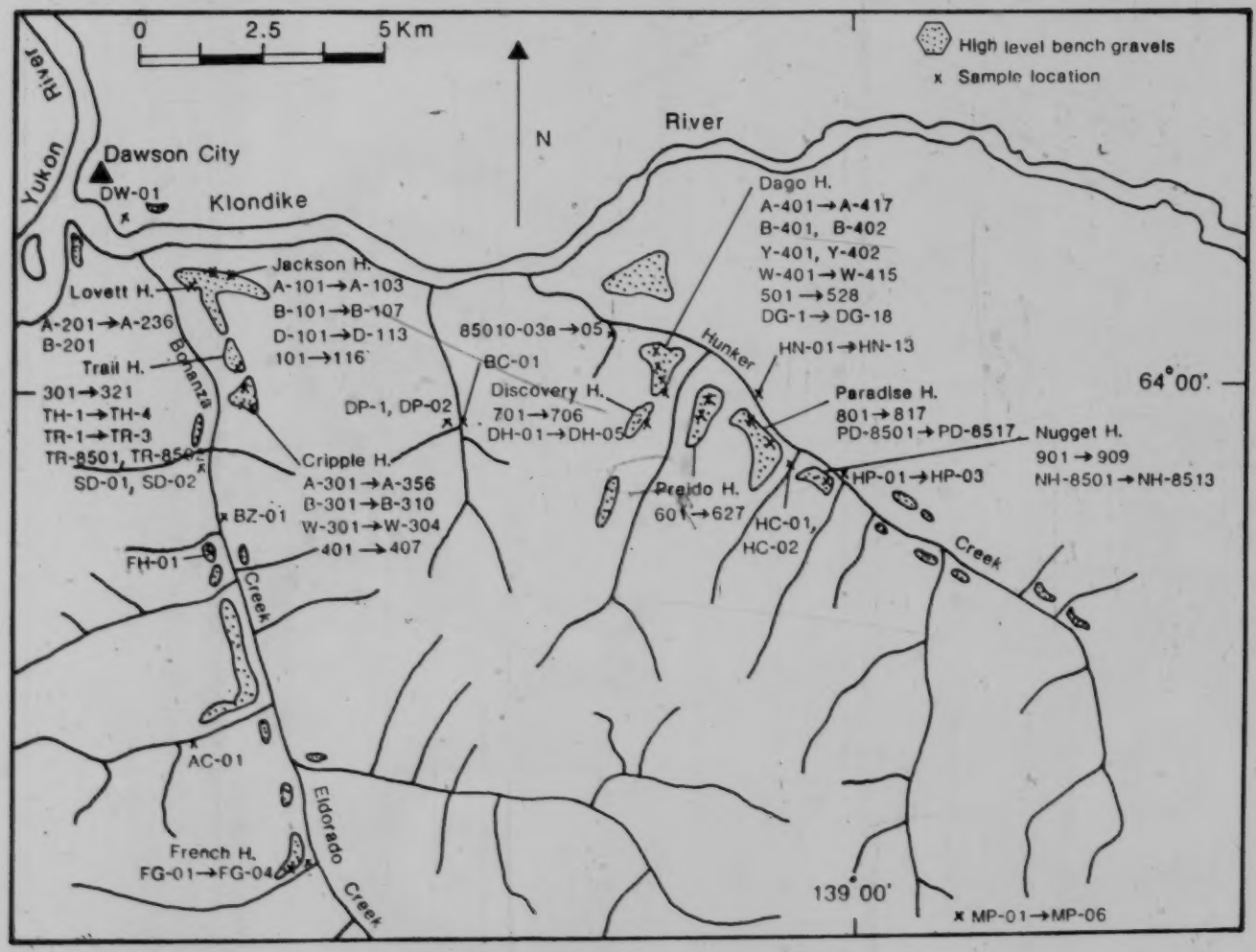

Figure 5.23 Location map for samples collected from the Klondike district.

5.3 Hydrometer Analysis

5.3.1 Background

Hydrometer analysis of grain size distribution is based upon particle settling rates in a fluid medium such as water. The rate of particle settling is dependant upon particle size, shape, density and the fluid viscosity. The maximum diameter of the particles in solution at any given time can be calculated based upon Stokes' Law of settling:

$$\omega = ([\rho_s - \rho_l]g / 18\mu) \times d^2$$

where,

ω = settling velocity of the particle (constant)
ρ_s = particle density
ρ_l = fluid density
μ = fluid viscosity
g = particle acceleration due to gravity
d = particle diameter

A hydrometer (a weighted glass cylinder) is introduced into the suspension and the solution density is obtained at various time intervals. Since the settling velocity of a particle is constant and the viscosity of the solution is assumed to be constant, the maximum diameter for a particle in solution can be calculated. Stokes' Law is valid for clay- to silt-size particles as the settling velocity of particles in this size range is dependant upon the fluid viscosity. Viscosity forces become negligible for particles greater than 0.3 to 0.4mm in diameter. As a result, the settling velocity of particles above this size range is not dependant upon viscosity of the fluid medium. The Impact Law (Krumbein and Sloss, 1963) describes the settling velocity of particles greater than 0.3-0.4mm diameter more accurately. Other basic assumptions of Stokes' Law include:

1. Particles are spherical.
2. Fluid/sediment mixture is infinitely dilute.
3. Particle densities are known.
4. Turbulence and currents are negligible.
5. Particles are completely disaggregated with no particle interaction during settling.
6. Temperature is constant.

A more detailed summary of the physics involved during particle settling is given in Blatt *et al.*, (1980).

5.3.2 Sample preparation

Samples of unconsolidated and/or clay-altered material were first dried at room temperature. Approximately 0.5 to 1kg of material was separated from each sample using a chute splitter. The material was then sieved using a No. 10 sieve (2mm). Competent (a) to breakable (b) samples of cobbles or bedrock were hand crushed using a steel mortar and pestal before being sieved Approximately 30 to 50 grams (accurately weighed) of the <2mm size fraction was placed in a 250ml beaker, the remaining amount of sample was stored for XRF analysis. Disaggregation of the sample was accomplished by adding 125ml of calgon (4% sodium hexametaphosphate) and allowing the sample to sit for 8 hours. After the soaking period the sample was then sonicated 3 to 4 times using distilled water. The suspended sediment and the solution were removed after each sonication and placed in a 1 liter graduated cylinder (settling column). After the final sonication the residue in the beaker was added and the cylinder was filled to the 1000ml line with distilled water. A control cylinder was prepared with 875ml of distilled water and 125ml of calgon. Both cylinders were allowed to equilibrate to room temperature (approximately 3 to 4 hours).

5.3.3 Procedure

To begin an analysis the settling column was agitated by shaking for approximately 1 minute. Hydrometer (density) measurements were taken at 0.25, 0.5, 1, 2, 5, 10, 15, 30, 60, 120, 240, 480 and 1440 minutes of elapsed time. The readings from 0.25 to 5 minutes were repeated several times and averaged. Temperature and density readings of the control solution were obtained periodically. Once the data was collected the following calculations were completed:

1. Hydrometer readings of the sample solution were corrected for variations in temperature and for the density of the calgon (temperature corrected density of the sample minus control density).
2. The corrected hydrometer readings were converted to effective depth (L) using calibrated tables.
3. The maximum particle diameter still in suspension was calculated by multiplying the average specific gravity of the particles (assume 2.65) by the square root of the effective depth (L) divided by the time.
4. The percentage of material in suspension at a specified time was calculated by dividing the corrected hydrometer reading by the weight of the sample.
5. A plot of maximum particle diameter versus the percentage of material still in suspension was constructed. Theoretically, the percentage of material in suspension at a specified time has a diameter less than the calculated maximum diameter for that specific time. As a result, the percentage of material in various size fractions can be determined from the graph.

5.4 Clay Mineral Analysis

5.4.1 Background

Clay minerals are hydrous layer silicates, part of the larger family phyllosilicates. Layered silicates are characterized by continuous two dimensional sheets (in the a and b directions) of SiO_4 tetrahedra bonded to sheets of octahedrally coordinated atoms. In the tetrahedral sheet 3 out of 4 oxygen atoms are bonded to neighboring tetrahedra forming a planar hexagonal network. The fourth oxygen points in a direction normal to the sheet and is shared by an octahedra in the octahedral sheet. The common plane of junction between the two sheets consists of shared apical oxygens plus unshared hydroxyl groups that lie at the center of each tetrahedral six-fold ring. Common octahedral cations include Al^{3+}, Fe^{3+}, Fe^{2+} and Mg^{2+}.

Groups and subgroups within the layered silicates are defined by their layer structure and chemistry. The 2 major groups of clay minerals are the 1:1 layered and 2:1 layered silicates. The 1:1 clay minerals are composed of repeated layers (built up in the c direction) of one tetrahedral sheet bonded to an octahedral sheet. Depending upon the valence of the octahedral cations the unit formula for the 1:1 clay minerals is $R_3^{+}Si_2O_5(OH)_4$ (trioctahedral) or $R_2^{+}Si_2O_5(OH)_4$ (dioctahedral). The 2:1 clay minerals are composed of repeated layers of two tetrahedral sheets bonded on either side of an octahedral sheet. The general unit formula for the 2:1 layered silicates (depending upon the valence of the cations in the octahedral sheet) is $R_3^{+}Si_4O_{10}(OH)_2$ (trioctahedral) or $R_2^{+}Si_4O_{10}(OH)_2$ (dioctahedral). More detailed information on the structure and chemistry of the clay minerals can be found in Brindley and Brown (1980), and Grim (1968).

Individual species of clay minerals can be identified by X-ray diffraction techniques based upon the structural and chemical differences between species. X-ray diffraction is based upon the diffraction of radiation (specifically Kα X-radiation) in accordance with Bragg's Law which states:

$$n\lambda = 2d\sin\theta$$

where

n = the order of the reflection (1, 2, 3, ...*etc.*),
λ = wavelength of the incident radiation,
d = the spacing of a parallel set of lattice planes,
θ = half the angle between the incident and diffracted rays.

An incident beam of radiation (of known wavelength) strikes a plane of points (of unknown spacing) that is a basic component of the Bravais space lattice (crystal structure) of the sample mineral. The angle between the incident and diffracted beams is measured (2θ) and the d-spacing (d) is calculated using:

$$d = n\lambda/2 \sin (2\theta/2)$$

The reflections are assumed to always be first order reflections (n). Almost all minerals have a distinctive set of d-spacings depending upon their crystal structure. Clay minerals can be identified by their integral basal spacings ($00l$) which are a reflection of their unit layer thickness in the c direction. Using well oriented samples the basal reflections are enhanced, while other hkl reflections are surpressed. This aids in the indentification of the clay minerals. For a more detailed account of the structure of clay minerals and their identification using X-ray techniques refer to Brindley and Brown (1980), Grim (1968) and Thorez (1976).

5.4.2 Sample preparation

Samples were initially prepared using the same procedure outlined in the hydrometer analysis. Once the hydrometer measurements had been taken on the sample in the settling column the cylinder was then agitated once again for approximately 1 minute. The settling velocity was used to calculate the amount of time needed to settle material $>2\mu$m in diameter to a depth of 30cm in the column (at 20°C the time needed is 23 hours, 45 minutes). The solution (containing material $<2\mu$m in diameter) was then siphoned off (approximately 30cm or 900ml) into a 2 liter beaker and 150 to 200ml of bleach (1% sodium hypochlorite) was added to aid in flocculating the clay minerals. This procedure was repeated 3 times to ensure that most of the material in the $<2\mu$m size fraction was extracted. The remaining residue (2μm-2mm size fraction) was dried and X-rayed using a random orientation technique (backpacked powder). The $<2\mu$m size fraction was then concentrated into a single beaker by draining the excess fluid after all the material had settled. The sample was then heated in a hot water bath at 60°C for 2 days to destroy any organic material present. This was followed by centrifuging until the sample was concentrated into 3 aliquots. The aliquots were then rinsed with distilled water and centrifuged several more times to remove the excess sodium hexametaphosphate and sodium hypochlorite. The presence of excess sodium in solution was detected by the formation of a cloudy precipitate upon the addition of silver nitrate ($AgNO_3$). Once the 3 aliquots had been rinsed thoroughly, one portion was saturated with potassium (20ml of 2M KCl solution for 3 hours) and another with calcium (20ml of 2M $CaCl_2$ solution for 3 hours). The third portion was left saturated with sodium. Excess potassium and calcium were removed using the same procedure described for the removal of excess sodium. All the aliqouts were then freeze-dried for 2 days to remove the excess fluid.

The next step involved the preparation of basal oriented samples on ceramic discs 2.5cm in diameter. Approximately 40-50mg of freeze-dried sample from the calcium and potassium saturated aliquots were each mixed thoroughly with 5-10ml of distilled water and then sonicated for 1 minute. The aliquots were then deposited onto ceramic discs using a suction apparatus following the method of Kinter and Diamond (1956). For each sample 2 discs were created; the $<2\mu$m size fraction calcium saturated and the $<2\mu$m size fraction potassium saturated. For a more detailed account of this and other sample preparation techniques consult Brindley and Brown (1980).

The residue, which consisted of material in the 2μm-2mm size fraction, was X-rayed using a backpack method in order to obtain random orientation of the minerals present. A dried powder was packed from the back into an aluminum sample holder approximately 1.5 x

2cm and 1mm in depth. The front portion of the sample holder was then irradiated. Identification of all the minerals present in sufficient quantities was accomplished by comparing the *d*-spacings of the observed peaks on the diffractogram with the *d*-spacings of common minerals in the JCPDS diffraction data files.

5.4.3 X-ray diffraction

It is generally accepted that most of the authigenic clay minerals occur in the <2μm size fraction (Grim, 1968). As a result, the potassium and calcium saturated discs were X-rayed using the following treatments to aid in the indentification of the clay minerals:

1. Calcium saturated (<2μm) disc: run from 2°2θ to 35°2θ in an atmosphere of 54% relative humidity (sample was first equilibrated to 54% relative humidity for 24 hours over a magnesium nitrate solution).
2. Calcium saturated (<2μm) disc: run from 2°2θ to 75°2θ in an atmosphere of 54% relative humidity after vapour solvating the sample with ethylene glycol (sample was equilibrated with atmosphere over ethylene glycol for 24 hours after heating the solution and sample to 65°C for 4 hours).
3. Potassium saturated (<2μm) disc: run from 2°2θ to 35°2θ in a nitrogen atmosphere (0% relative humidity) while still hot, after heating to 105°C for 24 hours.
4. Potassium saturated (<2μm) disc: run from 2°2θ to 35°2θ in an atmosphere of 54% relative humidity (sample was equilibrated to 54% relative humidity over a magnesium nitrate solution for 24 hours after 0% RH K$^+$ run).
5. Potassium saturated (<2μm) disc: run from 2°2θ to 22°2θ in a nitrogen atmosphere (0% relative humidity) after heating to 300°C for 3 hours.
6. Potassium saturated (<2μm) disc: run from 2°2θ to 22°2θ in a nitrogen atmosphere (0% relative humidity) after heating to 500°C for 2 hours.

These treatments are based upon the X-ray methods of Ignasiuk *et al.* (1983) and Longstaffe (1984). The X-ray diffractograms were obtained on a Philips vertical goniometer diffractometer equipped with a graphite monochromator filter using Co *k*α radiation produced by 50kV and 20mA. Diffraction patterns were obtained at 1°2θ/minute using a 1° divergent slit and chart speed at 600mm/hr (Ignasiuk *et al.*, 1983; Longstaffe, 1984). Identification of the clay minerals is based upon their basal spacings throughout these treatments. Brindley and Brown (1980), Grim (1968) and Thorez (1976) provide detailed summaries of the X-ray characteristics of the common clay minerals.

5.4.4 Clay mineral abundances

Semi-quantitative estimates of clay mineral abundances were calculated from the diffractograms of the <2μm size fraction using an internal standard (illite) and measuring peak heights. Appropiately weighted form factors were used in the calculations to account for differences in crystallinities and peak intensities between different species of clay minerals. The calculation procedure outlined below is modified after similar calculations by Biscaye (1965) and Johns *et al.* (1954).

1. A smooth baseline was drawn beneath the first order peaks on the <2μm size fraction

glycol and potassium saturated (550°C) diffractograms approximating the level of the background noise.

2. The 001 peak heights of kaolinite (7Å), illite (10Å), smectite (17Å) and the 002 of interstratified illite/smectite (≈13-14Å) or illite/chlorite (≈11-12Å) were measured on the <2μm size fraction glycol saturated diffractogram. Peak height was measured from the baseline established in step 1.
3. The 001 (14Å) chlorite peak height (if any was present) was measured on the diffractogram of the the <2μm size fraction potassium saturated sample after heating to 550°C for 2 hours. This eliminates interference from the smectite 001 or the 002 of the interstratified clay minerals. The same instrument settings used for the glycol diffractogram were used for this step.
4. The form factors were calculated as follows:

   a. Illite (10Å peak) was used as the internal standard and was assigned a form factor of 1.000.
   b. Smectite (17Å peak) = $\frac{\text{height of 17Å peak}}{4 \times \text{height of 10Å peak}}$
   c. Chlorite (14Å peak) = $\frac{\text{height of 14Å peak (550°C, K°)}}{3 \times \text{height of 10Å peak}}$
   d. Kaolinite (7Å peak) = $\frac{\text{height of 7Å peak}}{2.5 \times \text{height of 10Å peak}}$
   e. Illite/Smectite (≈13.5Å peak) = $\frac{\text{height of 002 (≈13.5Å) peak}}{2 \times \text{height of 10Å peak}}$

   The form factor values were summed. Individual form factors were divided by the sum and multiplied by 100 to estimate preliminary relative abundances of the clay minerals.
5. If chlorite was present then overlap occurred between the kaolinite 001 and the chlorite 002 peaks. A percentage for kaolinite was then obtained by subtracting the preliminary chlorite percentage from the preliminary kaolinite percentage. The clay mineral percentages were then summed again. The individual percentages were divided by the new sum and multiplied by 100 to yield relative abundances of the clay minerals in the presence of chlorite.
6. The method is generally reproducible with ±10% error.

5.4.5 Clay mineral crystallinities

Crystallinity measurements were completed on the kaolin minerals, illite and smectite as follows:

1. Kaolin minerals: The sodium saturated <2μm size fraction powder was packpacked into an aluminum sample holder and X-rayed from 2°2θ to 35°2θ. Scaler and multiplier were set at 1×10^3, while the time constant was at 2. All other conditions of the Philips diffractometer were the same as outlined for analyses of oriented (<2μm size fraction) samples. The measurements were performed according to the prescribed method of Hinckley (1963). The Hinckley (1963) crystallinity index (HCI) is equal to the heights of the $1\bar{1}0$ and $11\bar{1}$ above the local background, divided by the total height of the $1\bar{1}0$.
2. Illite minerals: The illite crystallinity was measured by taking the width of the 001 (10Å) peak (in millimeters) at half the peak height on the diffractogram of the glycol saturated <2μm size fraction (Dunoyer de Segonzac, 1969).

3. Smectite minerals: Smectite crystallinity was measured by taking the depth of the valley (V) between the 001 (17Å) peak and the background curve on the low angle side of the 001 (17Å). This value (V) was then divided by the height of the 001 (17Å) peak above background. The method was devised by Biscaye (1965).

5.5 Geochemical Analysis

5.5.1 X-Ray Fluorescence Analysis

Whole rock analyses were performed by the X-ray fluorescence (XRF) technique at McMaster University. Sample preparations were completed at the University of Alberta.

5.5.1.1 Sample preparation

Samples of unconsolidated and/or clay-altered material were first dried at room temperature. Approximately 0.5 to 1 kilogram of material was separated from each sample, where possible, using a chute splitter. The material was then sieved using a No. 10 sieve (2mm). Samples of competent (a) to breakable (b) cobbles and bedrock were cut in half with a diamond saw. One half was saved for thin sectioning and as a reserve. The other half, to be used for analysis, was washed and then crushed using a steel mortar and pestal before being sieved. Samples of vein material were hand crushed using a steel mortar and pestal, however, these samples were not sieved. All of the samples were split in two after being hand crushed and sieved. One split of each sample was run through a tungsten carbide swing mill. The other half was saved or used for clay mineral analysis. The swing mill was cleaned between each sample using 20/30 mesh sandblasting sand, followed by washing with detergent and drying with compressed air. After crushing, each sample pulp was tumbled for 12 to 16 hours in order to homogenize the pulp. A 15 gram aliquot was taken from each sample and placed in plastic vials. The remaining pulps were stored in plastic containers. The sample aliquots were then packaged and sent to McMaster University for whole rock analysis. Several replicate samples were sent with each batch in order to test the analytical precision within each batch and between batches.

At McMaster University two grams from each whole rock sample were fused with lithium tetraborate. The fused samples were recrushed and pressed into pellets. Each pellet was then analysed for major, minor and selected trace elements using an XRF machine. The X-ray intensities were corrected for matrix and background effects. Each sample analysis was normalized to 100%. The error of measurement at one sigma level is ± 0.05 for major elements and nearly $\pm 5\%$ for minor elements which are present in amounts less than 1%. The detection limit for the trace elements is 3ppm and the error of measurement is less than $\pm 5\%$. A detailed discussion of the procedure, accuracy and precision for this technique is presented in Longstaffe (1978).

5.5.2 Instrumental Neutron Activation Analysis

Selected vein samples collected during the 1985 field season were analysed by Instrumental Neutron Activation Analysis (INAA). All the irradiations were done in the University of Alberta SLOWPOKE II reactor, and all counting was done with the gamma spectroscopy equipment at this facility.

5.5.2.1 Sample preparation

Each vein sample was hand crushed using a steel mortar and pestal. Due to the small sample size only a small amount of sample was kept in reserve for fluid inclusion and stable isotope analysis. All the material that was hand crushed from each sample was ground to a

fine powder using an automated agate mortar and pestal. This unit was cleaned between each sample using 20/30 mesh sandblasting sand, followed by washing with detergent and drying with compressed air. Each sample pulp was tumbled for 12 to 16 hours in order to homogenize the pulp. Approximately 100 mg of rock powder from each sample ws sealed in a plastic irradiation vial, irradiated, and counted with Ge (Li) detectors. Counting was done after a short decay period (between 5 and 8 days). As a result, only certain elements such as the rare earth elements, Fe, Na, Cr, Co, As, Sb and Au were detectable due to high background activities. A detailed discussion of the procedure, accuracy and precision is given in St. Louis (1984). Four gravel matrix samples were analysed using this method, three of which were prepared for and analysed by the XRF method. These three samples (Table 3.13) had extremely high background activities due to the presence of tungsten aquired during crushing in the tungsten carbide swing mill.